

NUREG/CR-1099  
PNL-3177

---

---

# Depleted Uranium Dioxide Power Flow Through Very Small Openings

---

---

Prepared by S. L. Sutter, J. W. Johnston, J. Mishima, P. C. Owzarski,  
L. C. Schwendiman and G. B. Long, Editor

Pacific Northwest Laboratory

Prepared for  
U. S. Nuclear Regulatory  
Commission

POOR ORIGINAL

8008250

385

912

## NOTICE

This report was prepared as an account of work sponsored by an agency of the United States Government. Neither the United States Government nor any agency thereof, or any of their employees, makes any warranty, expressed or implied, or assumes any legal liability or responsibility for any third party's use, or the results of such use, of any information, apparatus product or process disclosed in this report, or represents that its use by such third party would not infringe privately owned rights.

POOR ORIGINAL

Available from

GPO Sales Program  
Division of Technical Information and Document Control  
U. S. Nuclear Regulatory Commission  
Washington, D. C. 20555

and

National Technical Information Service  
Springfield, Virginia 22161

DEPLETED URANIUM DIOXIDE POWDER  
FLOW THROUGH VERY SMALL OPENINGS

S. L. Sutter  
J. W. Johnston  
J. Mishima  
P. C. Owzarski  
L. C. Schwendiman  
G. B. Long, Editor

Manuscript Completed: January 1980  
Date Published: February 1980

Prepared for  
the U.S. Nuclear Regulatory Commission  
Division of Safeguards,  
Fuel Cycle and Environmental Research  
Office of Nuclear Regulatory Research  
Under a Related Services Agreement  
with the U. S. Department of Energy  
Contract EY-76-C-06-1830  
NRC Fin No. B2093

Pacific Northwest Laboratory  
Operated for the U.S. Department of Energy  
by Battelle Memorial Institute

## ABSTRACT

The report presents the results of experiments that measured the leakage of depleted uranium dioxide (DUO) powder through microorifices in a vessel approximately the same dimensions as a plutonium dioxide shipping container. Leaks were measured as a function of upstream pressure (15 psig to 1000 psig) and above and below the static powder level.

An equation was developed to predict powder transmission from leaks using  $\ln(A\sqrt{P}) > 10.5$  ( $A$  = area;  $P$  = pressure). Maximum DUO transmission values were calculated for leaks where  $\ln(A\sqrt{P}) < 10.5$ .

Conclusions of the study were: 1) diameter was the most important parameter in powder leakage; diameter and pressure were both significant; 2) the duration of a run had no statistically discernible effect on powder transmitted in times ranging to 24 hr; 3) the opening orifice or capillary types and location above or below the static powder level affected powder transmission; 4) agitation did not influence the flow from a leak below the static powder level; 5) the amount of powder covering a leak did not affect the leak below the static powder level; 6) leakage below the static powder level maximized at 100 psig for openings less than approximately 100  $\mu\text{m}$ ; 7) plugging was a frequent occurrence: 6% of the orifices and 17% of the capillaries plugged immediately upon pressurization (above powder leaks); and 8) efforts to increase the powder leakage by various procedures were unsuccessful.

## CONTENTS

ABSTRACT . . . . .	iii
FIGURES . . . . .	ix
TABLES . . . . .	xiii
INTRODUCTION . . . . .	1
OBJECTIVE . . . . .	5
SUMMARY AND CONCLUSIONS . . . . .	7
DESCRIPTION OF PLUTONIUM OXIDE SHIPPING CONTAINER SIMULATED IN EXPERIMENTS . . . . .	11
PHYSICAL PROPERTIES OF PARTICLES AFFECTING POWDER FLOW . . . . .	15
PARTICLE DIAMETER/APERTURE DIAMETER . . . . .	15
PARTICLE DIAMETER . . . . .	16
VOIDAGES . . . . .	16
MOISTURE CONTENT, HYGROSCOPICITY . . . . .	17
"HEAD" . . . . .	17
ANGULAR PROPERTIES . . . . .	17
EXPERIMENTAL: APPARATUS AND EXPERIMENTS PERFORMED . . . . .	19
APPARATUS . . . . .	19
Leak Path Above the Static Powder Level Apparatus (APLA) . . . . .	19
Vessel . . . . .	19
Sample Collection Chamber . . . . .	22
Pressure Measurements . . . . .	22
Agitation Airflow . . . . .	23
Orifices and Capillaries . . . . .	27
Flowmeters . . . . .	27
Depleted Uranium Dioxide Simulant . . . . .	29
Experimental Procedure . . . . .	31
Uranium Analysis . . . . .	31
Leak Path Under the Static Powder Level Apparatus (UPL) . . . . .	32
EXPERIMENTS PERFORMED . . . . .	32
Leak Path Above the Static Powder Level (APL) Experiments . . . . .	34

Leak Path Under the Static Powder Level (UPL) Experiments . . . . .	35
RESULTS AND DISCUSSION: LEAK PATH ABOVE THE STATIC POWDER LEVEL . . . . .	37
PLUGGING . . . . .	37
EXTRANEOUS LEAKAGE . . . . .	41
BACKGROUND DUO LEVELS . . . . .	41
RESULTS: FIRST SERIES . . . . .	42
APLA Preliminary Statistical Analysis . . . . .	43
DUO Transmitted During Pressurization/Depressurization . . . . .	47
Statistical Matrix Work . . . . .	48
Thirty-Minute Runs . . . . .	50
Eighteen "Zero"-Time Runs . . . . .	50
POWDER LEAKAGE WITH UNAIDED AIRFLOW . . . . .	50
EXTENDED TIME RUNS . . . . .	52
PRESSURE DECAY RUNS . . . . .	55
SLOW PRESSURIZATION . . . . .	56
APLA CAPILLARY LEAKS . . . . .	57
RESULTS AND DISCUSSION: LEAK PATH UNDER THE STATIC POWDER LEVEL . . . . .	59
LEAKS UNDER THE STATIC POWDER LEVEL . . . . .	59
DEPTH (WEIGHT) EFFECTS . . . . .	59
LEAKAGE FOR AN EXTENDED TIME . . . . .	61
PRESSURIZATION TIME . . . . .	62
RESERVOIR ORIENTATION AND SLOW PRESSURIZATION . . . . .	63
UPL CAPILLARY LEAKS . . . . .	66
MAXIMUM LEAKAGE . . . . .	66
REFERENCES . . . . .	69
APPENDIX A - TABULATION OF ANALYTICAL RESULTS . . . . .	A-1
APPENDIX B - STATISTICAL ANALYSIS OF DUO EXPERIMENTS . . . . .	B-1
SUMMARY . . . . .	B-1
DATA BASE . . . . .	B-8
Data Collection . . . . .	B-8
Data Organization . . . . .	B-9
Orifice Characterization . . . . .	B-9
DATA ANALYSIS . . . . .	B-10
Thirty-Minute Experiment . . . . .	B-12

"Zero"-Time Experiment . . . . .	B-16
Pressure Decay Runs . . . . .	B-20
Measured Flow Runs . . . . .	B-22
UPL Orifices . . . . .	B-27
UPL Time Comparisons . . . . .	B-30
Analysis of Variance for UPL Data . . . . .	B-32
UPL Orifices - Grams DUO Varied . . . . .	B-36
APL Capillary Runs . . . . .	B-40
SENSITIVITY ANALYSIS . . . . .	B-43
Apparatus Type . . . . .	B-45
Opening Type . . . . .	B-45
Aerosolization Mechanism . . . . .	B-50
Flow Mechanism . . . . .	B-50
PREDICTION EQUATIONS . . . . .	B-51
Statistical Models . . . . .	B-51
Correlations . . . . .	B-53
Statistics for $\ln$ DUO Data . . . . .	B-55
Number of Observations . . . . .	B-58
Averages . . . . .	B-58
Standard Deviations . . . . .	B-59
Multiple Correlation Coefficients . . . . .	B-59
Expected Transmissions for Low Airflows . . . . .	B-60
Expected Transmission for Higher Airflows . . . . .	B-65
REFERENCES . . . . .	B-83
APPENDIX C - ORIFICE FLOW DURING "ZERO"-TIME RUNS . . . . .	C-1
APPENDIX D - TOTAL MASS DUO TRANSMITTED AS A FUNCTION OF TOTAL AIRFLOW . . . . .	D-1
APPENDIX E - ORIFICE LENGTH-TO-DIAMETER RATIO . . . . .	E-1
APPENDIX F - RHEOLOGICAL TEST . . . . .	F-1

## FIGURES

1	Plutonium Air Transportable Package (PAT-1)	12
2	Cutaway Drawing of TB-1 Containment Vessel	13
3	Leak Test Pressure Vessel	20
4	APLA Flow/Pressure Control and Measurement Components	21
5	Schematic of the Above Powder Leak Test Vessel	22
6	Schematic of APL Airflow System	23
7	Sampler Detail for Above Powder Leaks	24
8	Orifice 1-100 After APLA 2 (Before and After Cleaning in Sonic Bath)	26
9	DUO and PuO <sub>2</sub> Particle Size Distributions	30
10	Under Powder Leak Rate Apparatus	33
11	The Second Powder Reservoir and Sample Collection Chamber	34
12	Plugged Apertures, Orifices (Top) and Capillaries (Bottom)	38
13	Scanning Electron Micrographs of Capillary Core Casts Showing Surface Roughness	40
14	Efficiency Test of Cement Seal of Orifice Plate	42
15	APLA Powder Flow Rates Through Characterized Leaks as a Function of Airflow Rates, $\mu\text{g}/\text{cc}$	44
16	APLA Powder Flow Rates Through Characterized Leaks as a Function of Airflow Rates, $\mu\text{g}/\text{min}$	45
17	Comparison of APLA Treatments Indicating Diameter Relationships	46
18	Total DUO Transmitted in 1000 psig APLA Experiments Compared with "Zero"-Time DUO Transmission	48
19	Total DUO Transmitted Through Orifices as a Function of Pressure and Diameter, 30-Min Experiments	51
20	Comparison of 30-min and "Zero"-Time Runs by Orifice Size	51
21	Comparison of DUO Transmitted Through Orifices By Maintained and Measured Airflow	52
22	APLA Airflow Rate as a Function of Time During a 24-hr Run, Orifice 1-110, 100 psig	53
23	Total DUO Transmitted Through 110- $\mu\text{m}$ Orifice During APLA Runs at 100 psig, as a Function of Time	54
24	DUO Leak Rate Through 110- $\mu\text{m}$ Orifices During APLA Runs at 100 psig, as a Function of Time	55



25	Comparison of Pressure Decay and Other Runs at 1000 psig . . . . .	56
26	DUO Powder Transmission Through Capillaries as a Function of Pressure (Top) and Diameter (Bottom) . . . . .	58
27	Total DUO Transmitted from Leaks Below the Static Powder Level as a Function of Pressure (Top) and Diameter (Bottom) . . . . .	60
28	Total DUO Transmitted From Leaks Below Different Quantities of Powder . . . . .	61
29	Total DUO Transmitted Through Orifices for Different Experimental Treatments, UPL . . . . .	64
30	Total DUO Transmitted from Leaks Below Powder Level, 2 Reservoirs, 25 g Powder, 1.5-cm Depth, 2-110 Orifice . . . . .	65
31	Reservoir Shapes . . . . .	66
32	Total DUO Transmitted Through Capillaries as a Function of Pressure (Top) and Diameter (Bottom) for UPL Experiments . . . . .	67
B1	Plots of Treatment Means, 30-min Experiment . . . . .	B-15
B2	Comparison of 30-min and "Zero"-Time Runs by Orifice . . . . .	B-20
B3	Comparison of Pressure Decay and Other Runs at 1000 psig . . . . .	B-22
B4	Plots of Treatment Means, Measured Flow Runs . . . . .	B-25
B5	Comparison of Maintained and Measured Flow Averages . . . . .	B-27
B6	UPL Comparisons Over Time . . . . .	B-31
B7	Pressure by Orifice Means, UPL Data . . . . .	B-35
B8	Cell Means for Weight-Varied UPL Runs . . . . .	B-39
B9	APLA Capillary Data . . . . .	B-42
B10	UPL vs. APLA at 500 psig . . . . .	B-46
B11	UPL vs. APLA at 1000 psig . . . . .	B-46
B12	Apparatus by Opening Type Comparison - Cell Means . . . . .	B-48
B13	Plot of All Data Used to Select Best Fit . . . . .	B-56
B14	Region for Which $\ln(A\sqrt{P})$ is Greater than 10.5 . . . . .	B-69
B15	Comparison of Prediction Equations Based on UPL-0, APL-0 and Capillaries Data Sets at 1000 psig . . . . .	B-71
B16	Estimated Values for UPL-0 . . . . .	B-72
B17	Estimated Values for APLA-0 . . . . .	B-73
B18	Estimated Values for Capillaries . . . . .	B-74
B19	Estimated Values for All Data . . . . .	B-76
B20	Confidence Limits for 1000 psig Estimates Based on Fit to All Data . . . . .	B-77

B21	Observed vs. Estimated Values for Fit to All Data . . . . .	B-78
B22	Observed vs. Estimated Values for UPL-0 Data . . . . .	B-80
B23	Observed vs. Estimated Values for APLA-0 Data . . . . .	B-81
B24	Observed vs. Estimated Values for Capillaries Data . . . . .	B-82
D1	Relationship Between Total Mass of Particles and Total Airflow Through Orifices for APLA Experiments . . . . .	D-2
D2	Relationship Between Total Mass of Particles and Total Airflow Transmitted Through Capillaries for ALPLA Experiments . . . . .	D-3
D3	Relationship Between Total Mass of Particles and Total Airflow Transmitted Through Orifices for UPL Experiments . . . . .	D-4
D4	Relationship Between Total Mass of Particles and Total Airflow Through Capillaries for UPL Experiments . . . . .	D-5
F1	Bin-Flow Test Vessel . . . . .	F-2
F2	Area Where DUO Dropped from Bin . . . . .	F-2
F3	Core Formed in Powder to Allow Ejection of DUO . . . . .	F-2
F4	Morphology of DUO Powder . . . . .	F-4

TABLES

1	Measured Orifice Diameters . . . . .	28
2	Measured Capillary Diameters . . . . .	28
3	Times Required for Pressurization/Depressurization of APLA Vessel . . . . .	47
4	Original and Final Orifice Sizes . . . . .	49
5	Total DUO Transmitted at Immediate Pressurization and 80-min Pressurization . . . . .	57
6	Total DUO Collected from Leaks Underneath the Static Powder Level for Different Collection Times . . . . .	62
7	Maximum Total DUO Transmitted for APLA and UPL Capillary and Orifice Experiments . . . . .	68
A1	Depleted Uranium Dioxide Transmission for Leak Paths Above the Static Powder Level . . . . .	A-1
A2	Depleted Uranium Dioxide Transmission for Leak Paths Under the Static Powder Level . . . . .	A-17
B1	Summary Table . . . . .	B-5
B2	Definition of Data Sets . . . . .	B-10
B3	Orifice Identification . . . . .	B-11
B4	Data, Sums and Averages for 30-min Experiment ( $\ln$ DUO $\mu$ g) . . . . .	B-13
B5	Analysis of Variance for 30-min Experiment ( $\ln$ DUO $\mu$ g) . . . . .	B-15
B6	Data, Sums and Averages for "Zero"-Time Experiment ( $\ln$ DUO $\mu$ g) . . . . .	B-17
B7	Comparison of 30-min and "Zero"-Time Treatments ( $\ln$ DUO $\mu$ g) . . . . .	B-17
B8	Analysis of Variance Comparing 30-Min and "Zero"-Time Runs . . . . .	B-18
B9	Data for Pressure Decay Comparisons All Runs at 1000 psig ( $\ln$ DUO) . . . . .	B-21
B10	Data, Sums and Averages for Measured Flow Runs . . . . .	B-23
B11	Analysis of Variance for Measured Flow Runs . . . . .	B-25
B12	Comparison of Maintained and Measured Flow Runs . . . . .	B-26
B13	Analysis of Variance Comparing Maintained and Measured Flow Runs . . . . .	B-26
B14	Numbers of Runs for UPL Orifices . . . . .	B-28
B15	Numbers of UPL Runs - Orifice by Time by Pressure . . . . .	B-29
B16	UPL Orifices Time Comparisons, $\ln$ DUO $\mu$ g . . . . .	B-31
B17	Averages and Standard Deviations for Orifice by Pressure . . . . .	B-32
B18	UPL Orifices Data for Analysis of Variance, $\ln$ (DUO $\mu$ g) . . . . .	B-33

B19A	Treatment Averages and Sums of Averages for UPL Orifices	. . .	B-34
B19B	Treatment Averages and Sums of Averages for UPL Orifices	. . .	B-34
B20	Analysis of Variance on UPL Orifices Treatment Means	. . .	B-35
B21	Data for UPL Grams DUO, Varied Runs (Orifice 13 at 111 $\mu\text{m}$ )	. . .	B-37
B22	Data, Sums and Averages for UPL Grams - DUO Varied Runs ( $\ln$ DUO)	. . . . .	B-38
B23	Analysis of Variance for UPL - Grams DUO Varied Runs	. . .	B-38
B24	APLA Capillaries Data, $\ln$ DUO	. . . . .	B-41
B25	Cell Means for UPL and APLA Comparisons	. . . . .	B-44
B26	Two-by-Two Tables Comparing APLA and UPL Dominance	. . .	B-47
B27	Correlations	. . . . .	B-54
B28	Statistics for $\ln$ DUO Data Used in Regression Equations	. . .	B-57
B29	Combinations of Pressure and Opening Diameter Required for $\ln$ ( $\text{AVP}$ ) = 10.5	. . . . .	B-61
B30	Stem and Leaf Displays of $\ln$ DUO for $\ln \text{AVP} < 10.5$	. . .	B-62
B31	Confidence Limits on Average $\ln$ DUO	. . . . .	B-64
B32	Comparisons of $R^2$ for Some Prediction Equations	. . . . .	B-66
B33	Statistics for Fits to the Prediction Equation $\ln \text{DUO} = a + b_1$ $\ln A + b_2 \sqrt{P}$	. . . . .	B-70
C1	Pressurization/Depressurization Times for APLA Runs	. . .	C-1
C2	Pressurization/Depressurization Gas Flows	. . . . .	C-2

## INTRODUCTION

Shipping containers for plutonium oxide have been designed to withstand severe postulated accidents. Stringent requirements have been placed on the integrity of plutonium shipping containers, but under severe impact some very small leaks may occur. These leaks can be tolerated if research can show that the powder contents do not leak to a significant degree. Specifications for leak tightness of radioactive material shipping containers are generally defined in terms of a leak rate for a gas, such as helium, that can be measured with great sensitivity. Because anticipated shipments of plutonium will be in the form of a fine plutonium oxide powder, it is necessary to know the potential leakage of this powder from leaks in the containers.

The first task of this powder leakage study was to review information in literature related to particle transport through very small apertures (Schwendiman and Sutter 1977). The literature review demonstrated that relatively few studies have been undertaken either theoretically or experimentally to determine the rate at which particles may be transported through narrow passageways. However, the literature review suggested that a rather small quantity of very small particles would leak through a very small channel as a result of many interacting mechanisms preventing particle passage. Subsequently, the present experiments reported here were designed to investigate particle losses through very small openings.

The experiments were to investigate a specific leak problem: the loss of fine plutonium oxide powder from a shipping container whose integrity has been breached under the stresses of an accident. These accident conditions were suggested in the Safety Analysis Report of the Plutonium Air Transportable Package (NRC 1978). The peak temperature for the qualification fire test was 1080<sup>o</sup>F, resulting in an internal pressure less than 1110 psia. However, we did not conduct elevated temperature tests because of experiment difficulties and safety considerations. In addition, airflow measurements (Sutter, Bander, Mishima and Schwendiman 1978; Owzarski et al. 1979) indicated less flow at elevated temperatures, which suggested that elevated temperature tests were of lesser importance. Therefore, tests selected and performed for our study measured powder leakage from a container pressurized to 1000 psig at room temperature.

Since the location of a leak in the shipping container may be above the powder level, or the bulk powder may completely cover the leak, particles could be jetted or vibrated through leak passageways under appropriate conditions. Therefore, the tested leaks were located above and below the static powder level.

A leak path can assume a variety of shapes and sizes. We studied leakage of very fine depleted uranium dioxide (DUO) powder through round orifices and capillaries. Although a narrow, tortuous leak path may simulate a more realistic leak, we believed that our selected configurations should give the maximum powder flow for the leak diameters and could be adequately described mathematically. The nominal leak diameters selected ranged from a 20- $\mu\text{m}$  orifice to a 250- $\mu\text{m}$  capillary.

The orifices and capillaries involved in these tests were characterized (Sutter, Bander, Mishima and Schwendiman 1978; Owzarski et al. 1979) in experiments measuring the airflow rates to verify flow prediction capability.

The shipping container simulated was designed specifically for  $\text{PuO}_2$  and mixtures of natural or depleted uranium dioxide and plutonium oxide. Depleted uranium dioxide was selected as the surrogate powder for these tests since DUO is a heavy metal with density and particle size similar to  $\text{PuO}_2$ , although different in morphology. For the quantity of powder used in these tests, approximately 3 kg, the use of  $\text{PuO}_2$  would have required special equipment and procedures. These difficulties precluded the use of  $\text{PuO}_2$  and depleted uranium dioxide was selected instead.

The results from the powder leak-rate study have been compiled in a series of quarterly reports (Schwendiman et al. 1976 to 1979). These reports can be consulted to follow the historical development of the project. The structure of this final report has been based on the project development reported in the series of quarterly reports. The information presented in the quarterly reports was evaluated, and a statistical analysis of the data was completed. In many instances the conclusions reached in the quarterly reports were invalidated as new information was developed and analyzed. For use in predicting powder flow resulting from the conditions of the DUO experiments,

we suggest using the values presented in this final report rather than the earlier reported observations.

All of the experimental results have been tabulated in Appendix A, with separate listings for leaks above and below the static powder level. The quantity of DUO measured for each experiment is reported as total  $\mu\text{g}$  DUO transmitted,  $\mu\text{g}$  DUO/min and  $\mu\text{g}$  DUO/cc air. Experimental parameters are included: aperture diameter, chamber pressure, length of run, airflow (cc/min), agitation (UPL only), and for some UPL experiments, the weight of DUO and sampler orientation. The complete statistical analysis of the results are discussed in Appendix B, and a summary is included.

In the overall study to quantify the relationship between the release of fine powder and specified gas leak rates through microopenings. Pacific Northwest Laboratory (PNL) defined gas leak rates and DUO powder transmission; Battelle Columbus measured  $\text{PuO}_2$  transmission. Both laboratories agreed that a uniform data presentation would facilitate relating the two sets of data. The format agreed upon was a tabulation of total mass of particles transmitted in micrograms versus a standard volume of gas leaked in each run. These values have been included as Appendix D and consist of plots of the total mass of particles transmitted in micrograms versus the total standard volume of gas leaked in each run. The total airflow through the orifices through the "zero"-time portion of the APLA runs was calculated using the methods in Appendix C.

Appendix E reports on the measurement of the length of the orifices. A length/diameter (L/D) of 1 or less had been specified for the orifices (Sutter et al. 1978). However, a nondestructive method to accurately measure the length of the orifices was not readily available at that time. One of the 20- $\mu\text{m}$  orifices was measured by destructive techniques after the powder flow tests were completed. The L/D ratio of this orifice was 28.

Appendix F describes a rheological test applied to the DUO powder to investigate its innate "flowability." The powder did not "flow" under the influence of gravity even through an opening 1.27 x 2.54 cm where the area equaled 3.23  $\text{cm}^2$ , many times the area of the largest orifice studied (with a diameter equalling 200  $\mu\text{m}$  and an area of  $3.1 \times 10^{-4} \text{ cm}^2$ ). This absence of "flowability" could account for much of the anomalous behavior in many of the powder leak tests.

## OBJECTIVE

The objective of this study is to develop experimental data that will be used to formulate calculational techniques to assess the potential powder passage through very small openings in shipping containers faulted in an accident.



## SUMMARY AND CONCLUSIONS

Parametric studies were conducted to indicate relationships that could be applicable to assessing powder flow through small apertures. Depleted uranium dioxide (DUO) was measured as a function of the following:

- pressure up to 1000 psig,
- aperture diameter,
- aperture length,
- time,
- leak orientation, i.e., above or below the static powder level.

A second document will encompass the predictive methodology developed from these experiments.

Seventeen thin-plate orifices with bore diameters ranging from 20 to 200  $\mu\text{m}$  and 12 capillaries, 0.76 cm and 2.54 cm long, with nominal diameters 50 to 250  $\mu\text{m}$ , were characterized in an earlier segment of this study. For the study reported here, two concurrent sets of experiments were conducted measuring the powder transmitted through these apertures in the Agitated (Above) Powder Leak Apparatus (APLA)<sup>(a)</sup> and Under Powder Leak (UPL) experiments. Depleted uranium dioxide was selected as a surrogate for plutonium oxide because of similarities in the powder characteristics of density and particle size. (The cost and difficulties of working with highly radioactive  $\text{PuO}_2$  were considered beyond the scope of this study.)

Initial experiments indicated aperture diameter and increasing pressure to be significant parameters for powder transmission, and in addition, seemed to indicate a correlation with airflow rate. Further investigation of powder transmission with a statistical matrix and pressurization/depressurization experiments led to the conclusion that there was no powder "leak rate" and that the duration of a run had no effect on the amount of DUO transmitted. The significance of the

---

(a) APLA Refers to both the Agitated (Above) Powder Leak Apparatus and to the above powder leak experiments.

diameter and pressure parameters was confirmed, and the influence of diameter was shown to be more important than pressure.

There was considerable variability in the powder transmitted (1 to  $7.92 \times 10^4$   $\mu\text{g}$ ), as might be anticipated. The coefficient of variation for the APLA experiments was 16%.

A statistical sensitivity analysis suggested that the relationship for DUO transmitted through a leak required a two-stage decision rule based on  $\ln(A\sqrt{P})$  values and leak location and aperture type, where  $A$  = area in  $\mu\text{m}^2$ ,  $P$  = pressure in psig. In the absence of information on leak location and opening configuration, statistics based on all the data may be used.

For  $\ln(A\sqrt{P}) < 10.5$  an estimated maximum DUO transmission value of 287  $\mu\text{g}$  for a leak path below the static powder level and 46  $\mu\text{g}$  for a leak path above the static powder level were calculated. If the leak is larger,  $\ln(A\sqrt{P}) > 10.5$ , the leakage can be predicted by an equation of the form:

$$\ln \text{ DUO} = a + b_1 \ln A + b_2 \sqrt{P}$$

where:

$A$  = Area,  $\mu\text{m}^2$

$P$  = Pressure, psig

DUO = depleted uranium dioxide,  $\mu\text{g}$

Coefficients  $a$ ,  $b_1$ , and  $b_2$  are dependent on leak configuration and location. Values to use are included in a summary table, page B-5 of Appendix B. Sets of values are suggested depending on: 1) orifice leak orientation above or below the static powder level, or 2) if the leak is an orifice or a capillary.

Time was not included in these equations since time was not a significant factor for apertures of the sizes investigated. This fact was determined by the statistical analysis of experiments up to 120 min long and confirmed by 6- and 24-hr runs using one selected orifice size.

Attempts to increase the powder transmitted using various strategies were not successful. Even turning the powder reservoir end for end and shaking, thereby alternately having the orifice covered with powder and not covered, did

not significantly increase the powder transmitted. For  $\ln(A\sqrt{P}) > 10.5$  (high airflow conditions), a capillary gave higher powder transmission than an orifice. At 1000 psig an orifice 38  $\mu\text{m}$  in dia has  $\ln(A\sqrt{P}) = 10.5$ . However, there was one seeming anomaly in capillary experiments: it appeared that a long capillary allowed greater powder flow than a short one of the same diameter. However, because the capillaries became plugged or broken, this anomaly could not be investigated further in the time and resource constraints of the study.

DESCRIPTION OF PLUTONIUM OXIDE SHIPPING CONTAINER  
SIMULATED IN EXPERIMENTS

The experiments described in this report respond to a need to define potential leakage of powder from a plutonium oxide shipping container involved in an accident. This container is designed and fabricated specifically for shipment of plutonium by air. The container is called the Plutonium Air Transportable Package, Model PAT-1, developed by Sandia Laboratories (Andersen, Duffey, Dupree and Nilson 1978). A Safety Analysis Report has been completed for the PAT-1 (NRC 1978), and it is fully described in the above documents. For the convenience of the reader, a brief description of the vessel has been included in this report since the vessel used for the leaks in the above the powder level (APLA) experiments simulated the inner TB-1 containment vessel of the Plutonium Air Transportable Package.

The PAT-1 is composed of three parts:

- TB-1 stainless steel containment vessel
- AQ-1 protective overpack
- PC-1 stainless steel product can

Figure 1 shows the principal elements of the package. The AQ-1 overpack consists of a 65-gal drum that is fully lined with an inner drum; both drums are made of 304 stainless steel. The redwood assembly is made of three elements: 1) a removable plug with longitudinally oriented grain, 2) a cylindrical annulus with radial grain orientation (fabricated as a series of wedges arranged in a ring), and 3) a fixed plug with longitudinally oriented grain. The TB-1 containment vessel, Figure 2, is comprised of a body, a lid secured by bolts, a copper gasket, and an O ring. The vessel body and lid are fabricated from precipitation-hardened stainless steel and house the PC-1 product can that is fabricated from 304 stainless steel and is closed by crimping in a canning machine. After crimping, the can is sealed by welding or silver soldering.

The authorized contents of the PAT-1 package are : 1) plutonium oxide and its daughter products in any solid form, and 2) mixtures of natural or

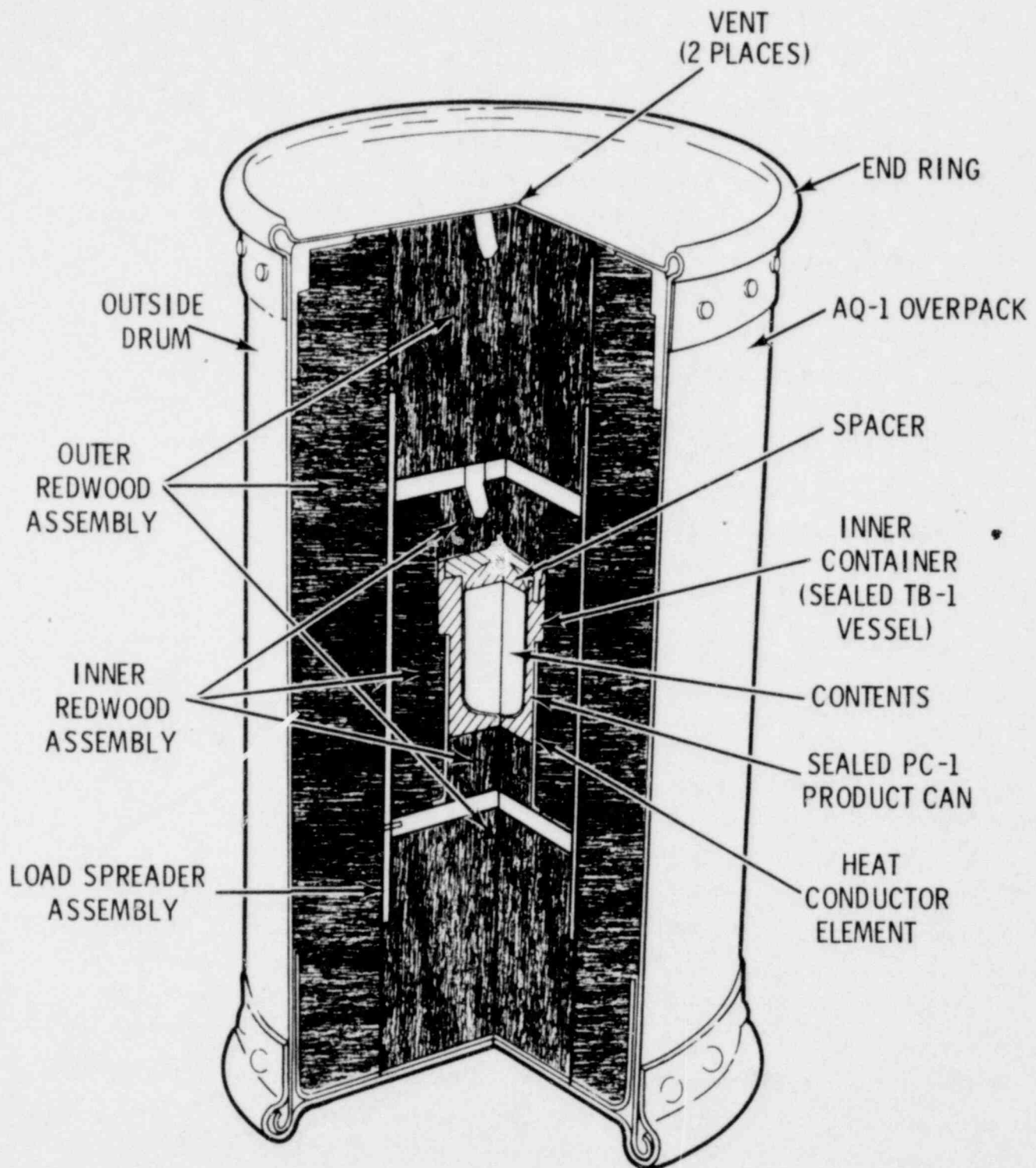


FIGURE 1. Plutonium Air Transportable Package (PAT-1)

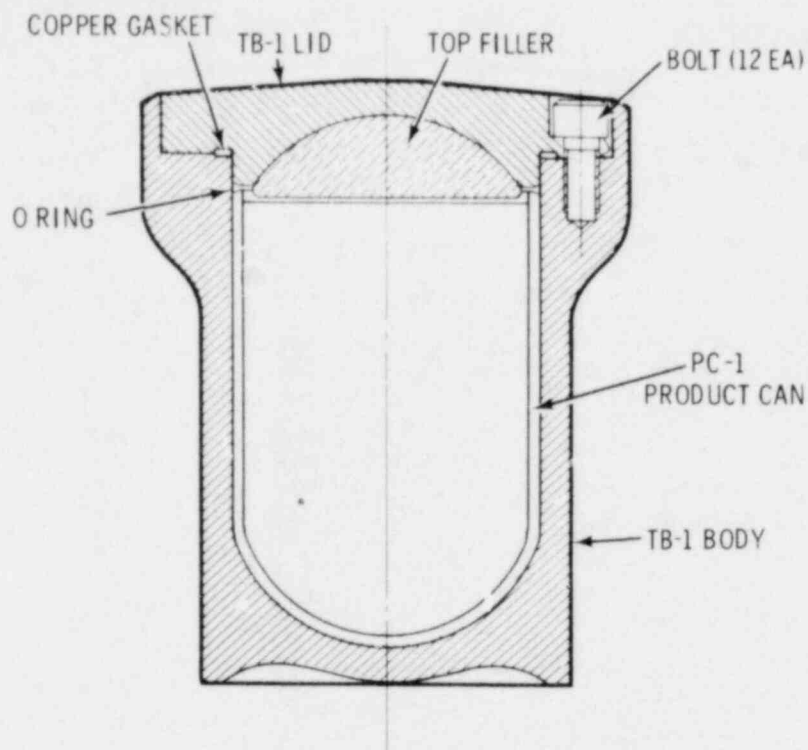


FIGURE 2. Cutaway Drawing of TB-1 Containment Vessel

depleted uranium dioxide and plutonium oxide and its daughter products, in any solid form. Additional permissible contents are: 1) maximum 16 g of water, and 2) two single-layer polyethylene bags weighing no more than 9 g, the bags taped closed or heat sealed.

The TB-1 meets the standards required for normal conditions of transport: a helium leak rate less than  $1 \times 10^{-10}$  atm cm<sup>3</sup>/sec. Under normal transport conditions, the maximum temperature of the TB-1 would be 215<sup>0</sup>F. Four of five TB-1 vessels within packages subjected to the fire test specified in the NRC Qualification Criteria (NRC 1978) reached 1080<sup>0</sup>F. The maximum air leakage rate was  $4.5 \times 10^{-5}$  atm cm<sup>3</sup>/sec and the internal pressure within the TB-1 vessel was calculated to range between 1144 and 1183 psia. This total pressure includes approximately 833 to 867 psia from superheated steam, 49 psia from heated air within the vessel, and 262 and 267 psia from decomposition of the polyethylene bags. The post-test pressure within the TB-1 vessel is bounded by 4 days at

1110 psia, followed by 3 days at 500 psia. The longest calculated fire duration is 4 days at 1080°F.

In the event of an accident, integrity of the PC-1 stainless steel product can may be breached and material released into the TB-1 vessel, and a leak in the TB-1 vessel in turn could release powder to the atmosphere. Our tests were designed to correlate powder leak rates and gas (air) leak rates under the accident conditions that are hypothesized for the TB-1 vessel. Powder leakage from the vessel was measured from leaks above and below the static powder level at pressures up to 1000 psig.

## PHYSICAL PROPERTIES OF PARTICLES AFFECTING POWDER FLOW

This section (based on Zenz and Othmer 1960) reviews some fundamental properties of powder that are important in understanding the behavior of the depleted uranium dioxide powder used in our experiments:

- Static and dynamic properties influence powder movement. Even at rest, a powder represents a two-phase system, and the movement of the powder involves interstitial fluid (in the case of our experiments, air).
- Interparticle and particle-to-bounding surface friction are important factors in particle movement. One example of powder flow, where solids flow freely, can be seen in an hourglass. A "sticky" powder placed in an hourglass would not flow.
- Powder ejecting from a leak initiates from a bed initially at rest, and the powder develops into moving flow. This study simulated leaks resulting from forces imposed by an accident.

### PARTICLE DIAMETER/APERTURE DIAMETER

The aperture should be sufficiently larger than the particle to allow the particle to flow. For flow of particulate solids in pipes (gravity), the internal diameter of the conduit should exceed the diameter of the largest particles by 5 to 7 times when the particles are present in high proportions (Zenz and Othmer 1960). The mass median diameter of the DUO powder under study was  $1\ \mu\text{m}$ , which suggests that the powder should flow freely through the openings used in the experiments, if the powder becomes airborne as discrete particles. However, free flow could be restricted if the DUO powder becomes airborne as agglomerates of particles, thereby increasing particulate diameter, or if there are a sufficient portion of large particles in the airborne concentration.

The DUO used in this study had 3% by mass of particles  $20\ \mu\text{m}$  and larger, which indicates that there might be sufficiently large particles in each microgram to restrict powder flow through an aperture smaller than  $100\ \mu\text{m}$  in diameter, if this particle diameter/aperture diameter relationship is valid.



## PARTICLE DIAMETER

Particle size also influences powder movement. Fine materials less than 76  $\mu\text{m}$  (.003 in.) in dia have a pronounced tendency to stick (Zenz and Othmer 1960), a property that would not facilitate particle flow under gravity. The mass median dia of the DUO powder used is 1  $\mu\text{m}$ , which indicates that these particles would be classified as "sticky" and would not flow freely.

For some fine powders such as kaolin, disaggregation cannot be achieved at all (Fuchs 1964), and airborne kaolin material would actually be in small aggregates. (Refined kaolin aggregates are 2 to 10  $\mu\text{m}$  in dia [Neumann 1953].) The actual configuration of the airborne DUO in our study was not known, but judging from its particle size (1  $\mu\text{m}$  MMD), the DUO might be hypothesized to have limited disaggregation.

## VOIDAGES

Void volume, the fraction of a static bed of particles occupied by air, can influence particle motion.

Irregular particle shapes and wider particle size distributions resist compaction. Fines reduce voidage, and coarse particles will randomly create interstices. Fluidization of powder can be caused by interaction of air and solids, i.e., if each powder particle is enclosed in a layer of air, the aerated powders flow almost like water. Local channeling can cause either rat holes or increased flow velocities. A highly arched bed is dynamically unstable, so that, upon shaking, the particles may reorient themselves and settle into a denser, lower voidage configuration. Some variation in powder flow rates might be expected as a function of void volume.

For randomly placed spheres, void volumes generally range from 0.38 to 0.47. Almost all naturally occurring random arrangements are believed to lie between these two limits.

For the under powder leak experiment, the original orientation of the DUO was a pour volume compressed with the application of pressure.

## MOISTURE CONTENT, HYGROSCOPICITY

Moisture greater than the moisture in equilibrium with surroundings would generally enhance "stickiness" of powders and prevent free flow. However, some tests of powder flow in air made with mixtures of tungsten powders 8 to 16  $\mu\text{m}$  showed the flow time to decrease with increasing relative humidity up to 45% and to increase again above this level (Hausner 1971). Up to this optimum humidity the moisture acted as a lubricant, lowered friction, and thus increased flow rate. Other powders would require a different relative humidity for optimum flow. The DUO leak tests in c r experiments were all run in an atmosphere with ambient relative humidity, about 40 to 50%. No attempt was made to control the powder humidity.

## "HEAD"

The "head" level of powder above a leak could be interpreted as the consolidation pressure on the powder. A decrease in "flowability" as a result of an increase in consolidation pressure is a common feature of powder behavior (Stainforth and Berry 1973). "Pelleting" and "tableting" processes are extreme examples of the diminution of "flowability" to zero under great pressure. The consolidation pressure of the 1000 psig in our study might be anticipated to limit powder flow.

## ANGULAR PROPERTIES

Angular properties are static and dynamic properties of powders. The degree of interparticle and particle-to-bounding-surface friction results in characteristic internal and surface phenomena that are important in particle flow (gravity). If the powder is "fluidized" by upward air movement at a sufficiently high velocity, the interparticle friction is negligible, and the powder will behave as a fluid. The angular properties would not be of significance in APLA experiments, therefore, but could play a role in a leak underneath the powder level. There are five commonly characterized properties for powdered materials: angle of internal friction  $\alpha$ , repose  $\beta$ , wall friction  $\gamma$ , rupture  $\delta$ , and slide  $\omega$ .

- a. Angle of internal friction  $\alpha$  is an internal phenomenon and is the friction condition as a powder starts to slide on itself at the outset of flow (Johanson 1975). In a test to determine the angle of internal friction of the DUO, the powder would not flow by gravity forces.
- b. Angle of repose  $\beta$ : Stability of mass of particles depends on mutual friction between grains. There are actually two different angles of repose: one occurs when a pile of solids is formed, and the other occurs when the solids are drained.
- c. Angle of rupture  $\delta$ : Angle formed with the horizontal by bulk solids sliding under forces of gravity against stationary solids.
- d. Angle of wall friction  $\gamma$ : angle formed by bulk solids with a wall.
- e. Angle of slide  $\omega$ : Frictional force between grains and an inclined solid surface.

This section has only touched upon the complexities of powder-fluid systems and other powder properties have not been considered, to name a few, sonic forces, electrical forces and permeability. Our tests yielded some results that might have been better explained with a better understanding of the basic properties of the DUO powder used. Of course, the absolute characteristics of a given powder depend strongly on the method and circumstances of use.

## EXPERIMENTAL: APPARATUS AND EXPERIMENTS PERFORMED

### APPARATUS

Experiments were performed measuring powder leakage above (APLA) and below (UPL) the static powder level, requiring two sets of apparatus. Both sets of apparatus are described here and equipment common to both are noted.

#### Leak Path Above the Static Powder Level Apparatus (APLA)

##### Vessel

Leaks above the static powder level were investigated in the Agitated Powder Leak Apparatus (APLA). Figure 3 is a photograph of the APLA pressure vessel installed in the Radioactive Aerosol Release Laboratory at PNL. A single sample collection chamber is shown attached to one of six available ports. The other ports are fitted with the plug shown on the right. The APLA flow/pressure measurement and control panel is shown in Figure 4. Figure 5 is a schematic of the APLA, and Figure 6 is a schematic of the airflow systems.

The internal dimensions of the vessel are about the same as for the primary TB-1 PuO<sub>2</sub> shipping container and has a volume of 3271.2 cc. High-pressure air from a 1A cylinder is regulated by a 0 to 1000 psig regulator and, if required, a 0 to 100 psig regulator in series. A manifold provides a capacity of five cylinders of air. The supply pressure gauge, high- and low-pressure regulator valve handles, and the four-way ball valve handle are visible on the left side of the panel in Figure 4. Air enters the pressure vessels containing the DUO powder via three lines visible in the schematic (Figure 6) and shown in Figure 3. These lines are:

- 2 lines to the powder aerosolization probes available that, in conjunction with throttling valve F, pressurize the vessel to the desired level.
- 1 line via valve C to pressurize the vessel independently of the aerosolization probes.

The remaining lines entering the vessel head in Figure 3 are to the pressure measurement system and the vessel exhaust. Each of the six individual panels

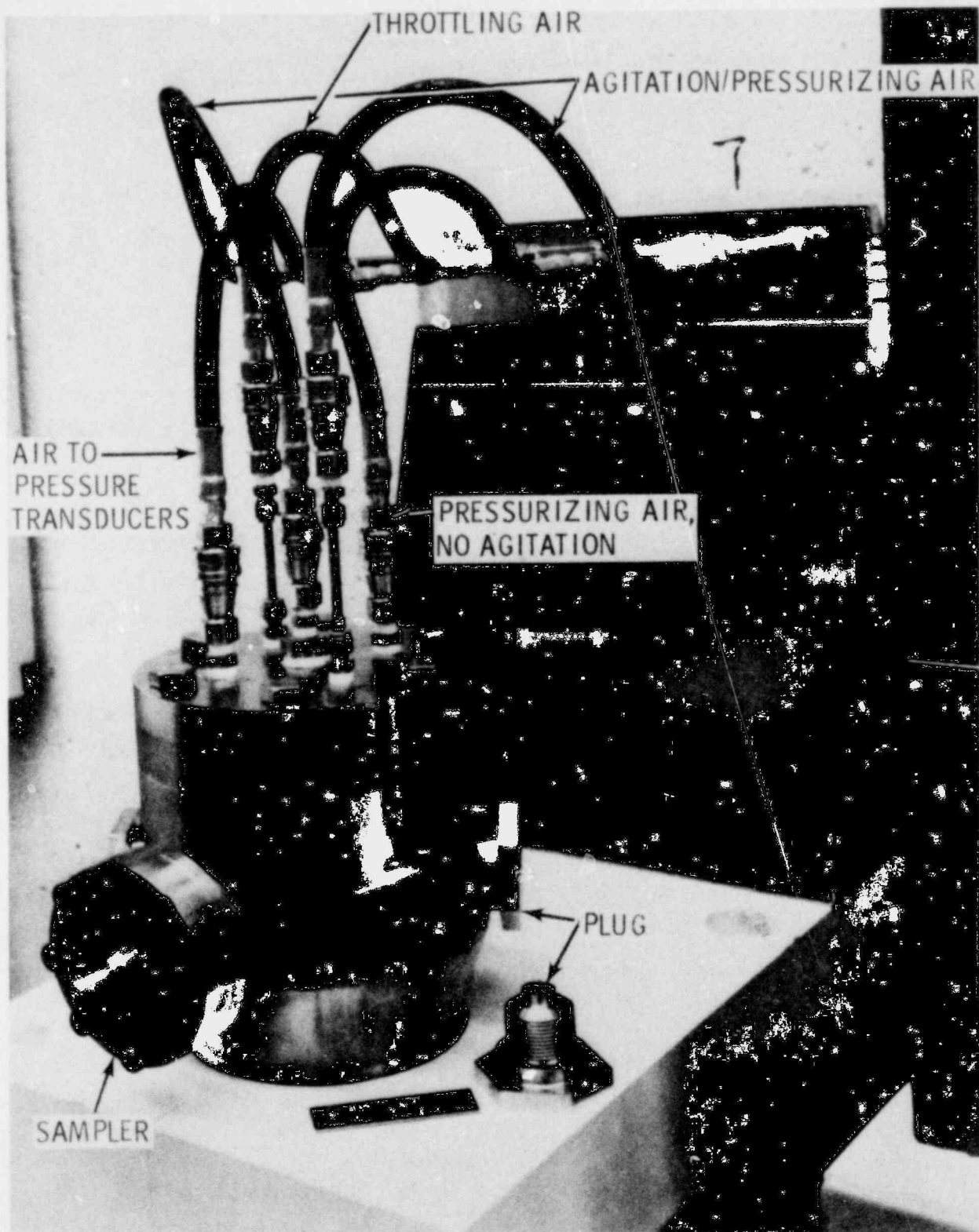


FIGURE 3. Leak Test Pressure Vessel

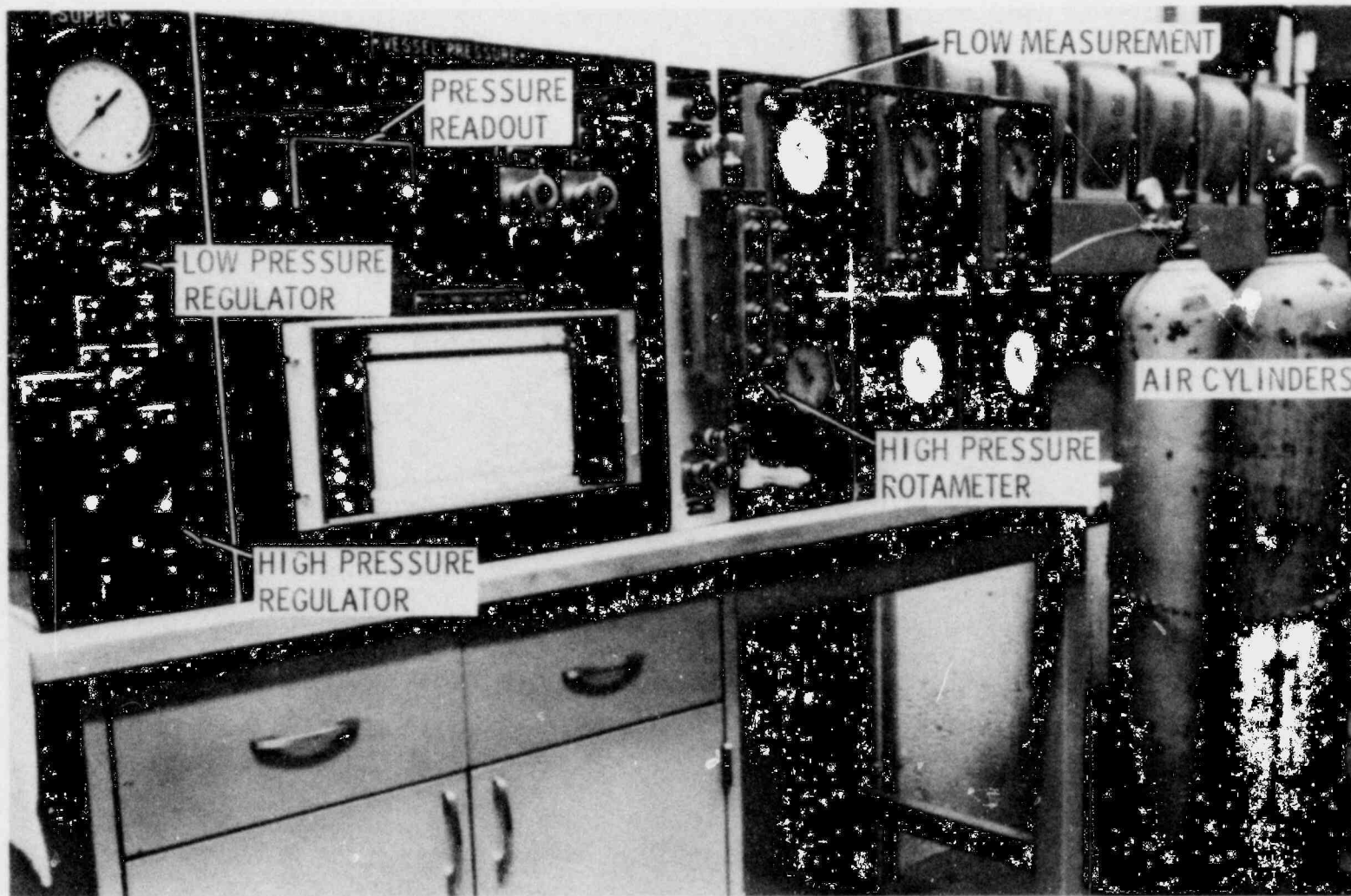


FIGURE 4. APLA Flow/Pressure Control and Measurement Components

POOR ORIGINAL

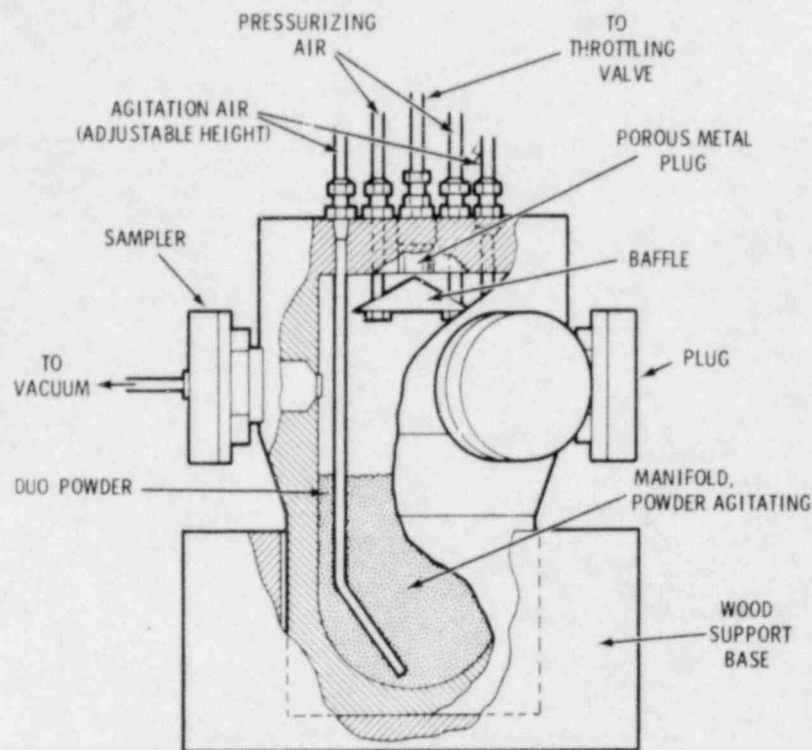


FIGURE 5. Schematic of the Agitated Powder Leak Test Vessel

visible on the right-hand side of the panel in Figure 4 provides flow measurement and control to leak paths attached to the six available ports.

#### Sample Collection Chamber

Figure 7 is a schematic of the sample collection chamber, showing the orifice plate cemented in place flush with the interior wall of the APLA vessel. A polycarbonate membrane filter 25, 47, or 76 mm in dia (0.1- $\mu$ m pore size) is supported on a sintered metal support plate in the appropriate location. A recoverable surface coating for the sampler chamber was formulated by dissolving gelatin capsules in hot water and painting the internal surfaces of the sampler with the solution. The coating retained flexibility and was easily removed after application. Particles were thus collected on the entire interior of the sampler chamber and all material passing through the aperture represented a sample. The gelatin and filter were combined for a single sample for each collection chamber.

#### Pressure Measurements

The pressure was monitored with a transducer indicator calibrated before use with an accuracy of 0.5% in the 100 to 1000 psig range and 0.1% in the 0 to

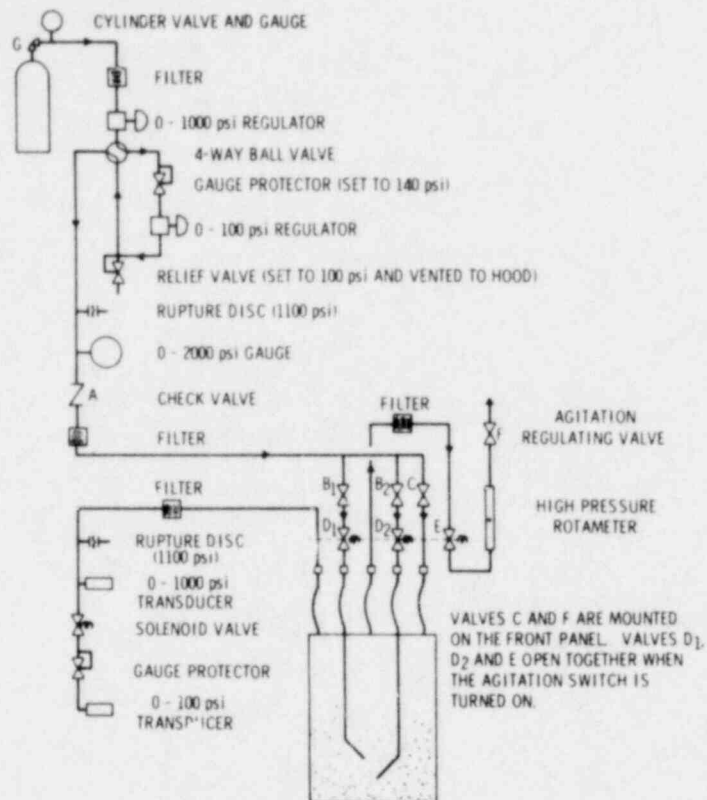


FIGURE 6. Schematic of APLA Airflow System

100 psig range. The pressure was displayed as a digital readout and recorded on a strip chart recorder.

#### Agitation Airflow

Compressed air was jetted through the powder in an attempt to induce aerosolizing forces greater than could be envisioned under accident conditions. This should maximize the airborne release to use a conservative estimate in accident analysis. The air entered the vessel through a probe at the bottom of the vessel about 7.6 cm below the powder level.

The efficiency of the aerosolization method was verified by visual observation using a clear plastic chamber having the same internal dimensions as the pressure vessel.<sup>(a)</sup> The airflow was monitored with a high-pressure rotameter with the same setting for every run. A baffle and glass wool filter backed up

(a) This vessel was inadvertently overpressured and fractured beyond repair following aerosolization tests of the system.



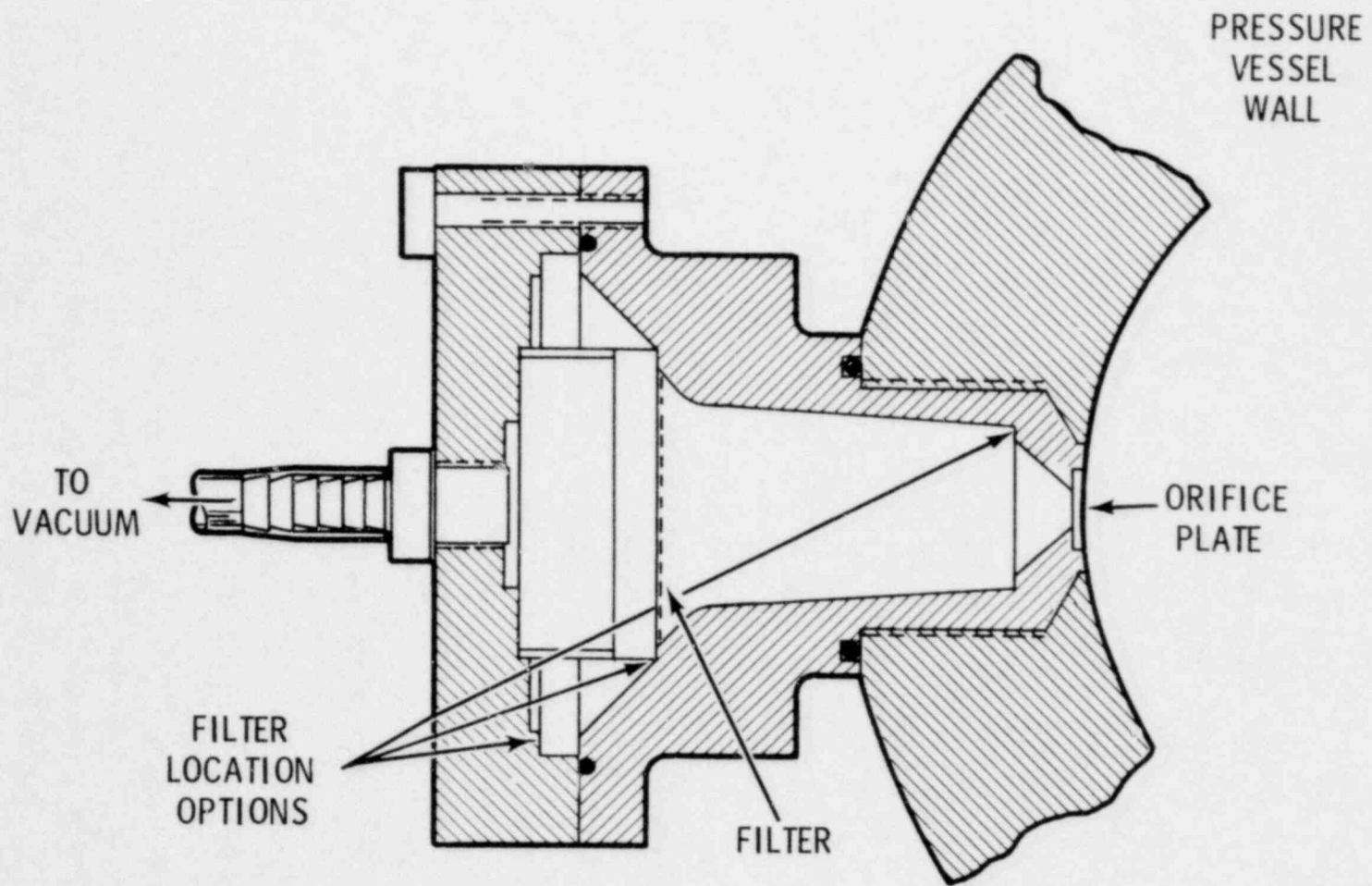


FIGURE 7. Sampler Detail for Above Powder Leaks

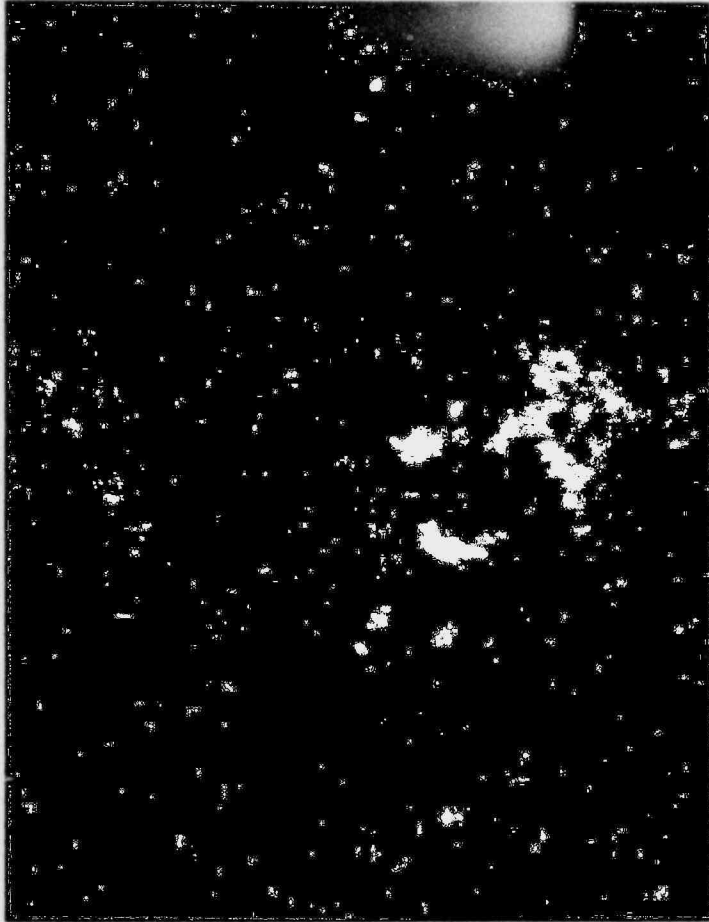
by a particulate filter prevented airborne particles from being carried out of the vessel and plugging the throttling valve.

The development of a fluidized system as a result of a gas blown through a bed of solids at increasing velocity in a continuous motion is a complex pattern (Parent et al. 1947; Newman 1953). After an abrupt initial expansion, the bed of solids expands continuously as the flow rate is increased and the solid and gaseous phases mix. If the gas velocity is relatively low, the appearance of the solids will be that of a boiling liquid. As the velocity increases, the gas entrains some particles, and entrainment increases with increasing gas flow rate. In the final stage of fluidization, particles become entrained in the gas stream as a dilute suspension. This process was observed in the plexiglass container before the experiments began, and the aerosolization method was corroborated.

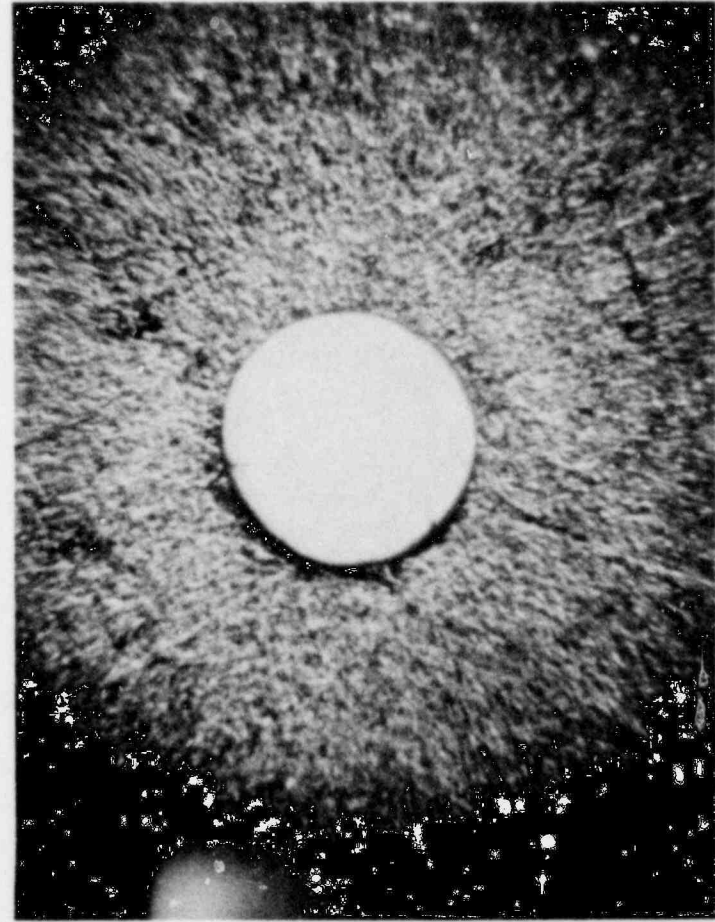
Additional corroboration of the efficiency of the aerosolization method is provided by the presence of DUO on the face of and visible in the orifice following an experiment, as seen in the photomicrograph in Figure 8. We had been additionally concerned that the aerosolized powder passing through an aperture would permanently lodge in the opening making the aperture useless. The right side of the photomicrograph shows that the orifice could be effectively cleaned using a sonic bath.

The airborne environment in the vessel was a mixture of interacting flow patterns--convective flow and turbulent flow. We have extrapolated observations from particle studies (Fuchs 1964) in an attempt to understand what occurred in the present experiments in regards to flow patterns.

In very intense convection with mean convection velocities much greater than the settling velocity of the particle, the aerosol concentration can be practically constant throughout the chamber, except near the walls, while the aerosol concentration decreases steadily with time. Investigations have established that the airborne weight concentration of particles in a chamber falls off rapidly when the concentration is stirred. This concentration phenomenon is partly caused by more rapid growth of particles as a result of accelerated coagulation of particles caused by stirring and by inertial deposition onto the chamber walls.



DIRTY



CLEANED IN SONIC BATH

FIGURE 8. Orifice 1-200 After APLA 2 (Before and After Cleaning in Sonic Bath)

POOR ORIGINAL

Turbulent flow in a circular tube (analogous to the circular vessel in our experiments) is usually accompanied by rotation of flow about the axis of the tube and by particle concentration maximized around the periphery of the tube. The gravitational deposition in turbulent flow is similar to deposition in convective flow.

Other forces at work in agitated airflow are deposition as a result of the turbulent flow, reentrainment of the particles, and coagulation and disaggregation of particles. These forces are not quantifiable. One observation has been made, however: when an aerosol of solid particles is subjected to sufficiently intense agitation, a stationary state can be reached when the rates of coagulation and disaggregation are equal. This stationary state was the desired airborne environment in the vessel which insured that replicate experiments were sampling from the same airborne particle environment.

Unfortunately, there was no way to verify the assumption that a stationary state was achieved in our experiments. During initial discussions related to the study, viewing windows with lasers and densitometers, etc., which would have been desirable as instrumentation to quantify the stationary state, were considered too costly. Also, a filter sample, in addition to the orifices, would still sample only from one point and would not give an adequate picture of the changing environment.

#### Orifices and Capillaries

The orifices and capillaries used for these investigations were characterized and described in an earlier segment of the leak rate study (Sutter, Bander, Mishima and Schwendiman 1978; Owzarski et al. 1979). The orifices ranged in diameter from 20 to 200  $\mu\text{m}$ . Two lengths of capillaries, 0.76 and 2.54 cm, ranged from 50 to 250  $\mu\text{m}$  in nominal internal diameter (ID). The diameters measured using a scanning electron microscope are listed in Tables 1 and 2.

#### Flowmeters

Variable area flowmeters provided interchangeable measurement units covering the entire flow regime from about 1 cc/min to 25 l/min. Before use, the flowmeters were calibrated using a bubble-test meter or a calibrated wet test

TABLE 1. Measured Orifice Diameters

<u>Nominal Diameter, <math>\mu\text{m}</math></u>	<u>Orifice Designation</u>	<u>Measured Diameter, <math>\mu\text{m}</math></u>
20	1-20	22
	1-20a	23
	2-20	20
36	3-20	23
	3-30	33
	1-36	43
	2-36	33
	3-36	38
	1-63.5	66
63.5	2-63.5	61
	3-63.5	65
	1-110	100
110	2-110	125
	3-110	100
	1-200	200
200	2-200	200
	3-200	200

TABLE 2. Measured Capillary Diameters

<u>Nominal Capillary Diameter, <math>\mu\text{m}</math></u>	<u>Measured Capillary Diameter, <math>\mu\text{m}</math></u>
50	48
75	78
100	114.3
150	182
200	229
250	275

meter, and calibration curves were prepared. The experimental flow values were read from these curves. An accuracy of  $\pm 2\%$  was anticipated after calibration. Some flows were maintained at the characterized airflow rate for the aperture using a vacuum; some were only measured.

#### Depleted Uranium Dioxide Simulant

Depleted uranium dioxide was used as a  $\text{PuO}_2$  simulant in these studies. About 3.5 kg filled the vessel to about 2.54 cm below the orifice. The particle size distribution of the DUO powder is shown in Figure 9 along with that of a Los Alamos  $\text{PuO}_2$  powder, a powder that might be shipped in the powder containers. There are many  $\text{PuO}_2$  size distributions available for comparisons, and the powder can range in size depending on the source and production method. The size data plotted represent the results of sizing using the same measurement techniques for all powders. All of the size distributions were determined using sedimentation methods that record the cumulative mass settled in a column of liquid. The DUO powder in Figure 9 has a Mass Median Diameter (MMD) of  $1 \mu\text{m}$ , which is a  $3.5 \mu\text{m}$  Aerodynamic Equivalent Diameter,<sup>(a)</sup> and 95% of its mass was associated with particles  $10 \mu\text{m}$  MMD or less. The MMD of the  $\text{PuO}_2$  powder is  $3.5 \mu\text{m}$ , and 85% of the mass is associated with particles  $10 \mu\text{m}$  MMD or less. Use of DUO, a fine material, provided conservative estimates for  $\text{PuO}_2$  powder leaks and mitigated the significance of possible selective depletion of fine particles by the aerosolization technique used.

The DUO particle size did not change significantly during the APLA experiments. The middle plot of Figure 9 shows the particle size distribution of the DUO after 103 APLA experiments using the same bulk powder. After 103 experiments the MMD was  $1.1 \mu\text{m}$ . Eight hundred grams of DUO were added to the APLA vessel at this time, and all of the bulk powder was replaced after 188 experiments. The size distribution of this material removed was the same as the original DUO powder.

---

(a) Showing aerodynamic characteristics of a unit-density sphere of the same diameter as the particle under consideration.

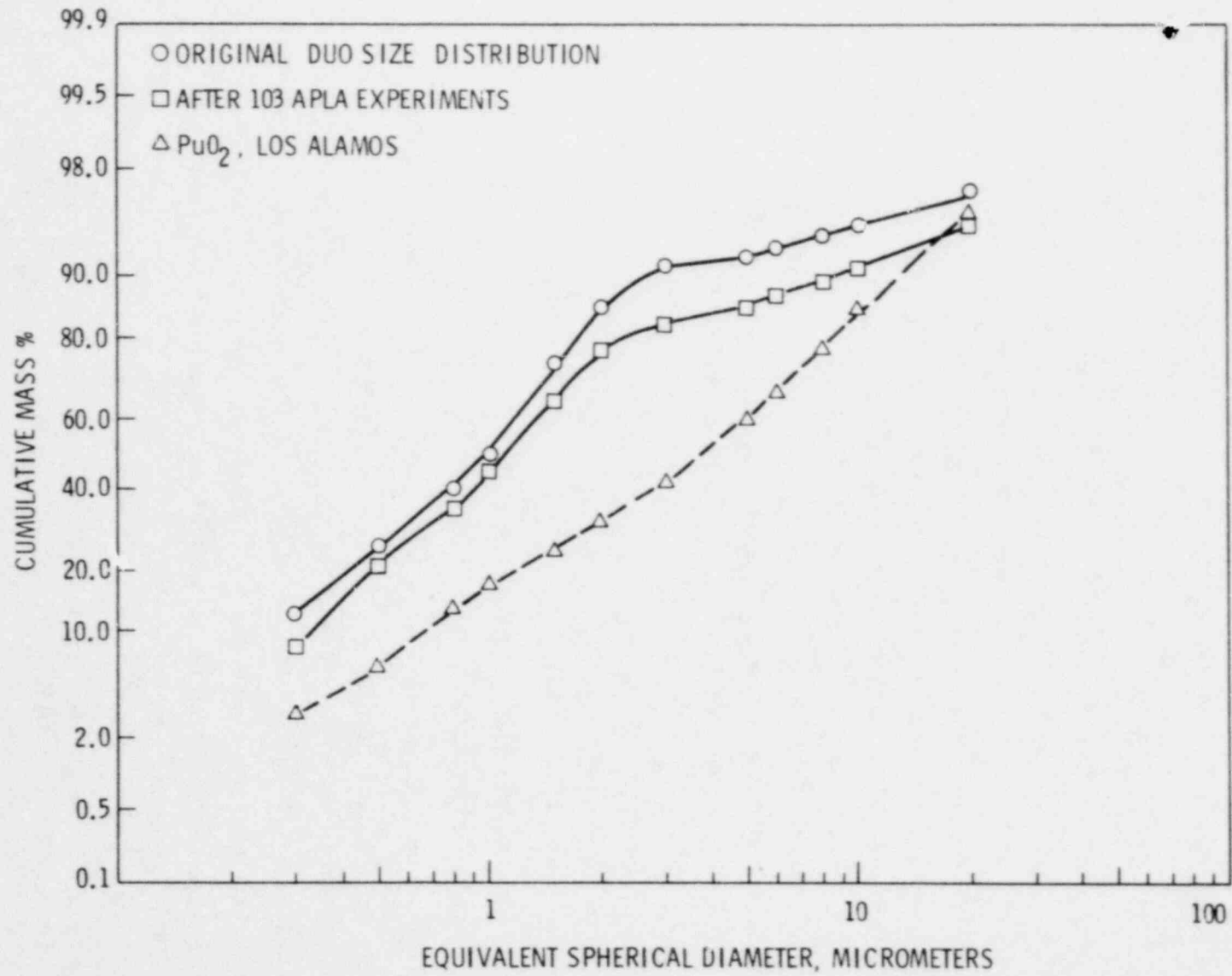


FIGURE 9. DUO and PuO<sub>2</sub> Particle Size Distributions

### Experimental Procedure

An aperture, either an orifice or a capillary, was cemented in the gelatin-coated, filter-loaded, sample collection chamber. The chamber was inserted in the test vessel and the upstream pressure increased to a predetermined level. Then the vessel was rapidly pressurized with agitation by opening the agitation control valves. (Agitation was regulated using the high-pressure rotameter.)

Airflow through the sampler was measured by a flowmeter on the control panel. The DUO powder was agitated, and the particle-laden air passed through the sampler for a designated time. The experiment was terminated by turning off the upstream air and allowing the vessel to depressurize.

### Uranium Analysis

The collected DUO samples were dissolved before analysis using a pyrosulfate fusion/organic extraction method with fluorophotometric or alpha-counting determination of uranium. General quality control procedures for the analysis were:

- Ten percent of the samples were analyzed in duplicate.
- "Spiked samples" were analyzed approximately 1 for every 10 samples analyzed.
- Blanks were analyzed approximately 1 for every 10 samples analyzed.

Quality control procedures for the fluorometric measurements were:

- Fluorometer was calibrated prior to use.
- Flux fusion times were controlled automatically to within a second.
- Concentration for each sample was determined by adding a known quantity of uranium to a second aliquot.
- Flux blanks were analyzed with each set of samples measured.
- Standard solutions of different concentrations of uranium were analyzed weekly.



Quality control procedures for counting were:

- Counter was calibrated before use.
- Background was determined before use.
- Plateaus were determined monthly.

The  $\pm$  reported in Appendix A is the uncertainty of the analysis at the 95% confidence limit.

#### Leak Path Under the Static Powder Level Apparatus (UPL)

The apparatus used to measure the airflow through orifices and capillaries, and reported as another segment of this study (Sutter, Bander, Mishima and Schwendiman 1978; Owzarski et al. 1979), was modified for use as the Under Powder Leak rate apparatus (UPL). A powder reservoir was incorporated in the design, as shown schematically in Figure 10, and was attached to the sample collection chamber.

The apparatus consisted of the powder reservoir attached to the sample collection chamber, a supply of high-pressure air, gauges for measuring pressures, and flowmeters. These are shown in Figure 10. A second larger powder reservoir fabricated to hold powder to a depth of 20.3 cm is shown in Figure 11. A weighed amount of powder was placed in the selected reservoir, and air at 15, 100, 500, or 1000 psig, was passed through the powder as indicated in Figure 10.

Most of the UPL apparatus was common to the APLA, e.g., the sample collection chamber, the flowmeters, the DUO simulant, and the uranium measurements. However, two pressure gauges were unique to the UPL--a gauge with an accuracy of  $\pm 0.1$  psig for the 0 to 100 psig range, and a second 0 to 1500 psig gauge that measured pressure within an accuracy of  $\pm 10$  psig.

#### EXPERIMENTS PERFORMED

Powder leaks from a shipping container can be the result of initiating forces from a variety of accident situations and have many parameters. Some conditions have been identified in the Safety Analysis Report for the shipping container (NRC 1978), including maximum pressure and temperature, pressurization time, and initial powder loading. Other conditions resulting from an

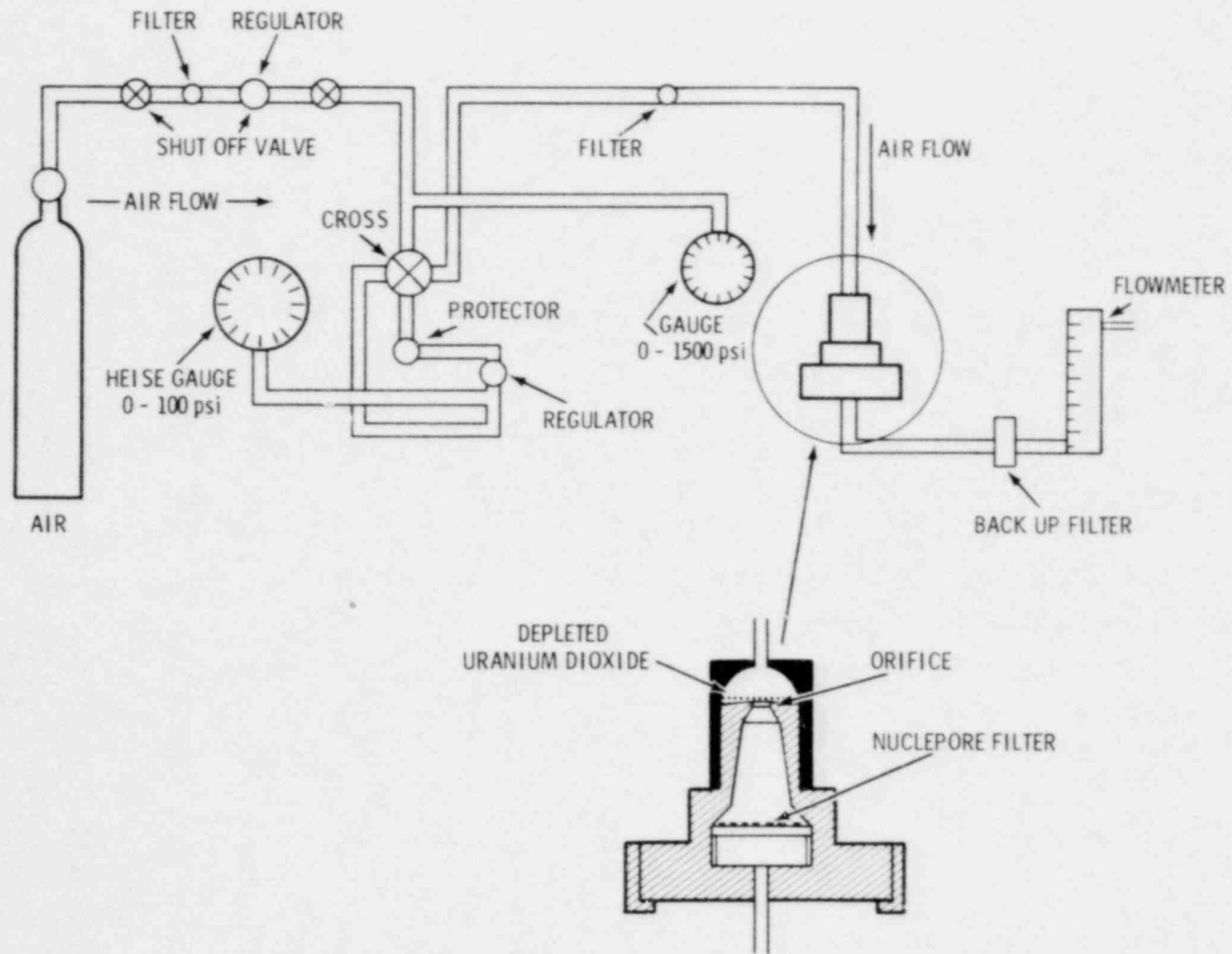


FIGURE 10. Under Powder Leak Apparatus

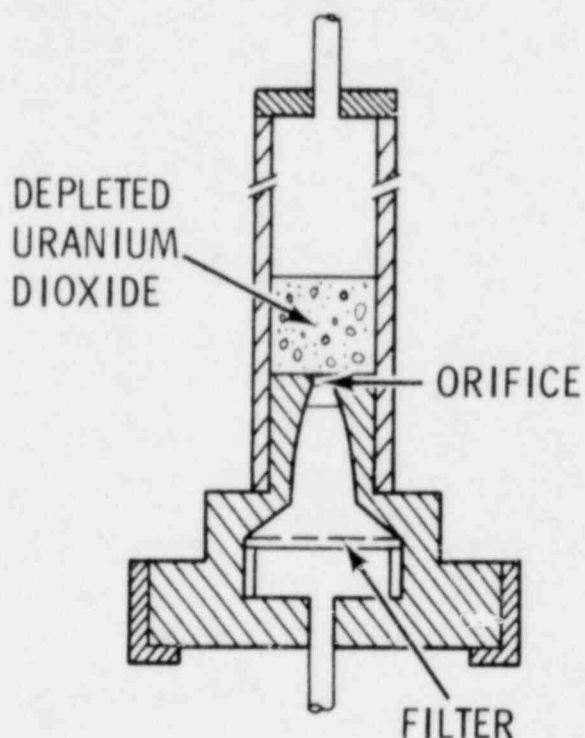


FIGURE 11. The Second Powder Reservoir and Sample Collection Chamber

accident cannot be identified: leak location and configuration, single or multiple leaks, quantity of powder covering the leak, and vibration or movement of the package to name a few. We conducted experiments that investigated a variety of parameters that could affect powder leakage. The experiments that were performed to describe specific powder leakage are listed below and are divided into two basic sets: leak path above and below the static powder level.

#### Leak Path Above the Static Powder Level (APLA) Experiments

- Single Aperture
  - 4 pressures: 30, 100, 500, 1000 psig; 5 orifices, 10 capillaries; flow maintained at the predetermined characterized airflow rate for each pressure (Sutter et al. 1978; Owzarski et al. 1979), or measured only with no attempt to achieve this predetermined flow rate.

- Multiple Orifices
  - Grouped by nominal orifice size; time constant or varying; 4 pressures
- Pressure Decay
  - 4 orifices: 1000 to 0 psig
- Statistical Matrix
  - 6 selected orifices; 3 pressures: 30, 500, 1000 psig
- Pressure Buildup ("Zero"-Time)
  - 3 orifices, 3 pressures (statistical matrix); 5 orifices, 4 pressures
- Extended Time
  - 1 selected orifice and pressure; runs for 6 and 24 hr,
- Slow Pressurization
  - 80 min to pressurize to 1000 psig
- Other (Limited)
  - Mixed orifices and capillaries; multiple sampling; multiple capillaries.

#### Leak Path Under the Static Powder Level (UPL) Experiments

All single aperture:

- 3 g DUO Above Leak
  - 5 orifices, 4 capillaries at 4 pressures, 15, 100, 500, 1000 psig, with and without agitation
- 25 g DUO Above Leak
  - 5 orifices, 2 capillaries, at 5 pressures: 15, 50, 100, 500, and 1000 psig
- Statistical Matrix (Powder Depth/Weight)
  - New reservoir, 1 orifice, 25 g, 100 g, or 250 g above leak.
- Slow Pressurization
  - 80 min to pressurize to 1000 psig
- Extended Time
  - 1 selected orifice, 1 pressure, 6 hr and 24 hr

- Orientation
  - 4 runs each with reservoir at  $180^{\circ}$ ,  $45^{\circ}$ ; slow and immediate pressurization to 1000 psig
- Rotation of Reservoir
  - End-for-end rotation of powder reservoir three times per min for 30 min, 1000 psig

## RESULTS AND DISCUSSION: LEAK PATH ABOVE THE STATIC POWDER LEVEL

All of the experimental results for leaks above the static level are included in Appendix A. The results from the runs with leaks above and below the static powder level will be discussed individually. Then, analogous behavior in the leaks will be observed.

Observations on plugging, extraneous leakage and background levels of DUO have been included since any of these can jeopardize the accuracy of the results.

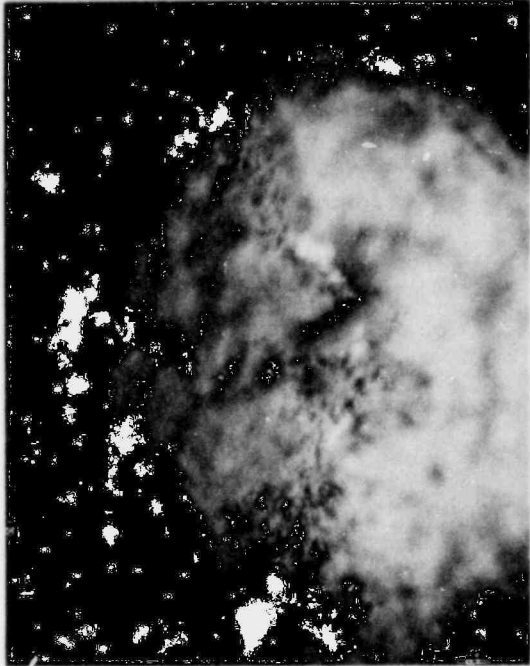
### PLUGGING

The clearance of each aperture was verified just before the aperture was used in each run. This examination was made by running a wire through the opening, shining a light through the opening and by visual observation, or by measuring the airflow through the orifice, or by using one or a combination of these methods, whichever was appropriate.

In some cases, apertures either plugged immediately when the sampling system was pressurized, or they became partially plugged with loss of powder flow although without complete cessation of airflow. Immediate plugging was ascertained when the flowmeter indicated no measureable airflow downstream of the sampler; partial plugging could be surmised from examination of the aperture after a run was completed. The immediate plugging samples that were sent for chemical analysis showed background levels of DUO. Since these apertures were known to be plugged, the results did not contribute to establishing any powder flow rate.

Twenty out of 319, or 6%, of the orifices used became totally plugged, and an additional 9, or 3%, became partially plugged during experiments. Seven of 41 capillaries, or 17%, plugged immediately, and 4, or 10%, were suspected of plugging.

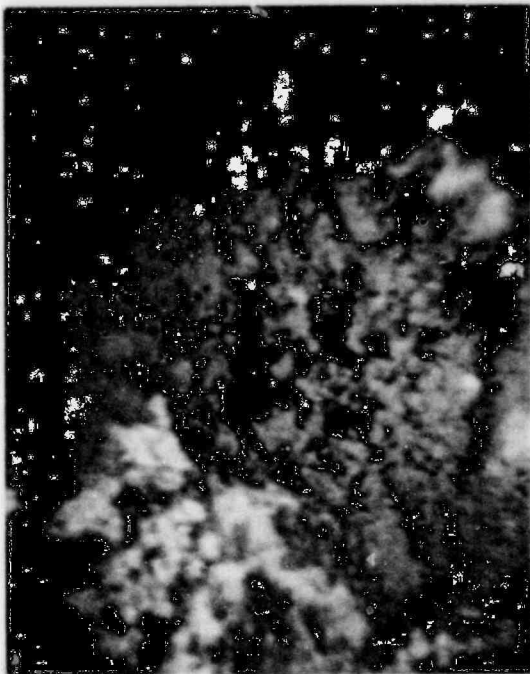
Plugging was additionally verified by microscopic examination of the aperture after a run. The photomicrographs in Figure 12 show orifice and capillary faces after plugging. These are the 200- $\mu\text{m}$ -dia orifice and the 250- $\mu\text{m}$  and 200- $\mu\text{m}$  capillaries, and can be compared with the 200- $\mu\text{m}$  orifice in Figure 8



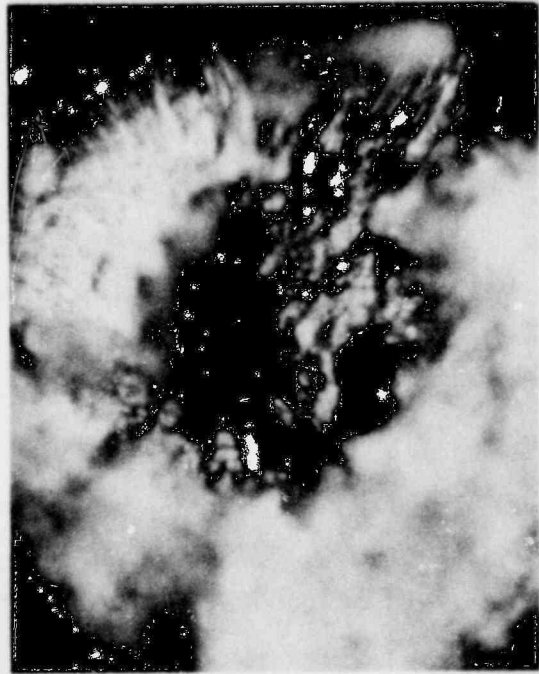
1-200



1-200



200S



250B

FIGURE 12. Plugged Apertures, Orifices (Top) and Capillaries (Bottom)

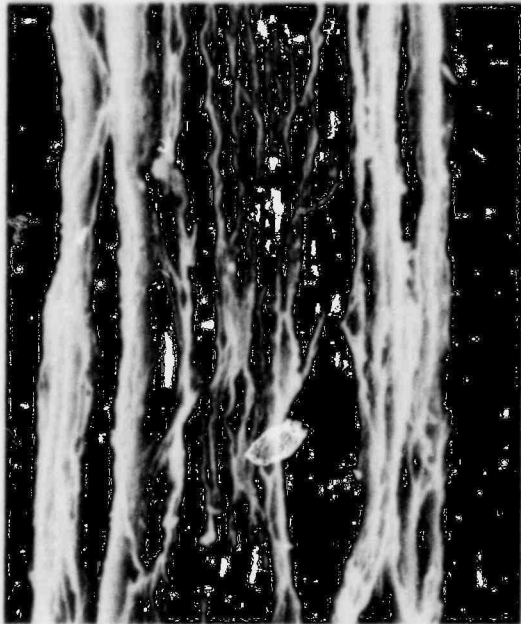
which has visible DUO powder on its face. Even with considerable powder deposition on the orifice in Figure 8, the orifice retained a large unrestricted leak path and showed little plugging.

During the runs, plugging was a random occurrence and happened at all pressures although the apertures usually plugged at the beginning of a run. For example, during a 24-hr run, one orifice began plugging 1 min into the run. Since more than 50% of the desired airflow had been achieved, the run was continued. The flow continued decreasing until the plug apparently released after 4 hr; the airflow stabilized and gradually returned to 95% of the initial flow. It is evident from this case that an aperture could have been both plugged and, subsequently, the obstructing material could have been blown free.

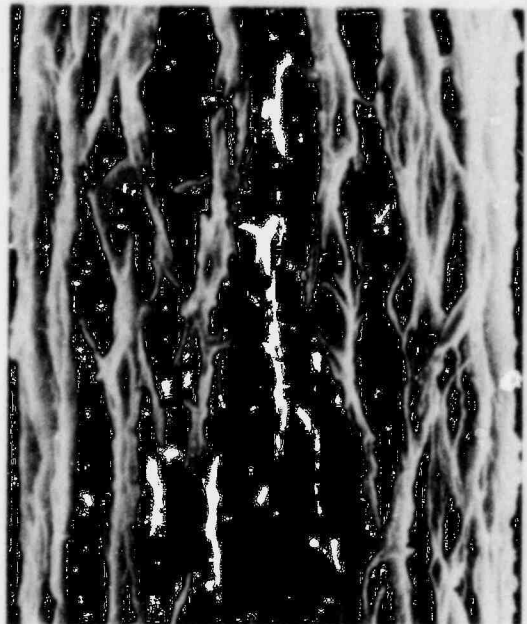
In the case of suspected partial plugging, powder could still flow through orifices. At the beginning of the extended time runs, several runs were started but aborted because only 7 to 15% of the desired flow could be achieved since we assumed that this condition could be evidence of plugging. The chemical analysis of the samples from these runs yielded 15.2 to 38.7  $\mu\text{g}$  DUO, even with partial plugging.

Capillaries, with more extensive surface area exposed to airborne powder than orifices, can plug at the face, or particles can deposit in the length of the leak path, leading to bridging and eventual flow blockage. This additional area available for deposition could account for the 17% plugging of capillaries compared to 6% for the orifices where plugging occurred primarily at the orifice face. Figure 13 is a photomicrograph of core samples from tubing used to fabricate the experimental capillaries. The core samples show an interior surface that would appear to facilitate particle deposition because of roughness. Since the capillary leak would be more representative of a leak subsequent to an accident than the orifice, the 17% rate of immediate plugging could be assumed to occur for small leaks under accident conditions.

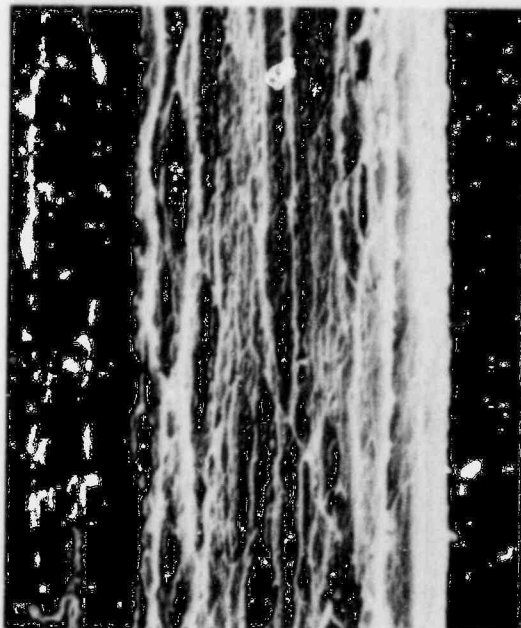




75 MICROMETERS  
800X



100 MICROMETERS  
700X



150 MICROMETERS  
1000X



200 MICROMETERS  
300X

FIGURE 13. Scanning Electron Micrographs of Capillary Core Casts Showing Surface Roughness

## EXTRANEOUS LEAKAGE

If an orifice plate were inadequately sealed in place in the sample collection chamber, extraneous powder leakage might have occurred around the circumference of the plate, giving erroneous results. To prevent leaks, each orifice plate was thoroughly cleaned with solvent, cement applied, and carefully sealed in place in the sample collection chamber. Since there were no means available to verify the condition of the seal when the chamber was inserted in the APLA, an extensive testing program verified the usefulness of this technique.

In a sealing test, a capillary leak supported in an orifice plate was cemented in place in the chamber, and the sampler attached to the UPL leak test apparatus (Figure 10) with the sampler in an upright position (see Figure 14). Leak-testing fluid covered the downstream face of the capillary support plate and the system was pressurized to 1000 psig for leak testing. Bubble formation indicated air leakage. These tests continued until a reliable sealing method was devised and verified.

A few seals failed during the powder leak tests. These failures were readily apparent by observing DUO powder streaked on the reverse side of the orifice plate, which verified high DUO transmission.

## BACKGROUND DUO LEVELS

Potential contamination of samples during handling is of concern in any experiment. To assure that the APLA sample analysis results represented the DUO collected in an experiment, background samples were prepared and sent for chemical analysis. The sampler was coated with gelatin, an orifice sealed on with glue, a filter fitted, and the unit screwed in place in the APLA. Chemical analysis showed that the average background of DUO was 2.66  $\mu\text{g}$ , 1  $\mu\text{g}$  above the reagent blank made from gelatin and a filter that was routinely analyzed for uranium with every group of samples. These results assured that background contamination during sample handling was not a problem in the APLA experiments.

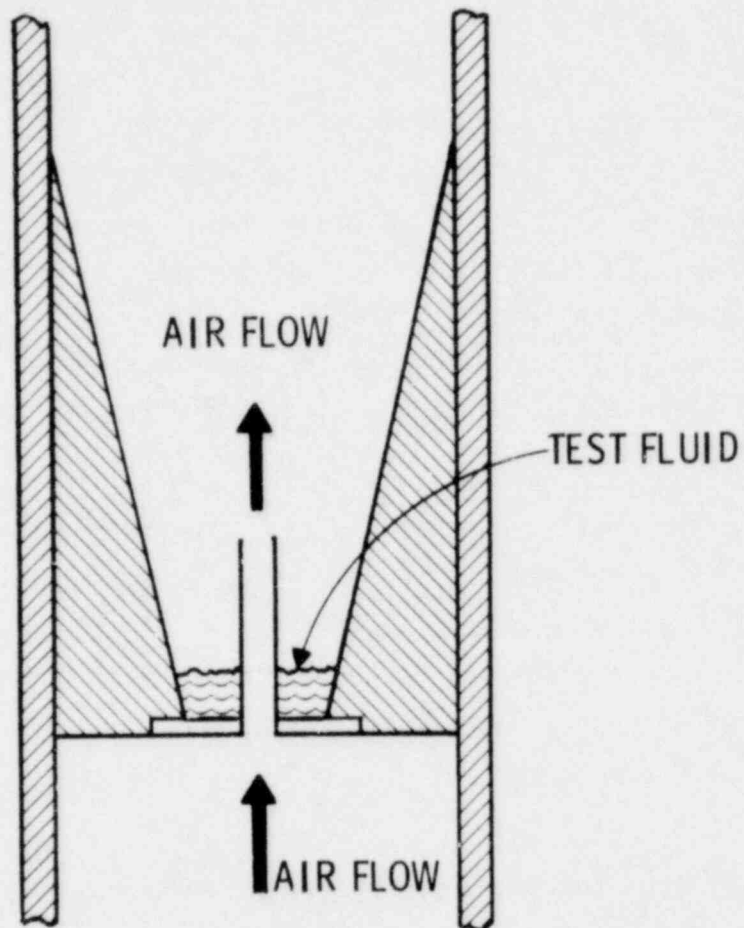


FIGURE 14. Efficiency Test of Cement Seal of Orifice Plate

Background contamination level determinations for the UPL were run by sealing an orifice in place in the sampler, covering the orifice with DUO (25 to ~250 g) fitting a filter and installing the unit in the UPL apparatus. The backgrounds averaged 2  $\mu$ g. As with the APLA, background contamination did not present a problem.

The majority of the DUO analysis results were well above background levels and represented real values for the powder transmitted. Some experiments with background levels of DUO were from small-diameter orifices at low pressures, which might be anticipated.

#### RESULTS: FIRST SERIES

The objective of the plutonium oxide leak rate study was to correlate powder transmission with known gas leak rates. The first experiments measured

the powders transmitted by airflows from less than 10 cc/min to 22  $\ell$ /min. Figures 15 and 16 are plots of the APLA powder flow through orifices and capillaries as  $\mu\text{g}/\text{cc}$  and  $\mu\text{g}/\text{min}$  as a function of airflow rate in cc/min. As the figures show, there appears to be a trend to a finite amount of DUO transmitted in each cc of air and increased  $\mu\text{g}/\text{min}$  DUO at higher flow rates.

#### APLA Preliminary Statistical Analysis

The first analysis of this initial APLA orifice data to establish a leak rate indicated that the natural logarithm ( $\ln$ ) DUO  $\mu\text{g}/\text{min}$  provided the best insight into the structure of the data. Eight different ways of analyzing the data were investigated as a function of airflow rate:

- DUO, total  $\mu\text{g}$  transmitted
- DUO/min, DUO per unit time
- DUO/ $\mu\text{m}^2$ , DUO per unit cross-sectional area
- DUO/min/ $\mu\text{m}^2$ , DUO per unit time per area,

and the natural logarithm ( $\ln$ ) of each.

The results of the single, multiple orifice-time constant, and multiple orifice-time varying runs are plotted in Figure 17 as a function of  $\ln$  (airflow) with specific nominal orifice size designated. The time-constant value is the average of all the orifices tested in one run. Since there was no assurance that shutting off the flow control downstream of the sampler shut off transmission to the sampler, the impact of the time of shut-off for the time-varying runs is questionable.

In conducting the time-varying runs, several samplers were turned off at successive time intervals. Pressure built up in the sampler when the sampler was shut off according to the sampler design, and the pressure was relieved to protect the gauge and flowmeter. Therefore, because there was always potential airflow through the sampler, there was an uncertainty as to the actual sampling time. For the time-varying runs,  $\bar{TV} = \ln [\Sigma \text{DUO}/\text{max time}]$  was selected as the best value to compare with the single and time-constant averages.

The data are plotted as a function of DUO  $\ln \mu\text{g}/\text{min}$  against the  $\ln$  of the characterized airflow rate. The relationships among the five orifices with three treatments, single, multiple, and time varying, are also shown.

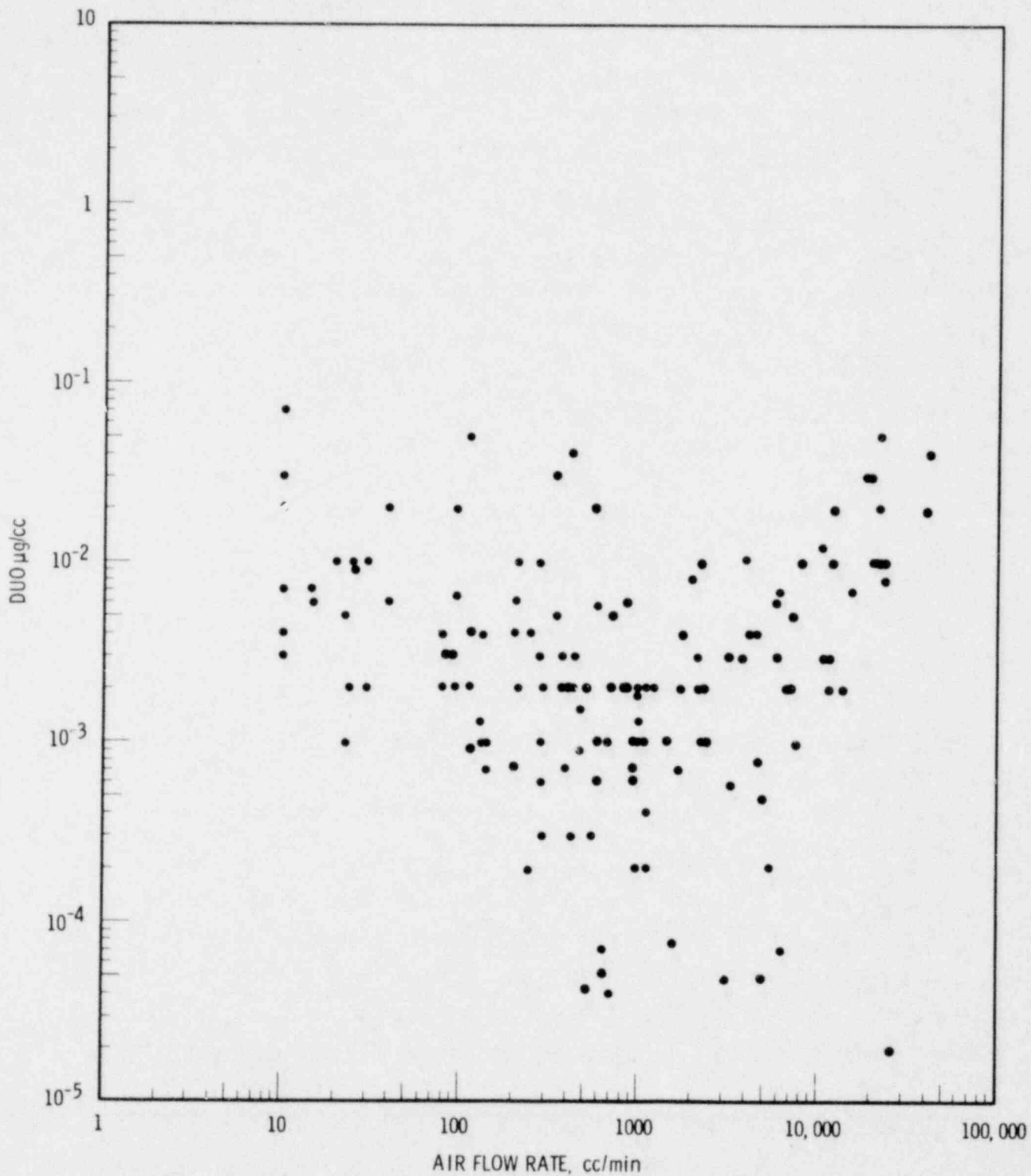


FIGURE 15. APLA Powder Flow Rates Through Characterized Leaks as a Function of Airflow Rates, µg/cc

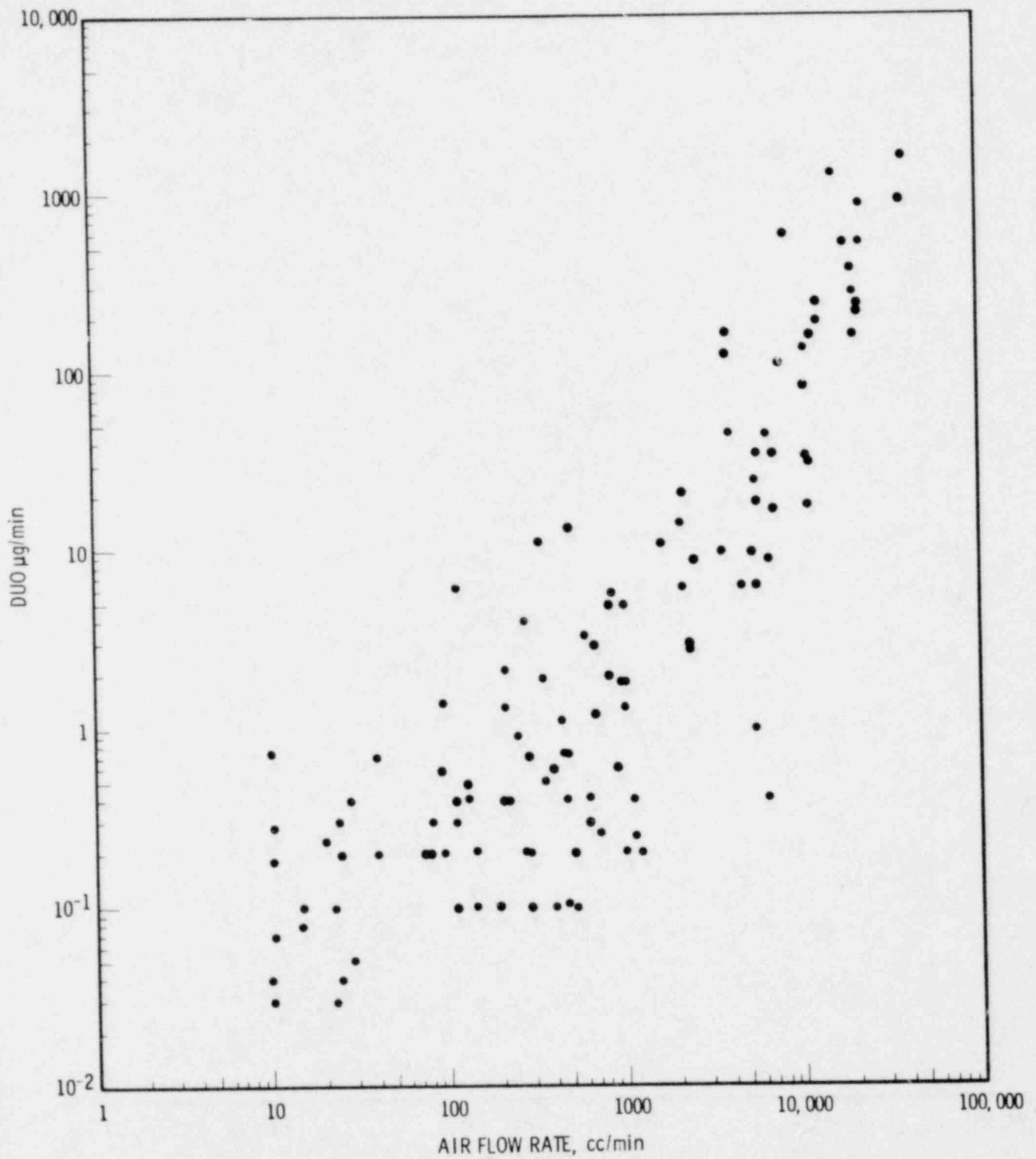


FIGURE 16. APLA Powder Flow Rates Through Characterized Leaks as a Function of Airflow Rates, µg/min

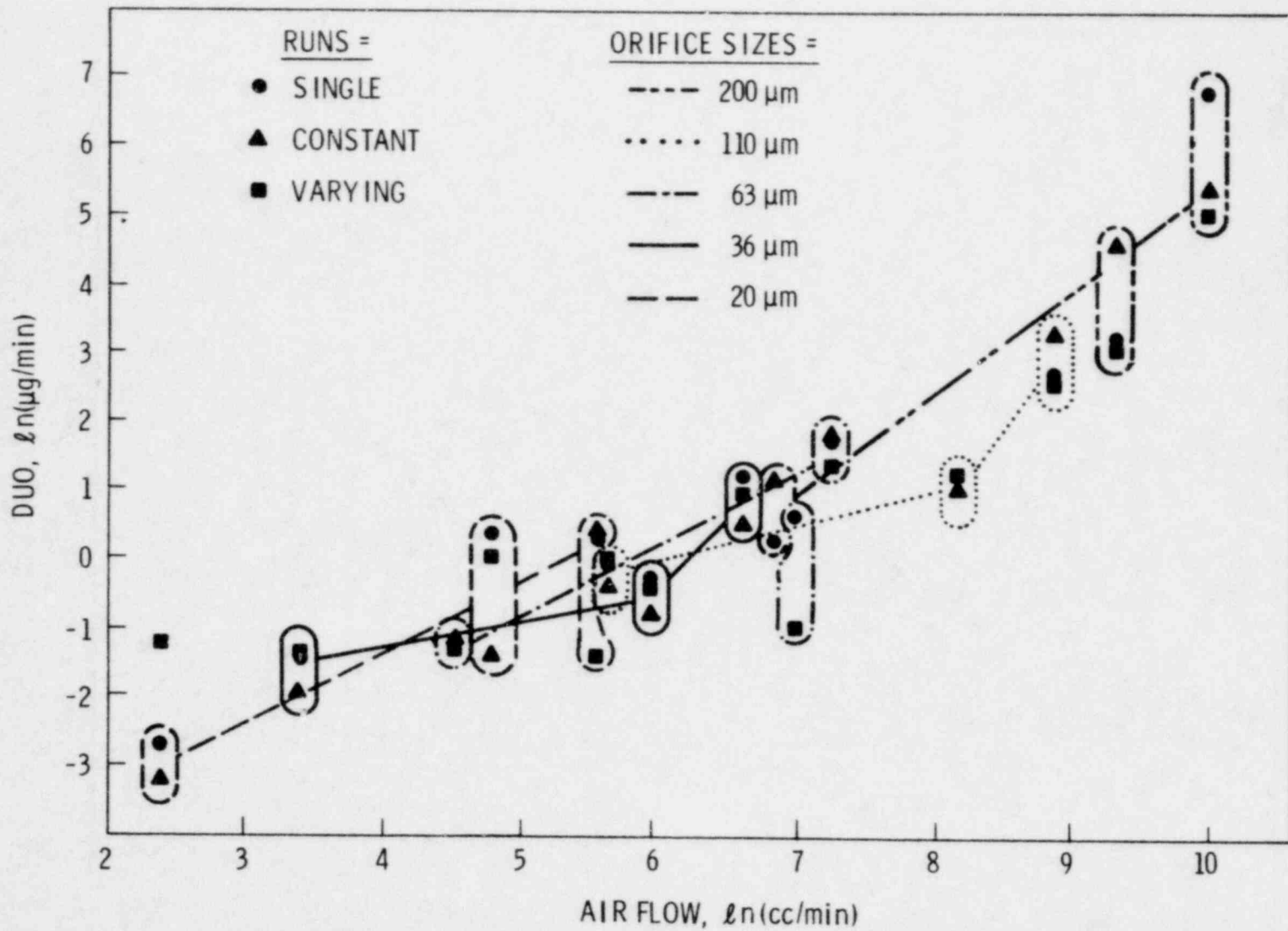


FIGURE 17. Comparison of APLA Treatments Indicating Diameter Relationships

The DUO flow rate increased with increasing airflow rate, and it appeared that a piecewise linear model (for the  $\ln$  data) might be appropriate to describe the results. The powder flow rate for the largest (200- and the 110- $\mu\text{m}$  dia) orifices at the higher airflow rates seemed to fit into a different flow regime.

#### DUO Transmitted During Pressurization/Depressurization

During these initial experiments, there were indications that DUO passed through the orifice during the time required for pressurization/depressurization, called "zero" time.

A few "zero"-time runs investigated the flow of powder into the powder collection chamber during the time required to bring the vessel to the experimental pressure and to return the vessel to ambient pressure. The flows during these times cannot be separated experimentally. The time required to pressurize and depressurize the vessel is short and is a function of pressure rather than orifice size since the bulk of the air exits through a throttling valve at the top of the vessel. Therefore, the time required to pressurize/depressurize is similar for all orifices at one pressure. Typical time requirements for pressurization/depressurization of the APLA vessel are shown in Table 3.

Results from these few experiments indicated that a large portion of the powder can be leaked during this pressurization/depressurization time, as indicated in Figure 18, with the total DUO transmitted at 1000 psig plotted as a function of  $\ln$  airflow rate. The solid lines indicate the standard deviation of the mean value.

TABLE 3. Times Required for Pressurization/Depressurization of APLA Vessel

Pressure psig	Time to Reach Pressure, sec	Total Time for Pressurization/ Depressurization, sec
1000	27 $\pm$ 3	190 $\pm$ 7
500	19 $\pm$ 4	132 $\pm$ 8
100	11 $\pm$ 2	68 $\pm$ 7
30	9.3 $\pm$ 2	40 $\pm$ 6



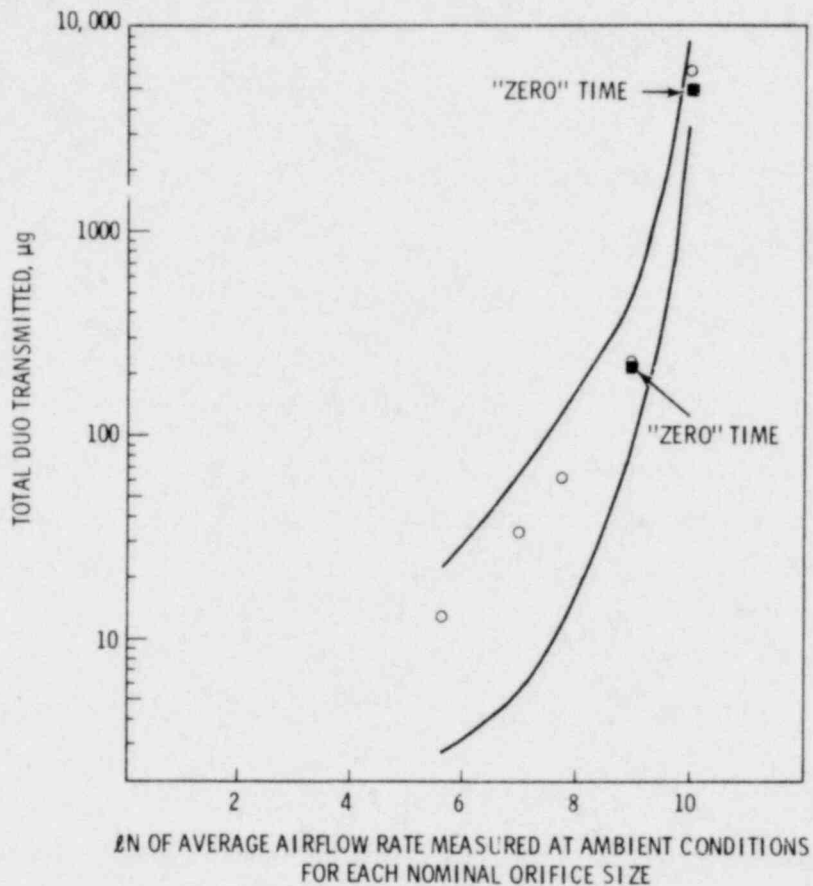


FIGURE 18. Total DUO Transmitted in 1000 psig APLA Experiments Compared with "Zero"-Time DUO Transmission

These runs led to a better understanding of the powder transmission problem. Subsequently, a statistical experimental matrix was designed to investigate "zero"-time powder transmission and to compare this transmission to 30-min runs.

#### Statistical Matrix Work

After the first series of runs indicated the potential structure of the data, two matrices of experiments were designed to investigate total powder flow and "zero"-time powder flow. A complete discussion of the statistical methods used is included in Appendix B. Thirty-six experiments investigated experiment-wide reproducibility, uniformity, and reproducibility of aerosolization of total powder flow. These experiments were all run for 30 min compatible with the air requirement of the system and judged long enough

to collect a sample adequate for analysis, since indications were that time had little effect on DUO transmission. The first results did not indicate significant differences in the DUO transmitted through the 20- and 36- $\mu\text{m}$  orifices and the 110- and 63.5- $\mu\text{m}$  orifices; therefore, the 36- 110-, and 200- $\mu\text{m}$  orifices were selected for use. Three pressures were used: 30, 500, and 1000 psig. Eighteen experiments investigated pressurization/depressurization effects.

The results of these two matrices of experiments were performed using a technique known as "analysis of the variance" (AOV). This technique divides the total variation in an experiment into the variation as a result of:

- the factors under investigation
- interactions between factors
- experimental error.

The variation of the factor under investigation is compared to the experimental error and a conclusion is reached. The techniques used are discussed more fully in Appendix B.

One complication arose during the experiments: the diameter of the orifices had changed. The sizes of the orifices as they were used in the matrix are shown in Table 4 and compared to the original orifice sizes. The variation between two orifices of the same nominal diameter was more than desired. However, there was no assurance that more satisfactory orifices could be fabricated and characterized within the project time scope, and therefore the study continued. The orifices in the table showing a decrease in diameter were all laser drilled, the others mechanically drilled. This fact was noted but not investigated.

TABLE 4. Original and Final Orifice Sizes

Orifice Designation	Original Diameter $\mu\text{m}$	Final Diameter $\mu\text{m}$
3-30	33	22
2-36	33	32
1-110	100	111
3-110	100	89
1-200	200	226
3-200	200	190

### Thirty-minute Runs

The results of the 36 30-min runs are plotted as a function of pressure and original and final orifice diameter in Figure 19.

The conclusions reached by the 36 experiments were:

- 1) both pressure and diameter have significant effect on the amount of powder transmitted,
- 2) diameter is more important than pressure,
- 3) the experimental error standard deviation was  $0.6782 \ln(\text{DUO } \mu\text{g})$
- 4) the coefficient of variation was 16.0%.

### Eighteen "Zero"-Time Runs

This matrix evaluated the powder transmission during pressurization/depressurization that had been observed in the initial experiments. The AOV table of the results and a comparison with the 30-min runs has been included in Appendix B. The  $\ln$  of the total DUO transmitted is plotted as a function of pressure and diameter in Figure 20.

The results of the 30-min runs are included in the plot. The conclusion from this matrix of experiments is that the duration of the run has no effect on the amount of DUO transmitted.

### POWDER LEAKAGE WITH UNAIDED AIRFLOW

In the initial experiments, the characterized airflow rates at the designated pressures for the apertures were maintained using a vacuum. This compensated for the buildup of back pressure that would lower the flows below the values characterized in the flow experiments. In contrast, this series of experiments did not use a vacuum to maintain flow and exhibited flows 6% to 98% of the characterized orifice flow. These experiments investigated the possibility that the vacuum was the major cause of powder transmission. The DUO measurements indicate powder transmission comparable to the transmission when flow was maintained by vacuum as shown in Figure 21 where the powder transmission is plotted as a function of  $\ln(A\sqrt{P})$ . These plots reflect the same trends as in all the results from the statistical matrix experiments, and

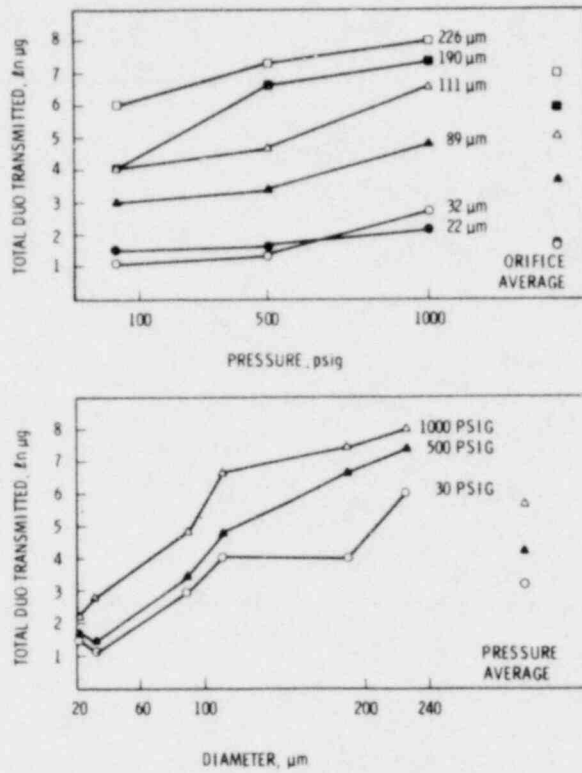


FIGURE 19. Total DUO Transmitted Through Orifices as a Function of Pressure (Top) and Diameter (Bottom) 30-Min Experiments

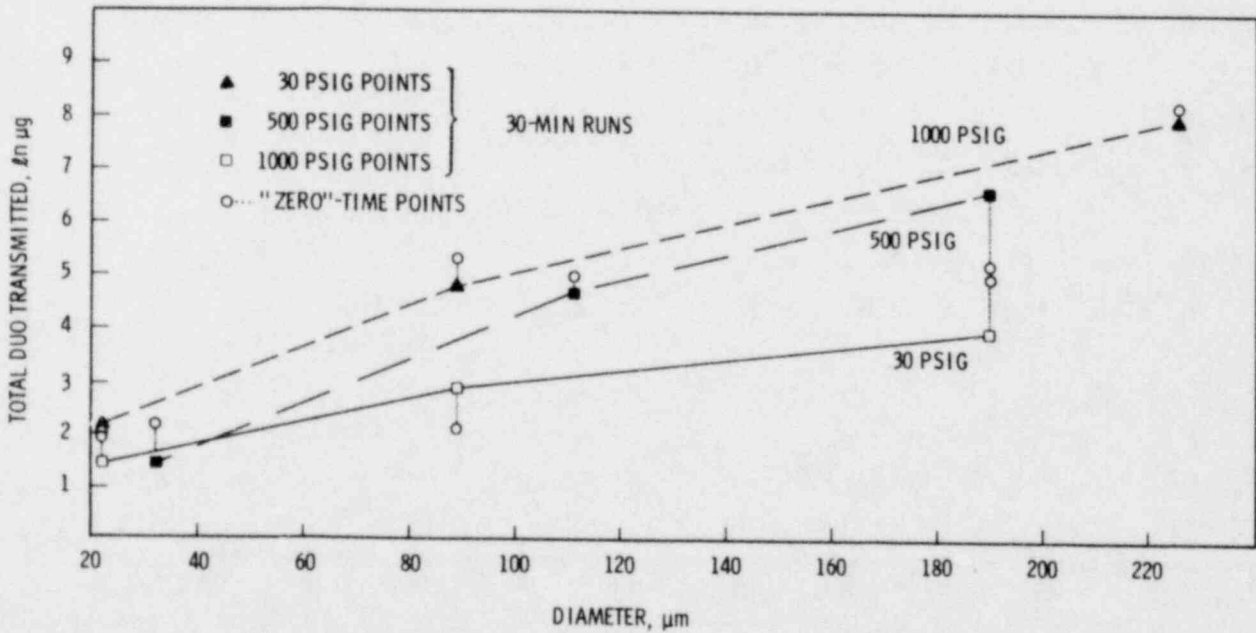


FIGURE 20. Comparison of 30-min and "Zero"-Time Runs by Orifice Size

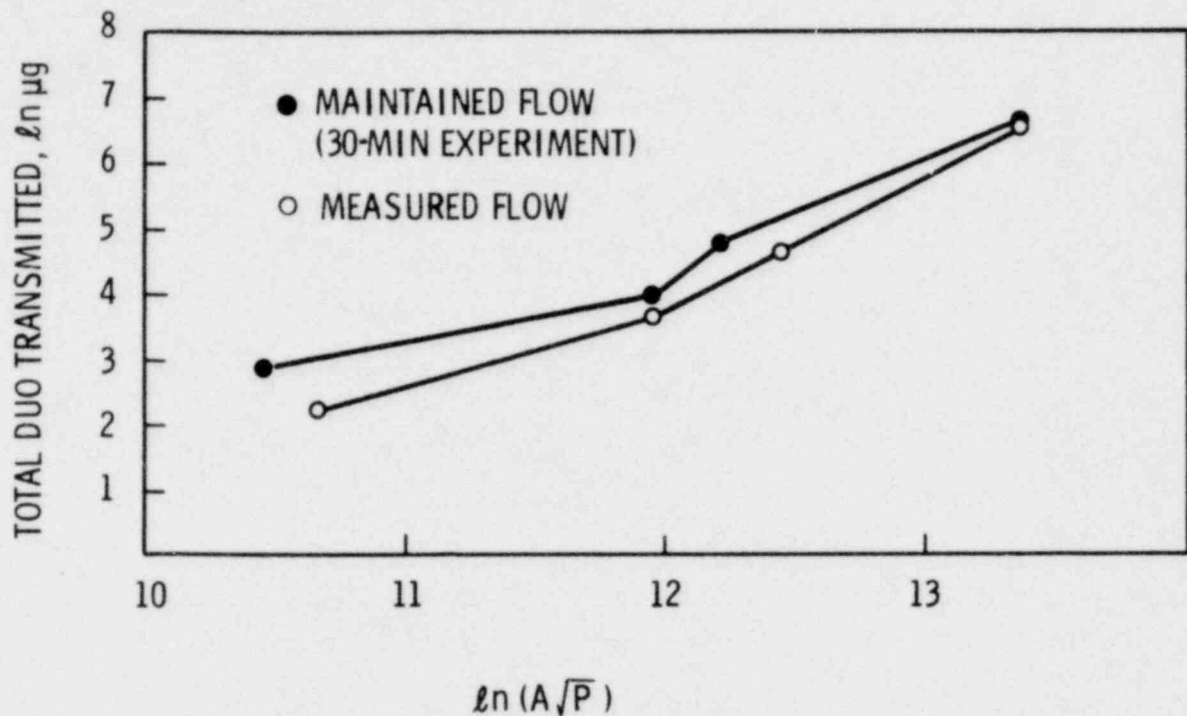


FIGURE 21. Comparison of DUO Transmitted Through Orifices by Maintained and Measured Airflow

the mean difference in the two plots is not statistically significant. The matrix indicated that the orifice diameter was the most important influence on flow rather than the actual air movement during the experiment. (Some of the under powder leak tests exhibited powder flow with no detectable airflow). The measured orifice diameter provided a better indication of the powder flow than the measured airflow rate during an experiment. The theoretical airflow rate through an orifice contains the factor  $A\sqrt{P}$ .

#### EXTENDED TIME RUNS

All of the work indicated that time was not of any significance in the powder transmission through the openings under investigation. To verify further this conclusion, the nominal 110- $\mu\text{m}$  orifice at 100 psig upstream pressure was used in runs to evaluate APLA powder transmission for extended

time periods. One experiment (and a replicate) were made at extended times of 24 and 6 hr.

The airflow rate during the first 24-hr run showed a gradual decrease during the first 4 hr, then a slow restoration of flow to 95% of the original flow rate, as illustrated in the plot in Figure 22. In this experiment, the orifice apparently plugged and a plug of powder built up, lessening flow. The plug subsequently seemed to erode as airflow was restored. At the minimum flow rate, the calculated apparent diameter of the orifice as a result of plugging was 85  $\mu\text{m}$ . Other runs were started but aborted because adequate airflow could not be achieved; flows were 50 and 100 cc/min ( $\sim 700$  cc/min was desired). Chemical analysis of samples from these runs yielded 15.2 to 38.7  $\mu\text{g}$  DUO, even with some plugging evident during microscopic examination of the orifice. However, an adequate flow was achieved with orifice 6-110, and a second 24-hr run was made. A constant airflow rate was maintained through the entire run with no evidence of plugging.

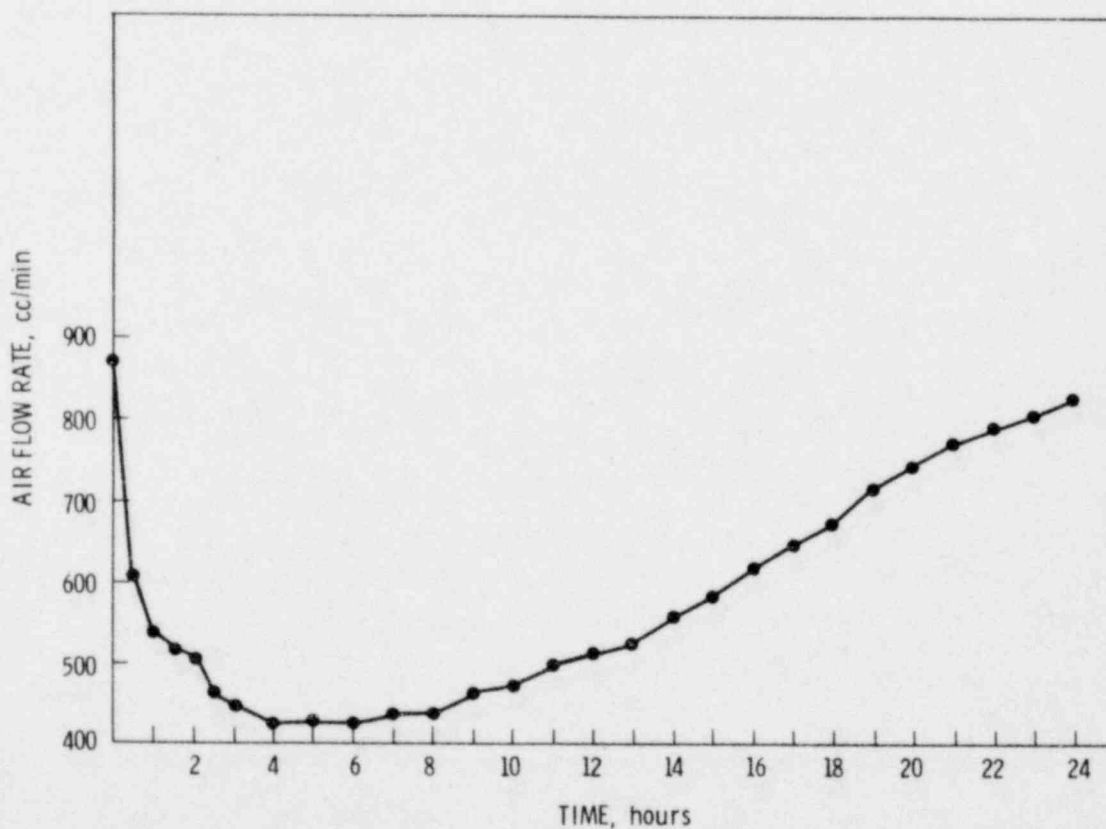


FIGURE 22. APLA Airflow Rate as a Function of Time During a 24-hr Run, Orifice 1-110, 100 psig

The total DUO transmitted in the extended time runs and shorter time experiments are compared in the plots in Figure 23. The DUO collected from the run exhibiting plugging and subsequent release of the plug showed the highest result for 24 hr, 305  $\mu\text{g}$ . The 105  $\mu\text{g}$  collected in the second 24-hr run is comparable to the highest collection from individual runs for shorter time periods, and therefore, it appears that maximum powder leakage occurred early in any run. The average leakage during a 1-min pressurization/depressurization time was 30  $\mu\text{g}$ . If this leakage had persisted for 24 hr,  $5.5 \times 10^4 \mu\text{g}$  DUO would have leaked, contrasted to the actual 305 and 105  $\mu\text{g}$ .

Figure 24 illustrates the maximum leakage occurring early in the 110- $\mu\text{m}$ -orifice run at 100 psig upstream pressure by plotting leak rate as a function of time. However, it is evident from Figure 23, showing total DUO transmitted, that there is no rate corresponding to an airflow rate.

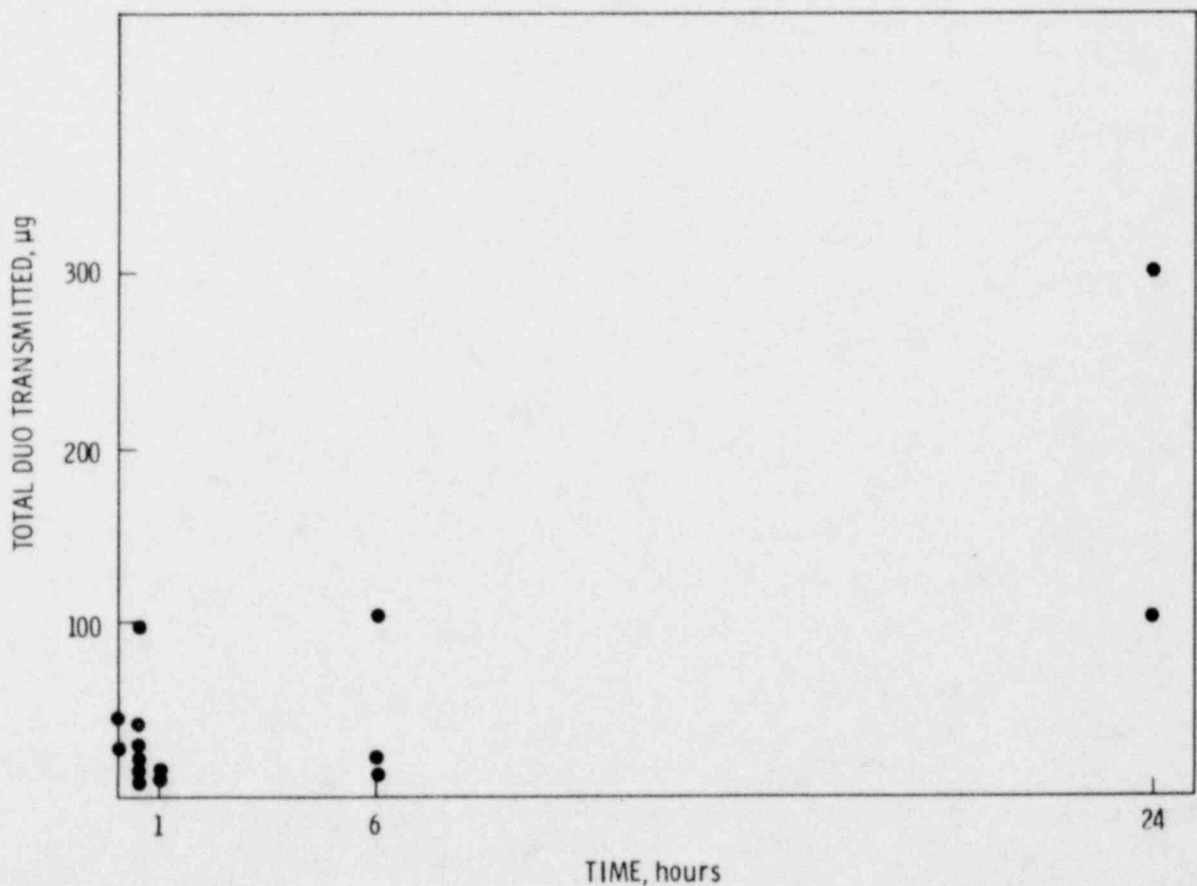


FIGURE 23. Total DUO Transmitted Through 110- $\mu\text{m}$  Orifice During APLA Runs at 100 psig, as a Function of Time

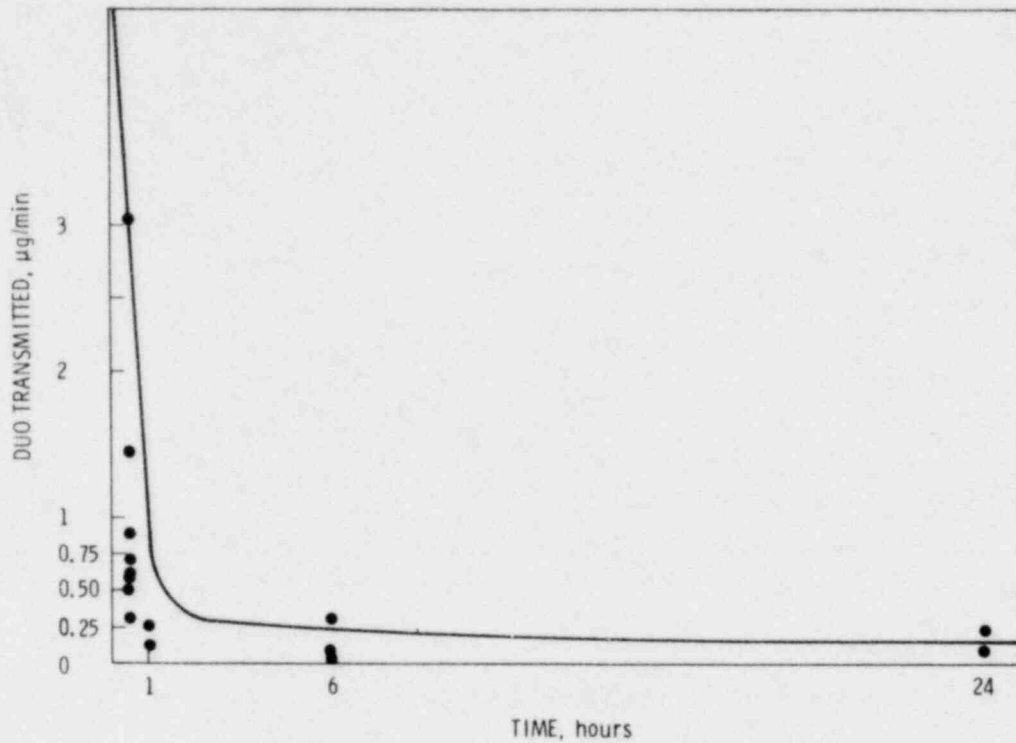


FIGURE 24. DUO Leak Rate Through 110- $\mu$ m Orifices During APLA Runs at 100 psig, as a Function of Time

#### PRESSURE DECAY RUNS

Pressure decay experiments measured powder transmission under a decaying pressure regime. The vessel was pressurized to 1000 psig and allowed to depressurize as the entire flow passed through the orifice. The time required for pressure decay varied from 0.45 hr for a 200- $\mu$ m orifice to 70 hr for a 20- $\mu$ m orifice. The results plotted in Figure 25 compare the DUO transmitted in pressure decay "zero"-time 30-min and 60-min runs for the same orifice. The results from the 63.5- $\mu$ m orifice were not included because they were questionable as a result of multiple pressurizations.

The data reinforce the hypothesis that duration of the run has little impact on DUO transmitted.



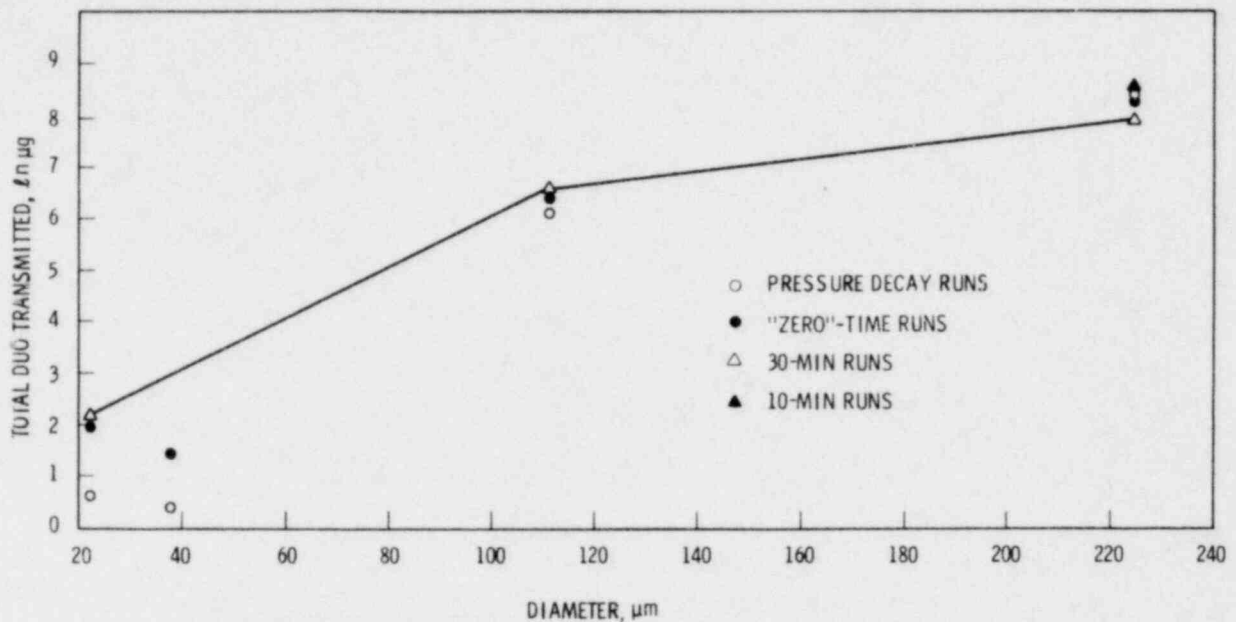


FIGURE 25. Comparison of Pressure Decay and Other Runs at 1000 psig

#### SLOW PRESSURIZATION

Since up to 80 min may be required for the TB-1 to be pressurized to 1000 psig after an accident, experiments using 1-110 and 1-200  $\mu\text{m}$  orifices investigated slow pressurization (80 min) in contrast to immediate pressurization. The results are compiled in Table 5.

The results of Table 5 infer that less powder is transmitted during slow pressurization; slow-pressurization DUO transmission through the 1-200 orifice is one third that of immediate pressurization. Although with the smaller-diameter orifice there is essentially no difference in DUO transmitted, the results of Table 5 seem to indicate that more powder can be airborne in immediate pressurization than 80-min pressurization. The 200- $\mu\text{m}$  orifice diameter is sufficiently large to allow powder flow. However, the same DUO transmitted during two runs using the smaller 110- $\mu\text{m}$  orifice diameter could indicate that this diameter does not allow free flow, and that even with powder flow from an environment with higher airborne concentrations (immediate pressurization), limited DUO can be transmitted.

TABLE 5. Total DUO Transmitted at Immediate Pressurization and 80-Min Pressurization

<u>Orifice</u>	Immediate Pressurization	80-Min Pressurization
	<u>µg</u>	<u>µg</u>
1-110	574	468
1-200	3705	1248

### APLA CAPILLARY LEAKS

The limited number of capillaries available for experimental use contributed to a lack of comprehensive data on capillary leaks. Several factors contributed to the problem of capillary availability:

#### 1. Fabrication Difficulties

The capillaries were fabricated from precision-bore stainless steel tubing mounted in a support plate (Schwendiman et al. 1976 to 1979). This fabrication proved to be difficult because of the size of the tubing (an internal diameter of 50 to 250 µm) and the rigorous conditions the capillaries would be required to withstand in an experiment (1000 psig, 1200<sup>0</sup>F). Fifty percent of the first shipment received were rejected because of suspected leaks, capillaries were not flush with their support plates and some capillaries were sealed. Subsequent fabrication attempts were no more successful than the first, but a complete set of units in two lengths was obtained. A second vendor was contracted. He had indicated familiarity with this type of fabrication but no other capillaries could be satisfactorily fabricated.

#### 2. Plugging

Capillaries often plugged and the material plugging the tubing could not be dislodged. For the smallest ID, 50 µm, no wire could be located of a diameter small enough to run through and clean the capillary. In any event, small-diameter wire would not have been sufficiently strong to dislodge extraneous material.

#### 3. Breakage

Small-diameter capillaries were fragile and had a high attrition rate during handling required for the experiment. Although a statistical

matrix could not be run because of the limited number of capillaries, at least one run was made with each capillary. Experiments continued until all the capillaries were plugged or broken.

The capillary data is plotted as a function of pressure and diameter in Figure 26. There is not enough data on capillaries to provide the basis for detailed statistical analysis, but descriptive results are possible. At 30 psig there was no increase in powder transmission with increasing diameter, except for the largest short capillary. There is a consistent drop in DUO transmitted at all pressure levels for the 100- $\mu$ m capillaries. With this exception, high pressure (1000 psig) produced increased DUO transmission. The transmissions for 30 psig were random for all apertures, except for the largest short capillary. There was an unexplained anomaly that could not be investigated further: it appeared that a long capillary could allow greater powder transmission than a short one of the same diameter.

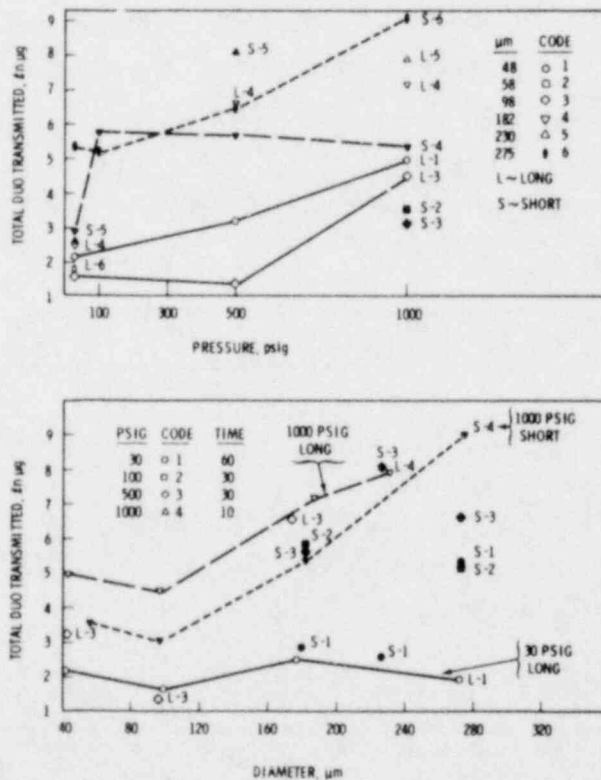


FIGURE 26. DUO Powder Transmission Through Capillaries as a Function of Pressure (Top) and Diameter (Bottom)

## RESULTS AND DISCUSSION: LEAK PATH UNDER THE STATIC POWDER LEVEL

In considering the location of a leak with respect to the contents of a container, it is apparent that the bulk powder can cover the leak partially or completely to various depths. When the leak geometry is favorable and when there is sufficient force, particles can pass through the leak path. The Under Powder Leak (UPL) experiments investigated some specific leak situations of the infinite variety that could result from an accident.

### LEAKS UNDER THE STATIC POWDER LEVEL

The first experiments investigated leakage from an orifice covered with 3 g DUO, the depth of coverage about 0.1 cm. For half of the experiments, agitation was applied using a mechanical vibrator. Almost all experiments used the same set of orifices.

The top of Figure 27 shows the transmission of DUO appearing to maximize at approximately 100 psig for all nominal sizes under 200  $\mu\text{m}$ . This maximization effect may indicate initial movement of the powder (at 100 psig), followed by compaction of the powder and bridging of the orifice which allows no further increase in flow. Agitation by a mechanical vibrator had no apparent effect on powder transmission. There were not enough data points to draw a statistical conclusion on the effect of time. The bottom half of Figure 27 shows the powder transmission increasing with orifice diameter.

### DEPTH (WEIGHT) EFFECTS

Bulk powder can completely cover a leak to various depths as the result of an accident. Therefore, an experimental matrix was completed that investigated pressure and depth effects on powder flow from a leak underneath the powder level. A new powder reservoir of the same internal diameter as the one used in the first experiments (Figures 10 and 11), enabled powder to cover the orifice to a maximum depth of 21.8 cm. Three pressures, 100, 500, and 1000 psig, were investigated. Three initial depths of DUO, 21.8, 7.4 and 1.5 cm, covered the orifice.

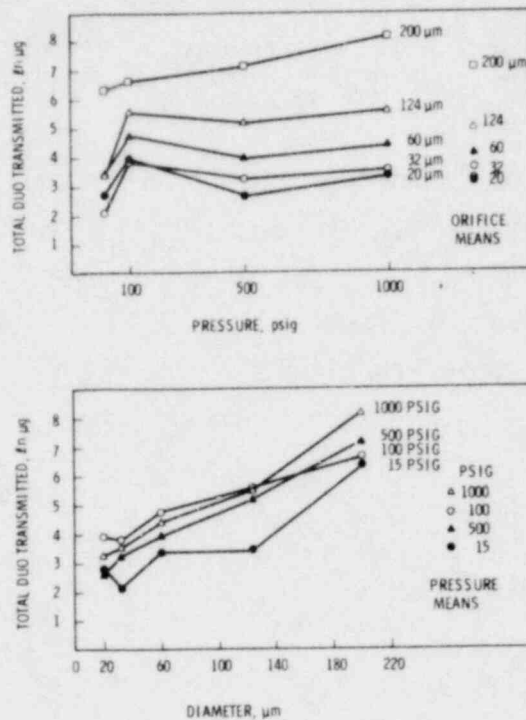


FIGURE 27. Total DUO Transmitted from Leaks Below the Static Powder Level as a Function of Pressure (Top) and Diameter (Bottom)

The powder was first weighed. Because of packing discrepancies (the packing was a pour volume and loose), the weight when DUO filled the reservoir to 21.8-cm was approximately 250 g. The DUO for 7.4-cm depth weighed 100 g; the DUO for 1.5 cm depth weighed 25 g. The powder exhibited compaction during the runs both at 100 psig and 1000 psig. For all pressures, a volume of powder with a depth of 21.8 cm before a run was 10.2 cm after a run. Thus, the final depth of powder in a run was about half the original depth. This compacted powder was caked, difficult to remove, and had to be scraped out of the chamber. The volumetric airflow rate was not changed as the packing occurred during a run. For the deepest powder, a depressurization time of about 40 min was required.

The DUO transmitted through the UPL leaks is shown in Figure 28 as a function of pressure. A summation of the statistical analysis is included in Appendix B.

The conclusions reached were:

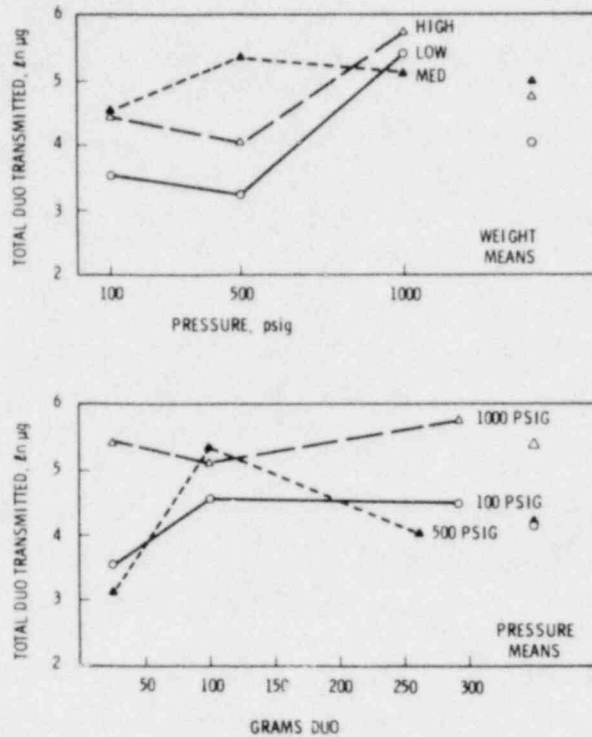


FIGURE 28. Total DUO Transmitted from Leaks Below Different Quantities of Powder

- Depth (weight) of coverage had no significant effect on powder transmission.
- Pressure had no significant effect on powder transmission.

#### LEAKAGE FOR AN EXTENDED TIME

The amount of DUO powder leakage from leaks underneath the powder level does not increase with time. Replicate experiments using the same 2-110 orifice used for all runs (100 psig pressure) and completed with 7.4-cm depth DUO over the orifice show that the amount collected in 24 hr was less than the collection in the 30-min runs. The results are shown in Table 6.

One of the replicate 360-min runs had the same powder passage as the 30-min runs; however, the amount collected in 24 hr was less than the 30-min runs. This "slow down" effect would indicate that the particles are first jetted through the leak passage, and then aggregates of small particles block

TABLE 6. Total DUO Collected From Leaks Underneath the Static Powder Level for Different Collection Times

<u>30 min</u> <u>µg DUO Transmitted</u>	<u>360 min (6 hr)</u> <u>µg DUO Transmitted</u>	<u>1440 min (24 hr)</u> <u>µg DUO Transmitted</u>
123	94.5	41.5
72.4	45.5	10.2

the transport of a significant number of other particles. Therefore, the precise orientation of the particles in the reservoir could contribute to the lower flow in the 24-hr runs.

It might be hypothesized that the pressure in the powder reservoir compresses the powder into a rigid form, preventing any further powder flow after the first particles jet through the orifice.

We conclude that there is no increase of powder transmission through a leak below the powder level as a function of time.

#### PRESSURIZATION TIME

As noted earlier, time up to 80 min could be required for the TB-1 vessel to reach an internal pressure of 1000 psig. Two experiments evaluated the impact of slow versus immediate pressurization on a leak below a 21.8-cm-deep powder bed. In the slow-pressurization experiments, the DUO compacted half as much as during immediate pressurization. The slow pressurization-compacted depth was 15.5 cm as opposed to 10.2 cm after immediate pressurization. The total DUO transmitted in each of two slow-pressurization runs was 933 and 210 µg contrasted to an average of 224 µg in two immediate pressurization runs. Whereas more powder can pass through an orifice during a longer span of pressurization time, the powder will not necessarily do so. Only one value is high (933 µg) and more data would be desirable to make a better assessment. The DUO compacted about the same amount in the two slow pressurization tests; however, one test had greater DUO transmitted through the orifice. The differences in powder transmittance is probably associated with initial packing as the powder was poured into the reservoir. One of the packings probably had interstices that encouraged fewer particle movements than the other, or there could be other controlling parameters.

## RESERVOIR ORIENTATION AND SLOW PRESSURIZATION

In an attempt to find effects that might maximize powder leakage, the orientation of the powder reservoir was changed. In earlier experiments the reservoir was in an upright ( $90^{\circ}$ ) position; this position was changed to horizontal ( $180^{\circ}$ ) and intermediate ( $45^{\circ}$ ) orientations. Twenty-five grams of DUO powder were placed in the reservoir while it was in the upright position; the reservoir was then tipped to the desired angle. In these positions, the DUO no longer covered the orifice. Half-hour runs at 1000 psig were made at slow and immediate pressurization. In a final set of experiments, the reservoir was equipped with a flexible high-pressure hose. The reservoir (25 g DUO at 1000 psig) was rotated end-for-end three times per min for 30 min, a  $180^{\circ}$  oscillation allowing the powder to drop from one end of the reservoir to the other.

None of these various orientation strategies yielded a significant increase in the DUO transmitted through the orifice. The results are displayed in a bar graph in Figure 29 that includes APLA and UPL results (110- $\mu$ m orifice) from experiments using two reservoirs, all at 1000 psig. The APLA results are from single orifice (S), time constant (TC), time-varying (TV), "zero", and statistical matrix (M) runs. The UPL runs are for Reservoir 1 with 0.5- and 1.5-cm powder coverage, and Reservoir 2 with 1.5-cm coverage in  $90^{\circ}$ ,  $180^{\circ}$ ,  $45^{\circ}$ , and turning-end-for-end orientations for 30 min after pressure was reached.

The average leak from Reservoir 1 (1.5-cm coverage), 1152  $\mu$ g, was the largest DUO transmission value. The other values were comparable, with an end-for-end leak of 522  $\mu$ g the closest to the highest value, which was still only half the leak from Reservoir 1. No efforts to maximize powder flow were successful. It appears that the configuration of 1.5-cm powder depth in Reservoir 1 can give the highest powder transmitted. This assumption is illustrated in the plot in Figure 30 that compares leaks below the powder level for the two reservoirs at tests of 1000 psig with 25 g DUO in the reservoirs. The 25 g of powder filled Reservoir 1 completely and left about 20 cm of void space in Reservoir 2. At every pressure the second powder reservoir transmitted less DUO.

A question arises from this experiment: does the DUO depth (completely full) or the shape of the reservoir (or an interaction of both) promote increased powder flow? Unfortunately, 1.5-cm DUO is the maximum capacity of



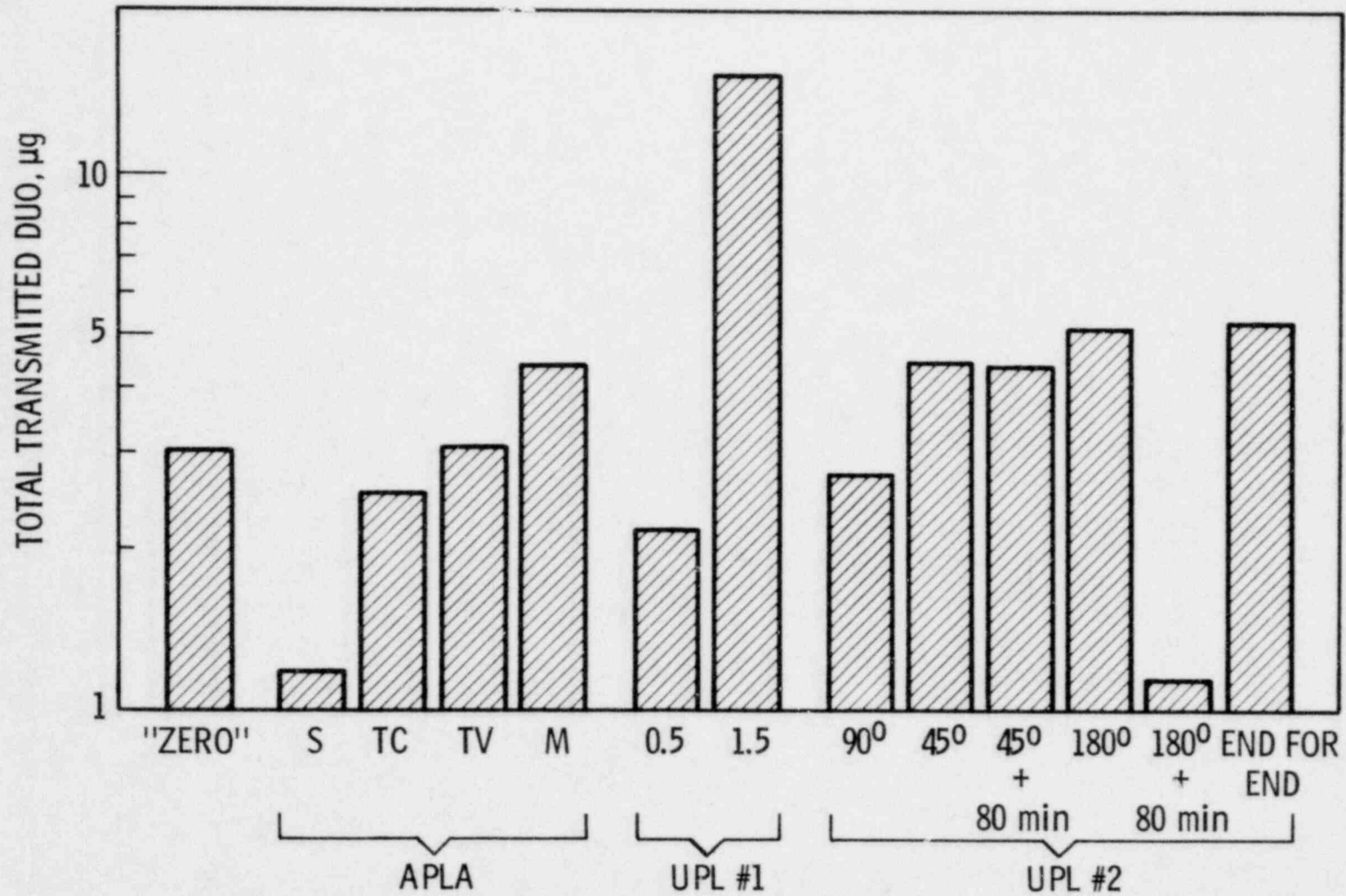


FIGURE 29. Total DUO Transmitted Through Orifices for Different Experimental Treatments, UPL

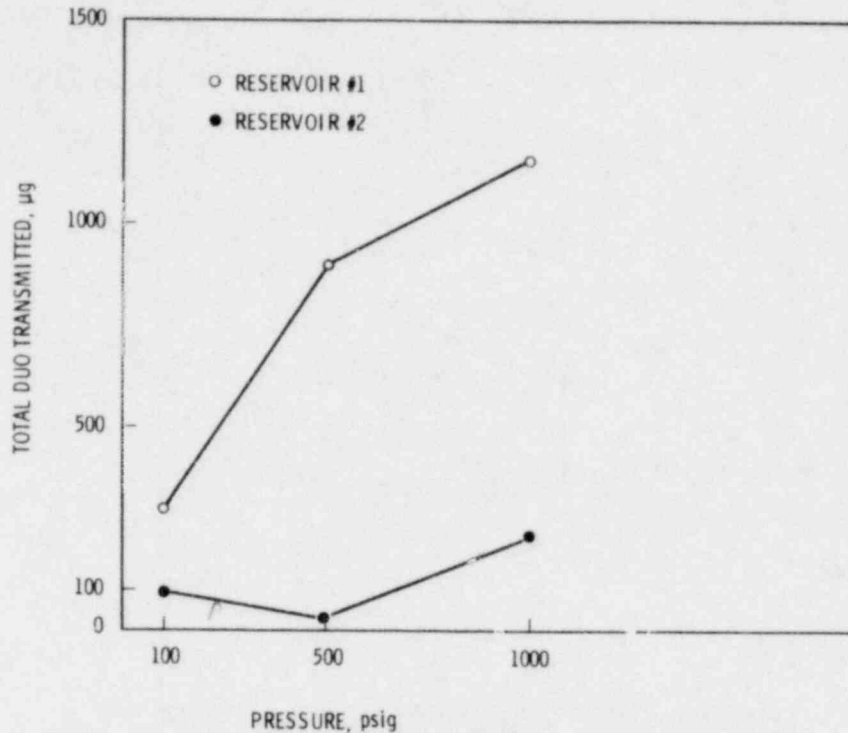


FIGURE 30. Total DUO Transmission from Leaks Below the Powder Level, Two Reservoirs, 25 g Powder, 1.5-cm Depth, 2-110 Orifice

Reservoir 1 and, thus, this problem could not be investigated. However, the statistical matrix used in investigating the effect of powder depth indicated powder depth had no effect on powder transmission. Therefore, the interior configuration might influence the leakage.

In order to speculate on the question of reservoir shape, the configurations of the reservoirs are sketched in Figure 31. Reservoir 1 has a bell-shaped expanding section, whereas Reservoir 2 has an abrupt expansion. The second reservoir has about 15 times the fetch from air entry to the orifice,  $D$ , than does the first reservoir. Airflow entering the chamber at 1000 psig would have a jet effect, setting up turbulent flow patterns. In the distance from the jet to the orifices, these patterns would be modified, and in Reservoir 2, with longer fetch and abrupt expansion, would have different flow patterns than those in Reservoir 1. Therefore, since flow would mix with the powder, DUO leakage might not be the same for each reservoir.

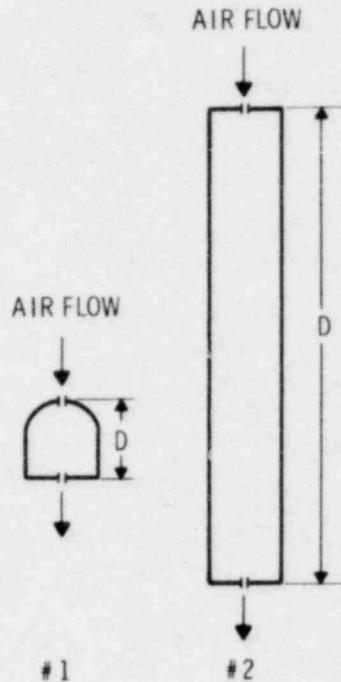


FIGURE 31. Reservoir Shapes

#### UPL CAPILLARY LEAKS

As a result of a limited number of available capillaries, the investigation of UPL capillary leaks was limited to two lengths of two diameters: 150  $\mu\text{m}$  and 250  $\mu\text{m}$  (nominal sizes). The results of these tests have been plotted as a function of pressure and diameter in Figure 32. The influence of pressure was similar to the initial experiments, with the diameter the most important variable of the three-length, diameter and pressure.

#### MAXIMUM LEAKAGE

The maximum orifice leaks were as anticipated from the 200- $\mu\text{m}$ -dia orifice. The short 250  $\mu\text{m}$  capillary had the greatest powder flow, with the exception of the UPL runs at 15 psig.

The maximum powder transmission for orifices and capillaries are shown in Table 7. However, the capillary and orifice flow data in this table cannot be compared since the capillary has an ID about 75  $\mu\text{m}$  larger than the orifice. However, the APLA and UPL leakage can be compared. The maximum orifice leakage for the APLA was greater than ( $\sim 2$  times) UPL measurements at 1000 psig. At

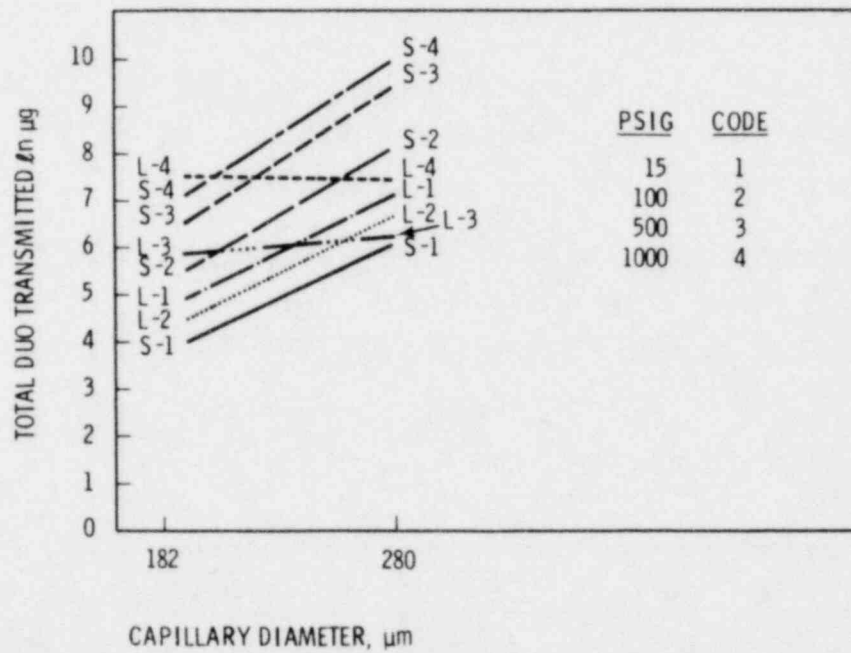
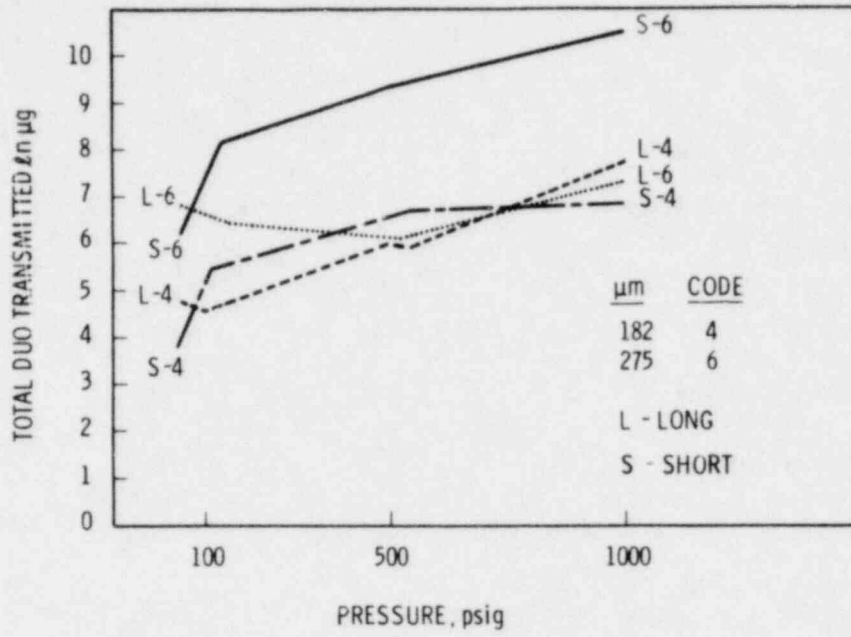


FIGURE 32. Total DUO Transmitted Through Capillaries as as Function of Pressure (Top) and Diameter (Bottom) for UPL Experiments

TABLE 7. Maximum Total DUO Transmitted for APLA and UPL Capillary and Orifice Experiments<sup>(a)</sup>

psig	Orifice		Capillary	
	APLA, $\mu\text{g}$	UPL, $\mu\text{g}$	APLA, $\mu\text{g}$	UPL, $\mu\text{g}$
1000	8730 <sup>(b)</sup>	4890	$1.58 \times 10^4$	$7.92 \times 10^4$ (c)
500	1300	4870	$1.15 \times 10^4$	$1.36 \times 10^4$ (c)
100	109	1240	188	1330(c)
30	323	--	217	--
15	--	734		1950(d)

(a) Before size increase, all 200- $\mu\text{m}$  dia orifices

(b) Run 2 had two pressurization/depressurization sequences; therefore, Run 2 was not considered representative. The run had a leakage of  $2.5 \times 10^4 \mu\text{g}$ .

(c) 250S

(d) 250B (long)

lower pressures, the maximum UPL measurements were greater. For the capillaries, the 1000 psig UPL leakage was 5 times the APLA, and at 500 psig, about the same. At lower pressures the UPL leak rate was larger.

Lowest values for both UPL and APLA orifice leakage could be background level values as a result of plugging. All of the UPL values were above background; however, no capillaries with less than 150- $\mu\text{m}$  ID were used in these tests.

## REFERENCES

- Andersen, J. A., T. A. Duffey, S. A. Dupree, and R. H. Nilson. 1978. PARC (Plutonium Accident Resistant Container) Program Research, Design, and Development. NUREG/CR-0030, SAND76-0587, Sandia Laboratories, Albuquerque, NM.
- Fuchs, N. A. 1964. The Mechanics of Aerosols. MacMillan Co., New York, NY.
- Hausner, H. H. 1971. Modern Developments in Powder Metallurgy. Plenum Press, New York, NY.
- Johanson, J. R. 1975. "Why Bulk Powders Flow or Don't." Chemtech. 572-576.
- Neumann, B. S. 1953. "Powders." Chapter X, Flow Properties of Disperse Systems, J. J. Hermans, ed., Interscience Publishers, pp. 382-422, New York, NY.
- Nuclear Regulatory Commission. 1978. Plutonium Air Transportable Package Model PAT-1. Safety Analysis Report. NUREG-0361, U.S. Nuclear Regulatory Commission, Washington DC.
- Owzarski, P. C., S. L. Sutter, L. C. Schwendiman, J. Mishima and T. J. Bander. 1979. Measured and Predicted Gas Flow Rates Through Rough Capillaries. NUREG/CR-0745, PNL-2623, Pacific Northwest Laboratory, Richland, WA.
- Parent, J. D., et al. 1947. "Fluidizing Processes-- Basic Observations from Laboratory Equipment." Chem. Eng. Prog. 43(8):429.
- Schwendiman, L. C. and S. L. Sutter. 1977. Transport of Particles Through Gas Leaks - A Review. BNWL-2218, Pacific Northwest Laboratory, Richland, WA.
- Schwendiman, L. C., et al. 1976-1979. Quarterly Progress Reports: The Study of Plutonium Oxide Leak Rates From Shipping Containers. PNL-2260-1 to PNL-2260-11, Pacific Northwest Laboratory, Richland, WA.
- Stainforth, P. T. and R. E. R. Berry. 1973. "A General Flowability Index for Powders." Powder Technology. 8, 243-251.
- Sutter, S. L., T. J. Bander, J. Mishima, and L. C. Schwendiman. 1978. Measured Air Flow Rates Through Microorifices and Flow Prediction Capability. NUREG/CR-0066, PNL-2611, Pacific Northwest Laboratory, Richland, WA.
- Zenz, F. A. and D. F. Othmer. 1960. Fluidization and Fluid Particle Systems. Reinhold Publishing Corp., New York, NY.

APPENDIX A

TABULATION OF ANALYTICAL RESULTS

TABLE A.1. Depleted Uranium Dioxide Transmission for Leak Paths Above the Static Powder Level

APLA	ORIFICE OR CAPILLARY DESIGNATION	MEASURED DIAMETER $\mu\text{m}$	CHAMBER PRESSURE psig	TIME min	AIR FLOW cc/min	TRANSMITTED <sup>(4)</sup> DUO, $\mu\text{g}$	DUO, $\mu\text{g}/\text{min}$	DUO, $\mu\text{g}/\text{cc}$
1	1-110	100	1000	20	7100 <sup>(2)</sup>	5.23 ± 1.6	0.26	4 × 10 <sup>-5</sup>
2	1-200	200	1000	20	16400 <sup>(2)</sup>	2.5 × 10 <sup>4</sup> ± 8.7 × 10 <sup>3</sup>	1.25 × 10 <sup>3</sup>	8 × 10 <sup>-3</sup>
3 <sup>(1)</sup>	1-110	100	1000	10	2100 <sup>(2)</sup>	140 ± 42	14	7 × 10 <sup>-3</sup>
4	2-110	125	500	30	4300-3800 <sup>(3)</sup>	1330 ± 410	44	1 × 10 <sup>-2</sup>
5	2-200	200	500	30	6200 <sup>(2)</sup>	1300 ± 340	43	7 × 10 <sup>-3</sup>
6	2-63.5	61	1000	10	2100	55.6 ± 17	6	3 × 10 <sup>-3</sup>
7								
7-1	1-20	22	500	10	111	60.7 ± 18	6	5 × 10 <sup>-2</sup>
7-2	1-20a	23	500	30	133	16.4 ± 4.9	0.5	3.8 × 10 <sup>-3</sup>
7-3	2-20	20	500	60	94	36.7 ± 11	0.6	6.5 × 10 <sup>-3</sup>
7-4	3-20	23	500	120	140	10.6 ± 3.2	0.1	7.1 × 10 <sup>-4</sup>
8	2-20	20	1000	10	210	13.2 ± 4	1.3	6 × 10 <sup>-3</sup>
9	2-36	33	1000	10	580	33.1 ± 9.9	3.3	6 × 10 <sup>-3</sup>
10	2-63.5	61	500	30	1000	54.7 ± 16	1.8	2 × 10 <sup>-3</sup>
11	3-36	38	500	30	470	21.7 ± 6.5	0.7	2 × 10 <sup>-3</sup>
12	2-20	20	500	30	94	42.8 ± 13	1.4	2 × 10 <sup>-2</sup>
13	1-200	200	1000	10	22000	5090 ± 2600	509	2 × 10 <sup>-2</sup>
14	250 A	274	500	30	5400 <sup>(2)</sup>	30.4 ± 9.1	1	2 × 10 <sup>-4</sup>
15	150 A	189	1000	10	10500	1280 ± 660	128	1.2 × 10 <sup>-2</sup>
16	2-200	200	1000	10	22000	8730 ± 4400	873	4 × 10 <sup>-2</sup>
17	1-200	200	30	60	1000	80.3 ± 24	1.3	1 × 10 <sup>-3</sup>
18	1-110	100	30	60	245	56.3 ± 17	0.9	4 × 10 <sup>-3</sup>
19	1-63.5	66	30	60	80	17.8 ± 5.3	0.3	4 × 10 <sup>-3</sup>

(1) DUPLICATE OF 1 BECAUSE OF POOR PRESSURE CONTROL IN RUN 1

(2) LESS THAN DESIRED FLOW

(3) DROPPED 1 MINUTE INTO RUN

(4) THE ± IS THE UNCERTAINTY IN THE URANIUM ANALYSIS AT THE 2 $\sigma$  CONFIDENCE LEVEL



TABLE A.1. (Continued)

APLA	ORIFICE OR CAPILLARY DESIGNATION	MEASURED DIAMETER $\mu\text{m}$	CHAMBER PRESSURE psig	TIME min	AIR FLOW cc/min	TRANSMITTED <sup>(4)</sup> DUO, $\mu\text{g}$	DUO, $\mu\text{g}/\text{min}$	DUO, $\mu\text{g}/\text{cc}$
20								
20-1	3-30	33	500	10	350	19.3 ± 5.8	1.9	5 × 10 <sup>-3</sup>
20-2	1-36	43	500	30	435	32.2 ± 9.7	1.1	3 × 10 <sup>-3</sup>
20-3	2-36	33	500	60	285	10.3 ± 3.1	0.2	6 × 10 <sup>-4</sup>
20-4	3-36	38	500	120	470	15 ± 4.5	0.1	3 × 10 <sup>-4</sup>
21	1-200	200	500	30	6400 <sup>(2)</sup>	12.8 ± 3.8	0.4	7 × 10 <sup>-5</sup>
22								
22-1	3-30	33	500	30	350	10.5 ± 3.2	0.5	1 × 10 <sup>-3</sup>
22-2	1-36	43	500	30	435	20.4 ± 6.1	0.7	2 × 10 <sup>-3</sup>
22-3	2-36	33	500	30	285	12.3 ± 3.7	0.4	1 × 10 <sup>-3</sup>
22-4	3-36	38	500	30	470	11.3 ± 3.4	0.4	9 × 10 <sup>-4</sup>
23	250 A	274	1000	10	0-1000 <sup>(2)</sup>	12.7 ± 3.8	1.3	1.3 × 10 <sup>-3</sup>
24								
24-1	1-20	22	500	30	111	7.9 ± 2.4	0.3	2 × 10 <sup>-3</sup>
24-2	2-20	20	500	30	94	5.5 ± 1.6	0.2	2 × 10 <sup>-3</sup>
24-3	3-20	23	500	30	140	4.5 ± 1.3	0.2	1 × 10 <sup>-3</sup>
24-4	1-20 a	23	500	30	133	10.9 ± 3.3	0.4	3 × 10 <sup>-3</sup>
25								
25-1	1-63.5	66	500	30	1100	75.6 ± 23	2.5	2 × 10 <sup>-3</sup>
25-2	2-63.5	61	500	30	1000	78.7 ± 24	2.6	3 × 10 <sup>-3</sup>
25-3	3-63.5	65	500	30	1200	87.3 ± 26	2.9	2 × 10 <sup>-3</sup>
26	150 B	176	500	30	5600	720 ± 330	24	4 × 10 <sup>-3</sup>
27								
27-1	1-63.5	66	500	10	1100	4 ± 1.2	0.4	4 × 10 <sup>-4</sup>
27-2	2-63.5	61	500	30	1000	6.1 ± 1.8	0.2	2 × 10 <sup>-4</sup>
27-3	3-63.5	65	500	60	1200	10.8 ± 3.2	0.2	2 × 10 <sup>-4</sup>
28	200 B	231	1000	10	20000	2690 ± 1100	269	1 × 10 <sup>-2</sup>

TABLE A.1. (Continued)

APLA	ORIFICE OR CAPILLARY DESIGNATION	MEASURED DIAMETER $\mu\text{m}$	CHAMBER PRESSURE psig	TIME min	AIR FLOW cc/min	TRANSMITTED <sup>(4)</sup> DUO, $\mu\text{g}$	DUO, $\mu\text{g}/\text{min}$	DUO, $\mu\text{g}/\text{cc}$
29								
29-1	1-20	22	1000	10	275	$36.5 \pm 11$	4.0	$1 \times 10^{-2}$
29-2	1-20 a	23	1000	10	275	$9.2 \pm 2.8$	0.9	$3 \times 10^{-3}$
29-3	2-20	20	1000	10	210	$20.9 \pm 6.3$	2.1	$1 \times 10^{-2}$
29-4	3-20	23	1000	10	290	$6.0 \pm 1.8$	0.6	$2 \times 10^{-3}$
30								
30-1	1-20	22	1000	10	275	$6.8 \pm 2$	0.7	$3 \times 10^{-3}$
30-2	1-20 a	23	1000	20	275	$3.3 \pm 1.2$	0.2	$7 \times 10^{-4}$
30-3	2-20	20	1000	30	210	$13.2 \pm 3.9$	0.4	$2 \times 10^{-3}$
30-4	3-20	23	1000	60	290	$5.8 \pm 1.7$	0.1	$3 \times 10^{-4}$
31								
31-1	1-20	22	30	10	10	$7.3 \pm 2.2$	0.73	$7 \times 10^{-2}$
31-2	1-20a	23	30	30	10.3	$8.5 \pm 2.5$	0.28	$3 \times 10^{-2}$
31-3	2-20	20	30	60	9.5	$10.9 \pm 3.3$	0.18	$2 \times 10^{-2}$
31-4	3-20	23	30	120	14.5	$9.8 \pm 2.9$	0.08	$6 \times 10^{-3}$
32	1-36	43	30	60	20	$14.2 \pm 4.3$	0.24	$1 \times 10^{-2}$
33								
33-1	1-20	22	30	60	10	$< 1.6 \pm 1.6$	$< 0.03$	$< 3 \times 10^{-3}$
33-2	1-20a	23	30	60	10.3	$2.4 \pm 1.6$	0.04	$4 \times 10^{-3}$
33-3	2-20	20	30	60	9.5	$< 1.6 \pm 1.6$	$< 0.03$	$< 3 \times 10^{-3}$
33-4	3-20	23	30	60	14.5	$6.0 \pm 1.8$	0.1	$7 \times 10^{-3}$
34	250 A	274	30	60	1180 (5)	$2.4 \pm 1.6$	0.04	$3 \times 10^{-5}$
35								
35-1	3-30	33	30	10	28	$3.8 \pm 1.6$	0.4	$1 \times 10^{-2}$
35-2	1-36	43	30	30	22	$2.9 \pm 1.6$	0.1	$5 \times 10^{-3}$

(5) Though flow was achieved wire could not be run through, appeared plugged after run

TABLE A.1. (Continued)

APLA	ORIFICE OR CAPILLARY DESIGNATION	MEASURED DIAMETER $\mu\text{m}$	CHAMBER PRESSURE psig	TIME min	AIR FLOW cc/min	TRANSMITTED <sup>(4)</sup> DUO, $\mu\text{g}$	DUO, $\mu\text{g}/\text{min}$	DUO, $\mu\text{g}/\text{cc}$
35 (CONT'D)								
35-3	2-36	33	30	60	24	$2.6 \pm 1.6$	0.04	$2 \times 10^{-3}$
35-4	3-36	38	30	120	39	$20.1 \pm 6$	0.2	$5 \times 10^{-3}$
36	1-20	22	30	60	10	$4.1 \pm 1.6$	0.07	$7 \times 10^{-3}$
37	250 B	274	30	60	520	$5.7 \pm 1.8$	0.1	$2 \times 10^{-4}$
38								
38-1	3-30	33	30	60	28	$3.1 \pm 1.6$	0.05	$2 \times 10^{-3}$
38-2	1-36	43	30	60	22	$2.0 \pm 1.6$	0.03	$1 \times 10^{-3}$
38-3	2-36	33	30	60	24	$17.5 \pm 5.3$	0.3	$1 \times 10^{-2}$
38-4	3-36	38	30	60	39	$43.7 \pm 1.3$	0.7	$2 \times 10^{-2}$
39								
39-1	1-63.5	66	1000 $\pm$ 0	1200	--	$303 \pm 91$	0.3	--
39-2	2-63.5	61	1000 $\pm$ 0	1200	--	$49.8 \pm .5$	0.04	--
39-3	3-63.5	65	1000 $\pm$ 0	1200	--	$326 \pm 98$	0.3	--
40								
40-1	1-63.5	66	1000	10	2300	$43.2 \pm 13$	4.3	$2 \times 10^{-3}$
40-2	2-63.5	61	1000	10	860 (2)	$20.3 \pm 6.1$	2.0	$2 \times 10^{-3}$
40-3	3-63.5	65	1000	10	1760 (2)	$76.8 \pm 23$	7.7	$4 \times 10^{-3}$
41	150 S	182	1000	10	14600	$212 \pm 64$	21.2	$1 \times 10^{-3}$
42								
42-1	1-63.5	66	1000	10	200 (2)	$17.8 \pm 5.3$	2	$1 \times 10^{-2}$
42-2	2-63.5	61	1000	30	1450 (2)	$61.9 \pm 19$	2	$1 \times 10^{-3}$
42-3	3-63.5	65	1000	60	2400	$167 \pm 50$	3	$1 \times 10^{-3}$
43	150 S	182	500	30	5600	$290 \pm 87$	9.7	$2 \times 10^{-3}$
44	150 B	176	30	60	520	$12.4 \pm 3.7$	0.2	$4 \times 10^{-4}$

TABLE A.1. (Continued)

APLA	ORIFICE OR CAPILLARY DESIGNATION	MEASURED DIAMETER $\mu\text{m}$	CHAMBER PRESSURE psig	TIME min	AIR FLOW cc/min	TRANSMITTED <sup>(4)</sup> DUO, $\mu\text{g}$	DUO, $\mu\text{g}/\text{min}$	DUO, $\mu\text{g}/\text{cc}$
45	150 S	182	30	60	640	$18.0 \pm 5.4$	0.3	$5 \times 10^{-4}$
46								
46-1	3-30	33	1000	10	695	$11.5 \pm 3.5$	1.2	$2 \times 10^{-3}$
46-2	1-36	43	1000	20	840	$97.3 \pm 29$	4.9	$6 \times 10^{-3}$
46-3	2-36	33	1000	30	580	$10.7 \pm 3.2$	0.4	$6 \times 10^{-4}$
46-4	3-36	38	1000	60	920	$32.6 \pm 9.8$	0.5	$6 \times 10^{-4}$
47								
47-1	3-30	33	1000	10	695	$33.6 \pm 10$	3.4	$5 \times 10^{-3}$
47-2	1-36	43	1000	10	840	$20.5 \pm 6.2$	2.0	$2 \times 10^{-3}$
47-3	2-36	33	1000	10	580	$1.35 \times 10^3 \pm 510^{(6)}$		
47-4	3-36	38	1000	10	920	$6.3 \pm 1.9$	0.6	$7 \times 10^{-4}$
48								
48-1	1-63.5	66	30	30	80	$6.19 \pm 1.9$	0.2	$3 \times 10^{-3}$
48-2	2-63.5	61	30	60	88	$15.3 \pm 4.6$	0.3	$3 \times 10^{-4}$
48-3	3-63.5	65	30	120	109	$11.0 \pm 3.3$	0.09	$9 \times 10^{-4}$
49								
49-1	1-63.5	66	30	57	80	$12.2 \pm 3.7$	0.2	$3 \times 10^{-3}$
49-2	2-63.5	61	30	57	88 (7)	$4.3 \pm 1.7$	0.08	$9 \times 10^{-4}$
49-3	3-63.5	65	30	57	109	$25 \pm 7.5$	0.4	$4 \times 10^{-3}$
50	100 B	99	1000	10	3140	$87.8 \pm 26$	8.8	$3 \times 10^{-3}$
51								
51-1	1-110	100	1000	15	7100	$259 \pm 78$	17.3	$2 \times 10^{-3}$
51-2	2-110	125	1000	30	500 (2)	$401 \pm 120$	13.4	$2 \times 10^{-3}$
51-3	3-110	100	1000	40	5800	$250 \pm 75$	6.3	$1 \times 10^{-3}$

(6) This orifice inadequately sealed, leaked DUO (results omitted)

(7) Lost flow after 30 min

TABLE A.1. (Continued)

APLA	ORIFICE OR CAPILLARY DESIGNATION	MEASURED DIAMETER $\mu\text{m}$	CHAMBER PRESSURE psig	TIME, min	AIRFLOW cc/min	TRANSMITTED <sup>(4)</sup>		
						DUO, $\mu\text{g}$	DUO, $\mu\text{g}/\text{min}$	DUO, $\mu\text{g}/\text{cc}$
52	100B	99	1000	10	400	6.2±1.9	0.6	2x10 <sup>-3</sup>
53								
53-1	1-110	100	1000	10	7100	350±110	35	5x10 <sup>-3</sup>
53-2	2-110	125	1000	10	2200 <sup>(2)</sup>	211±63	21.1	1x10 <sup>-2</sup>
53-3	3-110	100	1000	10	5800	187±56	187	3x10 <sup>-3</sup>
54	100B	99	500	30	195 <sup>(2)</sup>	4.07±1.7	0.1	7x10 <sup>-4</sup>
55	250S	276	1000	10	38800	9.21x10 <sup>3</sup> ±360	921	2x10 <sup>-2</sup>
56								
56-1	1-110	100	500	10	3060	23.3±7	2.3	8x10 <sup>-4</sup>
56-2	2-110	125	500	30	4500	119±36	4.0	9x10 <sup>-4</sup>
56-3	3-110	100	500	60	3100	55.3±17	0.9	3x10 <sup>-4</sup>
57	1-50	48	500	30	195	25±7.5	0.8	4x10 <sup>-3</sup>
58	250S	276	500	30	13300	675±200	22.5	2x10 <sup>-3</sup>
59								
59-1	1-110	100	500	30	3060	4.3±1.8	0.1	5x10 <sup>-5</sup>
59-2	2-110	125	500	30	4500	112±34	3.7	8x10 <sup>-4</sup>
59-3	3-110	100	500	30	3100	59±18	2.0	6x10 <sup>-4</sup>
60	200S	228	30	60	4800	13±3.9	0.2	5x10 <sup>-5</sup>
61	1-50	48	30	60	4	8.75±2.6	0.2	4x10 <sup>-2</sup>
62	100S	97	1000	10	4800	22.3±6.7	2.2	5x10 <sup>-4</sup>
63	200S	228	1000	10	25300	3.95±1.8	0.4	2x10 <sup>-5</sup>
64								
64-1	1-110	100	30	30	245	52.2±16	1.7	7x10 <sup>-3</sup>
64-2	2-110	125	30	60	365	52.4±16	0.9	2x10 <sup>-3</sup>
64-3	3-110	100	30	120	245	18.4±5.5	0.2	6x10 <sup>-4</sup>
65	2-75S	78	1000	10	2100	33.7±10	3.4	2x10 <sup>-3</sup>

TABLE A.1. (Continued)

APLA	ORIFICE OR CAPILLARY DESIGNATION	MEASURED DIAMETER $\mu\text{m}$	CHAMBER PRESSURE psig	TIME, min	AIRFLOW cc/min	TRANSMITTED <sup>(4)</sup>		
						DUO, $\mu\text{g}$	DUO, $\mu\text{g}/\text{min}$	DUO, $\mu\text{g}/\text{cc}$
66								
66-1	1-100	100	30	60	245	3.59±1.8	0.1	2x10 <sup>-4</sup>
66-2	2-110	125	30	60	365	36.0±11	0.6	2x10 <sup>-3</sup>
66-3	3-110	100	30	60	245	44.2±13	0.7	3x10 <sup>-3</sup>
67	1-50	48	1000	10	400	143±43	14.3	4x10 <sup>-2</sup>
68								
68-1	1-200	200	1000	10	23600 <sup>(9)</sup>			
68-2	2-200	200	1000	10	22000	2120±820	212	1x10 <sup>-2</sup>
68-3	3-200	200	1000	10	22000	2350±900	235	1x10 <sup>-2</sup>
69	200S	228	500	30	8000	3340±130	111	1x10
70	100B	99	500	30	1560	3.8±1.8	0.1	8x10 <sup>-5</sup>
71	250S	276	30	60	1650	217±65	3.6	2x10 <sup>-3</sup>
72								
72-1	1-200	200	500	10	12200	2380±910	238	2x10 <sup>-2</sup>
72-2	2-200	310 <sup>(10)</sup>	500	30	11200	1960±760	65	6x10 <sup>-3</sup>
72-3	3-200	200	500	60	11000			
73	100B	99	30	30	130	4.96±1.8	0.2	1x10 <sup>-3</sup>
74								
74-1	1-200	200	500	30	12200	3480±1300	116	1x10 <sup>-2</sup>
74-2	2-200	310 <sup>(11)</sup>	500	30	11200	2420±930	81	7x10 <sup>-3</sup>
74-3	3-200	200	500	30	11000			
75	1-110	100	100	30	640	19.3±5.8	0.6	1x10 <sup>-3</sup>
76								
76-1	1-200	200	1000	10	4000 <sup>(2)</sup>	1690±660	169	4x10 <sup>-2</sup>
76-2	2-200	310 <sup>(11)</sup>	1000	30	22000	4.31x10 <sup>4</sup> ±1.6x10 <sup>4</sup>	1436	7x10 <sup>-2</sup>
76-3	3-200	200	1000	60	4000-7000 <sup>(2)</sup>	7460±2800	124	2x10 <sup>-2</sup>

(8) PLUGGED IMMEDIATELY

(9) PLUGGED AFTER RUN; ENLARGED TO 310 $\mu\text{m}$  SQUARE DURING CLEANING(10) 310 $\mu\text{m}$ , FLOW NOT CORRECT, RESULT NOT USED

TABLE A.1. (Continued)

APLA	ORIFICE OR CAPILLARY DESIGNATION	MEASURED DIAMETER $\mu\text{m}$	CHAMBER PRESSURE psig	TIME, min	AIRFLOW cc/min	TRANSMITTED <sup>(4)</sup>		
						DUO, $\mu\text{g}$	DUO, $\mu\text{g}/\text{min}$	DUO, $\mu\text{g}/\text{cc}$
77	2-63.5	61	100	30	225	11.7±3.5	0.4	$2 \times 10^{-3}$
78	250S	276	100	30	4500	188±56	6	$1 \times 10^{-3}$
79								
79-1	1-200	200	30	60	1000	323±97	5	$5 \times 10^{-3}$
79-2	2-200(310)		30	60	960	9.11±2.7	0.2	$2 \times 10^{-4}$
79-3	3-200	200	30	60	1000	108±32	1.8	$2 \times 10^{-3}$
80	1-20	22	100	30	25	6.7±2	0.2	$9 \times 10^{-3}$
81	1-36	43	100	30	77	4.74±1.8	0.2	$2 \times 10^{-3}$
82								
82-1	1-200	200	30	30	1000	62.1±13	2.1	$2 \times 10^{-3}$
82-2	2-200	200	30	60	960			
82-3	3-200	200	30	90	1000	38.4±9.4	0.4	$4 \times 10^{-4}$
83	250B	274	100	30	3463	0.67±0.27	0.02	$6 \times 10^{-6}$
84	1-50A	48	100	30	1150	0.877±0.27	0.03	$2.6 \times 10^{-5}$
85	1-200	200	100	30	2300	80.8±15	2.7	$1 \times 10^{-3}$
86	150B	176	100	30	1150	0.462±0.27	0.02	$1.3 \times 10^{-5}$
87	200S	228	100	30	2430	1.04±0.31	0.03	$1.4 \times 10^{-5}$
88	150S	182	100	30	1640	320±43	10.7	$7 \times 10^{-3}$
89	1-50A	48	100	30	45	0.655±0.27	0.02	$4.9 \times 10^{-4}$
90								
90-1	250B	231	500	30	16080	2.00±0.60	0.07	$4 \times 10^{-6}$
90-2	250S	276	500	30	20000	11500±1400	383	$2 \times 10^{-2}$
91								
91-1	1-110	100	100	10	640	7.21±2.2	0.72	$1.1 \times 10^{-3}$
91-2	2-110	125	100	30	900	20.7±6.2	0.69	$7.7 \times 10^{-4}$
91-3	3-110	100	100	60	638	15.0±4.5	0.25	$3.9 \times 10^{-4}$

TABLE A.1. (Continued)

APLA	ORIFICE OR CAPILLARY DESIGNATION	MEASURED DIAMETER $\mu\text{m}$	CHAMBER PRESSURE psig	TIME, min	AIRFLOW cc/min	TRANSMITTED <sup>(4)</sup>		
						DUO, $\mu\text{g}$	DUO, $\mu\text{g}/\text{min}$	DUO, $\mu\text{g}/\text{cc}$
92								
92-1	1-110	100	100	30	640	8.71±2.6	0.29	4.5x10 <sup>-4</sup>
92-2	2-110	125	100	30	900	0.656±0.27	0.02	2.2x10 <sup>-5</sup>
92-3	3-110	100	100	30	638	20.6±6.2	0.69	1.1x10 <sup>-3</sup>
93								
93-1	1-63.5	66	100	10	255	0.788±0.27	0.08	3x10 <sup>-4</sup>
93-2	2-63.5	61	100	30	225	0.696±0.27	0.02	1x10 <sup>-4</sup>
93-3	3-63.5	65	100	60	265	1.75±0.53	0.03	1x10 <sup>-4</sup>
94								
94-1	1-63.5	66	100	30	255	1.03±0.31	0.03	1.3x10 <sup>-4</sup>
94-2	2-63.5	61	100	30	225	0.361±0.27	0.12	5.3x10 <sup>-4</sup>
94-3	3-63.5	65	100	30	265	2.50±0.75	0.08	3.0x10 <sup>-4</sup>
95								
95-1	250B	274	30	60	1200	8.55±2.6	0.14	1.2x10 <sup>-4</sup>
95-2	250S	274	30	60	1650	0.652±0.27	0.01	6.6x10 <sup>-6</sup>
96								
96-1	150B	176	30	60	520	0.883±0.27	0.015	2.8x10 <sup>-5</sup>
96-2	150S	182	30	60	640	9.65±2.9	0.16	2.5x10 <sup>-4</sup>
96-3	3-200	200	30	60	1000	16.7±5.0	0.28	2.8x10 <sup>-4</sup>
97								
97-1	250B	274	1000	10	31880 <sup>(2)</sup>	3.02±0.9	0.3	9.5x10 <sup>-6</sup>
97-2	250S	276	1000	10	38800	15800±2100	1580	4x10 <sup>-2</sup>
98								
98-1	150B	176	500	30	5600	959±140	32	6x10 <sup>-3</sup>
98-2	150S	182	500	30	7400	267±37	8.9	1x10 <sup>-3</sup>
98-3	3-200	200	500	30	11000	942±140	31	3x10 <sup>-3</sup>



TABLE A.1. (Continued)

APLA	ORIFICE OR CAPILLARY DESIGNATION	MEASURED DIAMETER $\mu\text{m}$	CHAMBER PRESSURE psig	TIME, min	AIRFLOW cc/min	TRANSMITTED <sup>(4)</sup>		DUO, $\mu\text{g}/\text{cc}$
						DUO, $\mu\text{g}$	DUO, $\mu\text{g}/\text{min}$	
100	1-110	100	1000 PRESSURE DECAY			449±58		
101								
101-1	1-20	22	100	30	25	8.23±2.5	0.27	$1 \times 10^{-2}$
101-2	1-20a	23	100	30	29	3.02±0.9	0.10	$3.5 \times 10^{-3}$
101-3	2-20	20	100	30	22	1.45±0.43	0.05	$2.2 \times 10^{-3}$
101-4	3-20	23	100	30	32	2.39±0.72	0.08	$2.5 \times 10^{-3}$
102	2-110	125	1000 PRESSURE DECAY					
103								
103-1	1-20	22	100	10	25	3.13±0.94	0.31	$1.3 \times 10^{-2}$
103-2	1-20a	23	100	30	29	3.33±0.99	0.11	$3.8 \times 10^{-3}$
103-3	2-20	20	100	60	22	1.26±0.38	0.02	$9.5 \times 10^{-4}$
103-4	3-20	23	100	120	32	1.52±0.45	0.01	$4 \times 10^{-4}$
104								
104-1	1-200	200	1000	10	18800	5690±960	569	$3 \times 10^{-2}$
104-2	3-200	200	1000	10	22300	1880±250	188	$8 \times 10^{-3}$
105	1-200	200	1000 PRESSURE DECAY			2670±340		
106								
106-1	3-30	33	100	30	74	3.26±0.98	0.11	$1.5 \times 10^{-3}$
106-2	1-36	43	100	30	77	3.04±0.91	0.10	$1.3 \times 10^{-3}$
106-3	2-36	33	100	30	64	4.62±1.4	0.15	$2.4 \times 10^{-3}$
106-4	3-36	38	100	30	106	4.51±1.4	0.15	$1.4 \times 10^{-3}$
107	3-20	23	1000	10	220*	3.18±0.95	0.32	$1.4 \times 10^{-3}$
108	3-36	38	1000	10	998*	3.76±1.1	0.38	$3.8 \times 10^{-4}$
109	3-20	23	1000	10	30*	4.02±1.2	0.40	$1.3 \times 10^{-2}$
110	3-36	38	1000	10	57*	6.85±2.0	0.68	$1.2 \times 10^{-2}$

\* MEASURED ONLY

TABLE A.1. (Continued)

APLA	ORIFICE OR CAPILLARY DESIGNATION	MEASURED DIAMETER $\mu\text{m}$	CHAMBER PRESSURE psig	TIME, min	AIRFLOW cc/min	TRANSMITTED <sup>(4)</sup> DUO, $\mu\text{g}$	DUO, $\mu\text{g}/\text{min}$	DUO, $\mu\text{g}/\text{cc}$
111	3-63.5	65	1000	10	660*	52.7±16	5.27	8.0x10 <sup>-3</sup>
112	3-110	100	1000	10	3650*	98.8±17	9.9	3x10 <sup>-3</sup>
113	3-200	200	1000	10	18500*	5110±880	511	3x10 <sup>-2</sup>
114	3-20	23	500	30	35*	2.88±0.87	0.10	2.7x10 <sup>-3</sup>
115	3-36	38	500	30	270*	4.09±1.2	0.14	5x10 <sup>-4</sup>
116	3-63.5	65	500	30	320*	8.3±2.5	0.28	8.6x10 <sup>-4</sup>
117	3-110	100	500	30	2250*	24.2±7.3	0.80	3.6x10 <sup>-4</sup>
118	3-200	200	500	30	10800*	535±68	17.8	2x10 <sup>-3</sup>
119	3-20	23	100	30	42.5*	1.13±0.34	0.04	8.9x10 <sup>-4</sup>
120	3-36	38	100	30	28*	2.77±0.83	0.09	3.3x10 <sup>-3</sup>
121	3-63.5	65	100	30	195*	8.09±2.4	0.27	1.4x10 <sup>-3</sup>
122	3-110	100	100	30	415*	14.0±4.1	0.47	1.1x10 <sup>-3</sup>
123	3-200	200	100	30	2260*	109.0±33	3.60	1.6x10 <sup>-3</sup>
124	1-36	43	1000 PRESSURE DECAY			1.45±0.43		
125								
126	3-36	38	30	30	28*	3.52±1.1	0.12	4.2x10 <sup>-3</sup>
127	3-63.5	65	30	30	98*	2.22±0.67	0.07	7.6x10 <sup>-4</sup>
128	3-110	100	30	30	120*	29.8±8.9	0.99	8.3x10 <sup>-3</sup>
129	3-200	200	30	30	860*	167±25	5.6	6x10 <sup>-3</sup>
130	3-20	23	1000	10	15.2*	2.78±0.83	0.28	1.8x10 <sup>-2</sup>
131	3-36	38	1000	10	385*	6.29±0.19	0.63	1.6x10 <sup>-3</sup>
132	3-63.5	61	1000	10	690*	34.6±10	3.46	5.0x10 <sup>-3</sup>
133	3-110	100	1000	10	335*	113±19	11.3	3x10 <sup>-2</sup>
134	3-200	200	1000	10	19200*	1570±210	157	8x10 <sup>-3</sup>
135	3-30	33	1000 PRESSURE DECAY			1.83±0.55		

\* MEASURED ONLY

TABLE A.1. (Continued)

APLA	ORIFICE OR CAPILLARY DESIGNATION	MEASURED DIAMETER $\mu\text{m}$	CHAMBER PRESSURE psig	TIME, min	AIRFLOW cc/min	TRANSMITTED <sup>(4)</sup>		
						DUO, $\mu\text{g}$	DUO, $\mu\text{g}/\text{min}$	DUO, $\mu\text{g}/\text{cc}$
136	3-20	23	500	STOPPED	PLUGGED	1.44±0.43		
137	3-36	38	500	30	230 *	6.56±2	0.22	9.5x10 <sup>-4</sup>
138	3-63.5	65	500	30	1020 *	14.3±4.3	0.48	4.7x10 <sup>-4</sup>
139	3-110	100	500	30	680 *	62.9±19	2.1	3.1x10 <sup>-3</sup>
140	3-200	200	500	30	10300 *	991±120	33	3x10 <sup>-3</sup>
141	3-20	20	100	STOPPED	PLUGGED	1.45±0.44		
142	3-36	33	100	30	19 *	1.92±0.58	0.06	3.4x10 <sup>-3</sup>
143	3-63.5	65	100	30	165 *	3.27±0.98	0.11	6.6x10 <sup>-4</sup>
144	3-110	100	100	30	370 *	20.3±6.1	0.68	1.8x10 <sup>-3</sup>
145	3-200	200	100	30	2300 *	89.2±27	3.0	1.3x10 <sup>-3</sup>
146	1-200	200	1000 PRESSURE DECAY			6850±820		
148	3-36	38	30	30	35 *	0.861±0.27	0.03	8.2x10 <sup>-4</sup>
149	3-110	100	30	30	177 *	2.91±0.87	0.10	5.5x10 <sup>-4</sup>
150	3-63.5	65	30	30	98 *	4.85±1.5	0.16	1.6x10 <sup>-3</sup>
151	3-200	200	30	30	870 *	9.18±2.8	0.31	3.5x10 <sup>-4</sup>
152	1-36	43	1000 PRESSURE DECAY			7.88±2.4		

\* MEASURED ONLY

TABLE A.1. (Continued)

APLA	ORIFICE OR CAPILLARY DESIGNATION	MEASURED DIAMETER $\mu\text{m}$	CHAMBER PRESSURE psig	TIME, min	AIRFLOW cc/min	TRANSMITTED <sup>(4)</sup> DUO, $\mu\text{g}$	DUO, $\mu\text{g}/\text{min}$	DUO, $\mu\text{g}/\text{cc}$
164	1-200	200	30	0		180±27		
165	1-110	100	30	0		11.1±3.3		
166	3-20	23	500	0		452±58		
167	1-20 <del>a</del>	23	PRESSURE DECAY			3.37±1.0		
168	1-20	22	1000	0		1.45±0.44		
169	1-36	43	1000	0		2.09±0.63		
170	1-63.5	66	1000	0		10.9±3.3		
171	3-110	100	1000	0		218±31		
172	3-200	200	1000	0		4740±580		
173	1-200	200	500	0		1680±220		
174	3-110	100	500	0		40.6±12		
175	1-63.5	66	500	0		9.53±2.9		
176	1-36	43	500	0		5.81±1.7		
177	1-20	22	100	0		1.81±0.54		
178	1-20 <del>a</del>	23	30	0		1.85±0.56		
179	1-110	100	100	0		26.5±8.0		
180	3-200	200	100	0		24.9±7.5		
181	3-63.5	65	100	0		6.92±2.1		
182	1-36	43	100	0		3.58±1.1		
183	1-63.5	66	30	0		5.27±1.6		
184	3-36	38	30	0		7.17±2.2		
185	1-200	226	1000	0		4.75x10 <sup>3</sup> +1.1x10 <sup>3</sup>		
186	1-110	111	1000	0		574±140		
187	1-2 <del>a</del>	22	1000	0		4.51±1.4		
188	3-20	20	1000	0		2.14±0.64		
189	1-110	111	500	30	10200	602±140 <sup>(11)</sup>		
190	2-36	20	1000	30	1300	6.85±2.1	0.23	1.6x10 <sup>-4</sup>

(11) LEAK AROUND SEAL

TABLE A.1. (Continued)

APLA	ORIFICE OR CAPILLARY DESIGNATION	MEASURED DIAMETER $\mu\text{m}$	CHAMBER PRESSURE psig	TIME, min	AIRFLOW cc/min	TRANSMITTED <sup>(4)</sup>		
						DUO, $\mu\text{g}$	DUO, $\mu\text{g}/\text{min}$	DUO, $\mu\text{g}/\text{cc}$
191	1-200	226	500	30	13,100	1430±330	47.7	$3.6 \times 10^{-3}$
192	3-110	89	1000	30	12,400	40.2±12	1.34	$1.1 \times 10^{-4}$
193	1-110	111	500	30	2150	124±32	4.1	$1.9 \times 10^{-3}$
194	2-36	32	1000	30	660	8.43±2.5	0.28	$4.3 \times 10^{-4}$
195	1-200	226	500	30	11,400	1260±290	42	$3.7 \times 10^{-3}$
196	3-110	89	1000	30	2200	73.3±21	2.4	$1.1 \times 10^{-3}$
197	1-200	226	30	30	1000	205±51	6.8	$6.8 \times 10^{-3}$
199	3-30	22	500	30	370	3.9±1.2	0.13	$3.5 \times 10^{-4}$
200	3-110	89	500	30	3360	46.7±14	1.56	$4.6 \times 10^{-4}$
201	1-110	111	1000	30	7100	607±140	20.2	$2.8 \times 10^{-3}$
202	3-30	22	1000	30	690	6.61±2.0	0.22	$3.2 \times 10^{-4}$
203	3-30	22	30	30	28	9.21±2.8	0.31	$1.1 \times 10^{-2}$
204	3-200	190	1000	30	22,000	2170±500	72.3	$3.3 \times 10^{-3}$
205	3-200	190	500	30	11,000	696±160	23.2	$2.1 \times 10^{-3}$
206	2-36	32	30	30	24	4.88±1.5	0.16	$6.8 \times 10^{-3}$
207	1-200	226	1000	30	28,000	2830±650	94.3	$3.4 \times 10^{-3}$
208	3-200	190	30	30	940	99±27	3.3	$3.5 \times 10^{-3}$
210	2-36	32	500	30	275	4.49±1.3	0.15	$5.4 \times 10^{-4}$
211	3-110	89	30	30	235	16.5±5.0	0.55	$2.3 \times 10^{-3}$
212	1-200	226	1000	30	25,200	3060±710	102	$4.0 \times 10^{-3}$
213	1-110	111	500	30	3060	103±28	3.4	$3.3 \times 10^{-2}$
214	3-200	190	30	30	1000	30.7±9.2	1.02	$1.0 \times 10^{-3}$

TABLE A.1. (Continued)

APLA	ORIFICE OR CAPILLARY DESIGNATION	MEASURED DIAMETER $\mu\text{m}$	CHAMBER PRESSURE psig	TIME, min	AIRFLOW cc/min	TRANSMITTED <sup>(4)</sup>		
						DUO, $\mu\text{g}$	DUO, $\mu\text{g}/\text{min}$	DUO, $\mu\text{g}/\text{cc}$
215	2-36	32	500	30	285	3.49±1.0	0.12	4.1x10 <sup>-4</sup>
216	3-110	89	500	30	3100	20.4±6.1	0.68	2.2x10 <sup>-4</sup>
218	1-110	111	30	30	245	105±32	3.50	1.4x10 <sup>-2</sup>
219	1-200	226	500	30	12,200	1710±40	57	4.6x10 <sup>-3</sup>
220	2-36	32	1000	30	580	33.2±10	1.11	1.9x10 <sup>-3</sup>
221	3-30	22	30	30	28	2.04±0.6	0.07	2.4x10 <sup>-3</sup>
222	3-200	190	500	30	11,000	822±1.90	27.4	2.5x10 <sup>-3</sup>
223	1-110	111	1000	30	7100	957±230	31.9	4.5x10 <sup>-3</sup>
224	3-30	22	1000	30	695	12.0±3.6	0.4	5.8x10 <sup>-4</sup>
225	1-200	226	30	30	1000	722±170	24.1	2.4x10 <sup>-2</sup>
227	3-200	190	1000	30	2200	1190±280	39.7	1.8x10 <sup>-2</sup>
228	2-36	32	30	30	24	1.93±0.58	0.06	2.7x10 <sup>-3</sup>
229	3-110	89	1000	30	5500	194±49	6.5	1.2x10 <sup>-3</sup>
230	3-30	22	500	30	350	6.82±2	0.23	6.5x10 <sup>-4</sup>
231	3-110	89	30	30	245	20.2±6.1	0.67	2.7x10 <sup>-3</sup>
232	3-200	190	30	0		189±47		
233	3-110	89	1000	0		245±60		
234	3-30	22	30	0		6.81±2.0		
235	2-36	32	500	0		8.18±2.5		
236	1-200	226	1000	0		3690±850		
237	3-200	190	500	0		276±68		

TABLE A.1. (Continued)

APLA	ORIFICE OR CAPILLARY DESIGNATION	MEASURED DIAMETER $\mu\text{m}$	CHAMBER PRESSURE psig	TIME, min	AIRFLOW cc/min	TRANSMITTED <sup>(4)</sup>		
						DUO, $\mu\text{g}$	DUO, $\mu\text{g}/\text{min}$	DUO, $\mu\text{g}/\text{cc}$
238	1-110	111	500	0		96.0±29.0		
239	3-110	89	30	0		10.2±3.1		
240	3-30	22	1000	0		8.91±2.7		
241	3-110	89	1000	0		175±44		
242	3-30	22	30	0		7.42±2.2		
243	3-200	190	500	0		131±34		
244	3-30	22	1000	0		5.79±1.7		
245	2-36	32	500	0		9.69±2.9		
246	3-200	190	30	0		110±30		
247	3-110	89	30	0		6.87±2.1		
248	1-200	226	1000	0		3720±860		
249	1-110	111	500	0		213±53		
250	1-110	111	30	30	245	26.4±7.9	1.0	$4.1 \times 10^{-4}$
251	1-110	111	100	360	640	10.5±3.2	0.03	$4.6 \times 10^{-3}$
252	1-110	111	100	360	640	23.2±7.0	0.06	$1.0 \times 10^{-4}$
253	1-110	111	100	30	870	42.9±13.0	1.43	$1.6 \times 10^{-3}$
254	1-110	111	100	0		49.0±15.0		
255	1-110	111	100	1440	700	305±77	0.21	$3.0 \times 10^{-4}$
256	6-110	111	100	1440	700	103±29	0.07	$1.0 \times 10^{-4}$
261	1-110	111	100	30	795	96.7±27	3.22	$4.1 \times 10^{-3}$
262	6-110	111	100	30	695	30.9±9.3	1.03	$1.5 \times 10^{-3}$
263	1-100	111	100	360	625	107±29	0.03	$4.8 \times 10^{-4}$
264	1-200	226	1000	8*		1890±460		
265	1-110	111	1000	80*		770±190		
266	1-200	226	1000	80*		992±240		
267	1-200	226	1000	80*		861±210		
268	1-110	111	1000	80*		166±44		

\*TO PRESSURIZE TO 1000 psig

TABLE A.2. Depleted Uranium Dioxide Transmission for Leak Paths Under the Static Powder Level

UPL	ORIFICE OR CAPILLARY DESIGNATION	MEASURED DIAMETER, $\mu\text{m}$	CHAMBER PRESSURE psig	AGITATION	TIME, min	AIR FLOW cc/min	TRANSMITTED <sup>(3)</sup>	DUO, $\mu\text{g}/\text{min}$	DUO, $\mu\text{g}/\text{cc}$
							DUO, $\mu\text{g}$		
1	2-200	200	1000	NO	5	12200-21000	$3.54 \times 10^3 \pm 1.3 \times 10^3$	(1)	(1)
2	2-200	200	1000	NO	5	13800	$1.61 \times 10^3 \pm 5.9 \times 10^2$	$3.2 \times 10^2$	$2 \times 10^{-2}$
3	2-200	200	1000	YES	5	6200	$4.89 \times 10^3 \pm 1.7 \times 10^3$	$9.8 \times 10^2$	$2 \times 10^{-1}$
4	2-200	200	5	NO	60	16.6	$6.96 \pm 2.1$	0.1	$7 \times 10^{-3}$
5	2-200	200	5	YES	60	18.2	$4.05 \pm 1.2$	0.1	$4 \times 10^{-3}$
6	2-110	125	1000	NO	20	4600	$118 \pm 35$	5.9	$1 \times 10^{-3}$
7	2-110	125	1000	YES	20	8000	$133 \pm 40$	6.7	$8 \times 10^{-4}$
8	2-110	125	15	YES	60	76	$37.2 \pm 11$	0.6	$8 \times 10^{-3}$
9	2-110	125	15	NO	60	18	$25.2 \pm 7.5$	0.4	$2 \times 10^{-2}$
10	2-63.5	61	1000	NO	20	1900	$58.9 \pm 18$	2.9	$2 \times 10^{-3}$
11	2-63.5	61	1000	YES	20	2000	$111 \pm 33$	5.6	$3 \times 10^{-3}$
12	2-63.5	61	15	NO	60	18	$51.5 \pm 1.5$	1.0	$5 \times 10^{-2}$
13	2-63.5	61	15	YES	60	16	$17.4 \pm 5$	0.3	$2 \times 10^{-2}$
14	2-36	33	1000	NO	20	21	$14.8 \pm 4$	0.7	$2 \times 10^{-2}$
15	2-36	33	1000	YES	20	26	$72.5 \pm 22$	3.6	$1 \times 10^{-2}$
16	2-36	33	15	NO	120	0.5	$4.5 \pm 1.8$	0.04	$1 \times 10^{-1}$
17	2-36	33	15	YES	120	1.1	$12.6 \pm 3.8$	0.1	$9 \times 10^{-2}$
18	2-20	20	1000	NO	20	30	$82.4 \pm 25$	4.0	$1 \times 10^{-1}$
19	2-20	20	1000	YES	20	61	$11.2 \pm 3.4$	0.6	$1 \times 10^{-2}$
20	2-20	20	15	YES	120	ND <sup>(2)</sup>	$21.2 \pm 6$	0.2	
21	2-20	20	15	NO	120	ND	$13.6 \pm 4$	0.1	
22	2-200	200	500	NO	20	6500	$812 \pm 220$	40.6	$6 \times 10^{-3}$
23	2-200	200	500	YES	20	5750	$1960 \pm 330$	98.0	$2 \times 10^{-2}$
24	2-110	125	500	NO	20	3250	$150 \pm 45$	7.5	$2 \times 10^{-3}$

(1) ALMOST ALL DUO EXPELLED IMMEDIATELY

(2) ND, NOT DETECTABLE, LESS THAN 0.2 cc/min

(3) THE  $\pm$  IS THE UNCERTAINTY IN THE URANIUM ANALYSIS AT THE  $2\sigma$  CONFIDENCE LEVEL



TABLE A.2. (Continued)

UPL	ORIFICE OR CAPILLARY DESIGNATION	MEASURED DIAMETER, $\mu\text{m}$	CHAMBER PRESSURE psig	AGITATION	TIME, min	AIR FLOW cc/min	TRANSMITTED <sup>(3)</sup> DUO, $\mu\text{g}$	DUO, $\mu\text{g}/\text{min}$	DUO, $\mu\text{g}/\text{cc}$
25	2-110	125	500	YES	20	2550	86.3 $\pm$ 26	4.3	2 $\times$ 10 <sup>-3</sup>
26	2-63.5	61	500	NO	30	470	71.8 $\pm$ 22	2.4	5 $\times$ 10 <sup>-3</sup>
27	2-63.5	61	500	YES	30	275	37.0 $\pm$ 11	1.2	4 $\times$ 10 <sup>-3</sup>
28	2-36	33	500	NO	60	225	20.4 $\pm$ 6	0.3	1 $\times$ 10 <sup>-3</sup>
29	2-36	33	500	YES	60	75	36.1 $\pm$ 11	0.6	8 $\times$ 10 <sup>-3</sup>
30	2-20	20	500	NO	60	14	15.0 $\pm$ 5	0.3	6 $\times$ 10 <sup>-3</sup>
31	2-20	20	500	YES	60	0.75	13.0 $\pm$ 4	0.2	3 $\times$ 10 <sup>-1</sup>
32	250 B	274	1000	NO	5	32500	379 $\pm$ 110	75.8	2 $\times$ 10 <sup>-3</sup>
33	250 B	274	1000	YES	10	32000	2830 $\pm$ 400	283	9 $\times$ 10 <sup>-3</sup>
34	150 B	176	1000	NO	5	9600	1270 $\pm$ 220	254	3 $\times$ 10 <sup>-2</sup>
35	150 B	176	1000	YES	10	7400	498 $\pm$ 120	50	7 $\times$ 10 <sup>-3</sup>
36	250 B	274	500	NO	30	14100	311 $\pm$ 98	10	7 $\times$ 10 <sup>-4</sup>
37	250 B	274	500	YES	30	11500	585 $\pm$ 140	20	2 $\times$ 10 <sup>-3</sup>
38	150 B	176	500	NO	30	3950	374 $\pm$ 100	12	3 $\times$ 10 <sup>-3</sup>
39	150 B	176	500	YES	30	5400	395 $\pm$ 120	13	2 $\times$ 10 <sup>-3</sup>
40	250 B	274	15	YES	60	410	1950 $\pm$ 300	33	8 $\times$ 10 <sup>-2</sup>
41	250 B	274	15	NO	60	28	78.3 $\pm$ 23	1.3	4 $\times$ 10 <sup>-2</sup>
42	150 B	176	15	YES	60	29	122 $\pm$ 37	2	7 $\times$ 10 <sup>-2</sup>
43	150 B	176	15	NO	60	50	129 $\pm$ 39	2	4 $\times$ 10 <sup>-2</sup>
44	2-200	200	100	NO	30	820	740 $\pm$ 400	25	3 $\times$ 10 <sup>-2</sup>
45	2-200	200	100	YES	30	485	578 $\pm$ 320	19	3 $\times$ 10 <sup>-2</sup>
46	2-110	125	100	NO	30	325	464 $\pm$ 140	15	5 $\times$ 10 <sup>-2</sup>
47	2-110	125	100	YES	30	280	120 $\pm$ 36	4	1 $\times$ 10 <sup>-2</sup>
48	2-63.5	61	100	NO	30	26.6	68.4 $\pm$ 21	2.3	9 $\times$ 10 <sup>-2</sup>

TABLE A.2. (Continued)

UPL	ORIFICE OR CAPILLARY DESIGNATION	MEASURED DIAMETER, $\mu\text{m}$	CHAMBER PRESSURE psig	AGITATION	TIME, min	AIR FLOW cc/min	TRANSMITTED <sup>(3)</sup> DUO, $\mu\text{g}$	DUO, $\mu\text{g}/\text{min}$	DUO, $\mu\text{g}/\text{cc}$
49	2-63.5	61	100	YES	30	66.4	190 ± 57	6.3	0.1
50	2-36	33	100	NO	30	6.8	139 ± 42	4.6	0.7
51	2-36	33	100	YES	30	15	69 ± 21	2.3	0.2
52	2-20	20	100	NO	30	ND	97.4 ± 29	3.2	
53	2-20	20	100	YES	30	ND	59.2 ± 18	2.0	
54	250 B	274	100	NO	30	1550	1160 ± 600	38.7	$3 \times 10^{-2}$
55	250 B	274	100	YES	30	2780	338 ± 100	11.3	$4 \times 10^{-3}$
56	150 B	176	100	NO	30	ND	94 ± 28	3	
57	150 B	176	100	YES	30	900	90.6 ± 27	3	$3 \times 10^{-3}$
58	150 S	182	100	NO	30	660	395 ± 12	13.2	$2 \times 10^{-2}$
59	150 S	182	100	YES	30	1180	118 ± 35	3.9	$3 \times 10^{-3}$
60	250 S	276	100	NO	30	660	1330 ± 580	44	$7 \times 10^{-2}$
61	250 S	276	1000	NO	10	19900	$7.92 \times 10^4 \pm 3.4 \times 10^4$	7920	0.4
62	250 S	276	500	NO	10	20200	$1.36 \times 10^4 \pm 5.6 \times 10^3$	1360	$7 \times 10^{-2}$
63	250 S	276	500	YES	10	13900	$1.22 \times 10^4 \pm 5 \times 10^3$	1220	$9 \times 10^{-2}$
64	150 S	182	1000	NO	10	10800	1640 ± 730	169	$2 \times 10^{-2}$
65	150 S	182	1000	YES	10	12200	1330 ± 580	133	$1 \times 10^{-2}$
66	150 S	182	500	NO	30	4200	666 ± 320	22	$5 \times 10^{-3}$
67	150 S	182	500	YES	30	6800	85.2 ± 380	28.4	$4 \times 10^{-3}$
68	150 S	182	15	NO	60	67	85.8 ± 26	1.4	$2 \times 10^{-2}$
69	2-200	200	15	NO	60	90	618 ± 190	10.3	$1 \times 10^{-1}$
70	2-220	200	15	YES	60	210	567 ± 170	9.5	$5 \times 10^{-2}$
71	150 S	182	15	YES	60	28	61.5 ± 18	1	$4 \times 10^{-2}$
72	250 S	276	15	YES	60	96	454 ± 140	7.6	$8 \times 10^{-2}$
73	250 S	276	15	NO	60	210	302 ± 91	5	$2 \times 10^{-2}$
74	250 S	276	100	YES	50	1280	$2.15 \times 10^3 \pm 650$	43	$3 \times 10^{-3}$
75	250 S	276	1000	YES	10	40500	$9.78 \times 10^3 \pm 3.7 \times 10^3$	978	$2 \times 10^{-2}$
76	2-20 <sup>(4)</sup>	20	1000	NO	10	57	22.3 ± 6.7	2.2	$4 \times 10^{-2}$
77	2-20 <sup>(4)</sup>	20	1000	YES	10	27	25.7 ± 7.7	2.6	$1 \times 10^{-1}$
78	150 B <sup>(4)</sup>	176	1000	YES	10	1100	$1.05 \times 10^3 \pm 420$	105	$1 \times 10^{-2}$
79	150 B <sup>(4)</sup>	176	1000	NO	10	11000	$5.46 \times 10^3 \pm 2 \times 10^3$	546	$5 \times 10^{-2}$

(4) RERUNS

TABLE A.2. (Continued)

UPL	ORIFICE OR CAPILLARY DESIGNATION	MEASURED DIAMETER $\mu\text{m}$	CHAMBER PRESSURE psig	AGITATION	TIME, min	AIRFLOW cc/min	TRANSMITTED <sup>(3)</sup>		
							DUO, $\mu\text{g}$	DUO, $\mu\text{g}/\text{min}$	DUO, $\mu\text{g}/\text{cc}$
80	2-200	200	100	NO	30	760	1240±370	41	$5 \times 10^{-2}$
81	2-200	200	100	YES	30	540	709±210	24	$4 \times 10^{-2}$
82	2-36	33	100	NO	30	95	24.6±7.4	0.82	$9 \times 10^{-3}$
83	2-36	33	100	YES	30	9	19.8±5.9	0.66	$7 \times 10^{-3}$
84	2-110	125	100	NO	30	490	236±71	8	$3 \times 10^{-2}$
85	2-110	125	100	YES	30	645	360±87	12	$1.9 \times 10^{-2}$
86	2-20	20	100	NO	30	ND	15.5±4.7	0.5	
87	2-20	20	100	YES	30	19.5	83.7±25	2.79	$1 \times 10^{-1}$
88	3-63.5	61	100	NO	30	145	31.0±9.3	1.03	$7 \times 10^{-3}$
89	150S	182	100	NO	30	750	479±62	16	$2 \times 10^{-2}$
90	250S	276	100	NO	30	1050	1730±230	58	$6 \times 10^{-2}$
91	1-200	200	50	NO	60	495	153±24	3	$5 \times 10^{-3}$
92	250S	276	100	NO	30	775	5370±650	179	$2 \times 10^{-1}$
93	150S	182	100	YES	30	890	443±58	15	$2 \times 10^{-2}$
94	3-63.5	61	100	YES	30	ND	31.5±9.4	1.05	
95	2-110	125	50	NO	60	115	84.0±2.5	1.4	$1.2 \times 10^{-2}$
96	1-200	200	50	YES	60	480	3320±410	55	$1 \times 10^{-1}$
97	2-110	125	50	YES	60	180	70.1±14	1	$6 \times 10^{-3}$
98	250S	276	50	NO	60	360	2440±310	41	$1 \times 10^{-1}$
99	2-20	20	50	NO	60	3.7	26.5±8.0	0.44	$1.2 \times 10^{-1}$
100	250S	276	50	YES	60	365	3150±390	53	$9 \times 10^{-1}$

TABLE A.2. (Continued)

UPL	ORIFICE OR CAPILLARY DESIGNATION	MEASURED DIAMETER $\mu\text{m}$	CHAMBER PRESSURE psig	(5)		AIRFLOW cc/min	TRANSMITTED <sup>(3)</sup>		
				AGITATION	TIME, min		DUO, $\mu\text{g}$	DUO, $\mu\text{g}/\text{min}$	DUO, $\mu\text{g}/\text{cc}$
101	150S	182	50	NO	60	250	113±19	2	$4 \times 10^{-1}$
102	2-110	125	15	NO	60	23.5	17.2±5.2	0.29	$1.2 \times 10^{-2}$
103	2-36	33	50	NO	60	13	43±13	0.72	$5.5 \times 10^{-2}$
104	1-200	200	15	NO	60	99	734±91	12	$1 \times 10^{-1}$
105	250S	276	15	YES	60	155	481±62	8	$5 \times 10^{-2}$
106	2-110	125	1000	NO	10	3800	1760±230	176	$5 \times 10^{-2}$
107	250S	276	1000	NO	10	1000	$3.81 \times 10^4 \pm 4.7 \times 10^3$	3810	3.81
108	?-110	125	1000	NO	10	2930	544±69	54	$2 \times 10^{-2}$
109	2-110	125	500		30	2750	894±210	29.4	$1.1 \times 10^{-2}$
110	2-36	33	1000		10	106	18.5±5.6	1.85	$1.7 \times 10^{-2}$
111	1-200	200	1000		10	13,600	4520±1000	452	$3.3 \times 10^{-2}$
112	3-63.5	61	1000		10	425	80.6±22	8.1	$1.9 \times 10^{-2}$
113	1-20	22	1000		10	ND	4.95±1.5	0.50	$1.2 \times 10^{-3}$
114	1-200	200	500		30	4000	4870±1130	162	$4.1 \times 10^{-2}$
115	3-63.5	61	500		30	435	10.4±3.1	0.35	$8.0 \times 10^{-4}$
116	2-36	33	500		30	NO READING	17.1±5.1	0.57	
117	1-20	22	500		30	NO READING	7.48±2.2	0.25	
118	3-63.5	65	50		60	3.4	5.22±1.6	0.09	$2.6 \times 10^{-2}$
119	1-20	22	50		60	ND	2.83±0.85	0.05	
120	2-36	33	15		60	0.23	6.74±2.0	0.11	0.49
121	3-63.5	65	15		60	3.5	39.7±12.0	0.66	0.19
122	1-20	22	15		60	ND	5.20±1.6	0.09	

(5) AGITATION DISCONTINUED AT RUN 109

TABLE A.2. (Continued)

UPL	ORIFICE OR CAPILLARY DESIGNATION	WT DUO g	CHAMBER PRESSURE psig	TIME, min	AIRFLOW cc/min	TRANSMITTED DUO, $\mu\text{g}$	DUO, $\mu\text{g}/\text{min}$	DUO, $\mu\text{g}/\text{cc}$
123	2-110	100	1000	30	2000	75.1±21	2.5	$1.3 \times 10^{-3}$
124	2-110	247	500	30	770	69.7±20	2.3	$3.2 \times 10^{-3}$
125	2-110	25	100	30	210	157±40	7.0	$3.3 \times 10^{-2}$
126	2-110	100	100	30	305	123±32	4.1	$1.3 \times 10^{-2}$
127	2-110	300	100	30	147	55.1±14	1.8	$1.2 \times 10^{-2}$
128	2-110	300	1000	30	2090	304±74	10.1	$4.8 \times 10^{-3}$
129	2-110	25	1000	30	5600	196±49	6.5	$1.2 \times 10^{-3}$
130	2-110	100	500	30	2600	289±70	9.6	$3.7 \times 10^{-3}$
131	2-110	25	500	30	1080	37.2±1.1	1.24	$1.2 \times 10^{-3}$
132	2-110	25	1000	30	4800	258±63	8.6	$3.3 \times 10^{-3}$
133	2-110	100	500	30	2350	158±40	5.3	$2.2 \times 10^{-3}$
134	2-110	100	100	30	135	72.4±20	2.4	$7.8 \times 10^{-2}$
135	2-110	281.9	100	30	345	138±36	4.6	$1.3 \times 10^{-2}$
136	2-110	282.8	1000	30	5050	331±80	11.0	$2.2 \times 10^{-3}$
137	2-110	27.2	500	30	465	17.2±5.2	0.57	$1.2 \times 10^{-3}$
138	2-110	275.7	500	30	535	48.7±14.0	1.62	$3.0 \times 10^{-3}$
139	2-110	57.5	1000	30	3200	198±49	6.6	$2.1 \times 10^{-3}$
140	2-110	25	100	30	152	28.7±8.6	0.96	$6.3 \times 10^{-3}$
141	2-110	100	1000	30	4650	373±90	12.4	$2.7 \times 10^{-3}$
142	2-110	281	1000	80+30	5150	993±230	31.1	$6.0 \times 10^{-3}$
143	2-110	284	1000	80+30	5050	210±54	7.0	$1.4 \times 10^{-3}$
144	2-110	100	100	1440	225	41.5±12.0	0.03	$1.3 \times 10^{-4}$
145	2-110	100	100	1440	66	10.2±3.1	0.007	$1.1 \times 10^{-4}$
146	2-110	100	100	360	320	94.5±26	0.26	$8.2 \times 10^{-4}$
147	2-110	100	100	360	320	45.5±14	0.12	$3.8 \times 10^{-4}$

TABLE A.2. (Continued)

UPL <sup>(6)</sup>	ORIFICE	SAMPLER ORIENTATION	WT DUO g	CHAMBER PRESSURE psig	TIME, min	AIRFLOW cc/min	TRANSMITTED <sup>(3)</sup> DUO, $\mu$ g	DUO, $\mu$ g/min	DUO, $\mu$ g/cc
154	2-110	180 <sup>0</sup>	25	1000	30	5400	398±99	13.3	2.5x10 <sup>-3</sup>
155	H-110	180 <sup>0</sup>	25	1000	80+30	7400	2.55±0.76	0.09	1.15x10 <sup>-5</sup>
156	4-110	180 <sup>0</sup>	25	1000	30	3850	628±160	20.9	5.4x10 <sup>-3</sup>
157	4-110	45 <sup>0</sup>	25	1000	80+30	5400	476±120	15.9*	
158	2-110	45 <sup>0</sup>	25	1000	30	3200	764±190	25.5	8.0x10 <sup>-3</sup>
159	4-110	45 <sup>0</sup>	25	1000	30	7700	119±32	4.0	5.7x10 <sup>-4</sup>
160	2-110	45 <sup>0</sup>	25	1000	80+30	7900	396±99	13.2*	
161	4-110	180 <sup>0</sup>	25	1000	80±30	1400	215±55	7.2*	
162	2-110	{ TURNED END } { FOR END }	25	1000	30	2325	552±140	18.4	7.9x10 <sup>-3</sup>
163	4110		25	1000	30	8850	492±120	16.4	1.9x10 <sup>-3</sup>

\* $\mu$ g/min CALCULATED ON 30 MIN TIME ONLY

(6) RUNS 148 - 153 BLANKS

APPENDIX B

STATISTICAL ANALYSIS OF  
DUO EXPERIMENTS

James W. Johnston

## STATISTICAL ANALYSIS OF DUO EXPERIMENTS

### SUMMARY

This appendix gives the results of statistical analyses of the data from 370 experimental runs in the Above Powder Leak (APLA) and Under Powder Leak (UPL) apparatus containing depleted uranium oxide (DUO). Leak paths from the apparatus were formed by orifices, long capillaries or short capillaries. The amount of DUO reaching a sampler downstream of the opening was measured using alpha counting or chemical analysis. Openings ranged in diameter from 20 to 276  $\mu\text{m}$  and chamber pressures from 5 to 1000 psig. Each experimental run was defined by:

- the apparatus,
- opening type used,
- the opening diameter,
- the chamber pressure, and
- the duration for which pressure was maintained.

In addition to these five defining characteristics, some APLA runs were made with vacuum-maintained flow and some UPL runs had mechanical agitation. All APLA runs had the powder agitated by air pressure. Airflow downstream from the sampler was also measured. In addition, the airflows through the openings were measured in the opening calibration apparatus, and calculated theoretical mass and volume flows were available.

The data for experimental runs in which immediate plugging or airflow leaks occurred were excluded from the statistical analysis. In addition, seven runs that had anomalously low DUO transmitted for the pressure and diameter combination for the run were removed as the analysis progressed.

The goals of the statistical analysis were to determine the amount of DUO transmitted and to develop a prediction equation for estimating the amount of DUO transmitted when leak conditions are specified. The statistical methods used to attain these goals were:

- plots of the data,
- analysis of variance,



- contingency table analysis,
- analysis of ranks,
- product-moment sample correlation, and
- linear regression.

These methods are documented in most statistical methods textbooks. All of them can be found in Bernard Ostle's (1963) Statistics in Research. Draper and Smith's (1966) Applied Regression Analysis provides an excellent treatment of regression methods. Sidney Siegel (1956) provides clear explanations of the ranking methods used in his Nonparametric Statistics.

The impacts of the various experimental conditions were assessed by comparing the natural logarithms of the total  $\mu\text{g}$  DUO transmitted for subsets of the data designed or selected to answer specific questions. The experimental conditions can be divided into two groups: those that were categorical and those that were continuous measured quantities. The conditions in the first group are: apparatus type, opening type, aerosolization mechanism and flow mechanism. The second group consists of orifice diameter, chamber pressure and duration of run.

The analysis of the categorical variables resulted in these conclusions:

- Apparatus type may have an effect.
- Opening type may have an effect.
- UPL agitation had no effect.
- APLA maintained flow had no effect.

Results for the measured variables indicated that:

- orifice diameter has a pronounced effect,
- chamber pressure has a low pronounced effect,
- duration of run does not have a discernible effect, and
- the effects of diameter and pressure are additive on the logarithmic scale.

The prediction equation developed was based on the simple logic that the total DUO transmitted could be represented by an aerosolization variable  $a_0$  that was a function of chamber pressure times the airflow. Algebraically,

$$\text{Total DUO} = a_0 (\text{total } F)$$

Since the flow  $F$  is a multiplicative function of cross-sectional area,  $A$ , and upstream pressure,  $P_0$ , (along with some theoretical or empirical constants), and these were our most precisely measured variables, the transmitted DUO was characterized by:

$$\text{Total DUO} = a_0 A \sqrt{P_0} (T)$$

where  $T$  is the duration of the run;  $A$  is the area,  $\mu\text{m}^2$ ;  $P$  is pressure, psig; and DUO is depleted uranium dioxide powder,  $\mu\text{g}$ .

This formulation assumes that the particulate matter (DUO) in the aerosol was constant over the duration of the run. Despite the indications from previous analyses that time had no effect, the relationship between  $A\sqrt{P}$  and DUO/min as well as Total DUO were investigated. The conclusion was that the use of DUO/min did not explain the structure in the data as well as Total DUO did. It was also determined that apparatus type did have an effect as far as orifices were concerned, but the results for capillaries were not different for the APLA or UPL apparatus. The structure in the data can be summarized by three statistically homogeneous subsets of data: UPL orifices, APLA orifices, and capillaries (irrespective of apparatus type).

The final result was that three prediction equations were required. They were of the form

$$\ln \text{DUO} = a + b_1 \ln A + b_2 \sqrt{P}$$

or, equivalently by exponentiating each side,

$$\text{DUO} = \exp [a + b_2 \sqrt{P}] A^{b_1}$$

Least squares fits to this model accounted for more of the variability in the data and resulted in more precise estimates than many other models that were

tried. However, pooling the data to provide fewer than three equations resulted in a significant decrease in precision of estimation.

One further complication in the characterization of the data structure was that these prediction equations were appropriate for values of  $\ln A\sqrt{P}$  greater than 10.5. Below this value, total DUO transmitted appeared to be a random phenomenon, the results having little relationship to the diameter and pressure for the run. The standard deviation of all runs satisfying the constraint that  $\ln (A\sqrt{P})$  be less than 10.5 (for example, at 1000 psig, a diameter less than 38  $\mu\text{m}$  would make the run fall under the constraint) was 0.8362  $\ln$  DUO, which was not significantly different (in most cases) from the standard deviations obtained for sets of runs with pressure and diameter the same from run to run. That is, the standard deviation of all the 84 runs with diameter-pressure combinations resulting in  $\ln (A\sqrt{P})$  less than 10.5 was the same as the standard deviation due to experimental variability. This result makes it necessary to have a two-stage decision rule on how to estimate the expected DUO for future similar experiments:

- 1A) If  $\ln (A\sqrt{P})$  is less than 10.5, use the average or upper limit methods based on low airflows (given below).
- 1B) If  $\ln (A\sqrt{P})$  is greater than 10.5, the high airflows case, use the least squares regression estimates and confidence limits (given below).
- 2A) Within 1A use the statistics for UPL or APLA orifices<sup>(a)</sup> as appropriate.
- 2B) Within 1B use the statistics for UPL orifices, APLA orifices or capillaries as appropriate. In the absence of information on leak location and opening configuration, the total statistics may be used.

Most of the required numbers are given in the Summary Table B.1. the upper half is for flows characterized by  $\ln (A\sqrt{P}) < 10.5$ , that is, low airflows. The numbers given are total  $\mu\text{g}$  DUO irrespective of duration of the leak. The

---

(a) There were only two APLA capillary runs, and none for UPL, with  $\ln A\sqrt{P} < 10.5$ ; therefore, there is no data base for saying what to do with capillaries in this case.

TABLE B1. Summary Table

Total  $\mu\text{g}$  DUO  
For Low Airflow,  $\ln(\overline{AVP}) < 10.5$

	Under Powder Leaks (UPL)	Above Powder Leaks (APLA)
Expected Average	33	5
90% CL(a) on Average		
• Lower	24	4
• Upper	46	6
Expected Maximum Single Release In a Year at a Once-a-Month Rate with 90% Confidence	287	46

Total  $\mu\text{g}$  DUO  
For High Airflow,  $\ln \overline{AVP} > 10.5$   
 $\ln \text{DUO(EST)} = a + b_1 \ln A + b_2 \sqrt{P}$

Expected Average for 1000 psig	UPL Orifices	APL Orifices	Capillaries	Total
At 37.4 $\mu\text{m}$ ( $\ln \overline{AVP} = 10.45$ )	11	6	2	6
At 276.1 $\mu\text{m}$ ( $\ln \overline{AVP} = 14.45$ )	6,800	7,820	13,870	9,480

Natural Logarithm Scale

Coefficients a	-10.2848	-14.1959	-17.9875	-14.2790
b <sub>1</sub>	1.6080	1.7906	2.1658	1.8280
b <sub>2</sub>	0.0449	0.1095	0.1170	0.1052
sd(Residual)	0.8053	0.8718	1.1379	0.9842
R <sup>2</sup> %	77.09	82.62	66.34	78.43
N	28	91	37	156

(a) CL is confidence limit

expected average is the predicted value to use if one wants an estimate of the central value to expect for a rerun of the same experiment<sup>(a)</sup> that was conducted. The approximate 90% CL (confidence limit) on the average gives the interval that would contain the obtained average in about 90 out of 100 reruns of the experiment. Such statistics are rather bland because we do not plan to rerun the study, and they say nothing about the expected maximum total DUO leaked from a future instance of a real-life analogue of the experimental apparatus, that is, an accident. However, this type of CL statistic is not uncommonly reported in similar studies and the reader left in puzzlement about what is meant by "90% Confidence".

The expected maximum reported in the Summary Table is highly qualified by necessary modifiers. It is based on the characterizations of the UPL and APLA total  $\ln$  DUO transmitted distributions as being normal (Gaussian) with different means but the same variance. A necessary part of determining the probability associated with a maximum value is specification of the number of observations from which the maximum is to be selected. The answer in the Summary Table assumes that the maximum over a year with a once-a-month accident rate might be of interest. Statistically, we answer the question about the maximum of 12 instances at the 90% confidence level, and the answer is 287  $\mu\text{g}$  DUO. Here, 90% means in 90 years out of 100 with the same accident rate. If the rate were once a year, the 90% limit would be 87  $\mu\text{g}$  DUO. (We get a new start each year.) If the rate were one every two months, the answer would be 214  $\mu\text{g}$  DUO. For the APLA data, the numbers are considerably smaller. The possibility that this was due to larger  $\ln$  ( $A\sqrt{P}$ ) for UPL can be excluded by noting that the distributions for  $\ln$  ( $A\sqrt{P}$ ) less than 10.5 are quite similar, with the APLA average being 9.43, slightly larger than the 9.33  $\mu\text{g}$  DUO for UPL.

The high airflow,  $\ln$  ( $A\sqrt{P}$ ) > 10.5, part of the Summary Table gives examples of the expected average for 1000 psig pressure at orifice diameters of 37.4  $\mu\text{m}$  and 276.1  $\mu\text{m}$ . These are near the extreme values for the range of the data upon which the regression equations were based. The reversal of the ordering

---

(a) In this discussion, "experiment" means all of the runs done to estimate the particular parameter under discussion.

of the three data sets (UPL orifices, APLA orifices, capillaries) based on the 37.4  $\mu\text{m}$  estimated values to the ordering based on the 276.1  $\mu\text{m}$  estimated values indicates that the lines for the estimation equations cross. The lines are plotted for 1000 psig in Figure B.15.

The next part of the Summary Table gives: the coefficients,  $a$ ,  $b_1$  and  $b_2$  estimated by least squares, the residual standard deviation, the percentage of the total variability in the  $\ln$  DUO values for the data set that was accounted for by the model, and  $N$ , the number of observations. All three coefficients increase in absolute value with data sets from UPL-0 to APLA-0 to capillaries. The coefficients for the fit to all 156 observations are not significantly different from those for the APLA-0 data. The residual standard deviations also increase from left to right for the three data sets. The sd (Residual) for the orifices are near the values found for experimental variability, about 0.85  $\ln$  DUO, but in the Capillaries and Total columns they are near unity, indicating there may be significant misfit. The fit to the capillaries data accounted for only two thirds of the total variability, but the other  $R^2\%$  were about 80%.

Confidence limits on estimated values from regression equations are more complicated than for the single variable confidence limits discussed above. An idea of the expected precision can be given by discussing the approximate 90% confidence limits for the 1000 psig values based on the total fit.

The 90% confidence limits are:

<u>Diameter</u> <u><math>\mu\text{m}</math></u>	<u><math>\ln(\text{AVP})</math></u>	<u>Lower</u> <u>Limit, <math>\mu\text{g}</math></u>	<u>Estimated</u> <u>Value, <math>\mu\text{g}</math></u>	<u>Upper</u> <u>Limit, <math>\mu\text{g}</math></u>
40.5	10.6	1.1	8.5	62.8
124.0	12.9	71.5	507.9	3,608.5
276.0	14.5	1,311	9,468	68,369

Since the limits were obtained for the natural logarithmic scale and transformed back to the DUO  $\mu\text{g}$  scale, they are quite asymmetric. These upper limits are most appropriately applied to the expected maximum in a single future run using the experimental apparatus. The actually observed maximum was 79,200  $\mu\text{g}$

DUO for an under powder leak through the 276- $\mu$ m capillary at 1000 psig. The next largest was 38,100  $\mu$ g DUO for a repeat of the same experimental conditions.

## DATA BASE

### Data Collection

The 370 experimental runs using depleted uranium oxide (DUO) in the plutonium oxide leak studies were defined by type of apparatus and by type of opening (leak path) combined with chamber pressure and duration of run. There were two types of apparatus:

- Above Power Leak (APLA)
- Under Powder Leak (UPL)

Leak paths were through three types of openings:

- orifices
- short capillaries
- long capillaries.

These openings varied in diameter from 20 to 276  $\mu$ m. Selection of opening (s) and the appropriate apparatus determined the hardware characteristics for a run. For each run a chamber pressure between 5 and 1000 psig, and a duration of run (time during which the apparatus was at the selected pressure) between 0 and 360 min was preselected. Some runs with multiple openings were made on the APLA. For the UPL, some runs were made using mechanical agitation; others were not. All APLA runs had powder agitation.

Samples collected downstream of the orifices were sent to a commercial analytical laboratory, and micrograms of uranium were determined using alpha counting, or fluorometric analysis. The micrograms of DUO transmitted was the independent variable measured. The measured variables used to characterize each run were:

- diameter of the opening (capillary or orifice)
- chamber pressure
- downstream flow
- duration of run.

In addition, the flows for each opening over the range of pressures from 0 to 1000 psig were available from previous runs in the opening calibration apparatus. Calculated airflows based on theory using the opening diameter and chamber pressure were also available.

Some experimental conditions caused increased variability of the results or difficulty in data manipulation and statistical analysis. These were:

- the limited capacity of air cylinders made higher pressure runs shorter;
- the diameter of the mechanically drilled orifices tended to increase, but the diameter of the laser-drilled orifices shrank during the course of the experiment.

#### Data Organization

The data were keypunched and organized into six APLA data sets and six UPL data sets as defined in Table B2. The codes defining the data sets are given in the three columns under Card Codes:

- AP - Apparatus: APLA = 2, UPL = 1
- O,CS,CL - Opening Type: Orifice = 1, Capillary Short = 2, Capillary Long = 3
- S,TC,TV - Run Type: Single = 1, Time Constant = 2, Time Varying = 3
- A,NOTA - Agitation: Agitated = 1, Not Agitated = 2.

The last column contains the number of runs included in the basic data. The 21 UPL runs in U-7 were not keypunched.

#### Orifice Characterization

The actual orifice diameters measured by photomicroscopy did not correspond to the nominal diameters originally used to identify the orifices. Table B3 relates the orifice designations to the actual measured diameters and to the computer codes used to identify them for the statistical analysis. Orifices changed diameters during runs in about the middle of the experiment.



TABLE B2. Definition of Data Sets

<u>Data Set</u>		<u>Card Codes</u>			<u>Runs N</u>
		<u>AP</u>	<u>O,CS,CL</u>	<u>S,TC,TV</u>	
A - 1	Single Orifice	2	1	1	160
A - 2	Multiple Time-Constant Orifice	2	1	2	20
A - 3	Multiple Time-Varying Orifice	2	1	3	18
A - 4	Single Short Capillary	2	2	1	14
A - 5	Single Long Capillary	2	3	1	20
A - 6	Multiple Opening	2	1-3	2	5
	Total APLA Runs				237
				<u>A,NOTA</u>	
U - 1	Agitated Orifice	1	1	1	28
U - 2	Non-Agitated Orifice	1	1	2	51
U - 3	Agitated Short Capillary	1	2	1	11
U - 4	Non-Agitated Short Capillary	1	2	2	14
U - 5	Agitated Long Capillary	1	3	1	9
U - 6	Non-Agitated Long Capillary	1	3	2	9
U - 7	Grams DUO Varied	-	-	-	21
	Total UPL Runs				143
	Total Experimental Runs				370

Laser-drilled (with orifice designation prefix of 3) tended to get smaller, and mechanically drilled tended to get larger. The last column in Table B3 uses "OID" to mean "orifice identification," the unique number assigned to differentiate orifices (or capillaries).

DATA ANALYSIS

Many of the experimental runs were not included in the detailed data analysis. In particular, the 43 multiple opening runs (Data Sets A-2, -3 and -6 in Table B2) were excluded because of 1) the uncertain effect of closing the air-flow path downstream of the samplers for the time-varying runs, and 2) insufficient data on the sampling ports used by specific orifices in specific time-

TABLE B3. Orifice Identification

Orifice Designation	Measured Diameter, m		Run No. at Change	Computer Codes		OID
	First	Second		Nominal Diameter	Orifice Code	
1-20	22	26	159	1	1	1
2-20	20	20	NC <sup>(a)</sup>	1	2	2
3-20	23	20	147	1	3	3
1-20a	23	23	NC	1	4	4
1-36	43	38	124	2	1	5
2-36	33	32	NC	2	2	6
3-36	38	30	137	2	3	7
3-30	33	22	135	2	4	8
1-63.5	66	66	NC	3	1	9
2-63.5	61	60	NC	3	2	10
3-63.5	65	62	NC	3	3	11
1-110	100	111	51	4	1	13
2-110	125	123	NC	4	2	14
3-110	100	89	211	4	3	15
1-200	200	( 213 ) ( -226 )	( 72 ) ( -146 )	5	1	17
2-200	200	(310)	No Use <sup>(b)</sup>	5	2	18
3-200	200	190	118	5	3	19
<u>Selected Capillaries</u>						
150-S	182			6	1	21
150-B	176			6	2	22
250-S	276			6	3	23
250-B	274			6	4	24

(a) NC means no (significant) change.

(b) Orifice 2-200 was no longer used after its diameter was increased to 310 μm.

constant runs. In addition, some experimental runs had airflow leaks, immediate orifice plugging, or other problems that caused failure to attain the prespecified experimental conditions. These runs were also excluded from detailed analysis.

Some of the experimental runs were specified to provide data for statistically designed experiments. Details are given in the descriptions that follow.

### Thirty-Minute Experiment

Preliminary analyses indicated that duration of run had little effect on the amount of DUO transmitted. (This fact is partially explained by the statistical confounding of duration of run with diameter of orifice, which, in turn, was the result of the limited capacity of the air cylinders. For the larger orifices the cylinders were emptied sooner making longer runs impractical until an air manifold was constructed.) We decided to do a series of 36 experimental runs of 30-min duration each, using three pressures (30, 500 and 1000 psig) and three nominal orifice diameters (36, 110 and 200  $\mu\text{m}$ ). Two orifices of the same measured diameter at each of the three nominal diameters were used. The orifices selected had, respectively, orifice identification codes (see OID column in Table B3) and original diameters of 6 and 8 at 33  $\mu\text{m}$ ; 13 and 15 at 100  $\mu\text{m}$ ; 17 and 19 at 200  $\mu\text{m}$ . The statistical experiment originally designed treated the orifices of the same diameter as replicates, but the statistical analysis had to be changed when it was noted that the diameters of the orifices had changed.

The results of the 36 runs are given in Table B4 in the natural logarithm of the  $\mu\text{g}$  DUO transmitted. This two-way table shows that the design was a factorial experiment with two replicates (Rep) for each of the 18 treatments. A treatment was a combination of one of the six orifices run at one of the three pressures. The last column and bottom rows give the "marginal" totals for each orifice and each pressure respectively. The sum used to calculate the averages (Ave) and sums of squares for the analysis of variance are also given. Except for three runs using OID 15, all of the runs were after diameters had changed; therefore, the  $\mu\text{m}$  given in Table B4 is the second measured diameter.

TABLE B4. Data, Sums and Averages for 30-Min Experiment ( $\ln$  DUO  $\mu\text{g}$ )

OID	Orifice Designation	$\mu\text{m}$	Rep.	30 psig	500 psig	1000 psig	Orifice Total
8	3-30	22	1	2.2192	1.3510	1.8886	5.4688
			2	0.7130	1.9199	2.4849	5.1178
			Sum	2.9322	3.2809	4.3735	10.5866
			Ave	1.4661 Z(a)	1.6405	2.1868 Z	1.7644
6	2-36	32	1	1.5851	1.5019	2.1318	5.2188
			2	0.6575	1.2499	3.5026	5.4100
			Sum	2.2426	2.7518	5.6344	10.6288
			Ave	1.1213	1.3759 Z	2.8172	1.7715
15	3-110	89	1	2.8034	3.8437	4.2946	10.0417
			2	3.0057	3.0155	5.2679	11.2891
			Sum	5.8091	6.8592	9.5625	22.2307
			Ave	2.9045 Z	3.4296	4.7812 Z	3.7052
13	1-110	111	1	4.6540	4.8203	6.4085	15.8828
			2	3.4012	4.6347	6.8638	14.8997
			Sum	8.0552	9.4550	13.2723	30.7825
			Ave	4.0278	4.7275 Z	6.6362	5.1304
19	3-200	190	1	4.5951	6.5454	7.6825	18.8230
			2	3.4243	6.7117	7.0817	17.2177
			Sum	8.0194	13.2571	14.7642	36.0407
			Ave	4.0097 Z	6.6286 Z	7.3821	6.0068
17	1-200	226	1	5.3230	7.4442	7.9480	20.7152
			2	6.5820	7.1389	8.0262	21.7471
			Sum	11.9050	14.5831	15.9742	42.4623
			Ave	5.9525	7.2915	7.9871 Z	7.0770
Pressure Total		Sum		38.9635	50.1871	63.5811	152.7317
				3.2470	4.1823	5.5811	4.2425

(a) Z indicates the orifice by pressure treatment has a corresponding run in the "zero"-time experiment.

The treatment means (averages) are plotted in Figure B1. The top half plots the averages (of two runs) for each orifice against the three pressures. The bottom half plots the same averages for each pressure against the diameter of each orifice. Comparing these halves of Figure B1, we see that:

- DUO transmitted increases less with pressure than with diameter
- orifice averages cover a broader range than pressure averages.

Both of these observations indicate that diameter is a more important determinant of the amount of DUO transmitted than pressure.

The analysis of variance of Table B5 shows that these observations are statistically significant. The factorial arrangement of treatments was handled as repeated measurements (split plot) on the orifices at the three pressures with two replicates of the 18 treatment experiment.

In this design, the magnitude of the replicate and orifice effects are tested by forming an F-ratio with the Error A Mean Square. The F-ratio for replicates was 0.34 and  $P(>F)$ , meaning the probability of observing a greater F value is noted as being " $>0.1$ ". For this study, we decided that the probability of an F-ratio must be less than 0.1 for an effect to be called significant statistically. The conclusion is that the results for replicates do not differ significantly. Although the F-test is based on variances, it tests differences between means (averages) since the variances compared are measures of mean differences. In this case, the replicate 1 average was 4.2806 and the replicate 2 average 4.2045  $\ln$  DUO, and the nonsignificant F-ratio indicates that these averages are not significantly different and could be represented by the grand average 4.2425  $\ln$  DUO. This same logic is used for all analysis of variance tests.

The orifice effect is highly significant, indicating that diameter has a pronounced effect. (The actual upper 0.001 probability value for an F-ratio with 5 degrees of freedom, df, for both numerator and denominator is 29.75, and the calculated value is over six times as large, indicating a probability of occurrence under the assumption of equality of orifice means, much smaller than 0.001.) The pressure effect, tested by Error B, is also highly significant, the actual 0.001 point being 12.97, which is about half the observed value.

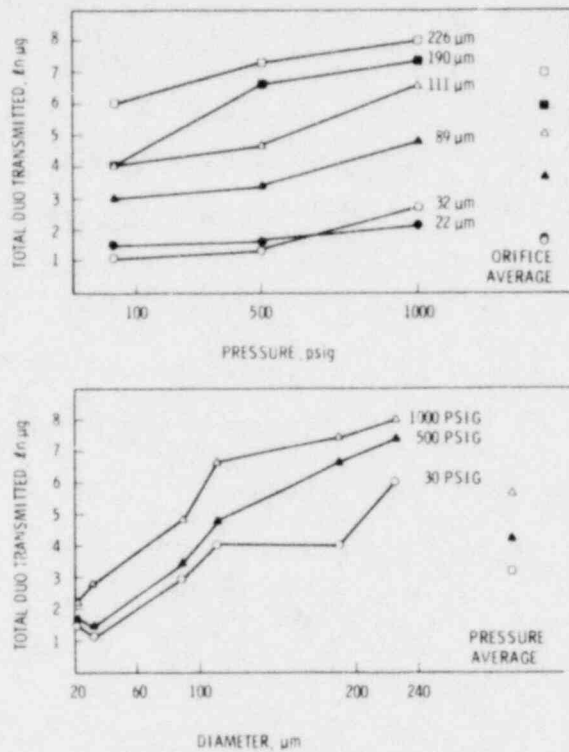


FIGURE B1. Plots of Treatment Means, 30-Min Experiment

TABLE B5. Analysis of Variance for 30-Min Experiment (ln DUO μg)

Sources	df	Sum of Squares	Mean Square	F	P(>F)
Replicate	1	0.05205	0.05205	0.34	>0.1
Orifice	5	146.8281	29.3656	192.56	<0.001
Error A	5	0.76273	0.1525		
Pressure	2	25.3165	12.6583	27.52	<0.001
O x P	10	6.4457	0.64457	1.401	>0.1
Error B	12	5.52021	0.46002		
Total	35	184.9253			

The orifice by pressure interaction, OXP, was nonsignificant, indicating that the changes in slope of the lines in Figure B1 were not significant. This means that the orifice and pressure averages adequately represent the data and that the orifice (diameter) and pressure effects can be considered to be additive on the logarithmic scale. The Error B Mean Square is an estimate of inherent experimental variability, and its square root provides an estimate of the standard deviation of the run-to-run random errors when orifice and pressure are the same. We can conclude that:

- both pressure and diameter have a significant effect on the amount of powder transmitted
- diameter is more important than pressure
- experimental error standard deviation was  $\sqrt{0.4600} = 0.6782 \text{ } \mu\text{n (DUO } \mu\text{g)}$
- the coefficient of variation was  $100 \frac{0.6782}{4.2425} = 16.0\%$

#### "Zero"-Time Experiment

We suspected that a significant proportion of the measured DUO transmitted could be sampled during the time the APLA was being brought up to pressure and depressurized. This time was usually less than 3 min compared to the 10- to 60-min duration of the run at pressure. A "zero"-time experiment was designed to check the hypothesis that as much DUO was transmitted during the time to reach pressurization as during the 30-min runs. This hypothesis could not be rejected.

The data, sums and averages are given in Table B6. Only half as many runs as used in the 30-min experiment were planned, and one of these produced unusable results (one of the 30 psig runs using Orifice 8). The diameters of the orifices were the same (within  $\pm 2 \text{ } \mu\text{m}$ ) as for the 30-min experiments. But the unexpected change in orifice diameters made the planned half replicate portion of the full design statistical analysis unbalanced. Therefore, a change in the planned analysis was necessary.

Table B7 compares the nine orifice-diameter by pressure-level treatment averages for the treatments common to the 30-min and "zero"-time experiments.

TABLE B6. Data, Sums and Average for "Zero"-Time Experiment ( $\lambda n$  DUO  $\mu g$ )

<u>OID</u>	<u>Orifice Designation</u>	<u><math>\mu m</math></u>	<u>Rep</u>	<u>30 psig</u>	<u>500 psig</u>	<u>1000 psig</u>
8	3-30	22	1	1.9184		2.1872
			2	-		1.7561
			Sum	1.9184		3.9433
			Ave	1.9184		1.9717
6	2-36	32	1		2.1017	
			2		2.2711	
			Sum		4.3728	
			Ave		2.1864	
15	3-110	89	1	2.3224		5.5013
			2	1.9272		5.1648
			Sum	4.2496		10.6661
			Ave	2.1248		5.3330
13	1-110	111	1		5.3613	
			2		4.5644	
			Sum		9.9247	
			Ave		4.9624	
19	3-200	190	1	5.2418	5.6204	
			2	4.7005	4.8752	
			Sum	9.9423	10.4956	
			Ave	4.9712	5.2478	
17	1-200	226	1			8.2134
			2			8.2215
			Sum			16.4349
			Ave			8.2174

The "Difference" column has six negative differences indicating that more often than not the "zero"-time average was greater than the 30-min average. The replicate-within-treatment-by-time (Rep/TxT) mean square from the analysis of variance (AOV) of Table B8 will be used to test the statistical significance of these differences. But first the AOV will be discussed.



TABLE B7. Comparison of 30-Min and "Zero"-Time Treatments (ln DUO µg)

Treatment	psig	µm	OID	Treatment Ave (of 2 Runs)		Difference 30-Zero	30 + Zero Ave
				30 min	Zero		
1	30	22	8	1.47	1.92 <sup>(a)</sup>	-0.4523	1.62
2	500	32	6	1.38	2.19	-0.7925	1.78
3	1000	22	8	2.19	1.97	0.2148	2.08
4	30	89	15	2.90	2.12	0.7795	2.51
5	500	111	13	4.73	4.96	-0.2353	4.84
6	1000	89	15	4.78	5.33	-0.5518	5.06
7	30	190	19	4.01	4.97	-0.9615	4.49
8	500	190	19	6.63	5.25	1.3808	5.94
9	1000	226	17	7.99	8.22	-0.2303	8.10
		Ave		4.0075	4.2323	-0.2248	4.1167
		sd		0.5331	0.3507	0.4564	
		sd (Ave)				0.1521	
		t				-1.478	

(a) Duplicate was missing; the result is for a single run.

TABLE B8. Analysis of Variance Comparing 30-Min and "Zero"-Time Runs

Source	df	Sum of Squares	Mean Square	F	P(>F)
Time	1	0.441920	0.441920	0.830	>0.1
Treatments	8	150.459690	18.807461	35.339	<0.001
Treatment x					
Time	8	4.257623	0.532203	2.555	<0.05
Rep/TxT	17	3.541175	0.208304		
Total	34	158.700408			

The analysis of variances showed a significant Treatment x Time interaction. The nature of this interaction is shown in Figure B2. The averages for the 30-min runs have a consistently increasing convex shape when the points for different orifices (diameters) are connected based on common pressure. But the 30 psig "zero"-time points would form a concave figure, and the 190- $\mu$ m orifice had only 0.29  $\mu$ g more DUO than the 111- $\mu$ m orifice at 500 psig. The plus and minus pattern of the difference column in Table B7 also shows the nature of the interaction.

The "Rep/TxT" mean square provides the estimate of experimental error variance, 0.2083, so that 0.4564 is the standard deviation, sd, and the coefficient of variation is:

$$100 \frac{0.4564}{4.1167} = 11.1\%$$

As expected, the differences between treatment means (the averages of four observations, two from the 30-min runs and two from the "zero"-time runs) were highly significant. The time means (4.01 and 4.23  $\mu$ g) were not significantly different.<sup>(a)</sup> This conclusion is also reached through use of the t-test given at the bottom of Table B7. The calculated t-value was -1.478, which is less than the 90th percentile of the t-distribution; therefore, there are no grounds for concluding that the "zero"-time runs produced significantly different DUO transmission than the 30-min runs on the average. The least significant difference (lsd), at the 95% level is

$$lsd = t_{0.975}(17) 0.208304 = 2.110 (0.4564) = 0.9630$$

where  $t_{0.975}(17)$  is the 97.5 percentile of the t-distribution with 17 degrees of freedom. Only the 500 psig difference for the 190- $\mu$ m orifice,

---

(a) For those who might object that the missing observation puts us in the unequal cell number situation and makes the main effects tests invalid, the required adjustment (e.g., Ostel 1963, p. 302) would only change the F-ratios by about 3%, which would not change the conclusion.

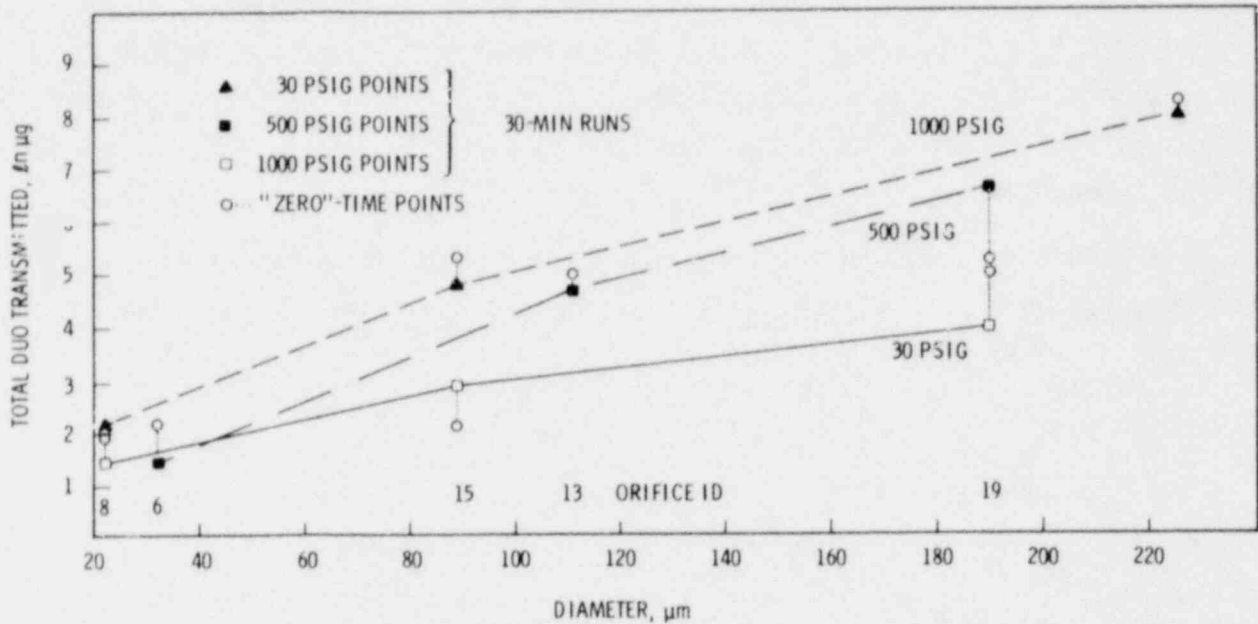


FIGURE B2. Comparison of 30-Min and "Zero"-Time Runs by Orifice

Treatment 8, exceeds this value. This single significant difference is not sufficient grounds to conclude that the transmission of DUO is different generally.

The final conclusion from this analysis is that duration of the run has no effect on the amount of DUO transmitted. There is no evidence to refute the hypothesis that the DUO was transmitted during the pressurization (and/or depressurization) phase of the experimental run. It follows that a transmission rate is meaningless for this set of experiments.

#### Pressure Decay Runs

These runs differed from the "zero"-time runs in that the APLA vessel was brought to pressure and then allowed to depressurize through the orifice instead of being exhausted through the relief valve. The total duration of the "zero"-time runs at 1000 psig was about 3 min, but the pressure decay runs took about 130 min.

The five pressure decay runs at 1000 psig were selected as the basis of the comparison since there were runs under other experimental conditions using the same orifices at that pressure. The data are given in Table B9 and plotted in Figure B3. For the 111- $\mu\text{m}$  dia and 226- $\mu\text{m}$  dia orifices there was no real difference in the log-transformed data. For the smaller orifices (22  $\mu\text{m}$  and 38  $\mu\text{m}$ ) the pressure decay runs resulted in slightly less transmitted DUO than for the "zero"-time or 30-min runs. The data are not numerous enough to provide quantitative statistical comparisons but do reinforce the hypothesis that duration of run has little impact on DUO transmitted.

TABLE B9. Data for Pressure Decay Comparisons, For Runs at 1000 psig ( $\ln$  DUO)

<u>OID</u>	<u><math>\mu\text{m}</math></u>	<u>Pressure Decay</u>	<u>30 Min</u>	<u>10 Min</u>	<u>"Zero" Time</u>	<u>Range of Averages</u>
5	38	0.3716			2.0643 0.7372 <u>1.4008</u>	1.0293
8	22	0.6043	1.9330 2.4849 <u>2.2090</u>		2.1872 1.7561 <u>1.9717</u>	1.6047
13	111	6.1070	6.4085 6.8638 <u>6.6362</u>		6.3526	0.5292
17	226	7.8898 8.8320 <u>8.3609</u>		8.5350	8.4659 8.2134 8.2215 <u>8.3003</u>	0.2347

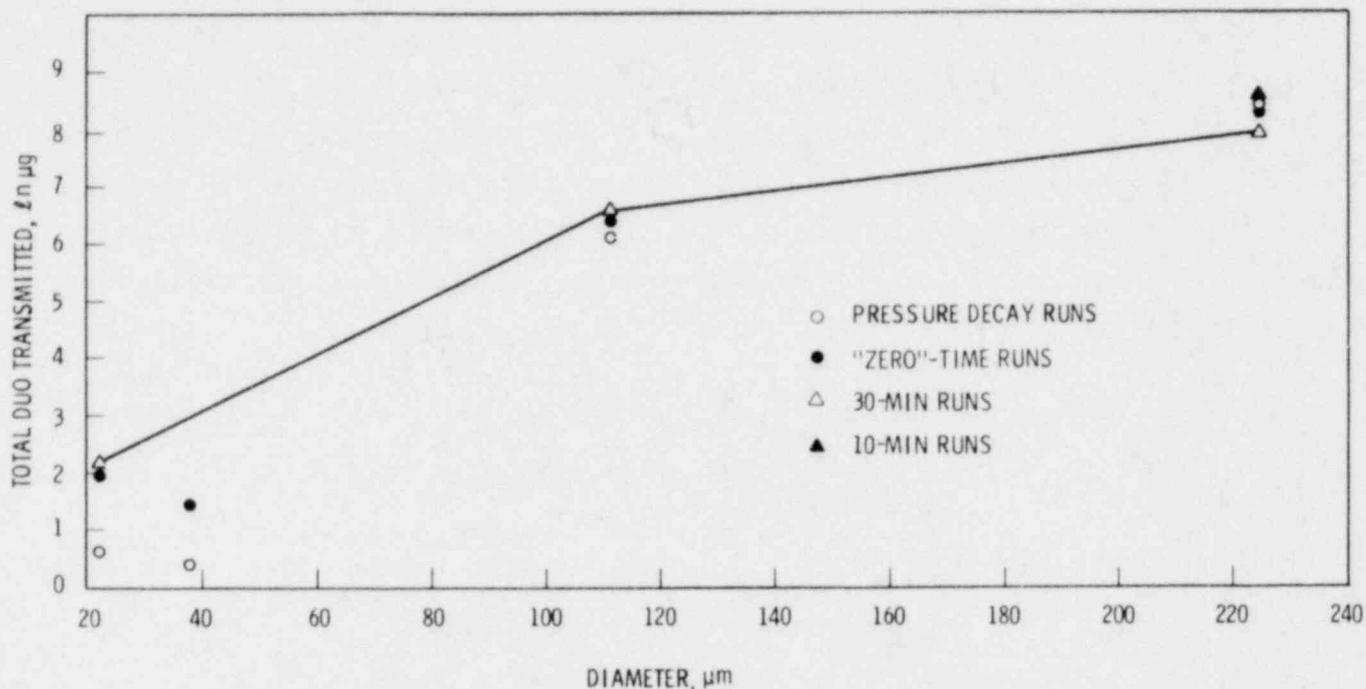


FIGURE B3. Comparison of Pressure Decay and Other Runs at 1000 psig

#### Measured Flow Runs

The APLA run numbers 107 through 152 were made without maintaining the flow by applying a downstream vacuum. The chamber-pressure induced flow was measured by reading a rotameter. These measurements were not as important as the change in experimental conditions. The purpose of using the downstream vacuum was to eliminate back-pressure, but the vacuum also applied another force that could affect powder transmission. Consequently, the APLA was modified to allow runs for which only the chamber pressure was the effective flow force. This was done to check the hypothesis that the downstream vacuum was a major contributing cause of powder transmission.

The  $\ln(\text{DUO})$  data, sums and averages for the measured flow runs are given in Table B10. All of the 1000 psig runs were of 10-min duration. Runs at the other pressures were for 30 min except for the second runs at 100 and 500 psig for the 23- $\mu\text{m}$  orifice, which were for 5 and 10 min, respectively. Another

TABLE B10. Data, Sums and Averages for Measured Flow Runs

OID	$\mu\text{m}$	$\ln(\text{DUC})$				Orifice
		Pressure				
		30	100	500	1000	
3	23		0.1222	1.0578	1.1569	
			0.3716	0.3646	1.3913	
				1.0225		
	Sum		0.4938	1.4224	3.5707	5.4869
	Ave		0.2469	0.7112	1.1902	0.7838
7	38	1.2585	1.0188	1.4085	1.9213	5.6071
	30	0.1508(a)	0.6523(a)	1.8810(a)	1.8390	4.5231
	Sum	1.4093	1.6711	3.2895	3.7603	10.1302
	Ave	0.7047	0.8356	1.6448	1.8802	1.2663
11	62	0.7975	2.0832	2.1163	3.9646	8.9616
		1.5790	1.1848	2.6603	3.5439	8.9680
	Sum	2.3765	3.2680	4.7766	7.5085	17.9296
	Ave	1.1883	1.6340	2.3883	3.7543	2.2412
15	100	3.3945	2.6391	3.1864	4.5931	13.8131
		1.0682	3.0106	4.1415	4.7274	12.9477
	Sum	4.4627	5.6497	7.3279	9.3205	26.7608
	Ave	2.2314	2.8249	3.6640	4.6603	3.3451
19(a)	190	5.1180	4.6913	6.2823	8.5390	24.6306
		2.2170	4.4909	6.8987	7.3588	20.9654
	Sum	7.3350	9.1822	13.1810	15.8978	45.5960
	Ave	3.6675	4.5911	6.5905	7.9489	5.6995
Pressure for (7, 11,15, 19)	Ave	15.5835	19.7710	28.5750	36.4871	100.4166
	Sum	1.9479	2.4714	3.5719	4.5609	3.1380

(a) Run after orifice diameter became smaller. All runs for Orifice 19 were at the reduced diameter of 190- $\mu\text{m}$ .

complication was that three of the runs for Orifice 7 were made after the orifice had shrunk from 38 to 30  $\mu\text{m}$ .

An analysis of variance was done on these data. The results for the 23- $\mu\text{m}$  orifice (OID 3) were not used since the missing data at 30 psig would complicate the analysis. The 23- $\mu\text{m}$  results were included in the plots of treatment means (as broken lines) of Figure B4, however. Comparing Figure B4 and Figure B1, the general picture is about the same, but the measured flow plots show more uniform trends than the maintained flow runs of the 30-min experiment.

The analysis of variance of Table B11 produced the same results as Table B5 for the maintained flow runs: there was no orifice-by-pressure interaction, and orifice diameter had a more pronounced effect than pressure as shown by the plots of Figure B4. The experimental error variance (Error B) was slightly larger (0.6813 versus 0.4600) but not significantly so. The standard deviation was 0.8254  $\mu\text{g}$  (DUO  $\mu\text{g}$ ) and the coefficient of variation (CV) was

$$100 (0.8254/3.1380) = 26.3\%$$

This value compares with 16.0% for the maintained flow (30-min experiment) CV based on the average of 4.2425  $\mu\text{g}$  (DUO  $\mu\text{g}$ ). The higher average for the maintained flow runs was partly the result of runs at the larger diameters.

The conclusion from the analysis of variance and overall plots comparisons is that no gross differences exist between the maintained and measured flow results.

A more precise comparison and conclusion is possible based on the following analysis. The measured flow runs used five of the six laser-drilled orifices. Only two of these orifices were used in the 30-min experiment, OIDs 15 and 19. The averages and data to be compared for these orifices are given in Table B12. There were comparable data in both data sets for only four treatments (pressure-by-diameter combinations). For OID 15, the diameter was 100  $\mu\text{m}$  for the measured flow runs, but had shrunk to 89  $\mu\text{m}$  for the maintained flow runs. The data were analyzed by the analysis of variance of Table B13 and the Treatment-by-Flow type means compared in Figure B5. A new variable was introduced for the plot. The abscissa is  $\mu\text{g} \sqrt{A}$  where A is the cross-sectional

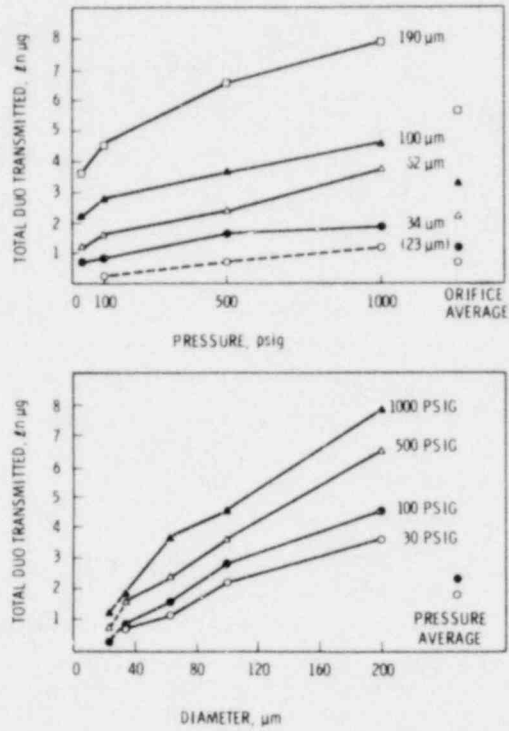


FIGURE B4. Plots of Treatment Means, Measured Flow Runs

TABLE B11. Analysis of Variance for Measured Flow Runs

Source	df	Sum of Squares	Mean Square	F	P(>F)
Replicate	1	0.98287	0.98287	3.060	>0.1
Orifice	3	87.2942	29.0981	90.597	<0.005
Error A	3	0.93684	0.31228		
Pressure	3	32.5880	10.8627	15.944	<0.001
O X P	9	6.1381	0.68201	1.001	>0.1
Error B	12	8.1757	0.68131		
Total	31	136.1157			



TABLE B12. Comparison of Maintained and Measured Flow Runs

Treatment	psig	$\mu\text{m}$	OID	Treatment Average		$\ln \text{AVP}$	
				Flow Maintained	Flow Measured	Early $\mu\text{m}$	Late $\mu\text{m}$
1	30	100	15	2.9045	2.2314	10.67	10.44
2	1000	100	15	4.7812	4.6603	12.42	12.19
3	30	190	19	4.0097	3.6675	11.95	
4	500	190	19	6.6286	6.5905	13.36	

Supporting Data

Treatment	1	2	3	4	Total
Measured Flow	3.3945	4.5931	5.1180	6.2823	
	1.0682	4.7274	2.2170	6.8987	
Sum	4.4627	9.3205	7.3350	13.1810	34.2992
Ave	2.2314	4.6603	3.6675	6.5905	4.2874
Maintained Flow	2.8034	4.2946	4.5951	6.5454	
	3.0057	5.2679	3.4243	6.7117	
Sum	5.8091	9.5625	8.0194	13.2571	36.6481
Ave	2.9045	4.7812	4.0097	6.6286	4.5810
Treatment Sum	10.2718	18.8830	15.3544	26.4381	70.9473
Ave	2.5680	4.7208	3.8386	6.6095	4.4321

TABLE B13. Analysis of Variance Comparing Maintained and Measured Flow Runs

Source	df	Sum of Squares	Mean Squares	F	P(>F)
Flow Type	1	0.3448	0.3448	0.44	>0.1
Treatment	3	34.6071	11.5357	14.84	<0.001
Flow Type x Treat.	3	0.2416	0.08052	0.078	
Rep/FTxT	8	8.3061	1.0383		
Total	15	43.4996			
Pooled Error	11	8.5477	0.7771		

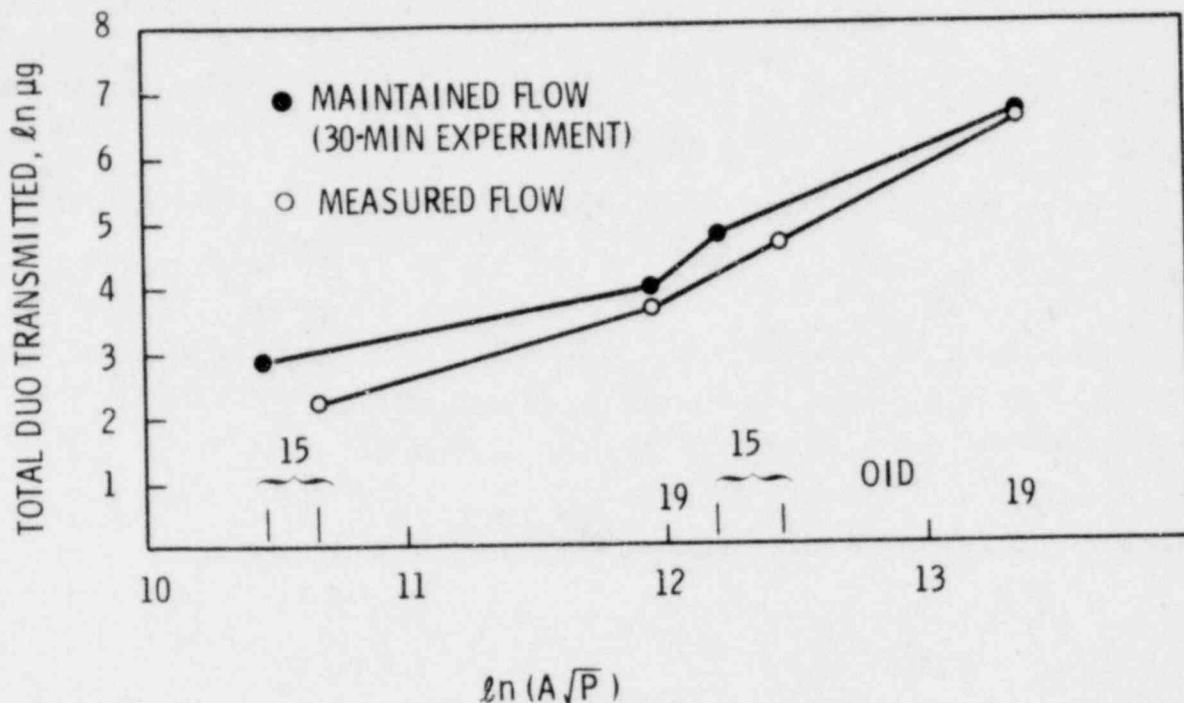


FIGURE B5. Comparison of Maintained and Measured Flow Averages

area of the orifice, and  $P$  is the pressure used for the run. Taking the natural logarithm of  $A\sqrt{P}$  linearizes the relationship with  $\ln$  DUO fairly well. Of course,  $A$  and  $\sqrt{P}$  are the basic theoretical determinants of flow. (The plots of Figure B5 do reflect the slightly concave quadratic shape that we could not explain or account for statistically.)

The analysis of variance of Table B13 shows that the mean difference (4.2874 - 4.4321) for the two flow types is not statistically significant. The Pooled Error Mean Square, 0.7771 is larger than for previous analyses, but not significantly so.

#### UPL Orifices

The results in the preceding sections were for runs using the APLA apparatus. For the UPL apparatus, there were 79 single orifice runs. The UPL apparatus had a mechanical agitator that could be activated for selected runs. The experimental treatments were determined by a combination of four factors:

- orifice (OID): 1, 2, 6, 10, 11, 14, 17, and 18
- pressure (psig): 5, 15, 50, 100, 500, 1000
- agitation: A (agitated);  $\bar{A}$  (not agitated)
- time: 5, 10, 20, 30, 60, 120 min.

The number of runs for the orifice-by-pressure-by-agitation treatments (ignoring time) are given in Table B14. There were four runs of 120 min duration at 15 psig; two runs for OID 2 and two runs for OID 6. There were also two runs of 60 min duration at 5 psig using OID 18 (200  $\mu$ m). The 70 remaining runs are allocated to the orifice-by-time-by-pressure treatments (ignoring agitation) in Table B15. This table shows that no 1000 psig run was longer than 20 min, all 100 psig runs were for 30 min and all 15 and 50 psig runs were for 60 min. Time is highly confounded with pressure, but some comparisons are possible.

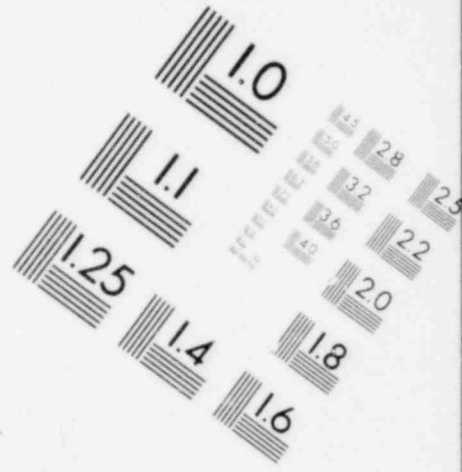
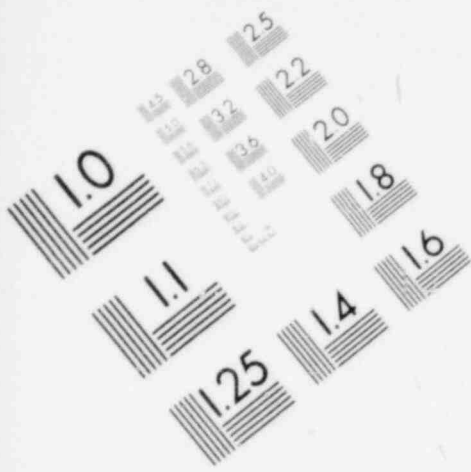
TABLE B14. Numbers of Runs for UPL Orifices

OID	Orifice	m	psig										Total	
			15		50		100		500		1000		A	$\bar{A}$
			A	$\bar{A}$	A	$\bar{A}$	A	$\bar{A}$	A	$\bar{A}$	A	$\bar{A}$	A	$\bar{A}$
1	1-20	24		1		1				1				3
2	2-20	20	1	1		1	2	2	1	1	2	2	6	7
6	2-36	32	1	2		1	2	2	1	2	1	2	5	9
10	2-63.5	60	1	1			1	1	1	1	1	1	4	4
11	3-63.5	64		1		1	1			1		2	1	6
14	2-110	124	1	1	1	2	2	2	1	2	1	3	6	10
17	1-200	213		1		2				1		1		5
19	2-200	200	2	2 <sup>(a)</sup>			2	2	1	1	1	2	6	7
Agitated			6		1		10		5		6		28	
Not Agitated				10		8		10		10		13		51
Total				16		9		20		15		19		79

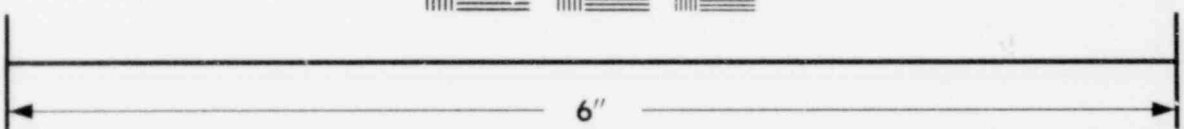
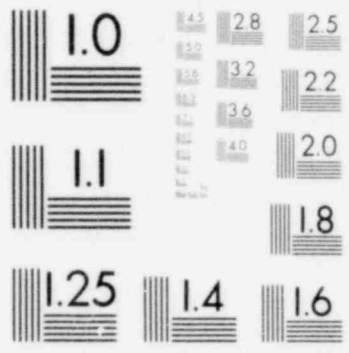
(a) The count includes an A and  $\bar{A}$  run made at 5 psig.

TABLE B15. Numbers of UPL Runs - Orifice by Time by Pressure

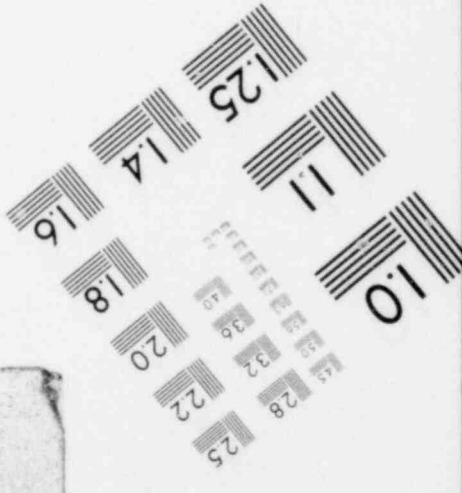
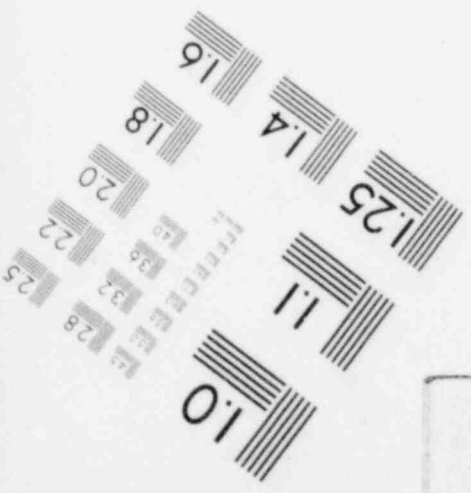
OID	60 min psig			30 min psig		20 min psig		10 min psig		Sum Over psig				
	15	50	500	100	500	500	1000	500	1000	60	30	20	10	Total
1	1	1			1					2	1			3
2		1	2	4			2		2	3	4	2	2	11
6	1	1	2	4	1		2		1	4	5	2	1	12
10	2			2	2		2			2	4	2		8
11	1	1		2	1				2	2	3		2	7
14	2	3		4		2	2	1	2	5	4	4	3	16
17	1	2			1				1	3	1		1	5
19	2			4		2				2	4	2		8
Totals	10	9	4	20	6	4	8	1	8	23	26	12	9	70



**IMAGE EVALUATION  
TEST TARGET (MT-3)**



**MICROCOPY RESOLUTION TEST CHART**



### UPL Time Comparisons

Table B16 gives the  $\ln$  DUO data for the available treatment (orifice-by-agitation-by-pressure-by-time) comparisons over time. These data are plotted in Figure B6. The results contradict expectations. Four of the five 10-to-20-min comparisons show a decline over time. The 30-to-60-min comparison shows a meager increase from 2.84 to 3.02  $\ln$  (DUO). The only appreciable difference between A and  $\bar{A}$  runs is for the 32- $\mu\text{m}$  orifice at 1000 psig for 20 min. Essentially the same results were obtained at 500 and 1000 psig for the 124- $\mu\text{m}$  orifice.

There are not enough data points to draw firm statistical conclusions about the effect of time for the UPL runs from these observations. Averages and standard deviation (sd) for the orifice by pressure data (averaged over agitation and time) are reported in Table B17. For Orifices 2 and 6 (20 and 32  $\mu\text{m}$ ), the standard deviations are not statistically different from the 0.6782  $\ln$  DUO standard deviation found for the 30-min APLA experiment. One can infer from this that the differences seen for the 20- and 32- $\mu\text{m}$  orifices in Figure B6 are within experimental variability; that is, agitation and time have no significant effect for these small orifices. The 10- and 20-min averages over A and  $\bar{A}$  are given at the bottom of Table B17, along with their differences, for the 124- $\mu\text{m}$  orifice. Using the standard deviation of the difference at 1000 psig:

$$\text{sd}(\text{diff.}) = 1/2[2(0.6215)]^{1/2} = 0.7884,$$

with 10 degrees of freedom, the t-value is

$$t = \frac{2.06}{0.7884} = 2.61$$

and for 500 psig,

$$\text{sd}(\text{diff.}) = 2(0.6215)^{1/2} = 1.1149$$

TABLE B16. UPL Orifices Time Comparisons  $\ln D'O$

OID	$\mu\text{m}$	Agitation	psig	Time (min)			
				10	20	30	60
2	20	$\bar{A}$	1000	3.2492	2.4159		
		A	1000	3.1046	4.4116		
6	32	A	1000		4.2836		
		$\bar{A}$	1000	2.9178	2.6946		
14	124	A	1000		4.8903		
		$\bar{A}$	1000	7.4731	4.7707		
		$\bar{A}$	1000	6.2989			
		$\bar{A}$	1000	6.8860			
6	32	A	500				3.5863
		$\bar{A}$	500			2.8391	3.0155
14	124	A	500		4.4578		
		$\bar{A}$	500	6.7957	5.0106		

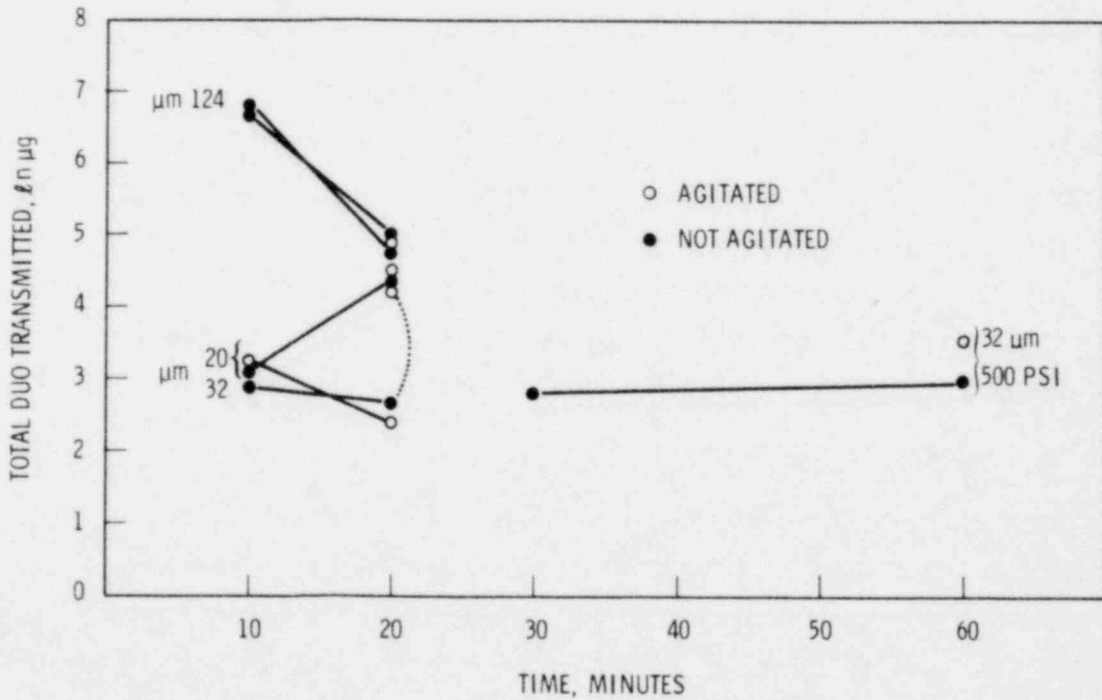


FIGURE B6. UPL Comparisons Over Time

TABLE B17. Averages and Standard Deviations for Orifice by Pressure

OID	$\mu\text{m}$	1000 psig		500 psig	
		Ave	sd	Ave	sd
2	20	3.29	0.8282		
6	32	3.30	0.8602	3.15	0.3906
14	124	5.86	1.2808	5.63	1.6531
14	124	10 min	6.89	6.80	
		20 min	4.83	5.01	
		Diff.	2.06	1.79	
		t	2.61	1.61	
		$\alpha (> t )$	0.05	>0.10	

so that

$$t = \frac{1.79}{1.1149} = 1.61$$

For ten degrees of freedom any t-value greater in absolute value than 2.23 should occur less than 5% of the time when the true difference is 0. The conclusion is that there is a significant time effect for the 124- $\mu\text{m}$  orifice at the 1000 psig level, but the effect is in the wrong direction. Total DUO transmitted is significantly less for a 20-min run than a 10-min run. The 1.79 difference at 500 psig is not significant statistically. The significant results are for one orifice at one pressure with replication for only the  $\bar{A}$  run at 1000 psig for 10 min and do not provide the data base required for inferences about the effect of time over all UPL runs.

Analysis of Variance for UPL Data

A subset of 57 of the 79 runs counted in Table B14 was selected for an analysis of variance on treatment means. The data for this analysis are given in Table B18. All the 50 and 5 psig data and the data for Orifices 1, 11 and 17 were ignored to provide a balanced design as far as treatment means were concerned. Sixteen of the treatments had replicate runs. Time was considered to be a source of experimental error and, therefore, was eliminated as a treatment factor.



TABLE B18. UPL Orifices Data for Analysis of Variance,  $\ln$  (DUO  $\mu\text{g}$ )

OID	$\mu\text{m}$	Pressure, psig							
		15		100		500		1000	
		A	$\bar{A}$	A	$\bar{A}$	A	$\bar{A}$	A	$\bar{A}$
2	20	3.0540	2.6101	4.0809	4.5788	2.5649	2.7081	3.2492	3.1046
				4.4272	2.7408			2.4159	4.4116
6	32	2.5337	1.9081	4.2341	4.9345	3.5863	3.0155	4.2836	2.6946
			1.5041	2.9857	3.2027		2.8391		2.9178
10	60	2.8565	3.9416	5.2470	4.2254	3.6109	4.2739	4.7095	4.0758
14	124	3.6163	3.2268	4.7875	6.1394	4.4578	6.7957	4.8903	7.4731
				5.8861	5.4638		5.0106		6.2989
									4.7707
18	200	6.3404	6.4265	6.3596	6.5067	7.5807	6.6995	8.4949	7.3840
				6.5639	7.1229				8.1719

The averages and sums of averages used for the analysis of variance are given in Tables B19A and B19B. The pressure-by-orifice averages are plotted in Figure B7. The analysis of variance is given in Table B20. The results of the AOV show that agitation did not have a significant effect. The average for the agitated runs was 4.52 and for the nonagitated it was 4.48  $\ln$  DUO. This 0.04  $\ln$  DUO agitation difference was not statistically significant. Consequently, the pressure-by-orifice averages, plotted in Figure B7 are sufficient to represent the structure in the data. The means for each orifice are plotted against pressure in the upper half of Figure B7 with orifice averages to the right. The only pronounced pressure effects are for the 20 to 100 psig points for orifices of 124- $\mu\text{m}$  dia or less, and a steady increase for the 200- $\mu\text{m}$  orifice. The bottom half of Figure B7 shows that diameter causes a steeper increase in  $\ln$  DUO transmitted than pressure does. It also shows that more  $\ln$  DUO was transmitted for 100 psig than for 500 or 1000 psig for the orifices of 124- $\mu\text{m}$  dia and smaller. Overall, the 100 and 1000 psig average transmissions are practically indistinguishable, 4.95 and 4.98  $\ln$  DUO, respectively (Table B19B).

TABLE B19A. Treatment Averages and Sums of Averages for UPL Orifices

OID	$\mu\text{m}$	Agitation	Pressure, psig				Orifice	
			15	100	500	1000	Total	Ave
2	20	A	3.0540	4.2540(a)	2.5649	2.8326	12.7100	3.18
		$\bar{A}$	2.6101	3.6598(a)	2.7081	3.7581	12.7631	3.18
		Sum	5.6641	7.9138	5.2730	6.5907	25.4416	
		Ave	2.83	3.96	2.64	3.30	3.18	
6	32	A	2.5337	3.6099(a)	3.5863	4.2836	14.0135	3.50
		$\bar{A}$	1.7061	4.0686(a)	2.9273	2.8062(a)	11.5062	2.88
		Sum	4.2398	7.6785	6.5136	7.0898	25.5217	
		Ave	2.12	3.84	3.26	3.54	3.19	
10	60	A	2.8565	5.2470	3.6109	4.7095	16.4239	4.11
		$\bar{A}$	3.9416	4.2254	4.2739	4.0758	16.5167	4.13
		Sum	6.7981	9.4724	7.8848	8.7853	32.9406	
		Ave	3.40	4.74	3.94	4.39	4.12	
14	124	A	3.6163	5.3368(a)	4.4578	4.8903	18.3072	4.58
		$\bar{A}$	3.2268	5.8018(a)	5.9032(a)	6.1809(a)	21.1127	5.28
		Sum	6.8431	11.1386	10.3610	11.0712	39.4139	
		Ave	3.42	5.57	5.18	5.54	4.93	
19	200	A	6.3404	6.4618(a)	7.5807	8.4949	28.8778	7.22
		$\bar{A}$	6.4265	6.8648(a)	6.6995	7.7780(a)	27.7688	6.94
		Sum	12.7669	13.3266	14.2802	16.2729	56.6466	
		Ave	6.38	6.66	7.14	8.14	7.08	
Pressure								
Total			36.3120	49.5299	44.3126	49.8099	179.9644	
Ave			3.63	4.95	4.43	4.98	4.50	

(a) Average based on more than one observation.

TABLE B19B. Treatment Averages and Sums of Averages for UPL Orifices

Agitation	Pressure		A	$\bar{A}$	Total
			15	Sum	18.4009
	Ave	3.68	3.58	3.63	
	100	Sum	24.9095	24.6204	49.5299
	Ave	4.98	4.92	4.95	
	500	Sum	21.8006	22.5120	44.3126
	Ave	4.36	4.50	4.43	
	1000	Sum	25.2109	24.5990	49.8099
	Ave	5.04	4.92	4.98	
Total			90.3219	89.6425	179.9644
Ave			4.52	4.48	4.50

Comparing Figure B7 to Figure B1, for the 30-min APLA experiment, the results for diameter are about the same, but pressure shows an increase only for the 200- $\mu\text{m}$  orifice for the UPL data. The declines between 100 and 500 psig and the lack of differences for the 100 and 1000 psig averages for all but the 200- $\mu\text{m}$  UPL orifice are further experimental anomalies with no obvious explanations.

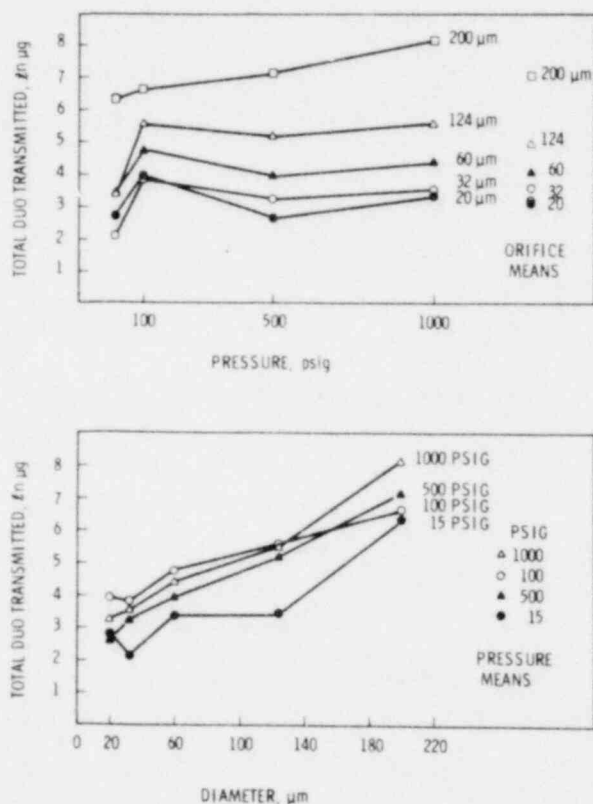


FIGURE B7. Pressure by Orifice Means, UPL Data

TABLE B20. Analysis of Variance on UPL Orifices Treatment Means

Source	df	Sum of Squares	Mean Square	F	P(>F)
Orifice	4	83.5714	20.8928	48.88	< 0.001
Pressure	3	11.9609	3.9870	9.33	< 0.001
Agitation	1	0.01154	0.1154	0.03	> 0.1
P X A	3	0.10886	0.03629	0.08	> 0.1
Error	28	11.96678	0.42739		
Total	39	107.6194			

### UPL Orifices - Grams DUO Varied

A series of runs (UPL runs 123 through 143) were made in the UPL apparatus to assess the effect of varying the amount of DUO between 25 and 300 g. This set of runs was not keypunched; therefore, a tabulation of the data, including flow (cc/min) and g DUO, is given in Table B21. All but the last two runs were of 30-min duration; runs 142 and 143 were for 80 min. Also, all runs used Orifice 13 at its 111- $\mu$ m dia.

A balanced subset of 18 of the 21 runs was selected for an analysis of variance. The treatments were defined by three weight levels by three pressure levels:

- Pressure (psig): 100, 500, 1000
- Weight of DUO:    Low: 25 to 27.2 g  
                      Medium: 100 g  
                      High: 247 to 300 g

There were two replicates of each of the nine treatments. Table B22 gives the data, sums and averages used for the analysis of variance of Table B23. The cell means are plotted in Figure B8.

The plots indicate an interaction caused mainly by the high (relative to theoretical expectation) mean for the 100 g-by-500 psig treatment. The analysis of variance did not find this apparent interaction significant. The small number of degrees of freedom combined with a large contribution to the error variances from a single cell caused the lack of sensitivity of the AOV. The 25 g-by-100 psig treatment accounted for almost 2/3 (65.7%) of the Error Sum of Squares. The next largest contribution was 18.1% from the 100 g-by-1000 psig cell. When the 25 g-by-100 psig cell was removed from the calculation of the error variance, the result was the adjusted error line of the AOV table. The weight by pressure (W x P) F-ratio was 2.785 with the 0.30399 error variances. Since the 90th percentile of the F-distribution with 4 and 8 degrees of freedom is 2.81, there are no grounds for judging the interaction statistically significant. The appropriate mean square for testing the main effects is that for the W x P interaction. This has only four degrees of freedom. Since the

TABLE B21. Data for UPL Grams DUO, Varied Runs (Orifice 13 at 111  $\mu\text{m}$ )

<u>DUO, g</u>	<u>psig</u>	<u>Run</u>	<u>cc/min</u>	<u>DUO <math>\mu\text{g}</math></u>	<u><math>\ln</math> (DUO <math>\mu\text{g}</math>)</u>
25	100	140	152	7.42	2.0042
25	100	125	210	157	5.0562
25	500	131	1080	37.2	3.6163
27.2	500	137	465	17.2	2.8449
25	1000	129	5600	196	5.2781
25	1000	132	4800	258	5.5530
57.5	1000	139	3200	198	5.2883
100	100	126	305	123	4.8122
100	100	134	135	72.4	4.2822
100	500	130	2600	289	5.6664
100	500	133	2350	158	5.0626
100	1000	123	2000	75.1	4.3188
100	1000	141	4650	373	5.9216
281.9	100	135	345	138	4.9273
300	100	127	147	55.1	4.0091
247	500	124	730	69.7	4.2442
275.7	500	138	535	48.7	3.8857
282.8	1000	136	5050	331	5.8021
300	1000	128	2090	304	5.7170
281	1000	142	5150	933	6.8384
284	1000	143	5050	210	5.3471

TABLE B22. Data, Sums and Averages for UPL-Grams DUO Varied Runs (n DUO)

Weight	g	Pressure, psig			Weight Total	
		100	500	1000		
Low	25		2.0042	3.6163	5.2781	10.8986
			<u>5.0562</u>	<u>2.8449</u>	<u>5.5530</u>	<u>13.4541</u>
		Sum	<u>7.0604</u>	<u>6.4612</u>	<u>10.8311</u>	<u>24.3527</u>
		Ave	3.53	3.23	5.42	4.06
Medium	100		4.8122	5.6664	4.3188	14.7924
			<u>4.2822</u>	<u>5.0626</u>	<u>5.9216</u>	<u>15.2664</u>
		Sum	<u>9.0944</u>	<u>10.7290</u>	<u>10.2404</u>	<u>30.0638</u>
		Ave	4.55	5.36	5.12	5.01
High	280		4.9273	4.2442	5.8021	14.9736
			<u>4.0091</u>	<u>3.8857</u>	<u>5.7170</u>	<u>13.6118</u>
		Sum	<u>8.9364</u>	<u>8.1299</u>	<u>11.5191</u>	<u>28.5854</u>
		Ave	4.47	4.06	5.76	4.76
Pressure Total		Sum	25.0921	25.3201	32.5906	83.0019
		Ave	4.18	4.22	5.43	4.61

TABLE B23. Analysis of Variance for UPL-Grams DUO Varied Runs

Sources	df	Sum of Sources	Mean Square	F	P(>F)
Weight	2	2.9288	1.4644	1.729	>0.1
Pressure	2	6.0641	3.0321	3.581	>0.1
W x P	4	3.3868	0.8467	1.075	>0.1
Error	9	7.0993	0.7877		
Total	17	19.4689			
Adjusted Error (a)	8	2.4319	0.30399		

(a) This is the variance of the within-W x P cell differences from the cell means with the large difference for the 25 g-by-100 psig runs removed.

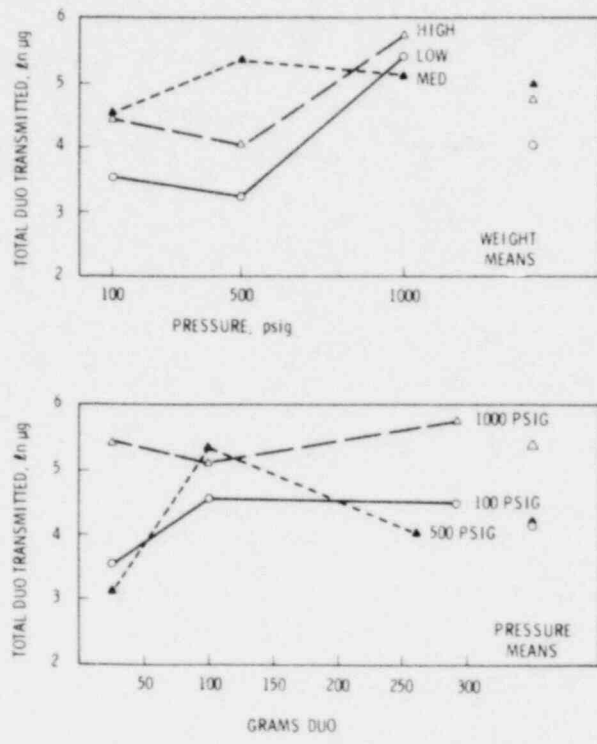


FIGURE B8. Cell Means for Weight-Varied UPL Runs

90th percentile of the F-distribution with 2 and 4 degrees of freedom is 4.19, neither the pressure nor the weight main effects can be judged to be significantly different.

The conclusion is that the AOV was not sensitive enough to detect any differences among the cell means or among the weight or pressure means.

This conclusion is reinforced by a nonparametric test of the hypotheses that the treatment means are randomly ordered. The test is based on comparing the ranking of cell means with a logical theoretical ordering of the cells. Assuming that amount of DUO, (weight), has a minor effect relative to pressure, a logical ordering of the cells is:

Weight	Pressure, psig		
	100	500	1000
25	1	4	7
100	2	5	8
280	3	6	9

The observed ordering based on cell means was:

Weight	Pressure, psig		
	100	500	1000
25	2	1	8
100	5	7	6
280	4	3	9

Kendall's rank correlation coefficient can be used to make the desired comparison. The corresponding ranks are set out below for more convenient comparison.

	psig								
	100			500			1000		
Theoretical	1	2	3	4	5	6	7	8	9
Observed	2	5	4	1	7	3	8	6	9

Kendall's rank correlation coefficient for this comparison is  $T = 0.055$ . The probability that  $T = 0.055$  under the null hypothesis that the theoretical and observed rankings are randomly related, i.e., there is no true association, is 0.460. There are no grounds for concluding that the means follow the assumed theory.

#### APLA Capillary Runs

The 34 experimental APLA runs using a single capillary resulted in useable data for 23 runs. Two sets of capillaries were used. One set had lengths ranging from 0.726 cm to 0.782 cm and average diameters from 58 to 276  $\mu\text{m}$  and were designated the Short Set. The second set, called the Long Set, was made up of longer capillaries, 2.54 cm to 2.95 cm, with average diameters between 48 and 274  $\mu\text{m}$ . The capillaries used and the pressures they were run at in the APLA are given in Table B24, which includes only the 23 useable runs. None of the samples through long capillary 250A were useable, and two of four 200S runs had negligible DUO values, as did two of the five runs using 100B. All four long capillary runs at 100 psig resulted in samples with less than 1  $\mu\text{g}$  DUO. Sixty-eight percent of the capillary runs produced valid data. The



TABLE B24. APLA Capillaries Data,  $\ln$  DUO

Capillary Designation	S or L	$\mu\text{m}$	Pressure, psig			
			30	100	500	1000
50-A	L	48	2.1691		3.2189	4.9628
75-S	S	58				3.5175
100-S	S	97				3.1046
100-B	L	99	1.6014		1.3350	4.4751
150-S	S	132	2.8904	5.7683	5.6699	5.3566
150-A	L	189				7.1546
150-B	L	176	2.5177		6.5793	
200-S	S	228	2.5649		8.1137	
200-B	L	231				7.8973
250-S	S	276	5.3739	5.2364	6.5147	9.1280
250-B	L	274	1.7750			
Duration of Run at Pressure (min)			60	30	30	10

usual reason for lower than expected sampled DUO was plugging of the capillary shortly after the run started.

There is not enough data on the capillaries to provide the basis for detailed statistical analysis. Ignoring the variability due to duration of the runs, the six nominal capillary diameters times the two lengths times the four pressures would require 48 experimental runs to have each possible treatment represented once (which would not provide an estimate of statistical experimental error). The 23 valid data points do not provide enough information to characterize the relative importance of diameter, length, and pressure for transport of DUO through capillaries. However, descriptive results are possible that might provide the basis for some questions for future study. All 30 psig runs were of 60-min duration; the 100 and 500 psig runs lasted 30 min; and the 1000 psig runs lasted 10 min.

The data are arranged in a nominal diameter by short-long by pressure matrix in Table B24, and the logarithms of the data are plotted in Figure B9.

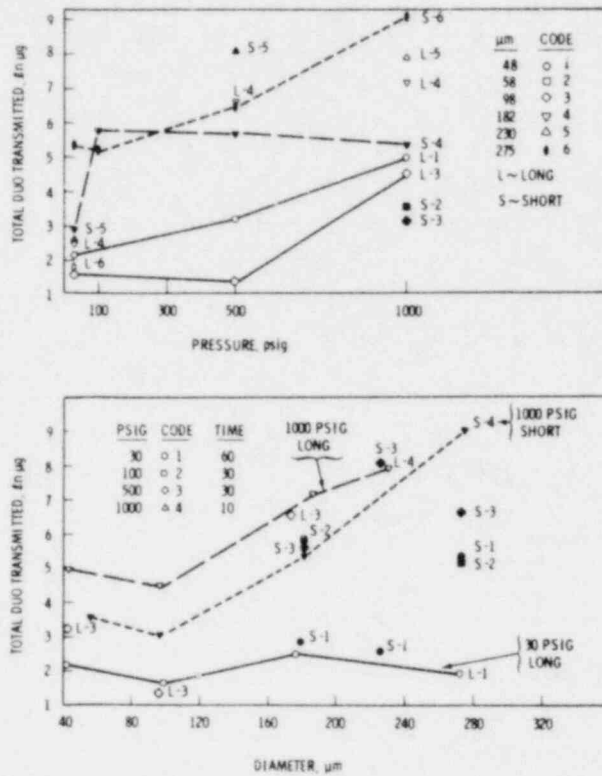


FIGURE B9. APLA Capillary Data

Since each of the 23 points is plotted in both parts of Figure B9, a code was used to designate the short or long by diameter combination in the upper part and the short or long by pressure treatment in the lower part. Only points for a treatment spanning the range of the abscissa are connected. Points are plotted at the average  $\mu\text{m}$  for the nominal diameter group. From the lower half of Figure B9 we see that the low pressure (30 psig) runs showed no steady increase with increasing diameter. The only exception is for the largest (276- $\mu\text{m}$ -diameter) short capillary (the point at 5.4  $\ln$  DUO). Another feature of Figure B9 is the consistent drop for all pressure levels for the 100- $\mu\text{m}$  capillaries. High pressure (1000 psig) does produce increasing DUO transmission for both long and short capillaries with increasing diameter if the drop at 100  $\mu\text{m}$  is ignored. At this high pressure the pattern is the same with the long having greater transmission than the short capillaries. The other data points show some relationships as expected, while other relationships are the reverse of the expected.

In the top half of Figure B9,  $\lambda_n$  DUO transmitted is plotted against pressure for each run. The results for the 98- $\mu\text{m}$  long capillary (L-3) are consistently lower than for the 48- $\mu\text{m}$  long capillary. The largest short capillary (275  $\mu\text{m}$ ) starts out high at 30 psig, then drops below the 182- $\mu\text{m}$  capillary at 100 psig, from which it follows the expected pattern. The 182- $\mu\text{m}$ -short capillary produced samples that were anomalously high at the 100 and 500 psig levels.

In terms of overall boundaries, the results for the capillaries are not different from those for the orifices. Both data sets were run at the same pressures, but the orifice diameters were between 22 and 226  $\mu\text{m}$ . For the 30-min experiment using orifices, the transmissions were between 2 and 3060  $\mu\text{g}$  DUO. Capillary transmissions were between about 5 and 3300  $\mu\text{g}$  DUO for diameters between 43 and 231  $\mu\text{m}$ .

The two most important observations about Figure B9 are:

- The transmissions for 30 psig were random for all capillaries except the largest short capillary as evidenced by the cluster of points at the 30 psig value in the psig plot and the locations of the 30 psig points in the  $\mu\text{m}$  plot.
- At 1000 psig, greater transmission was observed for long than short capillaries as evidenced by the lines for 1000 psig in the  $\mu\text{m}$  plot.

### SENSITIVITY ANALYSIS

The main reason for performing the preceding statistical analyses was to determine the impact of the experimental conditions on the amount of DUO transmitted. An experimental condition that had no significant impact on the amount of DUO transmitted would be of little use as a predictor of the amount of DUO transmitted. As a result of the lack of comparable treatments (opening-by-pressure combinations), these attempts at sensitivity analysis did not always provide conclusive results although some definite conclusions and tentative statements are possible.

The experimental conditions can be divided into two groups: those that were categorical and those that were continuous measured quantities. The

conditions in the first group are: apparatus type, opening type, aerosolization mechanism, and flow mechanism. The second group consists of orifice diameters, chamber pressure and duration of run. In the first group of conditions, only the APLA flow mechanism and the UPL aerosolization mechanism have been analyzed in detail. Table B25 provides the data that will be used to clear up the loose ends.

TABLE B25. Cell Means<sup>(a)</sup> for UPL and APLA Comparisons

OID	$\mu\text{m}$		UPL psig			APLA psig		
			100	500	1000	100	500	1000
2	20	L	3.96	2.64	3.30		3.76	2.58
3	21					0.12	1.06	1.08
4	23							1.21
1	24				2.01	0.94		
8	28	L					1.64	1.78
6	32		3.83	3.15	3.30		1.78	2.76
7	34	L				0.84	2.12	1.59
5	40					1.42	1.76	2.06
10	60	L	4.74	3.94	4.40		4.00	4.02
11	64		3.44	2.34	4.39	1.73	2.39	3.75
9	66					2.71	2.25	2.39
15	94	L				2.82	3.58	4.83
13	106					3.64	4.85	6.43
14	124		5.57	5.42	5.86			7.23
19	195	L				4.13	6.16	7.83
18	200		6.66	7.14	8.01			9.07
17	213			8.49	8.42	4.39	7.32	8.27
Capillaries								
22	149		4.52	5.95	7.23			
21	182		7.04	6.62	7.31	5.77	5.76	5.36
24	274		6.44	6.06	6.94			
23	276		7.91	9.47	10.34	5.24	7.82	

(a) Based on one to eight runs; averaging is over A and  $\bar{A}$  for UPL data.

## Apparatus Type

Figures B10 and B11 provide the basis for comparing the  $\ln$  (DUO) transmitted by the APLA and UPL apparatus using comparable orifices at 500 and 1000 psig. (The figures also have plots of the cell means for the capillary runs, C.A or C.U.) Table B26 has three 2 x 2 tables giving the number of times the UPL mean exceeded the APLA mean; the tables break the comparisons at 100  $\mu\text{m}$ . The Fisher exact probability test on the tables and the binomial test on the right marginals indicate that there is no reason to conclude that the 2 x 2 tables reflect anything other than random behavior. The most extreme marginals are in Table B26A. The probability that a 1-6 split occurs is 0.124, which is not small enough to reject the null hypothesis that  $U > A$  or  $A > U$  is equally likely. The conclusion is that the UPL and APLA transmissions of DUO do not differ significantly. That is, the apparatus used makes no difference. This implies that under powder leaks and above powder leaks could be characterized by the same prediction equation.

## Opening Type

All of the cell means for the capillaries runs and orifices of 94- $\mu\text{m}$  dia or larger listed in Table B25 are plotted in Figure B12. Because of the lack of balance in the orifice by pressure treatments, graphical interpretation is again used to provide indications of relationships. Since so much data is plotted in Figure B12, it requires considerable study to interpret. The points plotted are the orifice-by-pressure cell means for the four data sets: APLA orifices, APLA capillaries, UPL orifices, and UPL capillaries. Orifices of different diameters run at the same pressure are connected by the lighter lines and capillaries by the heavier lines.

The question of interest is: does transmission through orifices differ from transmission through capillaries? No consistent dominance is evident from the plot. At 1000 psig the high capillary value for UPL at 176  $\mu\text{m}$ , 7.23  $\ln$  DUO, contradicts the slight dominance of both the APLA and UPL orifices. Only a single APLA capillary mean is available at 1000 psig, 5.36  $\ln$  DUO at 182  $\mu\text{m}$ , and this value does not significantly differ from and is lower than the transmissions for 100 and 500 psig. At 500 psig the UPL capillaries and

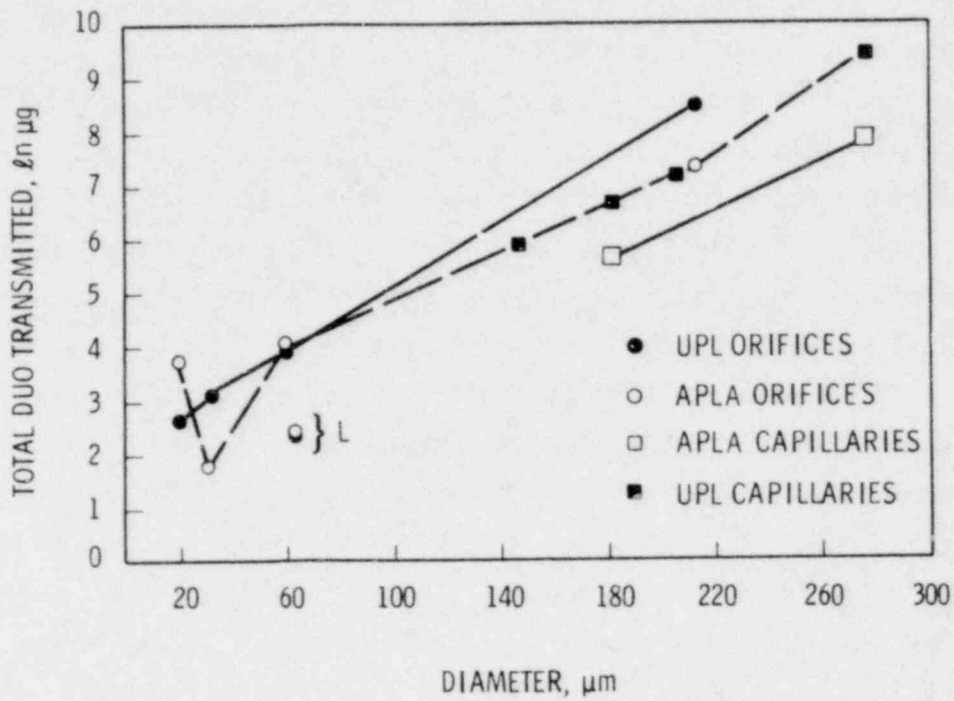


FIGURE B10. UPL vs APLA at 500 psig

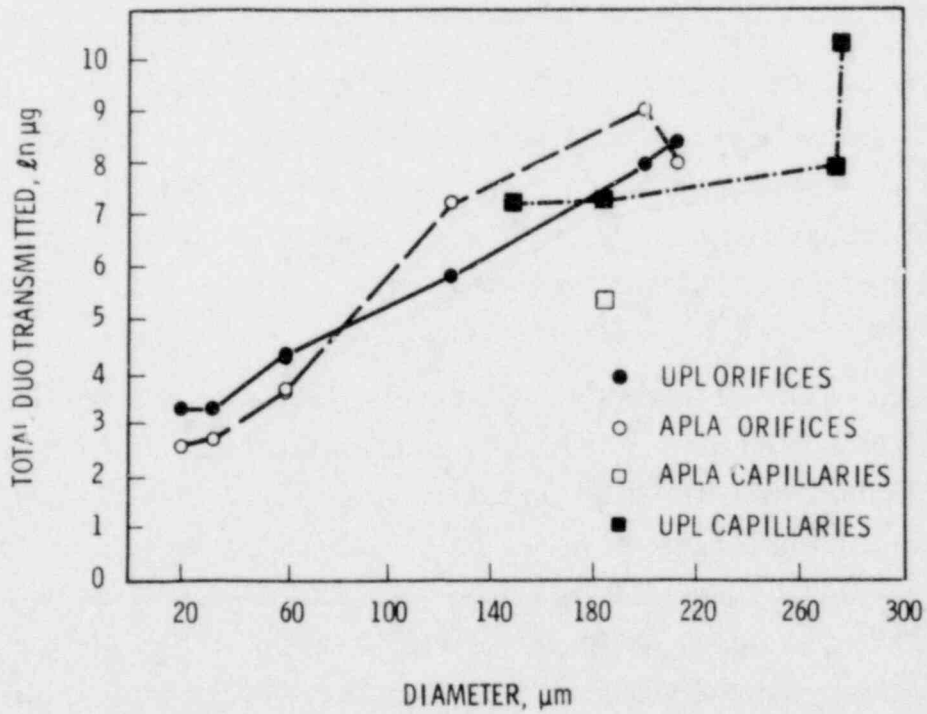


FIGURE B11. UPL vs APLA at 1000 psig

TABLE B26-A,B,C. Two-by-Two Tables Comparing APLA and UPL Dominance

A.	500 psig		
	$\mu\text{m} < 100$	$\mu\text{m} > 100$	Total
U>A	1	0	1
A>U	3	3	6
Total	4	3	

B.	1000 psig		
	$\mu\text{m} < 100$	$\mu\text{m} > 100$	Total
U>A	4	2	6
A>U	0	2	2
Total	4	4	8

C.	500 and 1000 psig		
	$\mu\text{m} < 100$	$\mu\text{m} > 100$	Total
U>A	5	2	7
A>U	3	5	8
Total	8	7	15

orifices had about the same  $\ln$  DUO means, except for the high orifice result at 213  $\mu\text{m}$ . Both the UPL orifices and capillaries results dominated the APLA orifices and capillaries at 500 psig. At 100 psig the APLA capillaries contradict theory by showing a slight decline in  $\ln$  DUO with increasing diameter. But the APLA capillary transmission does exceed that for the orifices. The dominance is reversed for the UPL comparison at 100 psig.

One way of clarifying these confusing results is to rank the lines for each of the four data sets at each pressure as is done in the following table. Ranking was done by overall dominance from lowest (rank 1) to highest (rank 4) so that the ranks have the same order as the lines:

psig	UPL		APLA	
	O	C	O	C
1000	3	2	4	1
500	4	3	2	1
100	4	3	1	2
Sum	11	8	7	4
Rank of Sum	4	3	2	1

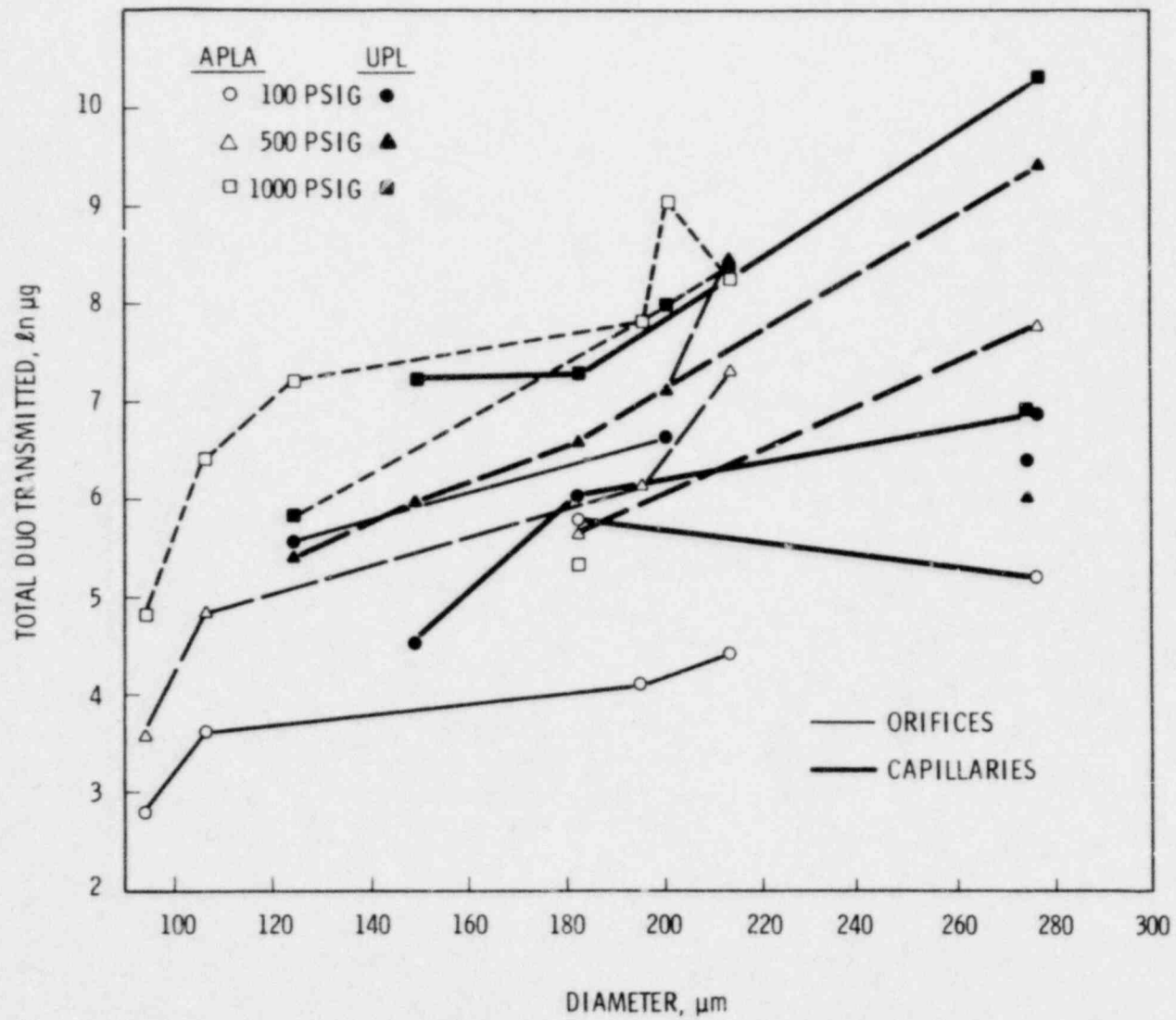


FIGURE B12. Apparatus by Opening Type Comparison - Cell Means



The ranks of the sums indicate the overall ordering of the data sets. The Friedman two-way analysis of variance by ranks can be used to test the null hypothesis that the results from each of the four data sets come from the same statistical population. The test is based on the sums for each data set. If the four data sets were from the same population then the sum of the ranks in each column would be close to 7.5, the expected value of the sum under the above null hypothesis. The test statistic is

$$\chi_r^2 = \left[ \frac{12}{Nk(k+1)} \sum_{j=1}^4 (\text{sum}_j)^2 \right] - 3N(k+1)$$

where

N = number of rows = 3

k = number of columns = 4

so that

$$\chi_r^2 = \frac{12}{3 \cdot 4 \cdot 5} \left[ (11)^2 + (8)^2 + (7)^2 + (4)^2 \right] - \left[ 3 \cdot 3 \cdot 5 \right] = 20$$

Siegel (1956, p. 281), gives a table of probabilities of the test statistics from which it was determined that a  $\chi_r^2$  value greater than 9.0 has a probability of occurrence under the null hypothesis of 0.0017. There is ample grounds for rejecting the null hypothesis on the basis of the observed test statistic that is more than twice as large as the most extreme value tabulated by Siegel. The chance that the four data sets come from the same statistical distribution is much less than one in a thousand. The conclusion is that the four data sets do produce significantly different transmissions of DUO.

This test reduced each data set to a mean rank for each of the three pressures. Points that might be anomalous or merely reflect experimental variability were ignored in the ranking of the lines. In particular, the three UPL capillary points at 174  $\mu\text{m}$  for 1000 psig were ignored. The conclusion based on this test must be taken cautiously, but there are grounds

for concern that both the apparatus type and opening type do have a significant effect on DUO transmitted. The UPL dominated the APLA, and orifices dominated the capillaries overall.

#### Aerosolization Mechanism

The APLA had an air-sparging mechanism for producing the aerosol. This mechanism was not changed during the course of the study, and, therefore, there is no reason to study it. Some multiple orifice runs were performed in the APLA to characterize the aerosol distribution in space and time, but the results were inconclusive.

The UPL used external agitation or no agitation, along with chamber pressure, as the forces to move powder to the sampler. The analysis of variance of Table B20 showed that agitation made no difference.

#### Flow Mechanism

The analysis of variance of Table B11 showed that the modification to the APLA allowing chamber pressure-driven flow, as opposed to vacuum-maintained flow, made no difference in the amount of DUO transmitted.

The sensitivity analysis of the categorical variables resulted in these conclusions:

- apparatus type may have an effect
- orifice type may have an effect
- UPL agitation had no effect
- APLA maintained flow had no effect.

Previous results for the measured variables indicated that:

- orifice diameter has a pronounced effect
- chamber pressure has a low pronounced effect
- duration of run does not have a discernible effect on the logarithmic scale.

## PREDICTION EQUATIONS

### Statistical Models

Many experimental and theoretical variables indicative of flow were considered as predictors of the amount of DUO transmitted. They included the natural logarithms of:

- $A\sqrt{P}$ , the average cross-sectional area times the square root of chamber pressure,
- cc/min, the typical rotameter reading during the run,
- $F_m$ , the average flow through the opening measured in the opening calibration apparatus,
- $M$ , the theoretically expected total mass flow during the pressurization and depressurization ramps,
- $V$ , the theoretically expected total volume flow for the pressurization and depressurization ramps

for the simple linear model; and  $A$  and  $\sqrt{P}$  for the multiple linear model. These variables were used as predictors of  $\ln$  DUO and  $\ln$  (DUO/min). The linear relationships for the raw (untransformed) data were also investigated.

The logic of the use of the transformation and the linear model is as follows. The transmitted DUO is a function of flow and aerosol concentration, that is, most simply,

$$\text{DUO} = aF$$

where:

- DUO is the micrograms of uranium transmitted,
- $a$  is an aerosolization constant, and
- $F$  is a measure of flow.

The flow itself is a function of cross-sectional area, chamber pressure and

orifice characteristics. In a previous project report<sup>(a)</sup> the theoretical flow measure, F, was defined as:

$$Q = \alpha A \psi \sqrt{2g\rho_0 P_0}$$

where:

- $\alpha$  is an orifice constant (equal to unity for theoretical flow and 0.80 to 0.88 for the orifice calibration runs),
- A is the cross-sectional area,
- $\psi \sqrt{2g\rho_0}$  is an airflow constant at an upstream pressure, and
- $P_0$  is the upstream pressure.

Since  $\alpha$  is also a function of upstream pressure, the flow equation can be written

$$Q = K_0 A \sqrt{P_0}$$

where  $K_0$  is the air flow constant for upstream pressure,  $P_0$ . Then,

$$\text{DUO/sec} = a \left[ K_0 A \sqrt{P_0} \right] \text{g/sec.}$$

Multiplying both sides by seconds gives

$$\text{DUO} = (aK_0) A \sqrt{P_0}$$

or setting a  $K_0$  equal  $a_0$ ,

$$\text{DUO} = a_0 A \sqrt{P_0}$$

---

(a) Appendix C of Sutter, S.L., T.J. Bander, J. Mishima, and L.C. Schwendiman. 1978. Measured Air Flow Rates Through Microorifices and Flow Prediction Capability, NUREG/CR-0066, PNL-2611, Pacific Northwest Laboratory, Richland, WA.

This multiplicative model can be linearized by taking the (natural) logarithm of each side,

$$\ln \text{DUO} = \ln a_0 + \ln A + 1/2 \ln P_0$$

In the experiment, four different upstream pressures,  $P_0$ , were routinely used: 30, 100, 500 and 1000 psig. A statistical model for the orifices (i) by pressure (j) by run (k) within the (i,j) treatment combination is:

$$\ln \text{DUO}_{ijk} = \alpha + \beta_1 \ln A_i + \beta_2 \ln \sqrt{P_j} + \epsilon_{ijk} \quad (1)$$

This model uses the upstream pressures,  $P_j$ , and allows separate assessment of the impact of area and pressure. Another model, combining the effects of area and pressure is

$$\ln \text{DUO}_{ijk} = \alpha + \beta \ln (A_i \sqrt{P_j}) + \epsilon_{ijk} \quad (2)$$

Least squares fits of these models to the data were used to estimate the parameters (the  $\alpha$ 's and  $\beta$ 's) in these models. Other models were also investigated. These models were of the same form as the above, but  $A\sqrt{P}$  was replaced by other indicators of flow and DUO by DUO/minute. The statistical problem was to select the best model from these logically tenable characterizations of the structure in the data.

### Correlations

Inspection of the simple correlation coefficients between the dependent variables,  $\ln \text{DUO}$  and  $\ln \text{DUO}/\text{min}$ , and the independent variables led to the conclusions that  $\ln A\sqrt{P}$  was the best candidate for predicting  $\ln \text{DUO}$  or  $\ln \text{DUO}/\text{min}$  and that  $\ln \text{DUO}$  characterizes the transmission slightly better than  $\ln \text{DUO}/\text{min}$ . The correlation coefficients are given in Table B27.

The correlations for the measured variables,  $A\sqrt{P}$  through  $F_m$  are based on 98 timed runs in the APLA. The four theoretical variables used the 150

TABLE B27. Correlations

Independent Variable	Dependent Variable		Description of Independent Variable
	$\ln \text{ DUO}$	$\ln \text{ DUO/min}$	
$\ln (A\sqrt{P})$	.8959	.8834	Measured area and pressure
$\ln A$	.8073	.7510	Measured area, $\mu\text{m}^2$
$\ln P$	.3277	.4220	Measured pressure, psig
$\ln (\text{cc/min.})$	.8577	.8495	Typical flow during run, rotameter reading
$\ln F_m$	.8610	.8801	Measured flow in calibration apparatus, cc/min
$\ln M$	.7920	.8572	Theoretical mass flow during pressurization ramps
$\ln V$	.8931	.8604	Theoretical volume flow during pressurization ramps
$\ln V'$	.6762		Theoretical volume flow for duration of run, standard conditions
$\ln V''$	.8087		Theoretical volume flow for duration of run, uncorrected

"zero"-time and timed runs in the APLA. The natural logarithm of  $(A\sqrt{P})$  has the highest correlations with both  $\ln \text{ DUO}$  and  $\ln (\text{DUO/min})$ ,  $r = 0.8959$  and  $r = 0.8834$  respectively. The difference between these  $r$ 's is not statistically significant, but the point is that use of duration of run does not improve the correlation. Cross-sectional area,  $\ln A$ , has substantial correlations taken by itself. Adjusting DUO for duration of run did not improve the correlation with area, but it did improve the correlation with pressure,  $\ln P$ . The actually measured flow during the run,  $\ln(\text{cc/min})$ , was not as highly correlated as the flow measured in the orifice calibration apparatus,  $\ln F_m$ .

Among the theoretical flow indicators,  $\ln V$  has a correlation with  $\ln \text{ DUO}$ , which is almost the same as  $\ln (A\sqrt{P})$ . Since  $\ln V$  is the total theoretical volume flow during the pressurization and depressurization ramps only, the

absence of a time effect is reinforced, particularly, when it is noted that the correlation drops from 0.8931 for  $\ln V$  to 0.6762 for  $\ln V'$ , the theoretical volume airflow for the total duration of the run standardized for pressure and temperature.

Based on this inspection of the correlations and the fits of the data to Model 2, above, it was decided to investigate the models using  $\ln A$ ,  $\ln \sqrt{P}$  and  $\ln (A\sqrt{P})$ . Since an effect for duration of run is difficult to exclude because of its strong theoretical foundation, both  $\ln DUO$  and  $\ln (DUO/\text{min})$  were tried as the dependent variables.

There were two reasons for not investigating the theoretical variables further. First, the data to be used included the results for the UPL apparatus and capillaries and the theoretical flow parameters would have to be determined and theoretical flows calculated for the physical and dynamic differences from APLA runs. Second, there was no improvement in the correlation for the theoretical variables over the correlation for the measured diameter and pressure correlation.

#### Statistics for $\ln DUO$ Data

Inspection of plots of the data led to the conjecture that there was a threshold mechanism operating. The 240 data points used are plotted as Figure B13. Each data set has its own symbol. When two or more points coincide, the numerosity of the coinciding points is plotted. This plot is intended to illustrate the randomness of the points with  $\ln (A\sqrt{P})$  less than 10.5, which are blocked off in the lower left hand corner, and the increasing trend for the higher flow points. It appeared that the  $\ln DUO$  sampled was independent of pressure and diameter for values of  $\ln (A\sqrt{P})$  less than 10.5 and that for higher values of  $\ln (A\sqrt{P})$ , the  $\ln DUO$  transmitted increased linearly. The separation at 10.5 is admittedly subjective, but it helped cure the non-linearity in the fits and so was practically useful. Also, random results at lower diameters and pressures do not seem unreasonable given the precision of measurement and degree of experimental control. Table B28 compares the statistics for the four data sets defined by apparatus type (UPL and APLA) and

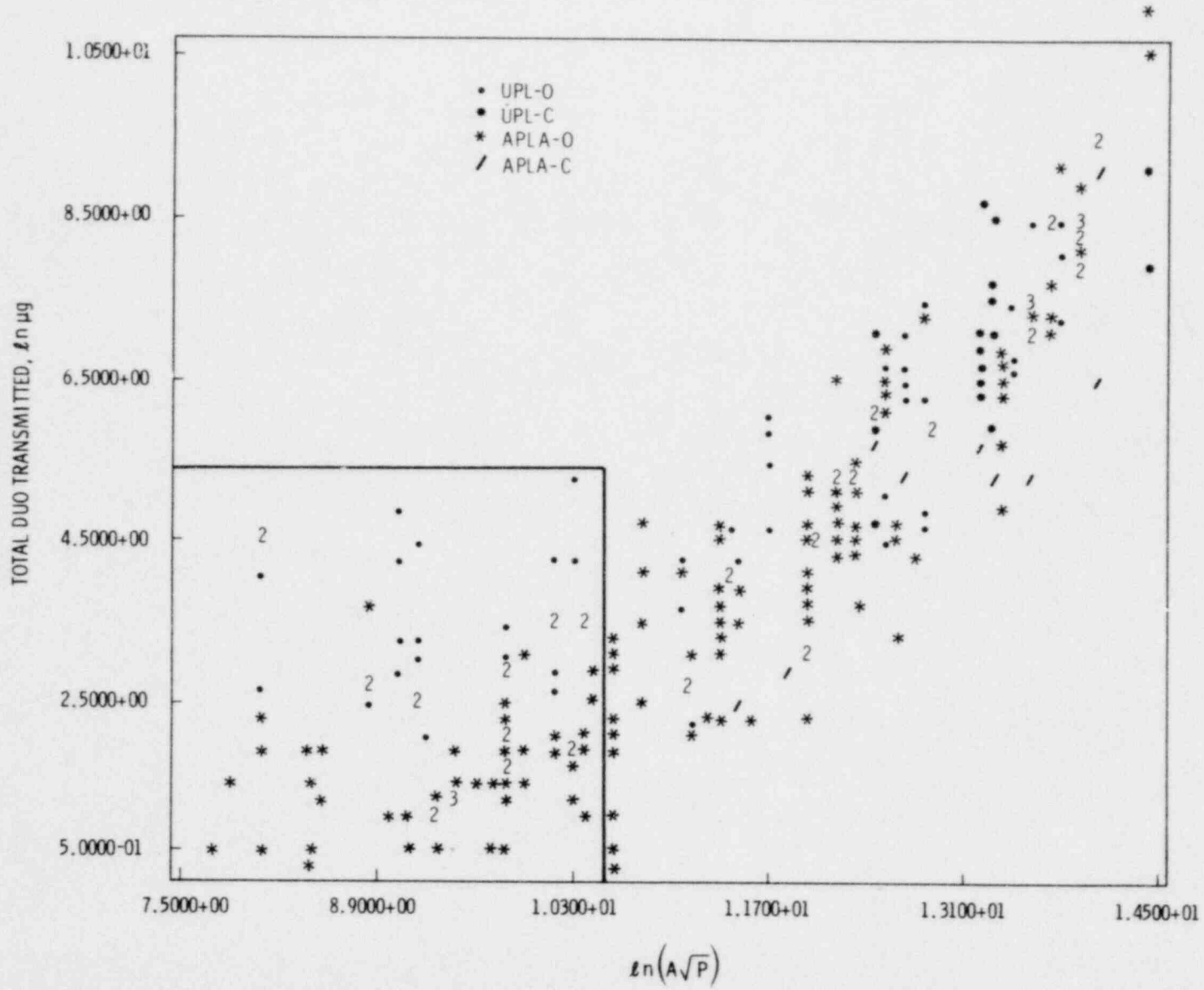


FIGURE B13. Plot of All Data Used to Select Best Fit



TABLE B28. Statistics for  $\ln$  DUO Data Used in Regression Equations

Total			Greater than 10.5			Less than 10.5		
N	UPL	APLA	N	UPL	APLA	N	UPL	APLA
0	53	150	0	28	91	0	25	59
C	28	9	C	28	9	C	0	0
Total	81	159	Total	56	100	Total	25	59
All	240		All	156		All	84	
Ave.	UPL	APLA	Ave.	UPL	APLA	Ave.	UPL	APLA
0	4.80	3.62	0	5.97	4.89	0	3.49	1.66
C	7.23	5.38	C	7.23	5.38	C	--	--
Total	5.64	3.72	Total	6.60	4.93	Total	3.49	1.66
All	4.37		All	5.53		All	2.21	
sd	UPL	APLA	sd	UPL	APLA	sd	UPL	APLA
0	1.8064	2.3138	0	1.6188	2.0680	0	0.8586	0.8268
C	1.6954	1.9359	C	1.6954	1.9359	C	--	--
Total	2.1068	2.3251	Total	1.7604	2.0521	Total	0.8586	0.8268
All	2.4271		All	2.1057		All	1.1772	
R <sup>2</sup> %	UPL	APLA	R <sup>2</sup> %	UPL	APLA	R <sup>2</sup> %	UPL	APLA
0	65.3	80.1	0	71.1	80.2	0	0.2	14.7
C	74.0	73.5	C	74.0	73.5	C	--	--
All	73.5		All	78.4		All	13.6	

opening type (O-orifice and C-capillary). For each data set, statistics are given for the total (all the data in the data set) and the two subsets consisting of the runs with  $\ln(A\sqrt{P})$  greater than 10.5 and less than 10.5 respectively. The statistics given are:

- N, the number of runs upon which the other statistics were based,
- Ave, the average of the N observations,
- R<sup>2</sup>% the squared multiple correlation coefficient giving the percentage of total variability of the  $\ln$  DUO data accounted for by the fit to the model  $\ln \text{ DUO} = a + b \ln(A\sqrt{P})$
- sd, the standard deviation of the N observation

### Number of Observations

A total of 240 runs were used in the search for the best prediction equation. Only 81 of the 122 UPL runs were included. There were two reasons for excluding runs after the runs with plugging or air leaks were excluded. First, 58 runs were removed because experimental conditions were not compatible with the bulk of the data. Second, during the analysis, 7 runs were removed because they caused excessive variability in the fits because the amount of DUO transmitted was too low for the potential airflow as measured by  $\ln(A\sqrt{P})$ . Twenty-five UPL orifice runs were excluded because they were run at 5, 15, or 50 psig and would require extensive recoding of the computer programs, if they were included. One more UPL orifice run was excluded because it had anomalously low  $\ln$  DUO transmission. This left 53 of the 79 UPL orifice runs. The number of UPL capillary runs were reduced from 43 to 31 by eliminating the 12 runs at 15 and 50 psig. Three more UPL-C runs with medium  $\ln$  DUO for high  $\ln(A\sqrt{P})$  were removed, leaving 28 runs in this data set. The 10 pressure decay and long duration runs were not included in the APLA orifices data set. For the APLA capillaries, the 23 runs of Table B24 were reduced to 12 by removal of 11 runs using capillaries that were not used in the UPL runs. This number was reduced to 9 by elimination of 3 runs with low  $\ln$  DUO. Note in Table B28 that there were no capillary runs used that had  $\ln(A\sqrt{P})$  less than 10.5 and that the APLA-C data set had only 9 runs. Had more time and funds been available, the computer coding required to include the 58 runs with noncompatible conditions would have been done. Most of the excluded runs were at the lower airflows, and so it was felt their inclusion would not contribute much to understanding the relationship between flow and DUO transmission.

### Averages

The averages are reported for completeness. The fact that the UPL averages are always greater than the APLA averages is not surprising since  $\ln(A\sqrt{P})$  was larger on the average for the total, 12.88 and 12.29 respectively. Capillary  $\ln$  DUO averages were also greater than orifice averages, again due to the larger diameter openings used.

### Standard Deviations

The standard deviations,  $sd$ , measure the variability of the data in each data set and subset. The most important comparison is for the  $\ln(\overline{AVP})$  less than 10.5 subtable. The standard deviations for the separate UPL and APLA total row are quite comparable in magnitude, 0.8586 and 0.8268  $\ln$  DUO respectively. This magnitude for the  $sd$  is also comparable with the standard deviations obtained for various within-treatment (opening diameter-by-pressure) standard deviations previously estimated:

- 0.6782 for the APLA 30-min experiment,
- 0.8254 for the APLA measured flow runs,
- 0.7897 for the UPL orifices

This comparison lends credence to the hypothesis that the variability for runs with  $\ln(\overline{AVP})$  less than 10.5 is not different from the experimental variability due to random error. Formal F-tests on the variances associated with these standard deviations resulted in the conclusion that they all estimated the same underlying experimental variability. However, when the UPL and APLA runs with  $\ln(\overline{AVP})$  less than 10.5 were combined, the resulting variability was significantly larger due to the significant difference between means [3.49-1.66 = 1.83  $\ln$  DUO].

The standard deviations for the runs with  $\ln(\overline{AVP})$  greater than 10.5 are about twice as large as those for runs at the lower airflows. The variances (standard deviation squared) are not statistically significantly different despite the range of  $sd$ 's from 1.6188 to 2.0680  $\ln$  DUO. But the differences between pairs of averages are significant statistically. These mean differences could reflect greater transmission for the UPL apparatus or through capillaries, but the cause of the differences could also be the larger average airflows for the UPL apparatus and for the capillaries. The decision on whether or not to pool the orifice and capillary runs within apparatus type and whether or not to pool the apparatus types will be deferred until the results of the fits for each data set are reviewed.

### Multiple Correlation Coefficients

The last set of subtables in Table B28 gives the squared multiple correlation coefficients,  $R^2\%$  for fits to the model

$$\ln DUO = a + b \ln (A\sqrt{P})$$

Again, the most important information is in the subtable for  $\ln (A\sqrt{P})$  less than 10.5. The linear fit accounts for practically none (0.2%) of the variability in the UPL data and only 14.7% of that in the APLA data. Accounting for 14.7% of the variability is adequate to make the fit statistically significant, but it is far less than the 70% to 80%  $R^2$  obtained for the data with  $\ln (A\sqrt{P})$  greater than 10.5. Inclusion of the data with  $\ln (A\sqrt{P})$  less than 10.5 also contributed to excessive curvilinearity in the plot of the residuals against the predicted values, which is indicative of a violation of the assumed linearity of the relationship. All of the above considerations led to the conclusion to investigate the fits for each data set based on the data for runs with  $\ln (A\sqrt{P})$  greater than 10.5

#### Expected Transmission for Low Airflows

By "low airflows," we mean airflows resulting from combinations of opening diameter and pressure that produces values of  $\ln (A\sqrt{P})$  less than 10.5.

Solving:

$$\ln (A\sqrt{P}) = 10.5$$

for  $\Delta$ , the opening diameter, we get:

$$\Delta^2 = \frac{4 e^{10.5}}{\pi \sqrt{P}}$$

$$\Delta = 215.0310 P^{-1/4}$$

Similarly, the pressure for a given  $\Delta$  is given by:

$$P = (2.137984 \times 10^9) \Delta^{-4}$$

Table B29 gives the solutions to these equations for the range of pressures and diameters used in the experimental runs. (See Table B3 for actual

diameters used.) Table B29 gives the upper limits to the diameter and pressure combinations, which were considered to result in random transmission of DUO. For example, at 5 psig, it would require a diameter of 144  $\mu\text{m}$  before structure was discernible in the results. At 30 psig, random results were observed for orifices with less than 92  $\mu\text{m}$  diameters. For the two smallest sets of orifices (OIDs 1-8), the required pressure for discernible structure was greater than the 1000 psig maximum used in the study. For 100  $\mu\text{m}$  or larger openings, pressures greater than 21 psig produced discernible structure.

Inspection of the Stem and Leaf displays and statistics of Table B30 reveal that UPL transmissions were larger than APLA. The Stem and Leaf Display, S/L D, is a type of frequency distribution characterization which uses the initial digit(s) of the observed values as the "stem" and the next following digit as the "leaf". The stems used in Table B30 use "h" for half to designate the item for leaves of 0.5 or greater so that each initial digit has two stems. The first value recorded for UPL is 2.0 and the second 2.4 for a total count of two values for the "2" stem. The "2h" stem has seven values, (2.5...,2.9). The resulting picture is a horizontal bar chart made by the numbers comparing the results for the 25 UPL and 59 APLA runs with  $\ln A\sqrt{P}$  less than 10.5.

It is obvious that the distribution for UPL is centered about a higher  $\ln$  DUO value than the distribution for the APLA values. The statistics bear this out. Using the t-test, the difference between averages is highly significant,

TABLE B29. Combinations of Pressure and Opening Diameter Required for  $\ln (A\sqrt{P}) = 10.5$

$\Delta = 215.03 P^{-1/4}$		$P = (2.14 \times 10^9) \Delta^{-4}$	
psig	$\Delta\mu\text{m}$	$\Delta\mu\text{m}$	psig
5	144	20	13,362
30	92	30	2,639
100	68	40	835
500	45	60	165
1,000	38	100	21
		150	4.2
		275	0.4

TABLE B30. Stem and Leaf Displays of  $\ln$  DUO for  $\ln (AVP) < 10.5$

Stem	UPL	APLA	Counts		
			UPL	APLA	Total
-0		1		1	1
0		13		2	2
0h		56666777		8	8
1		00011222233344		14	14
1h		555556778889999999		18	18
2	04	01112244	2	8	10
2h	5677899	5689	7	4	11
3	012244	04	6	2	8
3h	5	57	1	2	3
4	022244		6		6
4h	559		2		2
5	2		1		1

Statistics

Ave.	3.4938	1.6598
St. Deviation	.8586	.8268
Median	3.2	1.5
Min.	2.0122	-0.15
Max.	5.2470	3.7565
Range	3.2348	3.9065

the chance of a larger  $t$  being less than one in a thousand. The standard deviations are statistically the same with a pooled value of 0.8362  $\ln$  DUO, which has 82 degrees of freedom. Despite the single value of the "3h" stem for the UPL display, the distributions were assumed to be closely approximated by normal (Gaussian) distributions with the same variance but different means.

The possibility that the significant difference between  $\ln$  DUO averages was due to larger  $\ln (AVP)$  and so larger air flow potential for UPL than for APLA was excluded by inspecting the  $\ln AVP$  values less than 10.5. The APLA average was slightly (not significantly) larger at 9.43 than the 9.33 UPL average.

The practical conclusion is that UPL and APLA leaks should be treated separately for  $\ln AVP$  values less than 10.5.

Normal distribution theory can be used to develop confidence statements on the expected amount of  $\lambda n$  DUO in future experiments. Extrapolation of the experimental results to actual transmissions in an accident is dependent upon the theoretical similarity between the experimental conditions and actual conditions in the accident.

Confidence limits on the average  $\lambda n$  DUO transmitted are given by

$$\lambda n \text{ DUO} \pm t(1-\alpha/2;82) \text{ sd} / \sqrt{N}$$

where:

- $t(1-\alpha/2;82)$  is the 100(1- $\alpha/2$ ) percentile of the t-distribution with 82 degrees of freedom
- $\alpha$  is the complement of the confidence level,
- 100(1- $\alpha$ )=95 or 99 for  $\alpha = 0.05$  or 0.01
- N is the number of observations used to calculate the average  $\lambda n$  DUO.

The pooled standard deviation, 0.8362 and  $(0.025,80) = 1.990$ ,  $t(0.005;80)=2.639$  were used to obtain the limits in Table B31. These confidence limits can be translated to  $\mu\text{g}$  DUO by exponentiation.<sup>(a)</sup> The conclusions are:

For under powder leaks, we can be approximately 90% confident that average transmission will be between 24 and 46  $\mu\text{g}$  and 95% that the interval 21 to 51  $\mu\text{g}$  will contain the true mean. For above powder leaks, the 90% limits were 4.2 to 6.5  $\mu\text{g}$ , and the 95% limits were 3.9 to 7.0  $\mu\text{g}$ .

The reader might note that the confidence limits do not include the largest (nor the smallest) observed values. This is because they are for the average  $\lambda n$  DUO, that is the amount expected on the average. A more interesting statistic for accident analysis is the maximum amount expected. Table B30 gave the maximum amount observed for UPL as 5.2470  $\lambda n$  DUO and 3.7565  $\lambda n$  DUO for the

---

(a) For the standard deviation and number of runs for these data sets, 95% limits for the untransformed data obtained by this "naive transformation" (Land 1972) drop to about 90% confidence limits, and the 99% drop to about 95%.

TABLE B31. Confidence Limits on Average  $\ln$  DUO

<u>Apparatus</u>	<u>UPL</u>	<u>APLA</u>
N	25	59
$\frac{sd}{\sqrt{N}}$	0.1672	0.1089
$\ln$ DUO	3.4938	1.6598
95% Limits		
Lower	3.1610	1.4432
Upper	3.8266	1.8764
99% Limits		
Lower	3.0524	1.3725
Upper	3.9351	1.9471

APLA runs. These values translate to 190 and 43  $\mu\text{g}$  DUO respectively. Whenever one asks a question about the maximum expected, the statistician must ask the question, "The maximum of how many?" Intuitively, the more instances you have, the more likely it is that a value from the extreme tail of the distribution will be observed. A meaningful answer to the question of the expected maximum thus requires some information on the expected frequency of the events for which the maximum instance is required.

Since the expected frequency is not available, assume a once-a-month rate and ask the question: What will be the expected maximum for a given year? Statistically, the question is: What value of  $\ln$  DUO will be exceeded in less than 5%, or 1%, of the years during which 12 releases occurred due to airflows caused by leaks with  $\ln$  ( $\overline{AVP}$ ) less than 10.5? Our experiment characterized the distribution of such releases as being normal with a constant variance but different means for UPL and APLA. Pearson and Hartley (1962, Table 26) give the required coefficients for answering this question under normal theory. The required coefficient was obtained by interpolating between 60 and 120 degrees of freedom to get the values for the standard deviation with 82 degrees of freedom. The 5% value for an n of 12 was 2.59 and the 1% value, 3.12. We can thus conclude:

For under powder leaks, 95% of the years would be expected to have  $\ln$  DUO less than 5.6956 (equivalent to 287  $\mu\text{g}$  DUO) and 99% less than 6.1027 (or 447  $\mu\text{g}$  DUO). For above powder leaks, the expected 95% maximum is 3.8256  $\ln$  DUO (or 46  $\mu\text{g}$  DUO) and the 99% is 4.2687  $\ln$  DUO (or 71  $\mu\text{g}$  DUO). As an example of what would happen if the "accident rate" were cut in half, the UPL expected maximum



would be 5.3669  $\ln$  DUO (or 214  $\mu\text{g}$  DUO) at the 95% level and 5.8084  $\ln$  DUO (or 333  $\mu\text{g}$  DUO). The reduction in the probability (% level) associated with the  $\mu\text{g}$  DUO limits explained in the last footnote applies to these limits also.

#### Expected Transmission for Higher Airflows

The regression models described earlier were used to provide the expected transmissions for the runs with  $\ln$  DUO greater than 10.5. The selection of the best fit was quite circuitous. Decisions frequently had to be made on only marginal differences between model modifications. All the details will not be reported. Only the four most important decisions will be documented.

These were:

- use  $\ln$  DUO instead of  $\ln$  DUO/min
- use the three coefficient model  $\ln$  DUO = a + b<sub>1</sub>  $\ln$  A + b<sub>2</sub> [f(P)]
- use the square root of P without taking the logarithm.
- do not pool the data sets.

The squared multiple correlation coefficient, R<sup>2</sup>, carried the most weight in making the decisions. Inspection of residuals, magnitude of residual standard deviations and coefficient similarity were also considered. The decisions were also influenced by the desire to pool as much of the data as possible, and so minimize the number of prediction equations required to represent the structure in the data.

The R<sup>2</sup> values for the fits of four different models to the four data sets and the pooled data are given in Table B32. The numbers of observations, N, for each R<sup>2</sup> are given at the bottom of the table.

Comparing the results for equations 1 and 2 resulted in the decision to use  $\ln$  DUO instead of  $\ln$  (DUO/min) as the dependent variable. The R<sup>2</sup> for the four individual data sets are three to four percentage points better for  $\ln$  DUO/min for all data sets except APLA-0. This data set has the fit to  $\ln$  DUO dominating the fit to  $\ln$  (DUO/min) by 17.4 percentage points. The APLA-0 data set was the only data set with "zero"-time runs. Since division by zero is an undefined operation, zero was replaced by 2.72 min (equal to e, the base of the natural logarithm). This was about the duration of the pressurization

TABLE B32. Comparison of  $R^2$  for Some Prediction Equations

1. $\ln \text{DUO} = a + b \ln (A\sqrt{P})$			2. $\ln (\text{DUO}/\text{min}) = a + b \ln (A\sqrt{P})$		
$R^2$	U	A	$R^2$	U	A
0	71.13	80.22	0	74.83	62.80
C	73.69	73.54	C	77.41	77.49
O&C	74.59	78.52	O&C	75.51	60.02
All	78.43		All	66.47	

3. $\ln \text{DUO} = a + b_1 \ln A + b_2 \ln \sqrt{P}$				4. $\ln \text{DUO} = a + b_1 \ln A + b_2 \sqrt{P}$			
$R^2$	U	A	$\ln \sqrt{P}$	$R^2$	U	A	U&A
0	76.52	80.45		0	77.09	82.62	78.72
C	74.84	74.89		C	75.01	69.94	66.34
O&C	75.55	78.56		O&C	75.88	80.33	
All	78.57			All	78.43		

	N	U	A	U&A
0		28	91	119
C		28	9	37
O&C		56	100	
All			156	

and depressurization. The 32 APLA-0 "zero"-time runs with  $\ln (A\sqrt{P})$  greater than 10.5 could then be included in the  $\ln (\text{DUO}/\text{min})$  comparison. When the  $R^2$  were weighted by their N's and the average taken, the combined  $R^2$  were 77.03% for  $\ln \text{DUO}$  and 58.43 for  $\ln (\text{DUO}/\text{min})$ . Pooling the orifice and capillary data for each apparatus type resulted in the  $\ln (\text{DUO}/\text{min})$  dominating the  $\ln \text{DUO}$   $R^2$  by only one percentage point for UPL, but for APLA,  $\ln \text{DUO}$  was greater by 18.5 percentage points. For the combined data sets, "All," the  $R^2$  for  $\ln \text{DUO}$  was clearly best. Since the improvements due to using  $\ln (\text{DUO}/\text{min})$  were marginal for the three data sets with less than half the observations, but use of  $\ln \text{DUO}$  resulted in quite substantial improvement for the largest data set, the decision was made to use  $\ln \text{DUO}$  as the dependent variable.

The comparison between Equations 1 and 3 resulted in the decision to split out area and pressure and use a three coefficient model. All the  $R^2$

values in the subtable under Equation 3 are larger than those under Equation 1, although only slightly so. The major advantage was that this model eliminated most of the curvilinearity in the probability plot of the residuals.

The final comparison between the two for Equations 3 and 4 in Table B32 resulted in the decision to use the square root of pressure instead of the natural logarithm of the square root of pressure. The comparisons show only marginal improvement from using  $\ln \sqrt{P}$  to using just  $\sqrt{P}$ , the largest being 2.4 percentage points for the APL-0 data set. Pooling of the O and C data for each apparatus showed the same slight improvement. The pooling of all the data with  $\ln(A\sqrt{P})$  greater than 10.5 resulted in a marginal preference for the use of  $\ln \sqrt{P}$  instead of just  $\sqrt{P}$ . The pooling over apparatus type resulted in a 78.72% value for orifices but only 66.34% for capillaries. The weighted average of the four data sets  $R^2$  was 78.42% for Equation 3 and 79.54% for Equation 4.

Based on this analysis of the  $R^2$  values, it was decided to use the prediction equation:

$$\ln \text{DUO} = a + b_1 \ln A + b_2 \sqrt{P}.$$

When translated to  $\mu\text{g}$  DUO by taking the exponent of each side, this equation becomes:

$$\text{DUO} = \exp [a + b_2 \sqrt{P}] A^{b_1}$$

The prediction equations for the data with  $\ln A\sqrt{P}$  greater than 10.5 are given in Table B33. Each of the four data sets and the pooled data sets has a line giving the number of observations, N; the coefficients, a,  $b_1$ , and  $b_2$ ; the standard deviation of the residuals,  $\text{sd}(\text{Resid.})$ ; and  $R^2\%$  the squared multiple correlation coefficient.

These equations can be used to estimate the total  $\ln$  DUO (and  $\mu\text{g}$  of DUO) for given opening cross-sectional area and internal container pressure that satisfy  $\ln(A\sqrt{P})$  greater than 10.5.

The range of opening diameter and pressure combinations for which the prediction equations are appropriate is given in Figure B14. This figure shows, for example, that at 30 psig, the opening diameter should be at least 90  $\mu\text{m}$  and at 100 psig 68  $\mu\text{m}$  makes  $\ln(A\sqrt{P})$  greater than 10.5. After about 200 psig, the required diameter drops much more slowly with increasing pressure, declining from about 56  $\mu\text{m}$  at 200 psig to 28  $\mu\text{m}$  at 1000 psig. For diameter-pressure combinations in the region with  $\ln(A\sqrt{P})$  less than 10.5, the upper limit considerations of the previous section should be used.

The coefficients for nine equations are given in Table B33 and the question is which one to use for a particular application. The answer depends on the information specified to characterize the leak. At a minimum opening, diameter and internal container pressure need to be specified. The three asterisks in the data set column indicate the three equations recommended for use when the opening is characterized as an orifice or a capillary and the opening is specified as being above or under the powder. The coefficients for the fits to the two capillary data sets were not significantly different statistically. Consequently, the equation for the pooled capillary data is recommended for use with capillaries irrespective of where the leak is relative to the powder. The coefficients for the UPL and APLA orifice data sets are significantly different so that the orifice equations represent different transmission characteristics depending on the location of the leak. In particular, the magnitude of  $b_2$ , the coefficient for  $\sqrt{P}$ , is less than half as large for the UPL data as it is for the APLA data, indicating that pressure has a smaller impact for under powder leaks than for above powder leaks, at least after the effect of opening diameter is accounted for.

The lines with asterisks are projected from three-space ( $\ln \text{DUO}$ ,  $\ln A$ ,  $\sqrt{P}$  axes) to two-space by looking at the 1000 psig bundle in Figure B15. The lines for UPL-0 and APLA-0 converge and cross at  $\ln(A\sqrt{P})$  of about 13.6 as  $\ln(A\sqrt{P})$  increases. The line for capillaries has a steeper slope, the transmitted DUO initially being lower than for the orifices, equalling the orifices at about  $\ln(A\sqrt{P})$  of 13 and finally exceeding the orifice transmissions. Translating the extreme  $\ln \text{DUO}$  values to  $\mu\text{g DUO}$  at  $\ln A\sqrt{P}$  of 10.5 and 14.75, the results are:

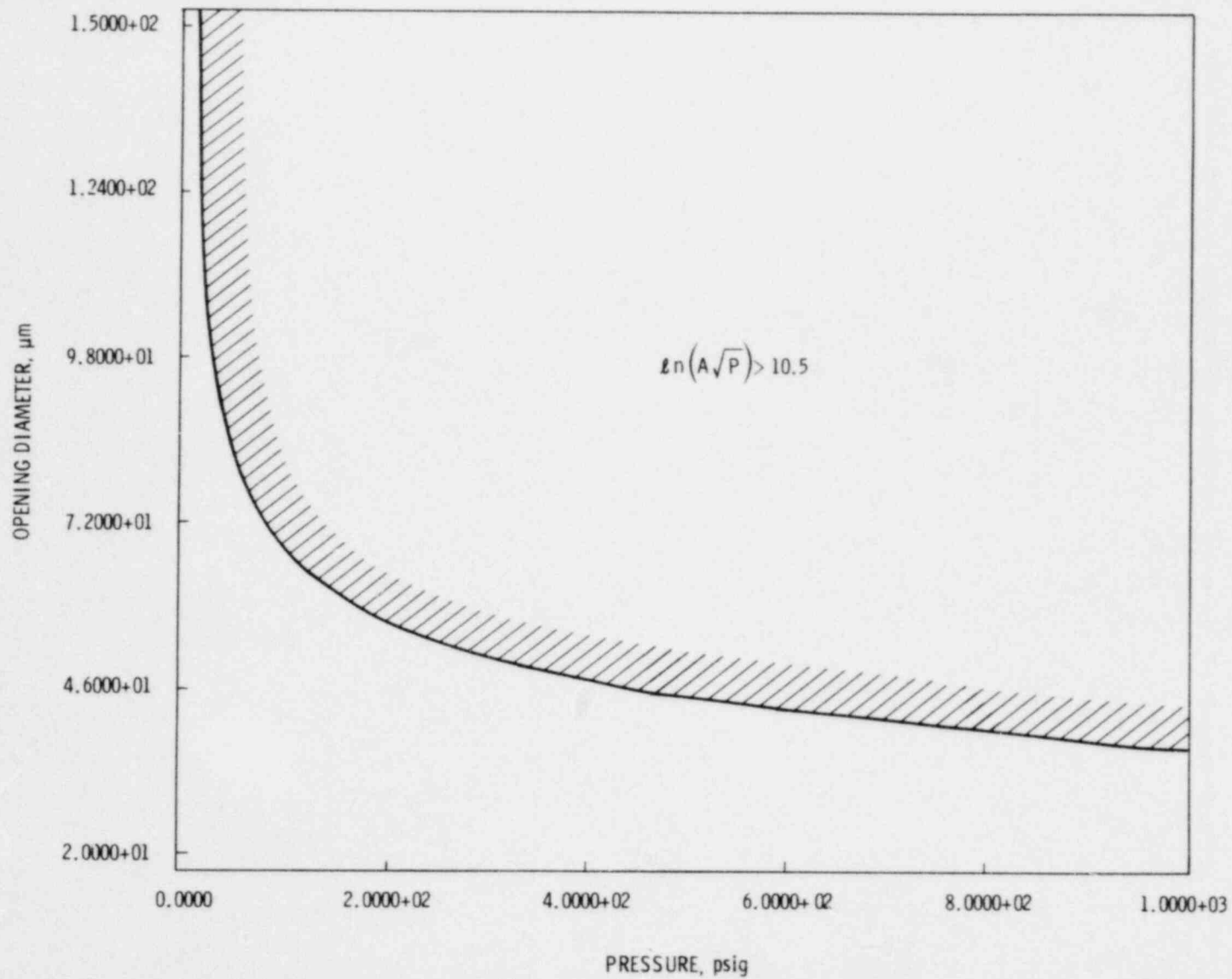


FIGURE B14. Region for which  $\ln(A\sqrt{P})$  is Greater Than 10.5

TABLE B33. Statistics for Fits to the Prediction Equation  
 $\ln \text{DUO} = a + b_1 \ln A + b_2 \sqrt{P}$  (Data with  
 $\ln \text{AVP} > 10.5$ )

Data Set	N	a	b <sub>1</sub>	b <sub>2</sub>	sd(Resid.)	R <sup>2</sup> %
*UPL-0	28	-10.2848	1.608028	0.044944	0.8053	77.09
*APLA-0	91	-14.1959	1.790593	0.109513	0.8718	82.62
UPL-C	28	-18.1034	2.243517	0.100656	0.8808	75.01
APLA-C	9	-20.9319	2.361245	0.102699	1.2256	69.94
UPL-O&C	56	-12.3951	1.748609	0.076221	0.8807	75.88
APLA-O&C	100	-13.6446	1.720591	0.111463	0.9192	80.33
O-UPL&APLA	119	-13.7516	1.77867	0.101787	0.9392	78.72
*C-UPL&APLA	37	-17.9875	2.165826	0.117040	1.1379	66.34
All(>10.5)	156	-14.2790	1.828047	0.105223	0.9842	78.43

\* These coefficients are the ones recommended for use with leak characteristics similar to those of the data set conditions.

- UPL-0; 12 to 10,400  $\mu\text{g}$  DUO
- APLA-0; 7 to 13,350  $\mu\text{g}$  DUO
- Capillaries 3 to 25,600  $\mu\text{g}$  DUO

When all the data with  $\ln \text{DUO}$  greater than 10.5 were pooled, the result closely paralleled the APLA-0 results with a range from 7 to 16,300  $\mu\text{g}$  DUO; ( $\ln \text{DUO}$  between 1.95 and 9.70).

Figures B16, B17 and B18 give the estimated  $\ln \text{DUO}$  values for each pressure used plotted against  $\ln A$  (cross-sectional area) for the three data sets. The estimated values for the actual data are plotted. All three plots have the same scale. Note that the pressure lines are parallel on each graph. (The 1000 psig lines were plotted against  $\ln (\text{AVP})$  in Figure B15 using different scales for the axes). Note that the three psig lines in Figure B16 form a closer bundle than the four lines of Figure B17. This greater separation for the APLA lines is indicative of the greater importance of pressure in the APLA runs. About the same degree of separation as for the APLA lines may be

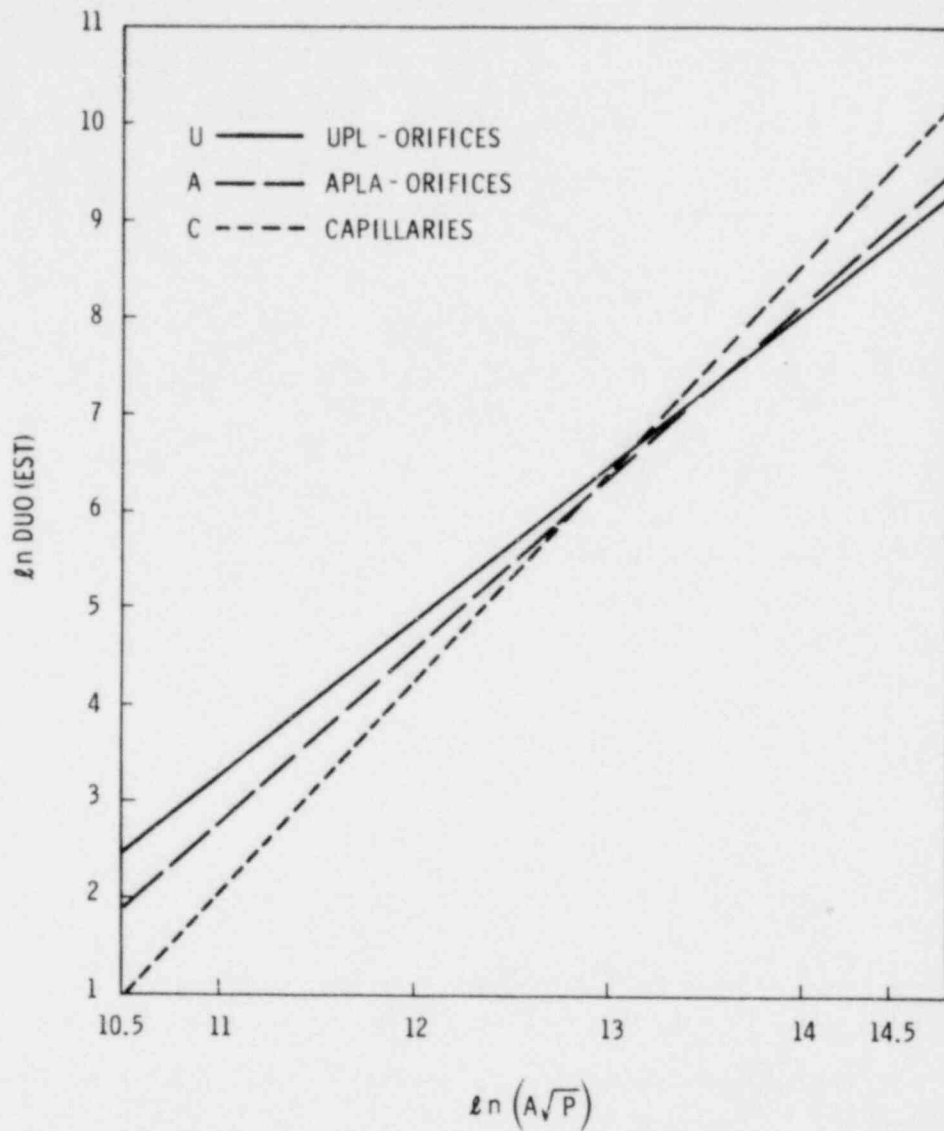


FIGURE B15. Comparison of Prediction Equations Based on UPL-0, APLA-0 and Capillaries Data Sets at 1000 psig

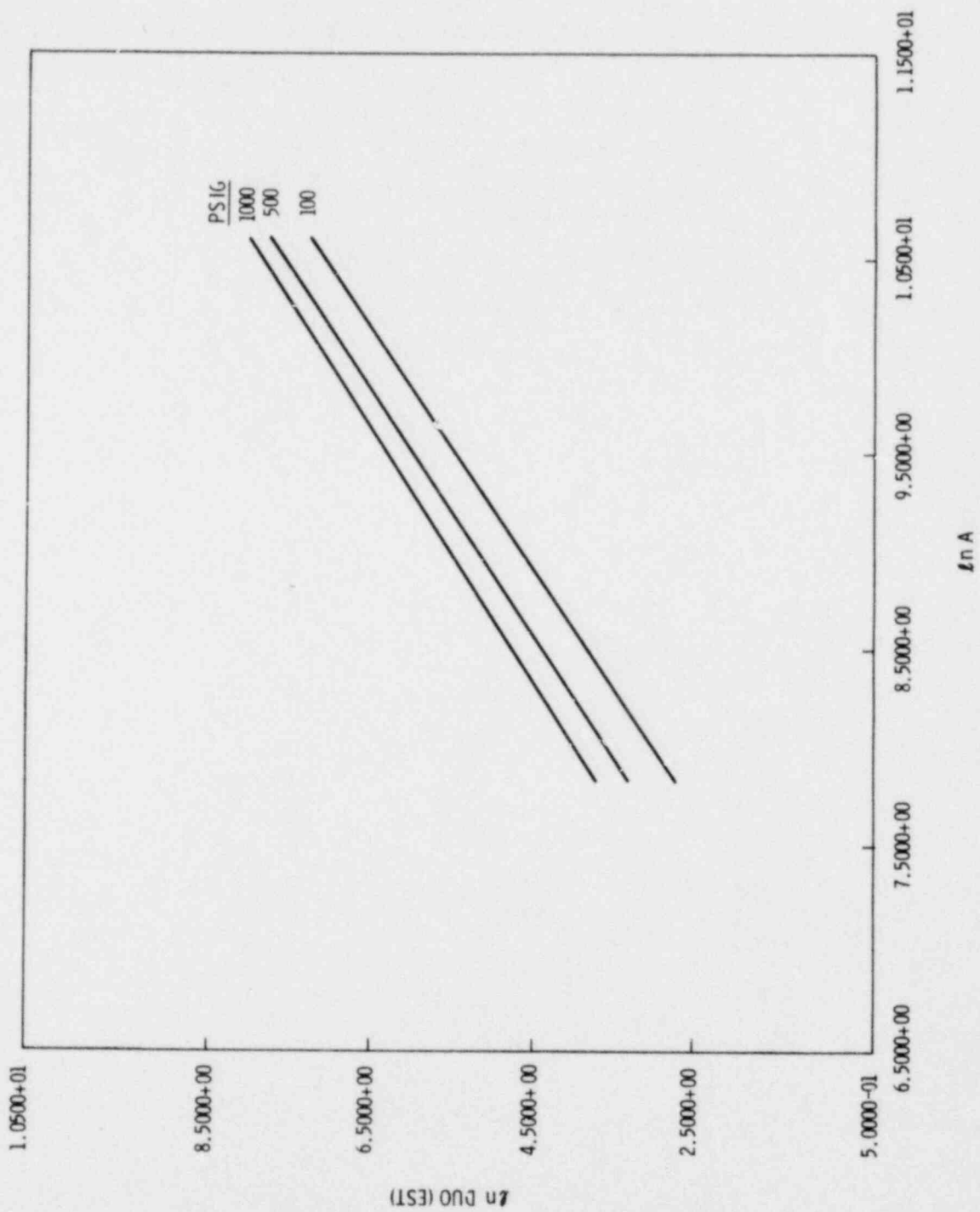


FIGURE B16. Estimated Values For UPL-0



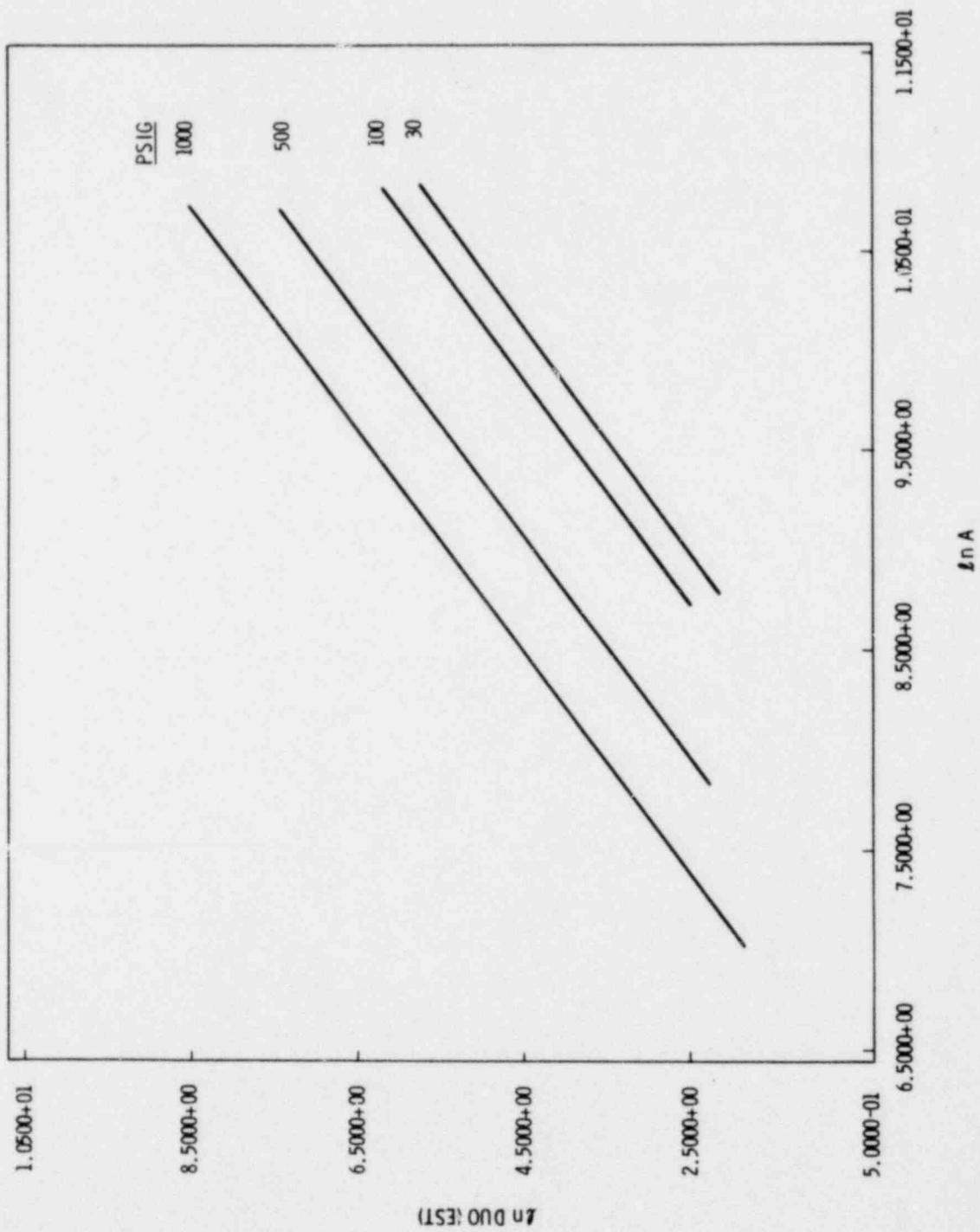


FIGURE B17. Estimated Values For APLA-0

B-74

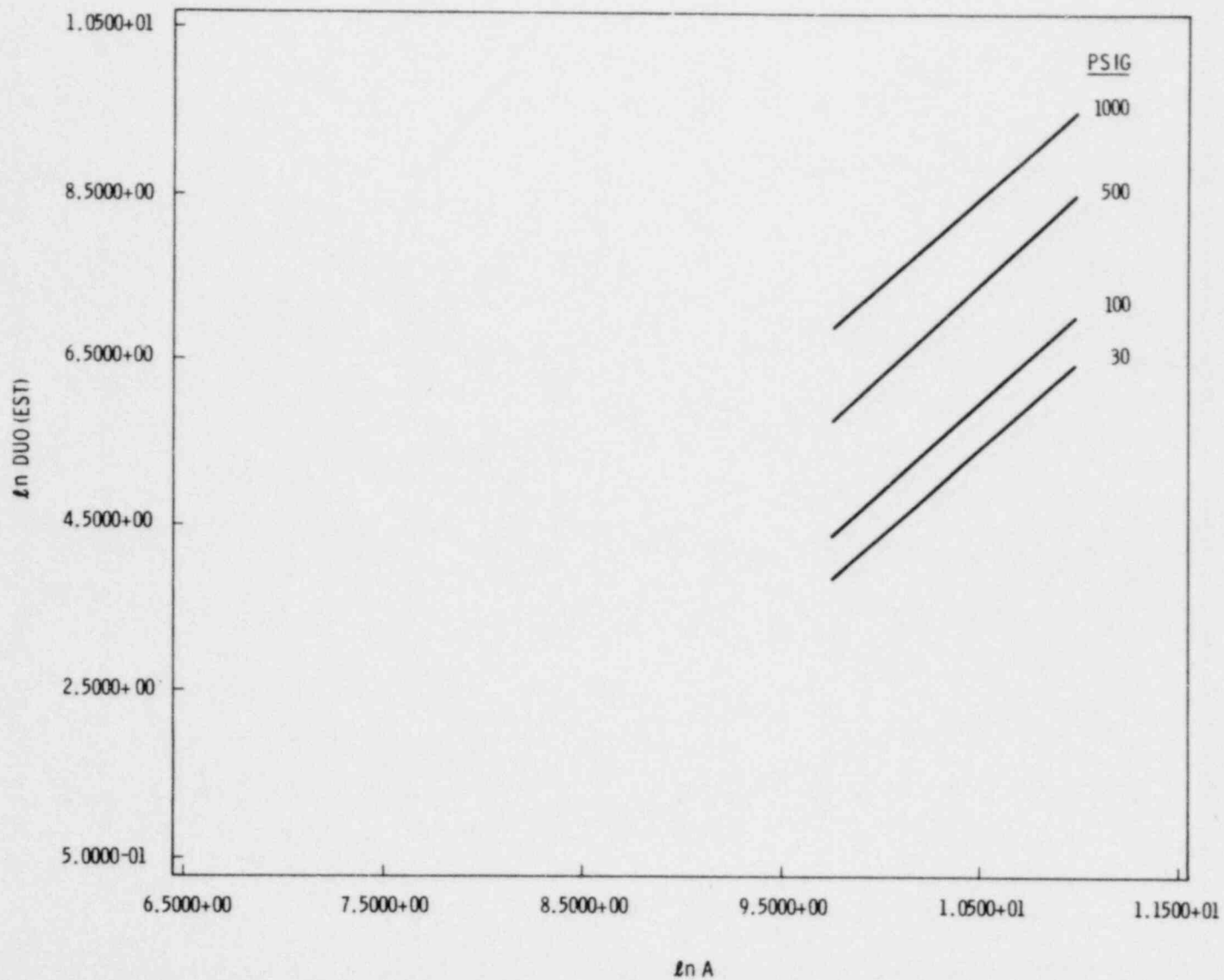


FIGURE B18. Estimated Values for Capillaries

observed for the capillaries plot, but the slope is more pronounced than for the APLA-0 data.

When all the data (N=156) with  $\ln(A\sqrt{P})$  greater than 10.5 were pooled, the plots of the estimated values against  $\ln(A\sqrt{P})$  in Figure B19 was nearly indistinguishable from the plots for the APLA-0 data in Figure B17. The slopes were the same, but the estimated values for the pooled data were slightly larger than for the UPL-0 based estimates.

The practical implication to be drawn is that the fit to all the data with  $\ln(A\sqrt{P})$  greater than 10.5 most closely reflects the transmission for above powder leaks through orifices, slightly over-estimates under powder leaks through orifices and under-estimates leaks through capillaries by a factor of two at the upper end of the diameter-pressure combinations used in the study. The over- and under-estimation is reversed at the lower end of the range, where  $\ln(A\sqrt{P})$  equals 10.5.

The precision of these fits can be compared by looking at the sd (Resid.) column of Table B33; the smaller the standard deviation of the residuals, the more precise the estimates will be. Among the three recommended prediction equations UPL-0 has the smallest sd (Resid.), 0.8053, followed by APLA-0 at 0.8718 and 1.1379 for the capillaries data set. When all data were pooled, the sd (Resid.) was 0.9842  $\ln(\mu\text{g DUO})$ .

The approximate 90% confidence limits for a predicted value are shown in Figure B20. These confidence limits are intended to provide the reader with a picture of the precision. They were calculated for the 1000 psig value at various  $\ln A$  values, and plotted against  $\ln(A\sqrt{P})$ . The estimated values for the four pressure levels are also plotted on Figure B20. The confidence limits would be slightly narrower for the UPL-0 and APLA-0 data sets and slightly broader for the capillaries data.

Another picture of how well the overall prediction equation fits the data is given in Figure B21. If the equation fit exactly, all data would fall along the OSB=EST line drawn on the plot. As it turns out, bands including the points would be about as broad as the confidence limits of Figure B20.

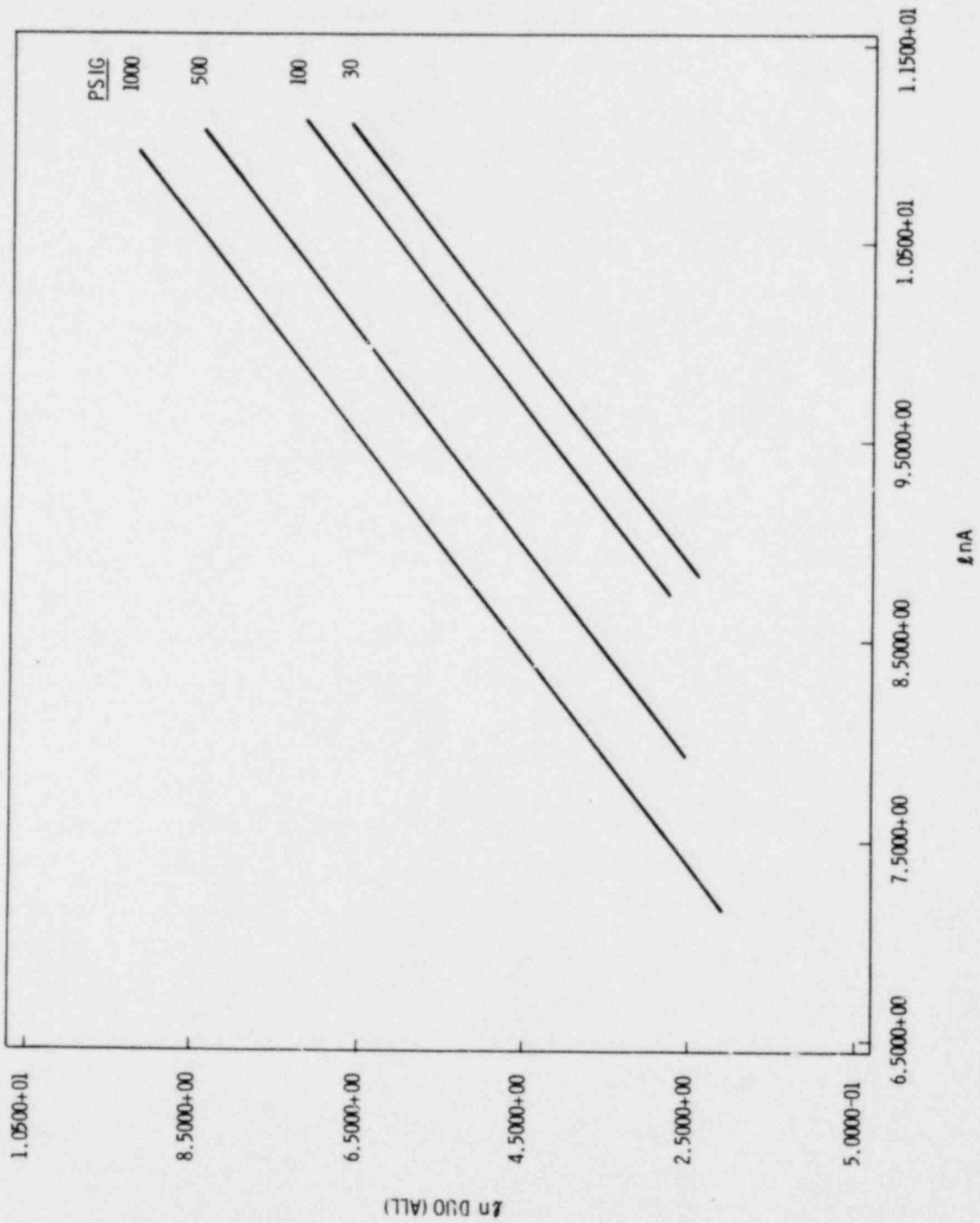
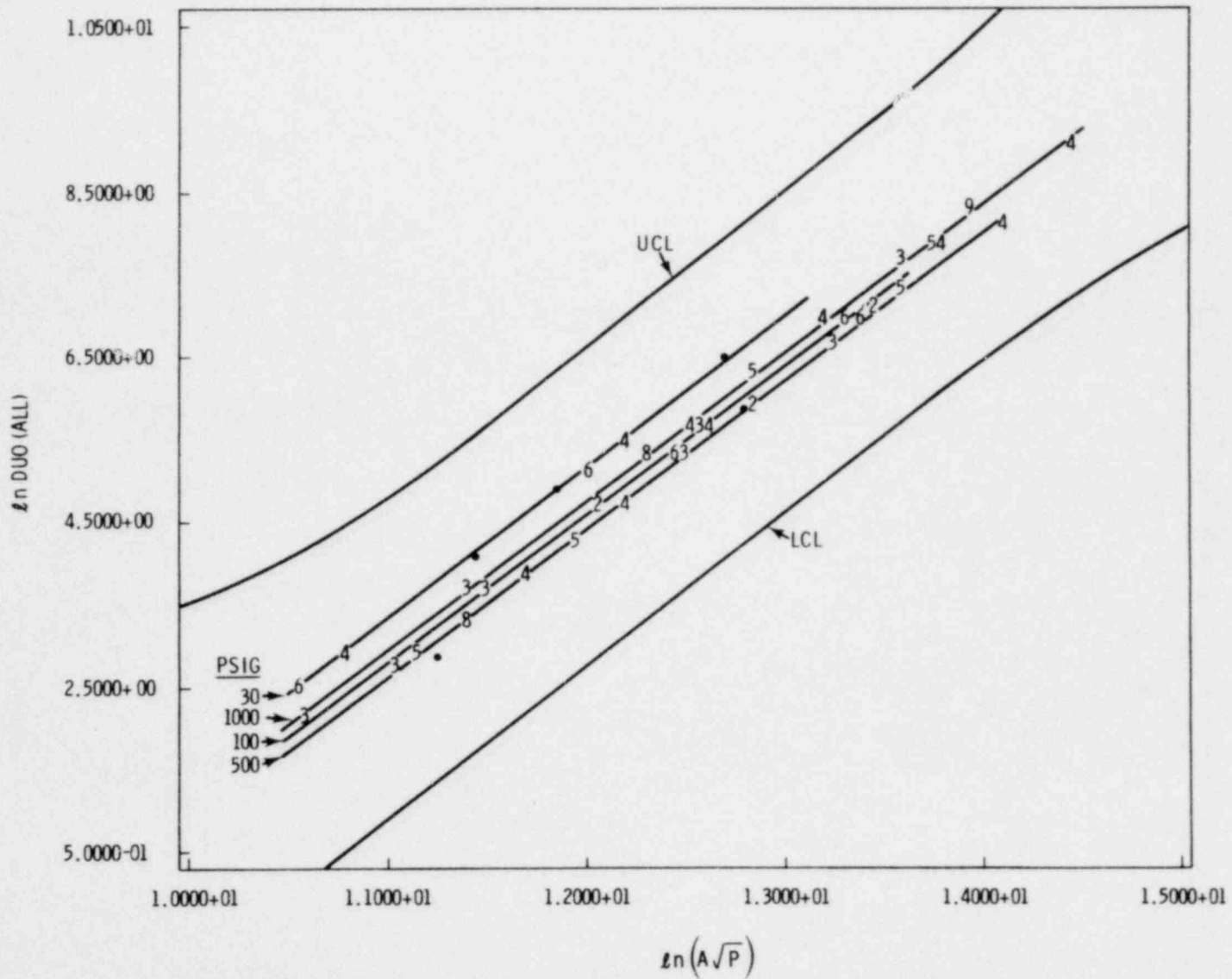


FIGURE B19. Estimated Values for All Data



**FIGURE B20.** Confidence Limits For 1000 psig Estimates Based on Fit to all Data

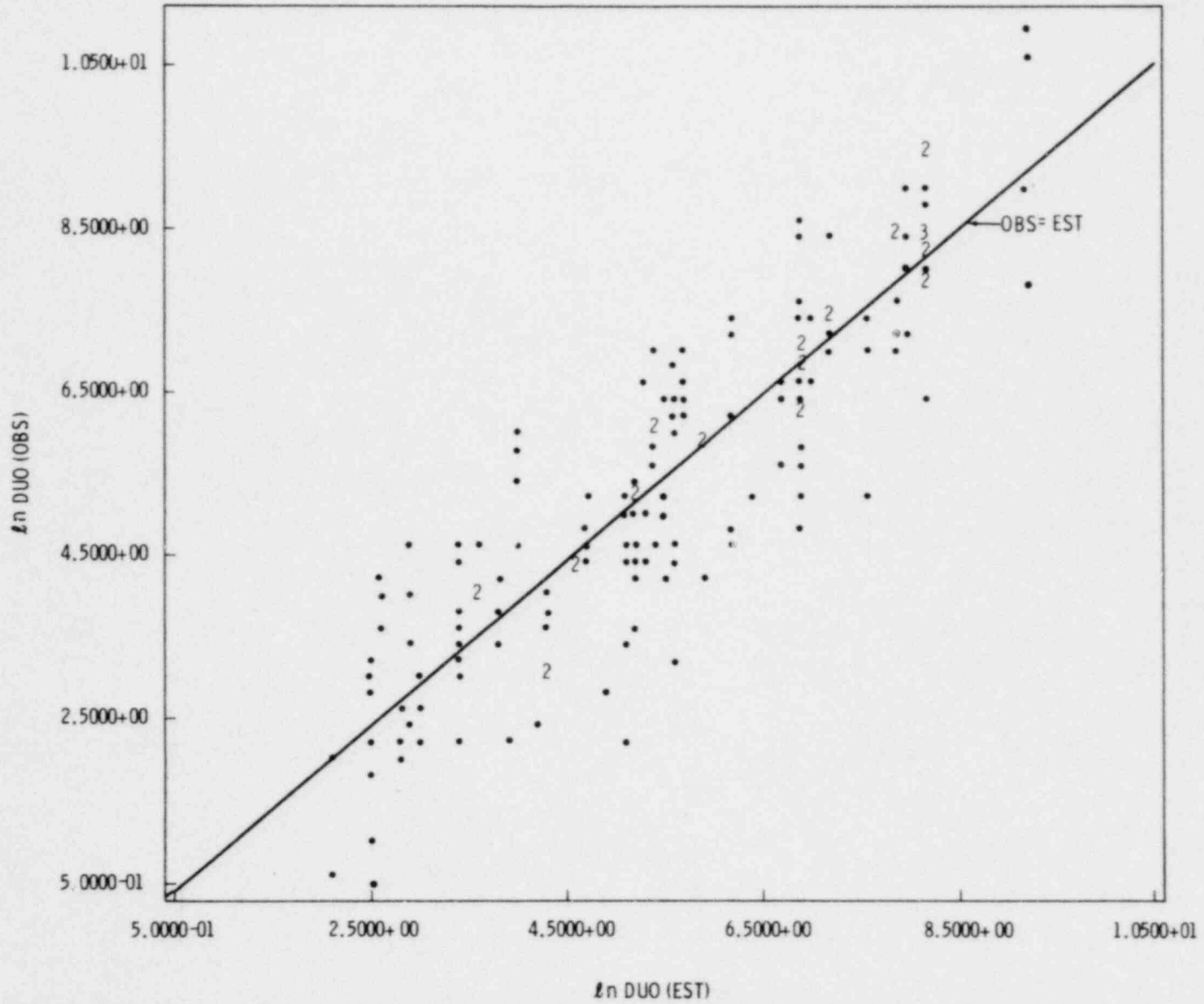


FIGURE B21. Observed vs. Estimated Values For Fit to All Data

Results for the three recommended equations are given in Figures B22, B23 and B24. These figures give the predicted psig lines drawn among the actual data points and plotted against  $\ln (AVP)$ . The degree of misfit is comparable in all cases.

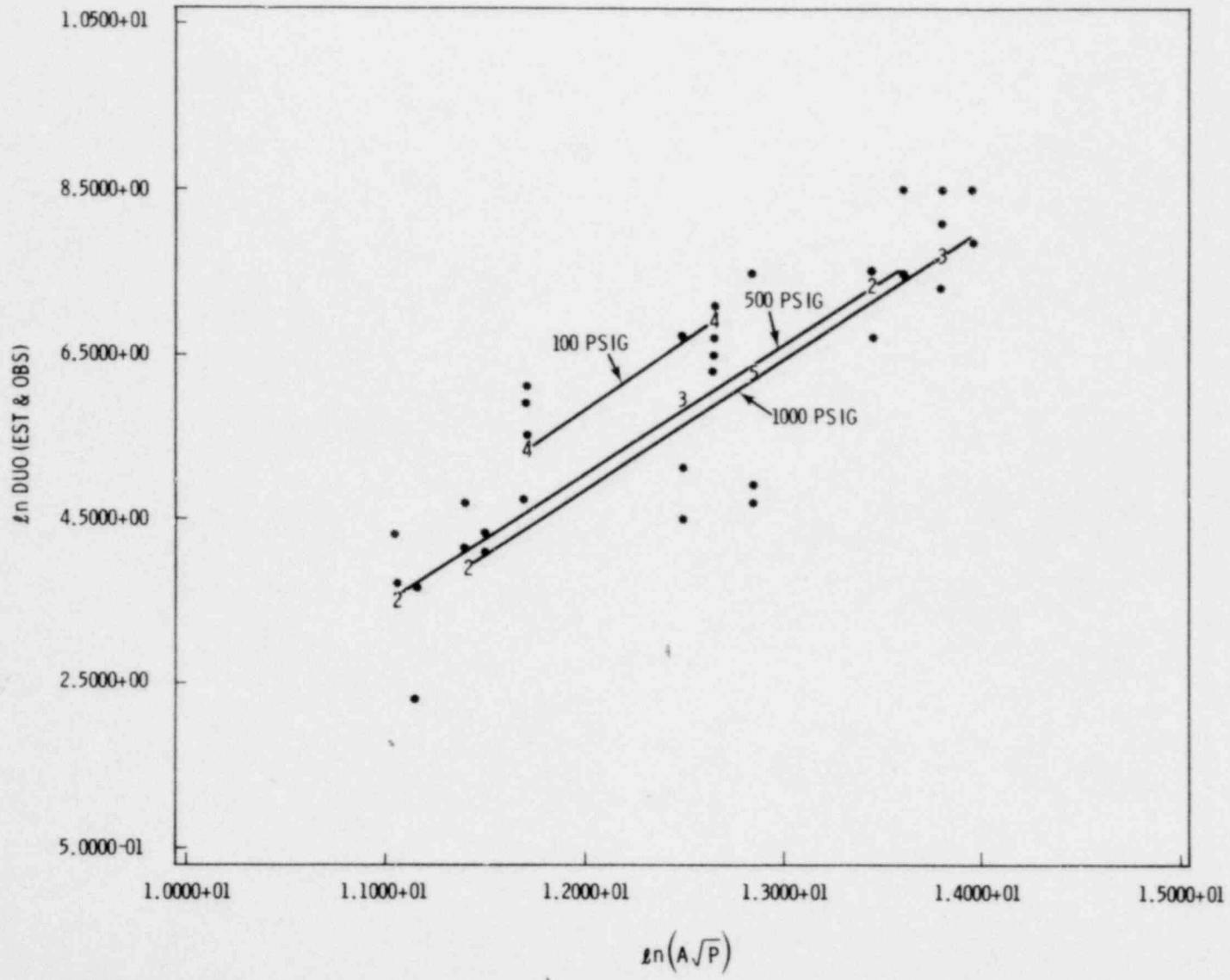


FIGURE B22. Observed vs. Estimated Values For UPL-0 Data



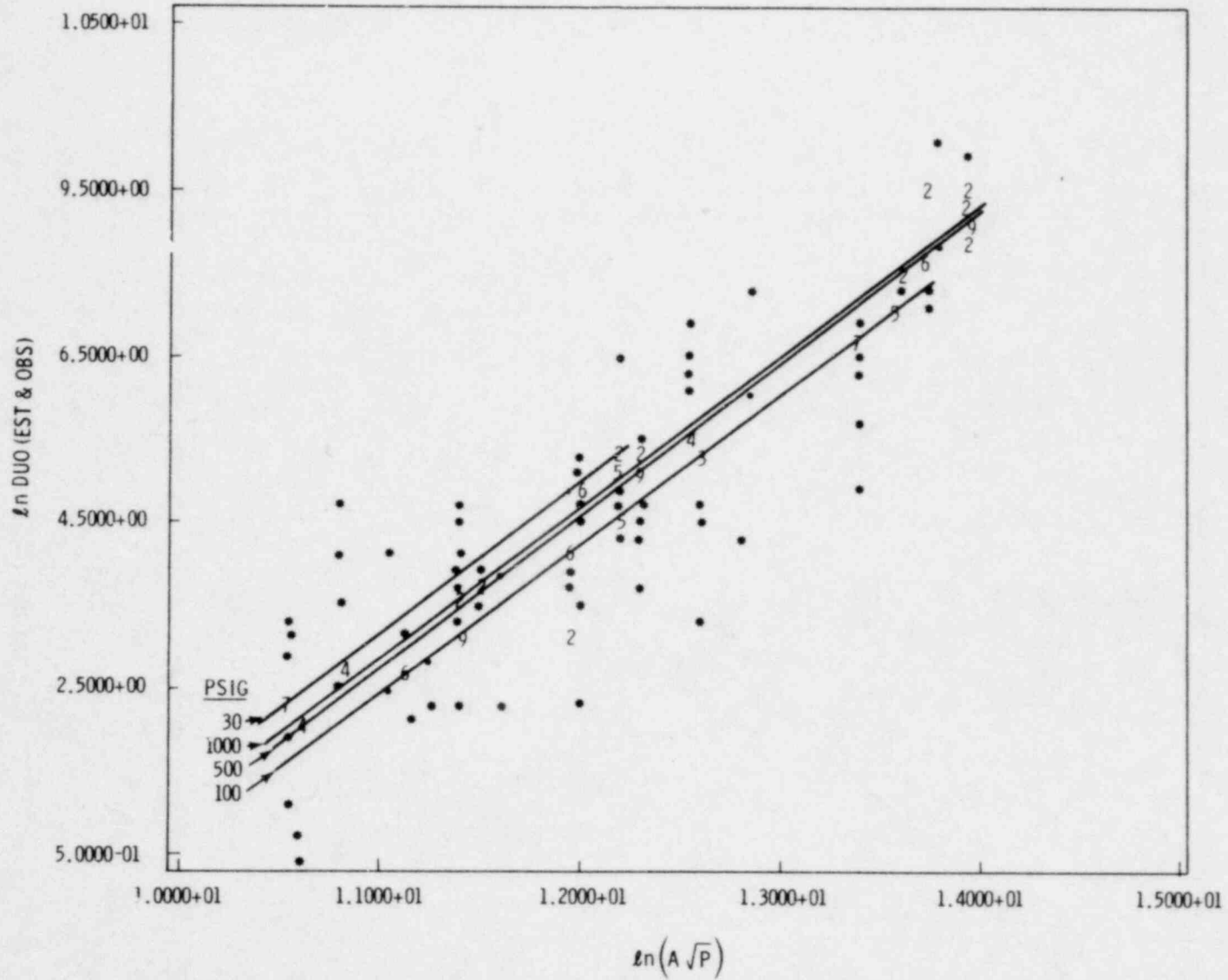


FIGURE B23. Observed vs. Estimated Values for APLA-0 Data

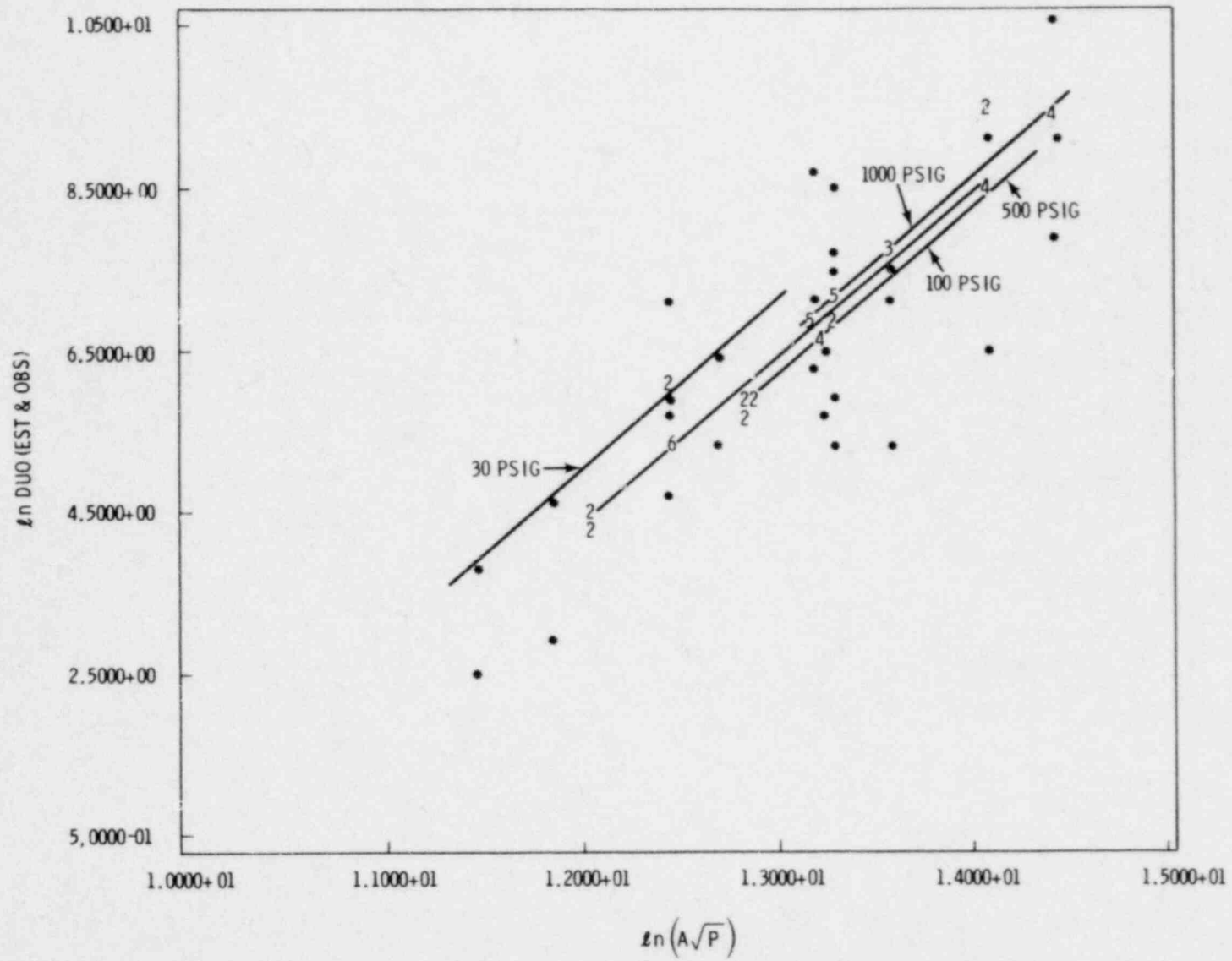


FIGURE B24. Observed vs. Estimated Values For Capillaries Data

## REFERENCES

- Draper, N. R. and H. Smith. 1966. Applied Regression Analysis. Wiley, New York, NY.
- Land, C. E. 1972. "An Evaluation of Approximate Confidence Interval Estimation Methods for Lognormal Means." Technometrics. 14:145-158.
- Ostle, B. 1963. Statistics in Research. Iowa State U. Press, Ames, IA.
- Pearson, E. S. and H. O. Hartley. 1962. Biometrika Tables for Statisticians. Vol. I, Cambridge U. Press, New York, NY.
- Siegel, S. 1956. Nonparametric Statistics. McGraw-Hill, New York, NY.

APPENDIX C

ORIFICE FLOW DURING  
"ZERO"-TIME RUNS

## ORIFICE FLOW DURING "ZERO"-TIME RUNS

During "zero"-time runs performed for orifice experiments, the volume of gas escaping the orifice was not measured since the flow rate varied rapidly during the complete pressurization/depressurization cycle. The best estimate arrived at for this flow was the result of the calculations described here.

The pressurization and depressurization periods were characterized by a linear buildup/decay of pressure with time. The following table gives the measured times required to build up and release the APLA vessel to and from the peak pressure.

TABLE C1. Pressurization/Depressurization Times for APLA Runs

<u>Pressure Range,</u> <u>psig</u>	<u>Pressurization Time,</u> <u>Sec</u>	<u>Total Time,</u> <u>Sec</u>
0 - 30	9.3	40
0 - 100	11	68
0 - 500	19	132
0 - 1000	27	190

The orifice mass flow rate,  $\dot{m}$ , at any absolute pressure,  $P$ , and density,  $\rho$ , is given by:

$$\dot{m} = \alpha A \psi [2 g_c P \rho]^{1/2}$$

where:

- $\alpha$  = orifice coefficient
- $A$  = orifice cross-sectional area
- $\psi = \left(\frac{P}{P_0}\right)^{1/\gamma} \left[ \frac{\gamma}{\gamma-1} \left( 1 - \left(\frac{P}{P_0}\right)^{\frac{\gamma-1}{\gamma}} \right) \right]^{1/2}$
- $P_0$  = ambient pressure
- $\gamma$  =  $C_p/C_v$  (heat capacity ratio)

and the volumetric flow is  $\dot{m}/\rho$  at density  $\rho$ . The following expressions were numerically integrated for  $P = 14.7 + a \cdot t$  (e.g.,  $a = 30/9.3$  for 30 psig pressurization period):

- total mass flow/ $\alpha A = \int_0^{t^*} \psi \left[ 2 g_c P \rho \right]^{1/2} dt$

( $t^*$  = time peak pressure  $P^*$  attained)

- total volumetric flow/ $\alpha A = \int_0^{t^*} \psi \left[ 2 g_c \frac{RT}{M_w} \right] dt$

at vessel conditions ( $M_w$  = gas molecular weight)

- total standard volumetric flow/ $\alpha A$  for  $\rho_0$  at 25°C, 1 atm =  $\frac{1}{\rho_0} \int_0^t \psi \left[ 2 g_c P \rho \right]^{1/2} dt$

The results of these integrals are tabulated below.

TABLE C2. Pressurization/Depressurization Gas Flows

Pressure Range, psig	Mass flow/ $\alpha A$ , g/m <sup>2</sup>	Volumetric Flow/ $\alpha A$ at P,T, m <sup>3</sup> /m <sup>2</sup>	Volumetric Flow/ $\alpha A$ at 25°C, 1 atm, m <sup>3</sup> /m <sup>2</sup>
0 - 30	4.312E+06 (1.855E+07)	1.734E+03 (7.458E+03)	3.605E+03 (1.551E+04)
0 - 100	1.147E+07 (7.091E+07)	2.147E+03 (1.327E+04)	9.593E+03 (3.014E+04)
0 - 500	8.148E+07 (5.661E+08)	3.761E+03 (2.613E+04)	6.812E+04 (4.733E+05)
0 - 1000	2.252E+08 (1.585E+09)	5.351E+03 (3.766E+04)	1.883E+05 (1.325E+06)

(a) Numbers in parentheses are depressurization flows

These flows were used for each orifice by multiplying the value by the average orifice coefficient and cross-sectional area.

APPENDIX D

TOTAL MASS DUO TRANSMITTED AS A FUNCTION OF TOTAL AIRFLOW

## TOTAL MASS DUO TRANSMITTED AS A FUNCTION OF TOTAL AIRFLOW

The total mass DUO transmitted as a function of total airflow were a part of the overall study to quantify the relationship between the release of fine powder and specified gas leak rates through microopenings. Pacific Northwest Laboratory defined gas leak rates and DUO powder transmission; Battelle Columbus measured  $\text{PuO}_2$  transmission. Both laboratories agreed that a uniform data presentation would facilitate relating the two sets of data. The format agreed upon was a tabulation of total mass of particles transmitted in micrograms versus a standard volume of gas leaked in each run. This standard volume is based on the best knowledge of the volume of leaked air (cc) or helium (cc) as an ideal gas at one atmosphere pressure (absolute) and at 25°C.

The plot in Figure D.1 shows the relationship between the total mass of particles transmitted and the best estimate of the total airflow through the orifices used in the APLA experiments.

The airflow during pressurization/depressurization was not measured since the flow rate varied rapidly during the complete pressurization/depressurization cycle. The best estimate of this flow for "zero"-time runs was calculated using the formulations in Appendix C. The value for the pressurization/depressurization occurring during other runs was calculated using this formulation and added to the measured flow during the run to make the best estimate of airflow.

The total capillary powder transmission has been plotted as a function of the best estimate of the total airflow during a run in Figure D.2. The final plots in Figure D.3 and D.4, relating the total mass of particles and total airflow for UPL experiments.



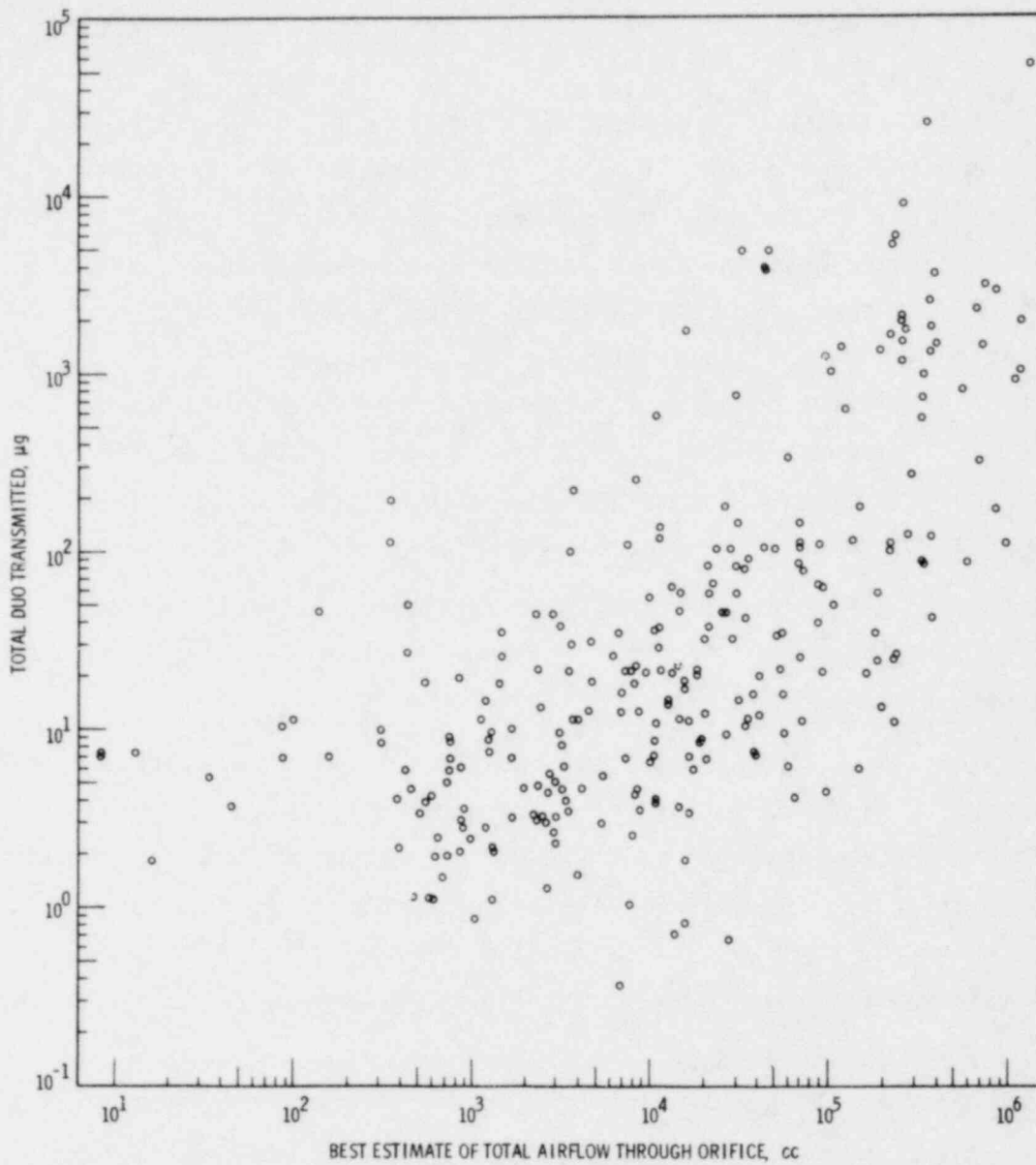


FIGURE D.1. Relationship Between Total Mass of Particles and Total Airflow Transmitted Through Orifices for APLA Experiments

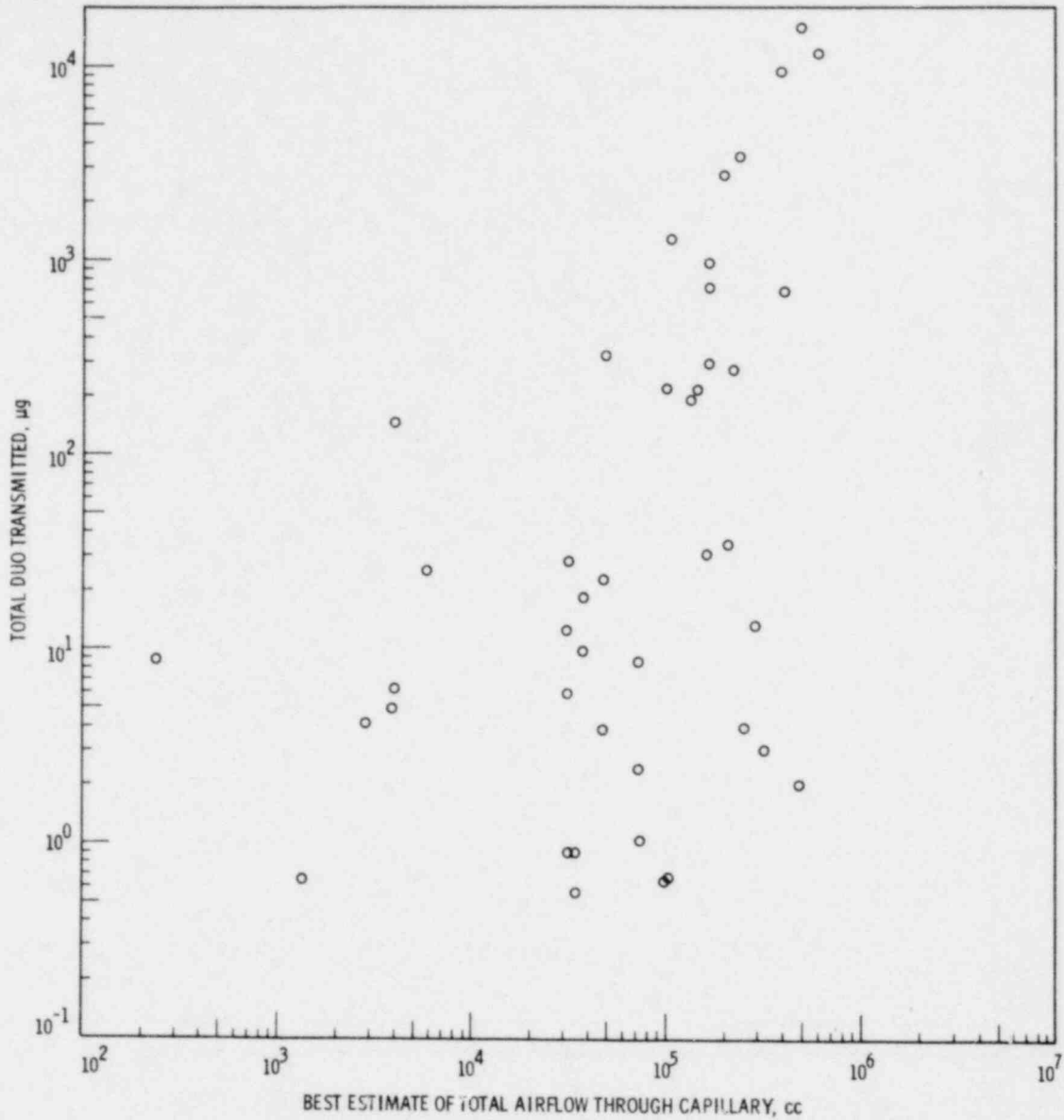


FIGURE D.2. Relationship Between Total Mass of Particles and Total Airflow Transmitted Through Capillaries for APLA Experiments

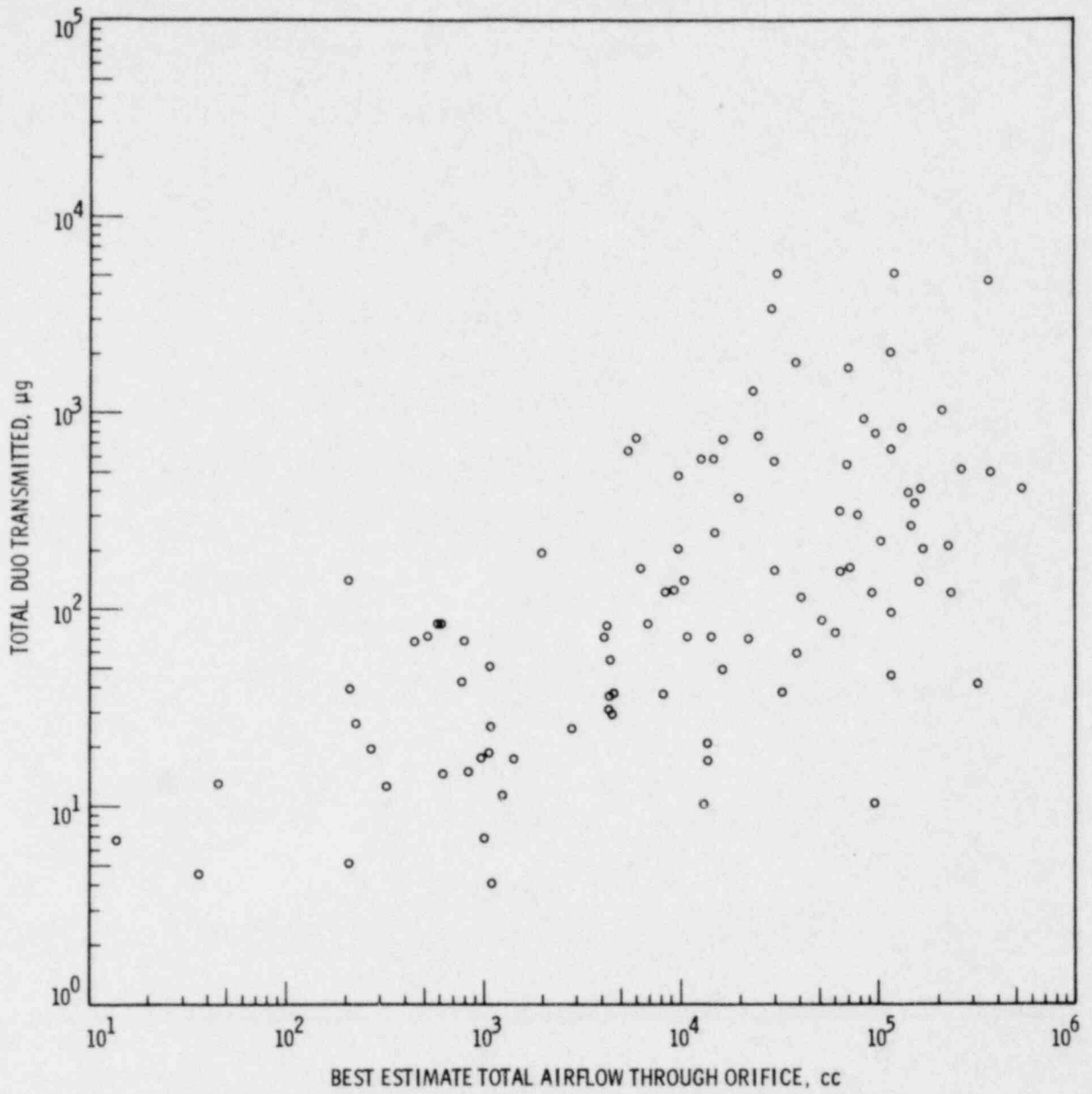


FIGURE D.3. Relationship Between Total Mass of Particles and Total Airflow Transmitted Through Orifices for UPL Experiments

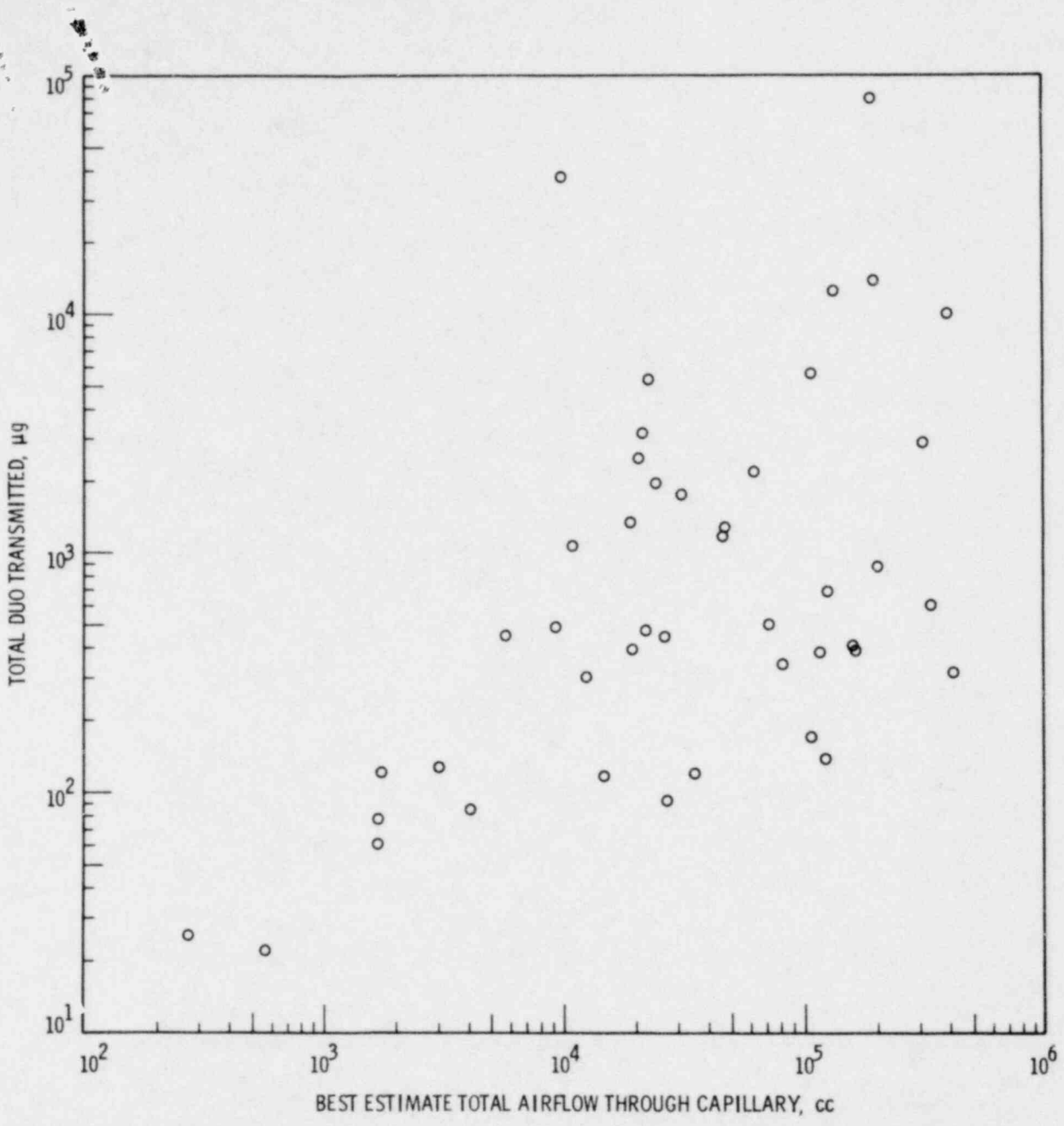


FIGURE D.4. Relationship Between Total Mass of Particles and Total Airflow Through Capillaries for UPL Experiments

APPENDIX E

ORIFICE LENGTH-TO-DIAMETER RATIO

### ORIFICE LENGTH-TO-DIAMETER RATIO

A length-to-diameter (L/D) ratio of 1 or less had been specified for orifices in the past (Sutter 1978). However, a nondestructive method to accurately measure the length of orifices was not readily available at that time. Use of the depth of focus of an optical microscope indicated that for one 20- $\mu\text{m}$  orifice the length of the orifice could have been up to 193  $\mu\text{m}$ . In the present investigation, one 20- $\mu\text{m}$  orifice impregnated with resin, was sectioned and the leak path measured after the powder leak experiments were completed. The measured leak path length was 560  $\mu\text{m}$ ; the L/D of this orifice was 28. This same path length would have an L/D ratio of 2.8 in a 200- $\mu\text{m}$  orifice. Time and funding restraints precluded a comprehensive investigation of the leak path length problem.

APPENDIX F

RHEOLOGICAL TEST

## RHEOLOGICAL TEST

During the DUO powder flow study, replicate results have often been disparate and difficult to predict. It has been assumed that much of this problem might be attributed to innate properties of the DUO powder. The DUO used in the experiments is a small (mass median diameter of 1  $\mu\text{m}$ ), easily packed, irregular powder that would tend to flow with difficulty.

In an effort to gain information on the innate "flowability" of the DUO powder, a rheological test (Zenz and Othmer 1960) was performed that demonstrated that the powder would not flow. A rheological test evaluates the interparticle friction (angle of internal friction,  $\alpha$ ) that is important in gravity flow and could play a role in leaks under the static powder level. The DUO powder was tested and compared to tests on sand with a mass median diameter of 64  $\mu\text{m}$ .

A bin-flow test measures the angle with the horizontal assumed by the moving core of solids in a vessel provided with a central opening in the bottom through which the contents can flow in free fall.

The vessel is rectangular with a clear front wall, as illustrated in Figure F1. The angle,  $\alpha$ , can be measured at the line of demarcation between stationary and flowing solids.

A clear, plastic bin 21.6 x 2.54 x 17.8 cm was fabricated. A 1.27 x 2.54 cm hole in the bottom of the bin was covered with a sliding plastic cover that could be opened to allow powder flow. The bin was filled with DUO powder to a depth of approximately 12.7 cm. As the bottom cover was removed, a marginal amount (<5 g) of DUO dropped out, as shown in Figure F2.

A swab was inserted to manually force the DUO out and a core was formed, as shown in Figure F3.

The bin was rapped briskly with a hammer and a flow formed, but continued only with constant agitation. Since the flow was really clumps of powder breaking off, no measurements of  $\alpha$  could be made on the DUO.

In order to compare DUO with powder that could flow, sand to a depth of 15.2 cm (mass median diameter of 64  $\mu\text{m}$ ) was tested in the same bin. As soon



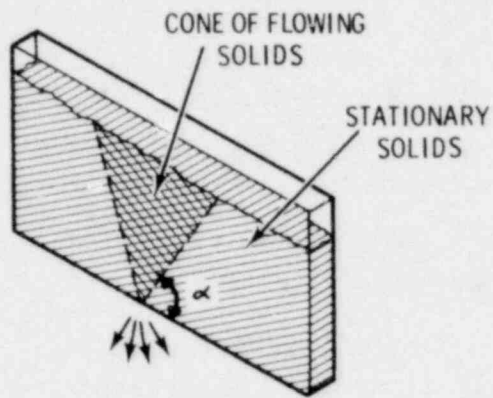


FIGURE F1. Bin-Flow Test Vessel

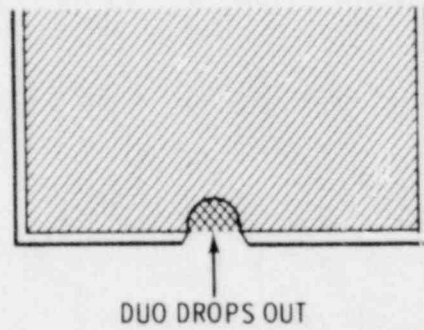


FIGURE F2. Area Where DUO Dropped from Bin

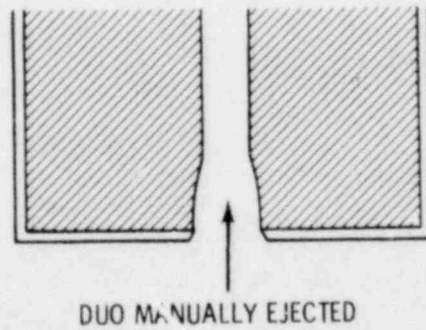


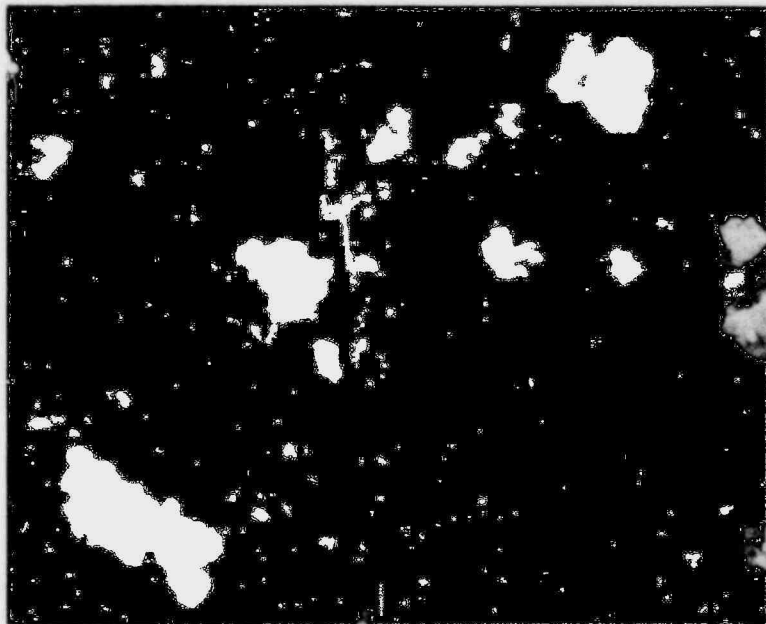
FIGURE F3. Core Formed in Powder to Allow Ejection of DUO

as the bottom hole was opened, fast flow became apparent, the line of demarcation between the core of flowing solids and the stationary solids was visible, and the angle of internal friction was measured as  $80^{\circ}$ .

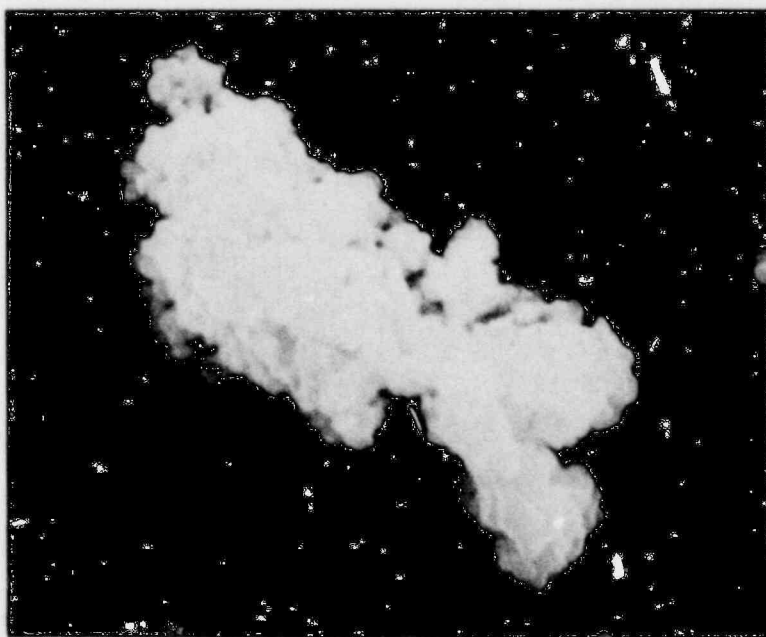
This test is a visual demonstration of the difficulty with which DUO flows and could, in turn, account for much of the anomalous behavior in many of the powder leak tests. This aperture had an area of  $3.23 \text{ cm}^2$ , whereas the largest orifice tested had an area of  $3.14 \times 10^{-4} \text{ cm}^2$ , and the largest capillary  $4.91 \times 10^{-4} \text{ cm}^2$ . Since DUO powder would not flow through an opening orders of magnitude larger than the tested apertures, unhampered flow through the apertures could not be expected.

Further insight into DUO flow behavior is provided by the scanning electron microscope photograph in Figure F4, which shows the morphology of the powder. This sample was briefly dispersed ultrasonically, and yet many apparent agglomerates are visible in the upper photo. The large particle in the bottom photo is  $6.5 \text{ }\mu\text{m}$  in diameter (Martin's Diameter) and appears to be an agglomerate of many smaller submicron particles.

This photograph represents a visible indication of the tendency of DUO to form agglomerates, making dispersion difficult. This powder property could account for many of the erratic results observed in these experiments.



3000 X



10,000 X

FIGURE F4. Morphology of DUO Powder

DISTRIBUTION

No. of  
Copies

No. of  
Copies

OFFSITE

OFFSITE

A. A. Churm  
DOE Patent Division  
9800 S. Cass Avenue  
Argonne, IL 60439

12 Office of Nuclear Regulatory  
Research  
Division of Safeguards, Fuel  
Cycle and Environmental  
Research  
NRC Division of Research  
Washington, DC 20555

J. J. Davis  
W. Lahs (10)  
Frank Swanberg, Jr.

3 NRC Office of Nuclear Material  
Safety & Safeguards,  
Transportation Branch  
Washington, DC 20555

Charles E. MacDonald  
C. Ross Chappell  
William H. Lake

240 NRC Division of Technical  
Information and Document Control  
Washington, DC 20555

NRC Division of Standards  
Washington, DC 20555

Donald R. Hopkins

2 DOE Technical Information Center  
U.S. Department of Energy  
P.O. Box 62  
Oak Ridge, TN 37830

2 Sandia Laboratories  
Albuquerque, NM 87115

John A. Andersen  
J. K. Cole

6 Battelle Memorial Institute  
505 King Ave.  
Columbus, Ohio 43201

M. Pobereskin  
W. J. Madia (3)  
E. W. Schmidt  
J. D. Yesso

ONSITE

50 Pacific Northwest Laboratory

T. J. Bander  
C. E. Elderkin  
R. L. Hadlock  
J. W. Johnston  
G. B. Long (2)  
J. Mishima  
P. C. Owzarski  
L. C. Schwendiman  
S. L. Sutter (33)  
R. K. Woodruff  
Publishing Coordination (2)  
Technical Information (5)

<b>NRC FORM 335</b> (7-77)		<b>U.S. NUCLEAR REGULATORY COMMISSION</b> <b>BIBLIOGRAPHIC DATA SHEET</b>		<b>1. REPORT NUMBER (Assigned by DDC)</b> NUREG/CR-1099	
<b>4. TITLE AND SUBTITLE (Add Volume No., if appropriate)</b> Depleted Uranium Dioxide Power Flow Through Very Small Openings				<b>2. (Leave blank)</b>	
<b>7. AUTHOR(S)</b> S.L. Sutter, J.W. Johnston, J. Mishima, P.C. Owzarski, L.C. Schwendiman, G.B. Long, Ed.				<b>3. RECIPIENT'S ACCESSION NO.</b>	
<b>9. PERFORMING ORGANIZATION NAME AND MAILING ADDRESS (Include Zip Code)</b> Battelle Pacific Northwest Laboratories P1 O. Box 999 Richland, WA 99352				<b>5. DATE REPORT COMPLETED</b> MONTH   YEAR December   1979	
<b>12. SPONSORING ORGANIZATION NAME AND MAILING ADDRESS (Include Zip Code)</b> Office of Nuclear Regulatory Research U. S. Nuclear Regulatory Commission Washington, D. C. 20555				<b>DATE REPORT ISSUED</b> MONTH   YEAR February   1980	
<b>13. TYPE OF REPORT</b>				<b>PERIOD COVERED (Inclusive dates)</b>	
<b>15. SUPPLEMENTARY NOTES</b>				<b>10. PROJECT/TASK/WORK UNIT NO.</b>	
<b>16. ABSTRACT (200 words or less)</b>  The objective of the report is to develop experimental data that will be used to formulate calculational techniques to assess the potential powder passage through very small openings in shipping containers faulted in an accident.  Results of experiments are presented that measured the leakage of depleted uranium dioxide (DUO) powder through microorifices in a vessel approximately the same dimentions as a plutonium dioxide shipping container. Leaks were measured as a function of upstream pressure (15 psig to 1000 psig) and above and below the static powder level. An equation was developed to predict powder transmission from leaks using $\ln(AVP) > 10.5$ ( $A$ = area; $P$ = pressure). Maximum DUO transmission values were calculated for leaks where $\ln(AVP) < 10.5$ .				<b>11. CONTRACT NO.</b>	
<b>17. KEY WORDS AND DOCUMENT ANALYSIS</b>				<b>17a. DESCRIPTORS</b>	
<b>17b. IDENTIFIERS/OPEN-ENDED TERMS</b>					
<b>18. AVAILABILITY STATEMENT</b> Unlimited			<b>19. SECURITY CLASS (This report)</b> Unclassified		<b>21. NO. OF PAGES</b>
			<b>20. SECURITY CLASS (This page)</b> Unclassified		<b>22. PRICE</b> S

UNITED STATES  
NUCLEAR REGULATORY COMMISSION  
WASHINGTON, D. C. 20555

OFFICIAL BUSINESS  
PENALTY FOR PRIVATE USE, \$300

POSTAGE AND FEES PAID  
U.S. NUCLEAR REGULATORY  
COMMISSION



120555031837 2 ANRT  
US NRC  
SECY PUBLIC DOCUMENT ROOM  
BRANCH CHIEF  
HST LOBBY  
WASHINGTON DC 20555

POOR ORIGINAL